TO MY BELOVED MOTHER

AND

TO THE MEMORY OF MY FATHER,

The Application of Physical Methods of Analysis to the Study of Surface Formed during Wear by Organo-Sulphur Compounds

Abderrahman AZOUZ

A Thesis Submitted for the Degree of Doctor of Philosophy

The University of Aston in Birmingham

December 1982

ACKNOWLEDGEMENTS

I would like to express my deep appreciation to the people who have contributed directly or indirectly to this research effort.

I wish to express my gratitude to my former supervisor Dr. D. M. Rowson for his guidance, encouragements and assistance shown throughout this project, and this, even after leaving the university. I am also indebted to my current supervisor Dr. T. F. J. Quinn for his interest and support shown after taking over the supervision. Their invaluable thoroughness and enthusiasm are deeply appreciated and admired. Mr. J. Sullivan is deeply thanked for his discussions and suggestions. My deep respect and special thanks to Professor S. E. Hunt (Head of the Physics Dpt.) for all his available help shown whenever problems threatening my studies have arisen. Mr. T. Kennedy and all the staff are thanked for their constant help and friendship.

I would like to acknowledge the Dynamitron Group (Birmingham Radiation Centre) and in particular Dr. L. G. Earwaker and A. J. Bentley for their assistance during the nuclear experiments.

It would be ingratitude on my part to forget the Algerian Government and the Algerian National Oil Company (Sonatrach) for their financial support. In this effect, my personal thanks and graditude towards Mr. Hamrour, Head of the Dpt. Research and Development (Sonatrach), for his encouragements and support.

Also, my special acknowledgements must go to Mr. O. Bencherif (Attache Culturel in the Algerian Embassy) for his valuable help during the final stage of this project.

A special thanks is given to Miss S. Clark for her continued support and understanding throughout this work, and also for being a source of pleasure to me.

I should not forget the encouragements received from my friends T. L. Brahimi, K. Zendagui, M. Toutaoui and M. Drouche, for boosting my moral whenever I needed it.

In addition, I also wish to thank Miss S. Gill and A. Purchase for their friendship.

Mrs M. Creighton is thanked for the excellence of her typing.

Finally I would like to express my love to my mother and my deepest gratitude to my brother Kamel whose sacrifice and patience are most appreciated. My love also goes to the rest of the family (Nasr-Eddine, Said, Abdelhak and Zineb).

Abderrahman AZOUZ

The Application of Physical Methods of Analysis to the Study of Surface Formed during Wear by Organo-Sulphur Compounds

A Thesis Submitted for the Degree of Doctor of Philosophy

By Abderrahman AZOUZ (December 1982)

SUMMARY

A variety of physical analytical techniques, among them Electron Probe Microanalysis, Scanning Electron Microscopy, X-ray Diffraction and Optical Microscopy, have already been used in the past to investigate the formation and role of surface films developed during wear tests using a four-ball machine to test extreme-pressure additives. Although the existence of such films has been confirmed by these techniques, and theories have been put forward in order to explain the reaction mechanisms of these additives, the actual surface composition is still not known precisely. This inability to define the chemical nature of these surface species is due mainly to the fact that the layers formed are extremely thin.

To this effect, an investigation of the possibility of applying nuclear microprobes such as Rutherford Backscattering using 2 MeV alpha-particles and Deuteron-proton stripping reactions [(d,p) reactions], alongside the more conventional techniques, has been undertaken so that a total picture of the thickness and chemical composition of the films generated by the action of the sulphur additives could be drawn. The combination of the results from these different techniques has led to the evaluation of the thickness and to a better understanding of the formation of such films.

Key Words

Additive Anti-Wear Extreme-Pressure Film Thickness

CONTENTS

LIST OF TABLES

LIST OF FIGURES

5.11/5.33: REACTION YIELD SPECTRUM INDUCED BY DEUTERON BEAM PROBING ON SELECTED E.P. FILMS:

5.34/5.45: R.B.S. SPECTRUM FOR:

SYMBOLS

a.w. = anti-wear

e.p. = extreme pressure

r.p.m = revolution per minute

A° = Angstrom and 1 A° = 10^{-10} metre

eV = Electron Volt; 1 MeV = 10^{6}eV.

keV = 10^{3} eV

h = Plank's constant = 4.13557 10^{-15} eV.s

t = thickness

"S" = stopping power

N_A = Avogadro's number

ρ = density ($g.cm^{-3}$)

$(N \triangle x)$ = Average number of sulphur atoms per square centimetre

E = Energy

1 μm = 10^{-6}m

1nm = 10^{-9}m

CHAPTER ONE

INTRODUCTION

1.1. Lubricants and Additives

1.1.1 Principle of Lubrication

When two solid surfaces are in sliding or rubbing contact both friction and wear usually occur (1, 2, 3, 4). The friction is the resistance to the motion, whilst the wear results from the loss or the destruction of the surface material. To reduce the coefficient of friction and the wear, it is necessary to prevent the asperity contact between the two solid surfaces. This can be achieved by interposing a substance (solid, liquid or gaseous) between them to facilitate their relative movements. This substance may be termed a lubricant. Therefore the process involved is termed lubrication and could be generally defined as the art of minimising both friction and wear at the interface between surfaces in relative motion.

1.1.2 Lubricants: Functions and Requirements

The effect of the lubricant on friction and wear occurring between two surfaces is an inherent part of the lubrication process. Therefore this is referred to as a primary function of a lubricant. Nevertheless there are some other functions expected to be achieved. These are assigned as the secondary functions of a lubricant and they are its removal of frictional heat taking place during the event, its prevention from any external contamination and its protection against corrosion. To perform efficiently the lubricant must possess some properties which are (2):

a) Low shear strength

During sliding operation, the shear strength of the lubricant must be lower than that of the material of the surfaces it separates. Thus the lubricant will be able to undergo lateral (shearing) displacement.

b) Good Thermal Conductivity

Any frictional heat generated, at the contact area during the rubbing or sliding process, must be quickly and effectively dissipated from the bearing region without causing damage to the sliding surface.

c) Good Cleansing and Prevention of Contamination

The deposition of external agents as wear debris, air-borne dust, combustion products etc..., could reduce the efficiency of the process. The lubricant must keep the system clean and also ensure a good protection of the bearings against the contaminants.

d) Good Protection

The rubbing wear depends on the distance separating the sliding surfaces and on the temperature of the asperity contact and, also, it is strongly dependant on the bearing load. Corrosive wear results from the environment surrounding the system, whether the bearing is in operation or is idle.

Consequently the lubricant should not initiate any active corrosion; on the contrary it should protect the surfaces of interest against any chemical corrosive attack.

Gases (air, helium, etc...,) solids (dry bearing or solid lubricants), semi-solids (greases) or liquids (oils, aqueous or synthetic products) have been used for lubricating surfaces. Among them oily lubricants form the largest category and are classified according to their source of origin as mineral, animal, vegetable or fish oils (5). With the expansion of the oil industry, mineral or petroleum oils are widely used. In addition to the essential requirements for a lubricant (primary and secondary functions) they possess some other important advantages:

- Inexpensive and abundant,
- Extensive period of life,
- Physical and chemical properties are closely controlled in manufacture,
- Operational temperature range is wide enough to cover the majority of industrial applications,
- Non-toxic,
- Miscible with a wide selection of chemical additives.

Finally, it is worth noting that the viscosity, which is an important property of an oil for determining its ability to lubricate, is defined qualitatively as the resistance of the fluid to flow under an applied pressure (6). Practically, the coefficient of viscosity (sometimes called dynamic viscosity) is evaluated by taking the ratio of the applied shear stress to the rate of shear.

1.1.3 Additives

The load-bearing capacity of straight mineral oils is often insufficient for many industrial applications. It is therefore necessary to incorporate suitable additives into the lubricant to impart additional properties not originally present in the oil, or to enhance an existing property. Only after this addition has been made can the expected results be achieved (1, 4).

Additives are classified according to their functions and each type is employed depending on the special lubrication needed (1, 4, 7). Some examples are given below:

Circumstances whereby lubricant is utilised	Correct type of additives required
- High temperature	- Anti-oxidant (or oxidation inhibitor)
- Corrosive attack	- Corrosive inhibitor
- Soot contamination	- Detergent and dispersant
- All applications (low and high temperature)	- Viscosity index improvers
- Low temperature	- Pour point depressant
- Presence of air	- Anti-foam
- Water contamination	- Emulsifier
- High load bearing (high pressure and high temperature)	- Anti wear and extreme pressure

1.2 Type of Lubrication

The distance between the surfaces in contact, the bearing loads and the speed of the motion are the essential factors of the thickness of the lubricating film which, in turn, defines the type of lubrication that might occur. Figure 1.1 (8) shows the order of magnitude of the separation between sliding surfaces under each condition. As a result of the interest given to investigate the surface layers in the anti-wear and extreme-pressure regions, only the situations related to these areas will be considered (a.w. and e.p.).

1.2.1 Boundary Lubrication (Anti-Wear Regime)

The regime of boundary lubrication (or anti-wear regime) occurs when, due to high loads or low velocities, an oil film between moving metal surfaces is no longer maintained and this results in a metal-to-metal (ie asperity) contact over a significant portion of the lubricated area (Figure 1.2).

1.2.2 Extreme-Pressure Lubrication

In the situation of highly loaded contact surfaces giving rise to the temperature above the limit of the effectiveness of the boundary lubrication, the bulk oil film breaks down resulting in catastrophic wear, usually followed by scoring or scuffing, or even welding of the surfaces. This regime is called extreme-pressure lubrication.

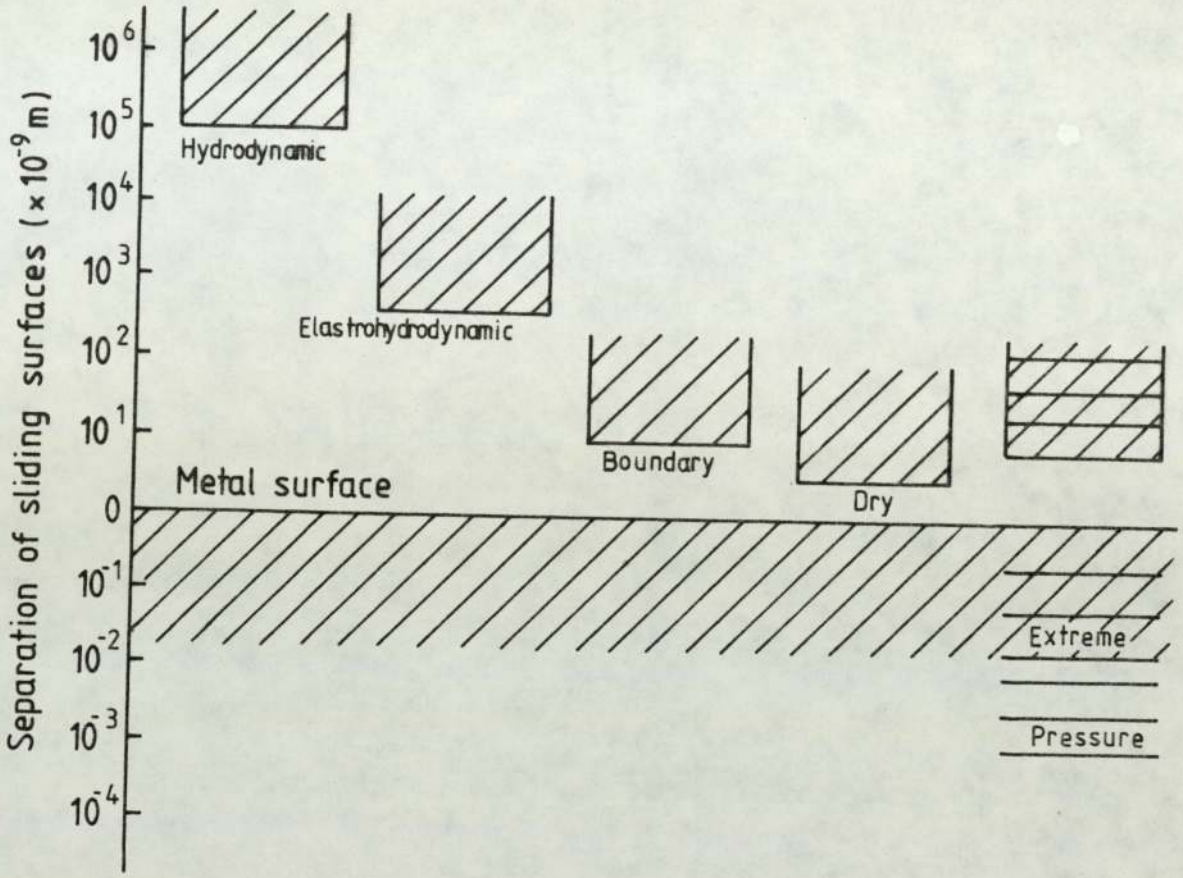

Fig 1:1 ORDER OF MAGNITUDE OF THE SEPARATION BETWEEN SLIDING SUFACES UNDER SPECIFIC TYPE OF LUBRICATION.

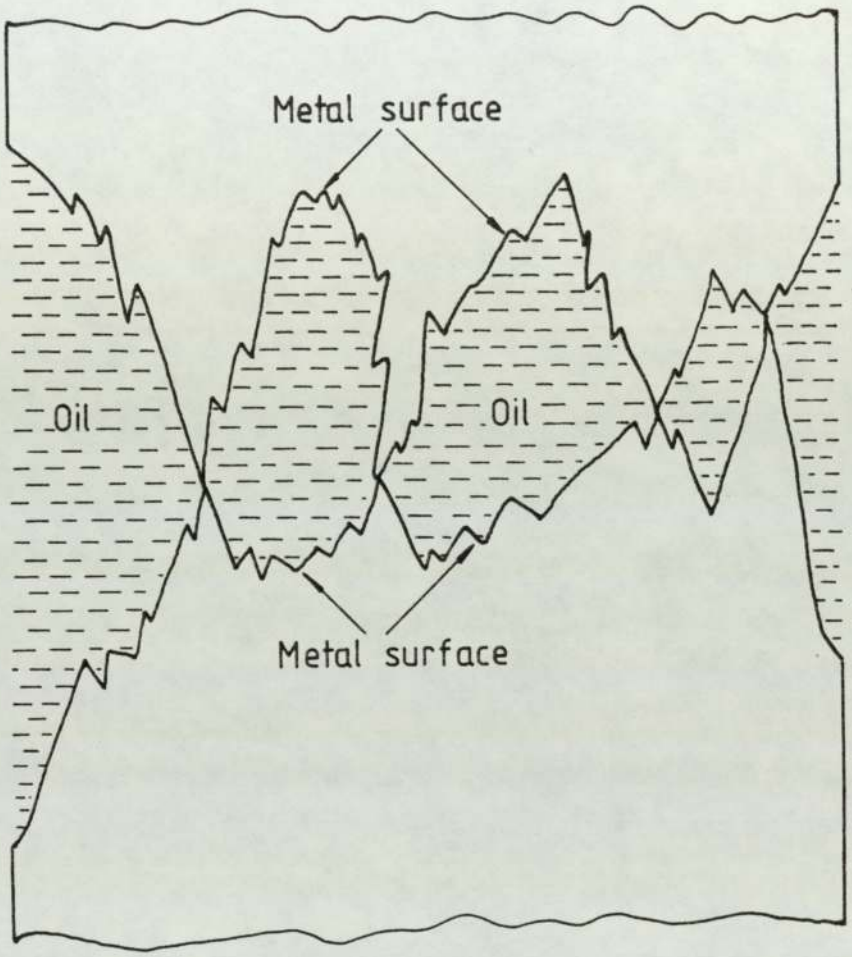

Fig 1:2 Boundary lubrication between two solid surfaces.

1.3 Anti-Wear and Extreme-Pressure Additives

As stated above when high loads or temperatures are involved during the lubrication process, normal lubricants cannot produce or maintain a continuous oil film between the interacting surfaces moving relatively to each other. It is therefore necessary to incorporate additives into the oil to prevent destructive metal-to-metal contact resulting in severe wear or welding. Anti-wear additives are used in the case of boundary lubrication whilst extreme-pressure additives (sometimes called anti-weld additives) are employed under the second condition.

1.3.1 Anti-Wear Additives

The most common anti-wear (a.w.) additives used are fatty acids and esters and they react chemically with the metallic surfaces to form a strongly adsorbed polar film between them. Consequently the metallic friction is reduced by the presence of this solid lubricant film formed which is effective at temperatures up to its melting point (Fig 1.3) (1, 4, 7).

1.3.2 Extreme-Pressure Additives

The use of extreme-pressure (e.p.) or anti-weld additives is necessary under the working conditions of high temperatures in which the oil film between the contacting surfaces has broken-down. Organic compounds containing one or more of the element sulphur, chlorine, phosphorus or lead are found to be the most suitable commercial e.p. additives. Only when the pressure becomes very high between the surface

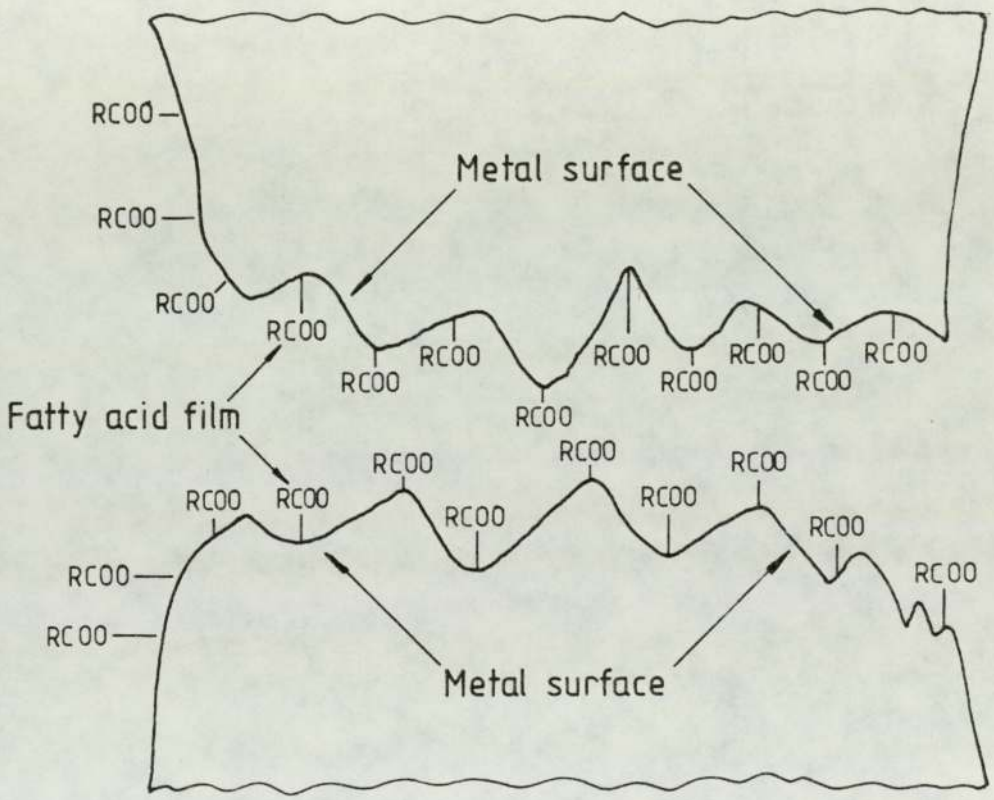

Fig 1:3 Surface Polar film formation.

asperities, do the additives undergo chemical reaction with the metallic surfaces, to form solid inorganic films of relatively low shear strength and high-melting temperatures. These films prevent seizure and welding of the bearing surfaces. Figure 1.4 shows a schematic representation of the sulphur film formation when the sulphur element is a part of the additive used. It is understood that during the process there will be some chemical wear appearing with the formation of e.p. films.

1.4 Previous Investigations

Since the introduction of the 4-ball machine as a device for testing the e.p. lubricants in 1933 by Boerlage (9), a variety of analytical methods have been applied either directly or indirectly for studying the mechanism and the e.p. efficiency of the organo-sulphur compounds. The most commonly accepted theory is that the organo-sulphur additives react with the metal surface to form mixed surface layers of organic and inorganic sulphides and/or iron oxide which prevent metal-to-metal contact and seizure.

By studying the coefficient of friction developed between two identical metallic surfaces under e.p. lubrication using sulphur-containing compounds as the additives, Greenhill (14), in 1948, suggested that a chemical reaction takes place between the moving surfaces and the additives. Assuming that sulphide films were formed during the process, he showed their existence by employing taper-section techniques.

From their 4-ball test results, Davey and Edwards (15) tried to explain the influence of chemical structure on the load-carrying

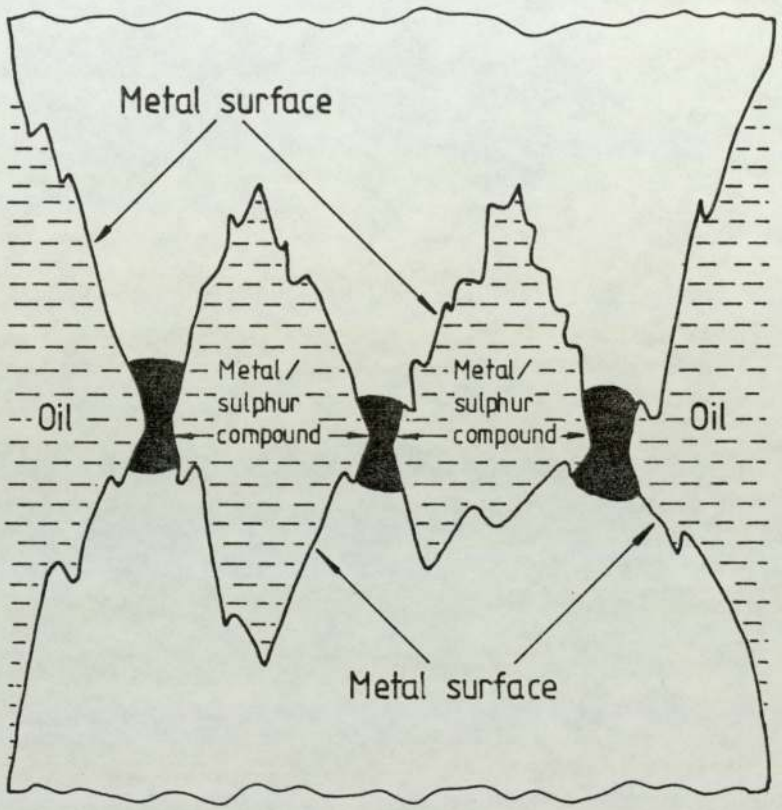

Fig 1:4 A simple representation of the Asperity sulphide formation.

properties of organo-sulphur compounds. They proposed that the reaction mechanism taking place on the steel surface of the balls, consisted of two or three steps, provided that the types of additives used were monosulphide or disulphide respectively.

i) Reacton of Monosulphide

The first step implies the formation of an adsorbed layer under mild loading and it is represented as follows:

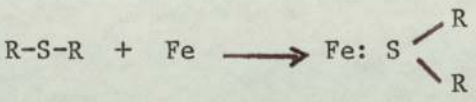

The second involves the formation of a mixed layer of ferrous sulphide and organic compound, vis:

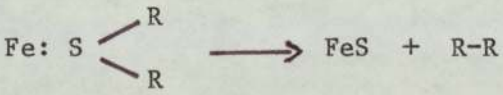

The effectiveness of this layer formed is reduced with the increase of load, and under severe conditions (ie extreme pressure) the film breaks down.

ii) Reaction of Disulphides

Similar to the action of the monosulphides, the first step involves the formation of an adsorbed layer under mild loading and the schematic representation is shown below:

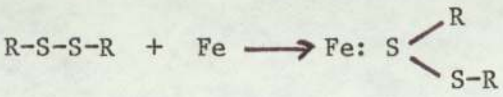

The second step indicates the formation of an iron mercaptide, namely:

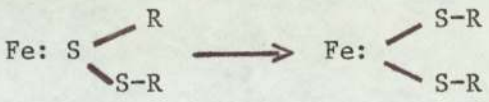

The iron mercaptide layer behaves as a soap film formed from a fatty acid under boundary lubricant conditions.

The third step occurs under very severe conditions and it involves the break down of the iron mercaptide film resulting in the formation of iron sulphide and organic sulphide layers, as shown below:

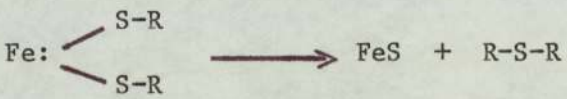

Loeser et al (16) used radioactive tracer technique and X-ray spectroscopy to analyse lubricant films on metal surfaces. Radioactive sulphur-35 (S-35) was employed to study the content and distribution of sulphur in e.p. films. The combination of the results from both techniques showed a positive identification of the sulphur element in or on the e.p. surface. Also they revealed that the additive or additive decomposition products react chemically with the surfaces to form a solid lubricant film.

From S.A.E. extreme pressure tests with sulphurised mineral oils, Godfrey (17) indicated that the e.p. mechanism consisted of the formation of a layer of 0.5 to 1.0 μm deep in the steel and the major constituent was Fe_3O_4, whilst iron sulphide was a minor constituent.

He speculated that the presence of sulphur in the mineral oil favourised the oxidation of steel under e.p. conditions. He also pointed out that although iron sulphides are a minor constituent in the final product, they are necessary for high load carrying capacities.

Electron Probe Microanalyser (E.P.M.A.) was introduced to the study of e.p. additives first by Allum and Forbes (10) when investigating the wear scars obtained during 4-ball tests on a series of oils containing organic disulphides. The authors showed the benefit of employing this technique for detecting the sulphur element and measuring its concentration together with its distribution over the worn surfaces. They found that in the mixed lubrication (ie a.w. region) very little sulphur was present, whilst in the e.p. region, large quantities of sulphur were detected. They postulated that this small detection of sulphur in the a.w. area was mainly due to the formation of an iron mercaptide. The results, also, showed that the sulphur distribution was uneven and the maximum film thickness was estimated between 0.3 to 0.5 μm. This investigation strongly supported to their earlier suggestion (18, 19) on the action of organo-sulphur compounds as load-carrying additives where they theorised that under e.p. conditions the activity of the additive is directly related to the ease of cleavage of the carbon-sulphur bond to form an inorganic sulphur containing layer.

Allum and Ford (18) observed from their e.p. results on monosulphides, disulphides and sulphoxides that the order of increasing e.p. activity was:

diphenyl $<$di - n -butyl$<$di-sec -butyl$<$di-tert -butyl$<$dibenzyl $<$diallyl

They concluded that the e.p. activity depended on the strength of the C-S bond which, consequently, made the e.p. performance of disulphides higher than that of the monosulphides.

The same kind of test was applied by Allum and Forbes (19) to determine the a.w. properties of these organo-sulphur additives and the results obtained were quite different from the e.p. results cited above. The following increasing order of activity was found:

di-tert-butyl $\ll$ di-n-butyl $<$ diallyl $<$ dibenzyl $<$ diphenyl

Also the a.w. performance of monosulphides was found to be less that that of the disulphides. The authors suggested that the a.w. activity was governed by the ease of scission of the S-S bond, so that an iron mercaptide could be formed.

In order to vindicate the two last conclusions drawn for the a.w. and e.p. activities, Forbes and Reid (11) investigated the adsorption/reaction of some disulphide compounds with metallic surfaces. They carried out liquid phase adsorption experiments on ground iron powder over a range of temperatures (25-170°C) and the results obtained for the reactivity of these organic disulphides was in the following order:

diphenyl $<$ di-n-octyl $<$ di-n-butyl $<$ di-tert-butyl $<$ dibenzyl

Furthermore, the test showed that the monosulphides and the mercaptans were less reactive than the corresponding disulphides. Consequently this investigation provided supporting experimental

evidence of the previous suggestions (18, 19) on the mechanism of the action of the organo-sulphur compounds in general, and as a result of this study an hypothesis was proposed to summarize the results obtained. The hypothesis can be simply represented in the following diagram:

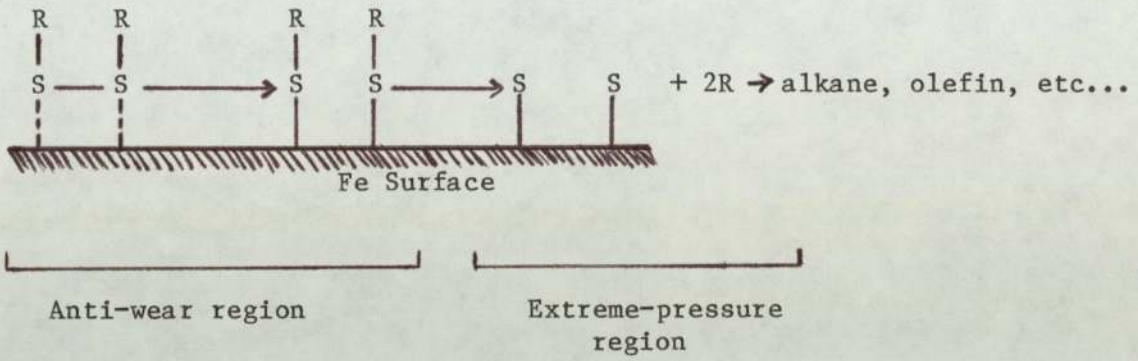

Instead of trying to evaluate the effectiveness of the additives by establishing the influence of their chemical structure and not giving any attention to the composition of the surface films formed, Coy and Quinn (8, 12, 13) decided to use a variety of physical methods of analysis to obtain as much information as possible about the composition of the films produced in actual wear tests using a 4-ball machine. The worn surfaces were analysed by the following methods:

i) glancing angle X-ray diffraction,

ii) electron probe microanalysis,

iii) scanning electron microscopy,

iv) optical microscopy combined with sectioning,

v) microhardness testing.

The authors demonstrated that a satisfactory analysis of the worn surfaces required several techniques. The combination of the

results from these analytical methods showed that the e.p. activity of the disulphides followed the order of the ease of scission of the C-S bond, viz:

diphenyl < di-tert -butyl < dibenzyl

also thick layers of iron sulphide (FeS) were the main chemical compound detected on the films formed by the good e.p. additives such as DBDS and DTBDS. In the a.w. region, FeS was not detected and the authors believed that the reason was probably due either to the thinness of the films formed on the wear scars or to the adsorption/reaction of the additives onto the surfaces as suggested by Forbes et al (10, 11, 18, 19). Consequently the investigators recommended further highly sensitive surface techniques (capable of analysing the outermost atomic layers) to be used as a complementary method for studying the reaction mechanisms occurring in the a.w. regime. However, as a general conclusion summarising the analyses carried out by Coy and Quinn (8, 12, 13), it was demonstrated that the load-carrying capacity was determined by the properties and the thickness of the films formed on the worn surfaces, and any further investigation of this interesting but difficult field should be based on the study of the real worn surfaces rather than films produced by static immersion tests previously used in the past.

The development of sensitive surface techniques such as X-ray Photoelectron Spectroscopy (X.P.S. or E.S.C.A.), Auger Electron Spectroscopy (A.E.S.), Low Energy Diffraction (L.E.E.D.), Secondary Ion Mass Spectroscopy (S.I.M.S.), etc..., led to the possibility of employing them in tribological research and in particular to the study of the films formed during wear tests using a 4-ball machine.

The feasibility of using A.E.S. with depth profiling to detect and examine the surface films formed by additives in lubrication processes was reported by Phillips, Dewey, Hall, Quinn and Southworth (20). X-ray Photoelectron Spectroscopy (X.P.S.) was engaged by Bird and Galvin (21) to examine films formed on the surfaces of EN31 steel specimens by oil solutions of e.p. additives, such as elemental sulphur and DBDS, in immersion and rubbing tests. Their investigation showed that X.P.S. was of great advantage by providing information on the elements associated with their respective chemical states to a depth profile of about 1 to 2 nm. In addition, the results obtained from the immersing and rubbing tests were quite different and this finding provided the experimental evidence that the previous immersion tests were not, in general, good guides in the study of the reaction mechanisms of the organo-sulphur additives.

Auger Electron Spectroscopy (A.E.S.) incorporated with argon-ion sputtering technique were utilised by McCarrol, Mould, Silver and Sims (22) to build up an approximate composition profile of the layers formed on the wear scars, which were produced during tests using a 4-ball machine with two sulphur-containing compounds, dibenzyl disulphide (DBDS) and di-tert-nonyl polysulphide, as the lubricant additives. The analyses showed that the sulphur level decreased gradually with increasing depth then stayed constant below a depth of around 100 A°. This result indicated that the additive-metal reaction was taking place over the first few Angstroms. The investigators also examined the influence of load on film formation and they found that the increment of the load increased the sulphur content in the surface layer.

In a two publications, Tomaru, Hironaka and Sakurai (23, 24) studied the effect of oxygen on the load-carrying action of some sulphur additives by combining several methods, namely:

i) 4-ball machine,

ii) hot wire technique (in air and in argon),

iii) E.P.M.A. and,

iv) Ion Microanalysis (I.M.A.).

They proposed that the effectiveness of the e.p. additives containing sulphur compounds could also be attributed to the presence of the oxygen occurring in the bearing zone, and not only to the sulphur element alone, as previously predicted.

The reaction kinetics of the film-forming reaction were observed by Okabe, Nisho and Masuko (25). Radioactive tracer technique, using radioactive dibenzyl disulphide labelled with sulphur-35, enabled them to measure the friction coefficient simultaneously with the amount of the surface reaction product on the friction surface. The interpretation of the results demonstrated that the chemical reactivity of the sulphur-type additives and their lubricating performance depended upon the adsorptive-action of the sulphide in the friction zone.

The phenomenon taking place during the interaction between organic sulphides and metallic powder of Fe, Cu and some oxides, was interpreted by Mayer, Berndt and Essiger (26) with the assistance of the Differential Thermal Analysis technique (D.T.A.) By this method the internal factors influencing the interaction of rubbing surfaces

under dynamic conditions were deduced. The D.T.A. measurements revealed that the starting temperature of the sulphidizing reaction was a relative criterion for the reactivity, independent of the reaction type. This observation purported that the e.p. efficiency of the organo-sulphur compounds was mainly governed by the temperature parameter.

Even though the idea of the great significance of the temperature effect in lubrication processes is not new, there is still much to be learned about the magnitude and distribution of the temperature originated at the contact point between the top ball and the three stationary balls during the running operation of the 4-ball wear tester. Thereby the knowledge of the surface temperature is of great importance and may add new elements of information in the comprehension of the mechanism by which lubricants and additives affect wear via chemical processes. Unfortunately, many practical obstacles arise in recording the contact temperature, however few (but different) approaches to overcome this difficulty have been reported up until now.

First, Blok (27) tackled the problem theoretically and proposed mathematical equations for calculating the contact temperature or "flash temperature" occurring at sliding surfaces under extreme pressure conditions. He later applied these equations to the case of the 4-ball machine (28). Following the same step, Jaeger (29) carried out the calculations into considerable numerical detail. Taking into account these two previous findings and starting from Blok's concept (28), which stated that the load carrying capacity of lubricant was characterised by a critical temperature for failure, Lane (30) used a

simple mathematical treatment to demonstrate that the maximum value of this critical temperature could be simply reduced to the following expression $W/d^{1.4}$, where W was the applied load in kg and "d" the wear scar diameter in mm. He designated this expression as "Flash Temperature Parameter (F.T.P.) representing the flash temperature occurring in the contact area between the balls, furthermore it was regarded as a measure of e.p. performance of lubricants. This assessment was accepted as one of the test procedures of the 4-ball machine and recommended by the Institute of Petroleum, I.P. 239/77 (31).

Fein (32) investigated the seizure phenomenon in the 4-ball wear machine by observing the effect of non-reactive lubricants on steel and by using Blok's equations (28) to estimate the surface temperatures corresponding to the bulk lubricant transition temperatures. He concluded that the relationship between bulk lubricant temperature, load and speed at the transition, depended entirely on load and speed, and this was due to the frictional heat generation.

By modifying the conventional ball holder and incorporating an iron-constantan thermocouple inside the pot, Manteuffel and Wolfram (33) were able to record automatically the temperature changes of the lubricant after it left the contact area. Thus a "temperature-load" chart was obtained. The interpretation of the wear scars at the transition points on the "temperature-load" curve suggested that very rapid wear occurred together with a rapid drop unit in pressure during these periods of severe boundary lubrication. They completed the investigation by using the radioactive tracer technique which revealed that at the transition points there was an increase in chemical activity between the metal surface and the active e.p. elements in the lubricant.

Sethuramiah, Okabe and Sakurai (34) regarded the temperature factor as the main contribution to the e.p. lubrication failure. Firstly they observed the friction coefficient (f) just before and at welding points during standard tests on five sulphur compounds at various concentrations, and the results displayed two distinct types of behaviour according to the concentration and the additives employed. In the first case welding occurred with a sudden transition (Tr 1) from a relatively low friction within two or three seconds, whilst in the second type the friction rose from a relatively low value (Tr 1) and remained constant for a period of time (Tr 2) before welding occurred. Figures 1.5 and 1.6 gave a schematic representation of these two types of behaviour (34). After completing the standard tests, the bulk temperatures at the transition times (Tr 1 and Tr 2) were recorded by means of a thermocouple probe inserted into the ball pot. The average values found for Tr 1 and Tr 2 were respectively 60°C and 125°C. With very simple assumptions made on Archard's theory (35) the contact temperatures at these points were calculated. These were then added to the corresponding recorded bulk temperature values. The quantities obtained were designated as the failure temperatures and their values were between 290°C to 390°C for Tr 1 and around 700°C for Tr 2. The investigators concluded that two types of failure governed by critical temperatures were taking place during the e.p. lubrication, namely these 1) lubricant failure and 2) e.p. film failure. The first type was attributed to the inefficacy of the carrier lubricant or its decomposition products beyond the critical temperature corresponding to the transition Tr 1. In the event of Tr 2, when the applied loads were being supported by the e.p. films formed, the second type was due to the break down of these protective films as a result of the chemical reactions occurring between them and the metal surface, and usually ending up by welding when the temperature approached 700°C.

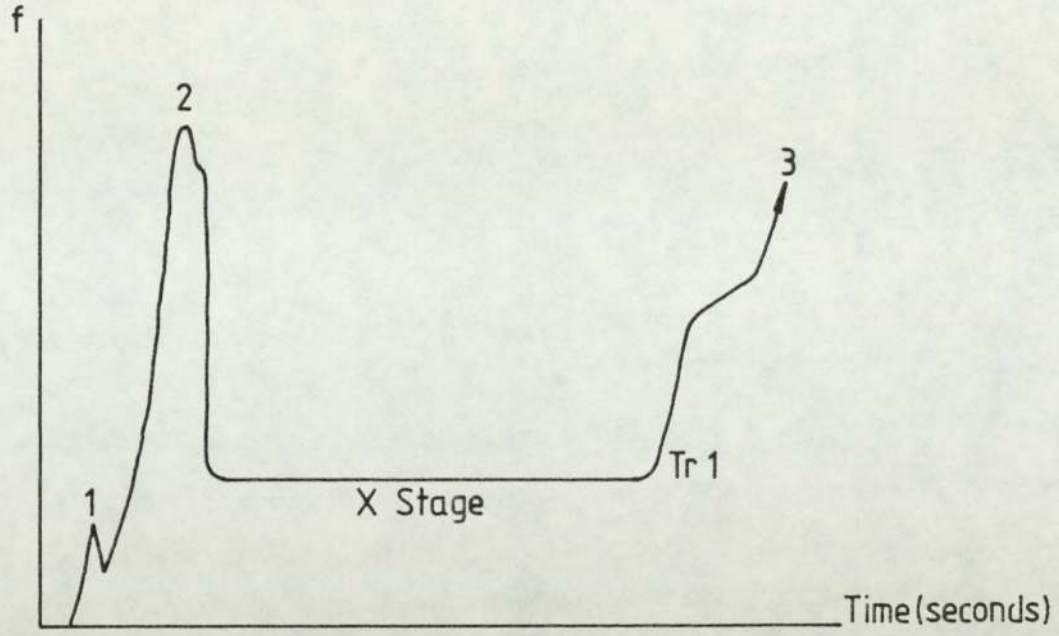

Fig 1:5 Type 1 behaviour at weld load (schematic representation)

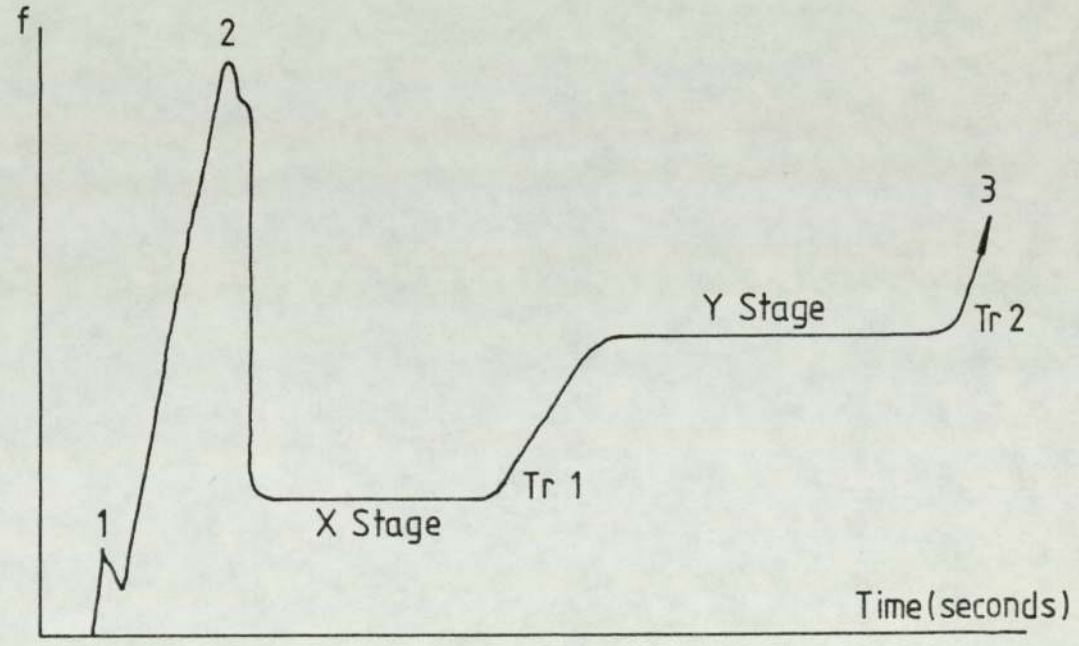

Fig 1:6 Type 2 behaviour at weld load (schematic representation)

KEY

1	Start	Tr 1	Transition point N° 1
2	Seizure	Tr 2	Transition point beyond Tr 1
3	Welding		

1.5 Aim of this research

The aim of this research was to investigate the formation and the role of surface layers developed during wear tests when organo-sulphur compounds were used as the additives. The emphasis was placed on the introduction of new techniques, for instance, nuclear analysis to study the structure of such surface films in order to gain further insight into the accepted theory of the reaction mechanism and the load-carrying properties of these additives. The additives studied were elemental sulphur and three aromatic sulphides namely dibenzyl disulphide (DBDS), dibenzyl monosulphide (DBMS) and diphenyl disulphide (DPDS) each at their various concentrations according to the test selected. The base lubricant used was a white mineral oil (Risella 32). Wear tests were performed on the well known Shell four-ball machine using either the conventional geometry of rotating ball on three stationary balls or the altered design of "ball-on-three-flats" in which the contact geometry was identical to the conventional mode. The balls or rollers, which were referred to as test specimens during the analytical methods employed throughout this work, were EN31 steel hardened to 850 $\pm$ 10 V.P.N. The operational time was either one minute for each load in the case of determining the additive performances, or for a time range of one minute to several hours in the case of investigating the dependence of a.w. and e.p. film formation on time, and on the temperature; and also to enable the colletion of a sufficiently large quantity of wear debris for the eventual X-ray diffraction analysis.

As stated earlier, the previous investigators applied a variety of physical analytical techniques to explain the 4-ball wear,

in terms of possible wear mechanisms. Although the findings were consistent with the formation of surface layers of iron sulphide, very little is known about the distribution and the thickness of these films. By introducing high energy charged particles, it was hoped that the present investigation would provide a means for studying the a.w. and e.p. surface films formed on EN31 steel during sliding wear tests. Two types of charged particles were used, namely
1) Rutherford Backscattering (R.B.S.) using 2 MeV alpha-particles and
2) Charged Particle Stripping Reactions using Deuterons [(d, p) reactions]. In addition, analyses using the more conventional techniques such as X-ray diffraction technique, S.E.M. coupled with an energy dispersive analyser, E.P.M.A. and X.P.S. were accomplished. Bulk temperatures were also recorded using thermocouples.

The combination of the results obtained from these different methods led to the evaluation of the thickness of the films formed during 4-ball tests and also to a better understanding of the mechanism of the action of the organo-sulphur additives used throughout this project.

Also as a part of this research, a survey and theoretical calculations were conducted to show that Neutron Activation Analysis was not suitable for detecting the sulphur element in the wear debris collected.

CHAPTER TWO

EXPERIMENTAL METHODS AND DETAILS

2.1 The 4-ball Machine

2.1.1 The Original Design

The 4-ball machine is a standard tribology test rig for testing the e.p. and a.w. properties of oils and greases (36). The one used throughout the project was a Shell 4-ball machine (Figure 2.1) given to the University of Aston by Shell Research Limited. The basic principle of the machine is that one load-bearing ball is rotated in contact with three fixed load-bearing balls immersed in the oils plus additives (Figure 2.2). The centres of the four balls form an equilateral tetrahedron.

The conditions of the experiments were chosen to satisfy the requirements made by the Institute of Petroleum (designation IP 239/77) concerning the use of the 4-ball machine as a lubricant testing device. Therefore during tests covering the determination of load-carrying activity for the a.w. and e.p. regions, the running time for each applied load was the standard time of one minute over a range of loads from 40 kg to 900 kg depending on the additive used. The rotation of the upper loaded-ball was fixed to 1500 r.p.m. The balls were made from EN31 steel and the size of each one was $\frac{1}{2}$ inch in diameter (Figure 2.3).

2.1.2 The "3-Flats" Modification

Due to the difficulty of analysis the $\frac{1}{2}$ inch diameter ball on the electron probe microanalyser available at the University, one-

FIG. 2.1 FOUR-BALL MACHINE

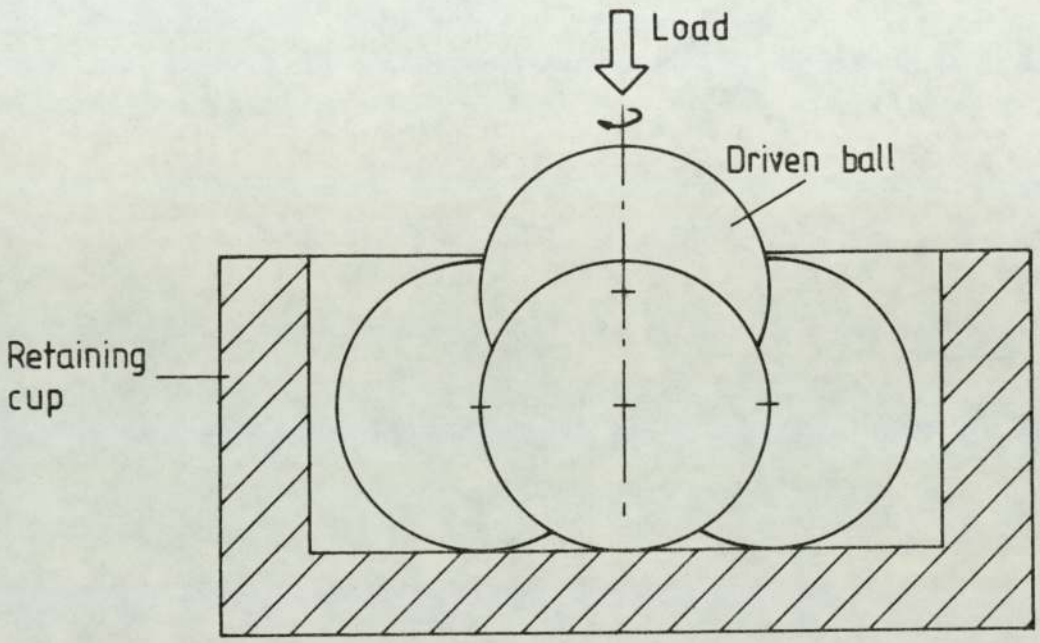

Fig 2:2 Basic arrangement of four-ball testing machine.

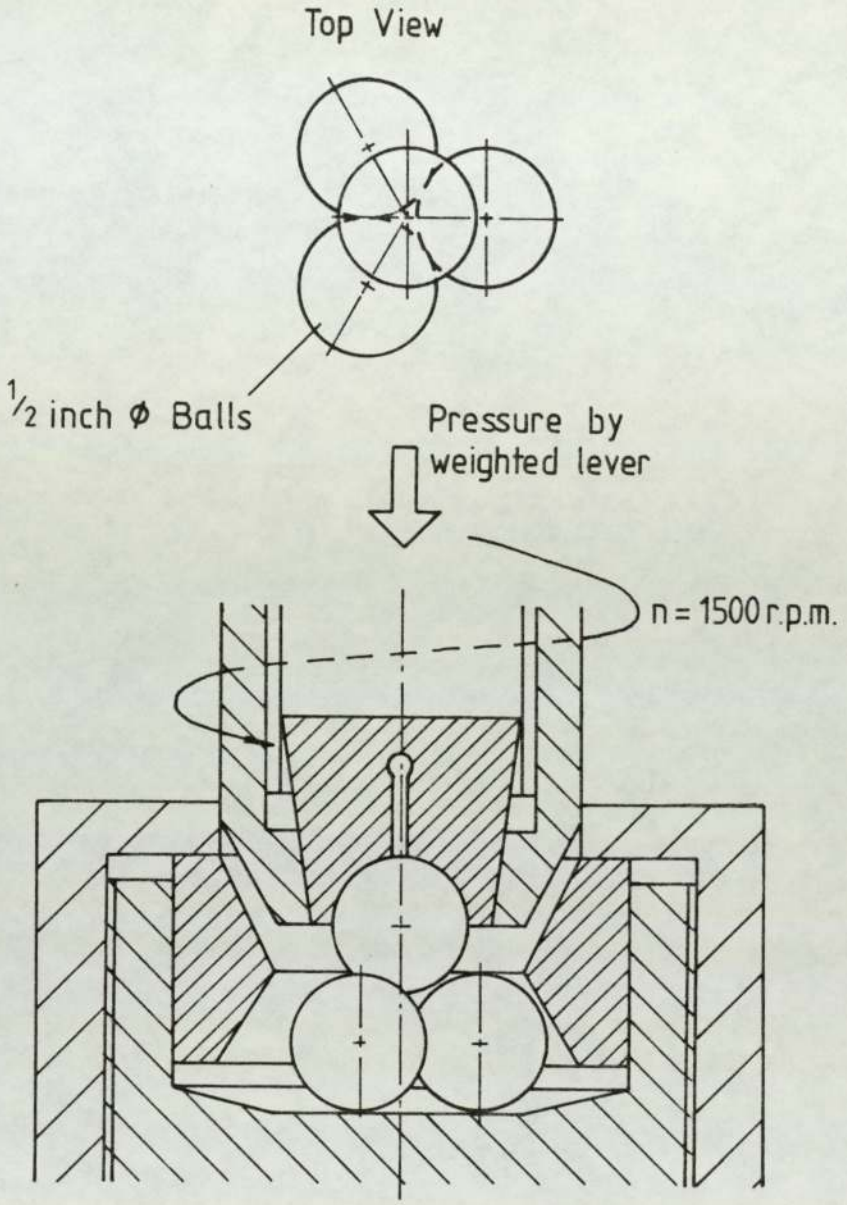

Fig 2:3 Diagram showing details of ball-cup inside the Four-Ball machine.

ball-on-three flats geometry as used by Coy (8) was utilised to produce suitable samples for the analysis. In this arrangement three $\frac{1}{4}$ inch diameter and $\frac{1}{4}$ inch long steel rollers are locked in a holder so that a top-rotating $\frac{1}{2}$ inch diameter ball rests at the centre of the flats. An alteration of the original design (8) of the holder for the rollers was made to ensure a better performance during the preparation of the specimens. The contact geometry between the top loaded ball and the rollers was identical to the ball-on-ball mode. Figure 2.4 shows the basic arrangement for the roller bearings. In addition the latter are also more suitable for analysing by means of the nuclear techniques to be described later.

2.1.3 Initial Cleaning Procedure

The balls were first washed thoroughly with a detergent and rinsed with ordinary water. After being dried they were cleaned with a commercial degreasing solution supplied by Shell and called SPB2. Then they were put in a water cooled vapour bath containing petroleum ether for at least two hours. At the end of the cleaning operation they were stored with great care, isolated from any kind of external contamination before being used in the 4-ball machine.

The procedure for cleansing the rollers was to commence by polishing the one end using different abrasive papers (grade 100, 180, 240, 400, 600 and 1200) and diamond papers (1 and 6 μm) and then to clean in an ultra-sonic bath using acetone. Afterwards the same procedure as described above for the cleaning of the balls was used on the rollers and also on the removable parts of the 4-ball machine.

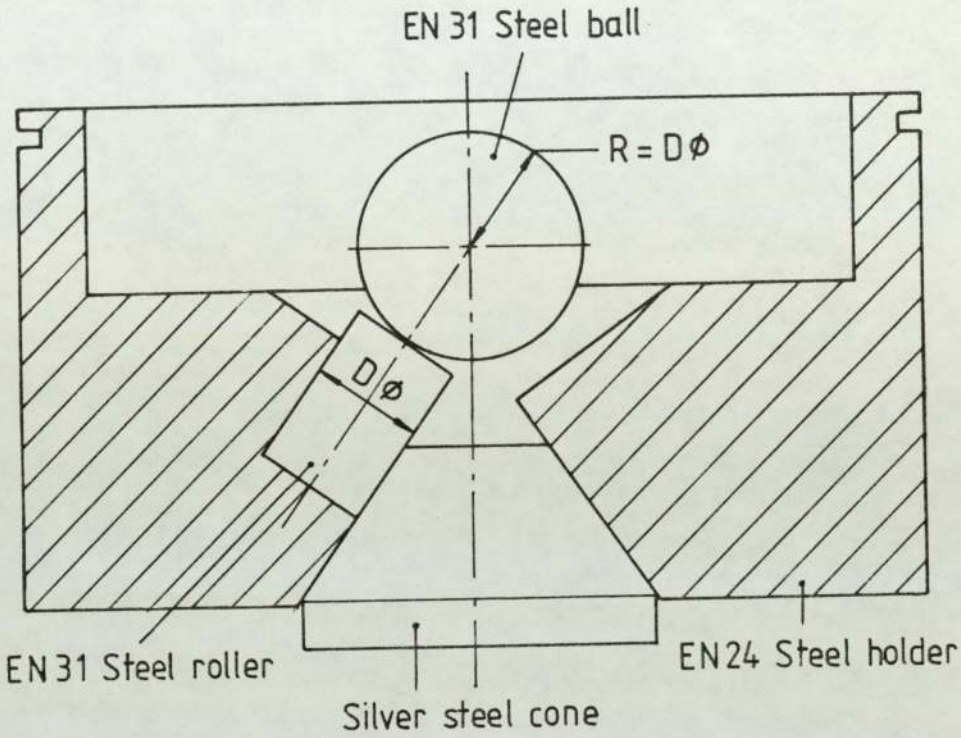

Fig 2:4 3-Flats holder

2.1.4 Procedure of the Test

At the beginning of each experimental procedure, the 4-ball machine was switched on for a period of fifteen minutes to warm up the motor ensuring constant speed and torque. Meanwhile balls or rollers were mounted in their respective holders. For each load, in the case of the conventional mode, three balls were placed into the bowl of the container (Figure 2.3) and then fixed together by a clamping ring. A clamping nut served to tighten them up. A fourth ball was put into a chuck (Figure 2.5) and the whole was thrust at the end of the drive shaft when the machine was ready for an experiment to begin. About 20 ml of the solution under test was poured into the cut containing the three clamped balls and the holder was put in the appropriate position, ie beneath the rotating ball in the chuck.

In the case of the one-ball-on three flats, the experiment was set up in a similar manner, except that there was no need to use the clamping ring with the altered holder (cf. figure 2.4).

Afterwards, the top ball was rotated under a specified load against the three lower balls (or rollers) for either one minute in the case of the standard test or for a time range of 1 minute to several hours in the case of investigating the dependence of a.w. and e.p. film formation on time and on the temperature of the lubricant.

At the end of the experiment, the lower test samples were degreased by SPB2. Then the diameter of the scars formed on their surfaces was measured by using a travelling microscope, parallel and at right angles to the direction of sliding. Therefore for each applied load, six readings were taken and a mean value was found.

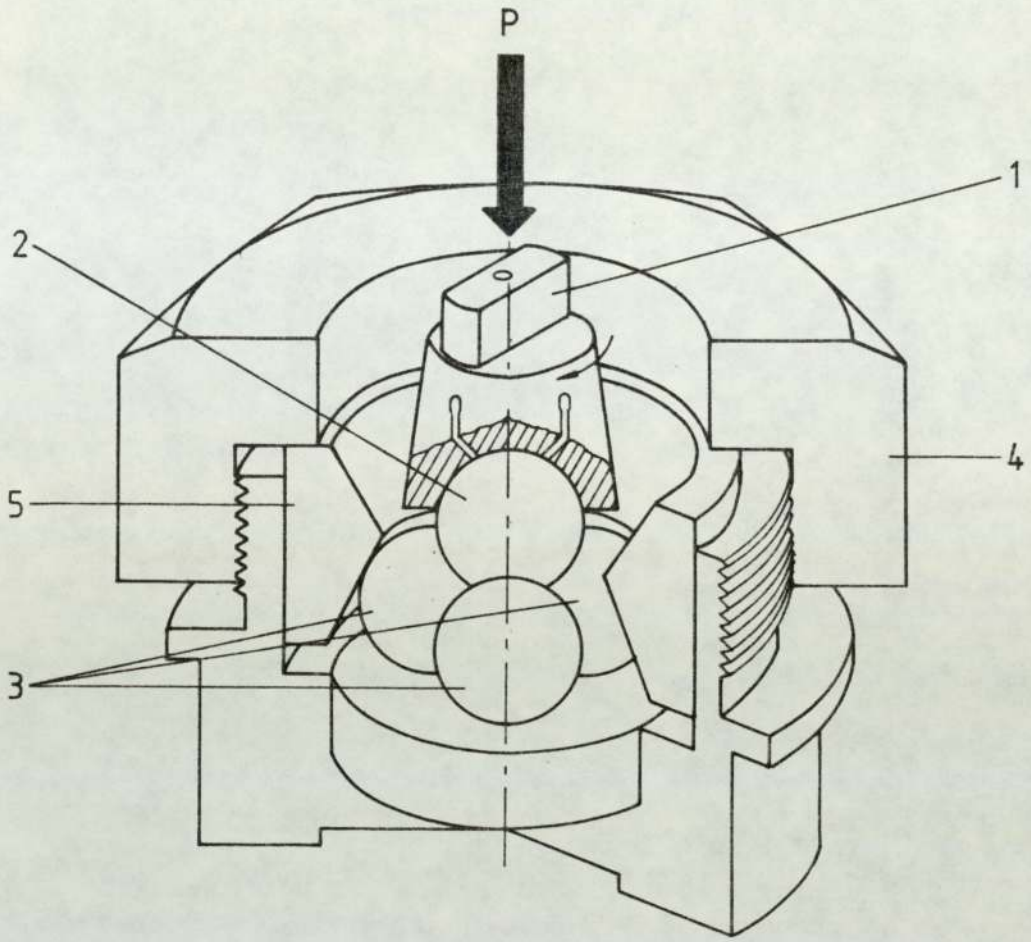

KEY

1 Chuck
2 Driven ball
3 Stationary balls
4 Clamping ring
5 Ball holder

Fig 2:5 Main elements of a four-ball machine

The "wear-load" curve was obtained by plotting the mean wear scar diameter against the load on a log-log scale. A typical log-log plot of the mean scar diameter versus the applied load, as shown in Figure 2.6, usually reveals three distinctive regions namely AB, BC and CD corresponding respectively to different operating modes of the lubricant:

i) Region AB: This region is called anti-wear (a.w.) in which due to the condition of low load and low friction, the wear causes only small smooth circular scars and their diameters are slightly larger than those of indentation caused by the static load and represented by the Hertz line.

ii) Region BC: This region is called the initial seizure (i.s.) and it is indicated by a sudden increase of the measured scar diameter due to the rapid increase of friction and wear. The phenomenon is recognised practically by a squeaky sound of the machine and it could be caused by a momentary failure of the oil film which separates the two surfaces involved.

iii) Region CD: This region is called extreme pressure (e.p.) and it is distinguished by the high load and the high friction involved in the process. This results in the visible evidence of rough and large scars on the three stationary balls. With the increase of the load (ie towards the point D), the bulk oil tends to break down due to the very high pressure imposed upon the contact areas, and this leads to the fusion of the metal between the rubbing surfaces. Hence the four balls weld together in the pyramid form.

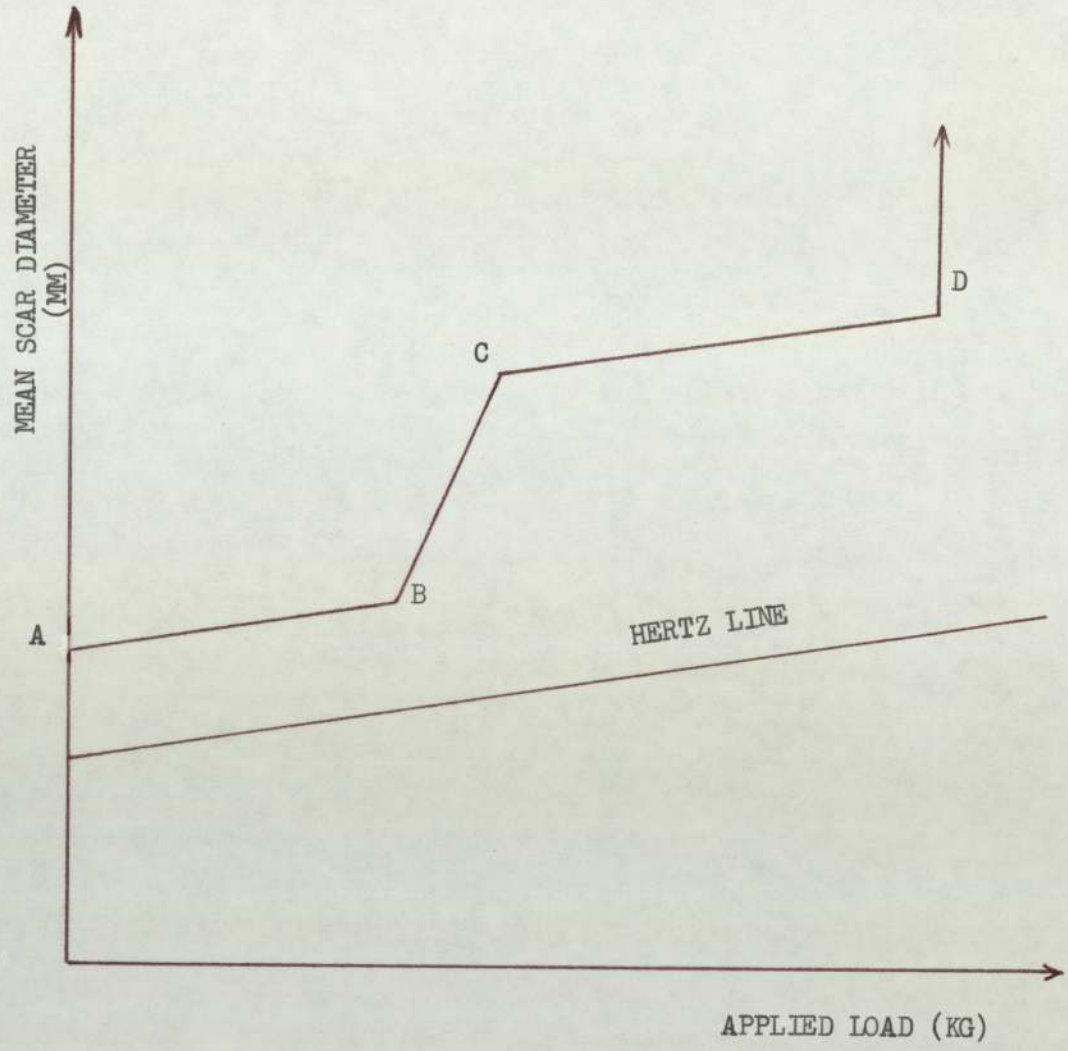

FIGURE 2.6 TYPICAL LOG-LOG PLOT OF THE MEAN SCAR DIAMETER VERSUS THE APPLIED LOAD.

2.1.5 Temperature Work

To study the temperature of the oil plus additives during wear test under a.w. and e.p. regimes, a thermocouple wire was immersed into the bowl holding the balls so that the temperature variations of the lubricant with time could be recorded. Thus, for each additive, a "temperature-time" chart was obtained for each region. Also the dependence between the temperature and the load, during the standard wear test, was investigated using the same procedure.

2.2 Description of the Material

2.2.1 Balls and Rollers

The balls and the rollers were made from EN31 steel hardened to 850 $\pm$ 10 V.P.N. with the following composition:

C: 0.90 up to 1.00%

Si: 0.10 up to 0.35%

Mn: 0.30 up to 0.75%

S: 0.050 maximum

P: 0.050 maximum

Cr: 1.00 up to 1.60%

Ni: 0.10%

Fe: balance ie 95.90% up to 97.50%

2.2.2 Lubricants

A white mineral oil called Risella 32 (Shell momenclature) was used throughout the project. It is a highly refined mineral oil

containing mainly saturated cyclic hydrocarbons with side chains and contains less than 100 p.p.m. sulphur. It is also a good lubricant for use in high temperature experiments. Some of its physical properties, measured at 30°C and 100°C, are presented in Table 2.1.

2.2.3 Additives

As the aim of this investigation was to study the surfaces formed during wear by organo-sulphur compounds only additives containing sulphur were employed. The additives studied were elemental sulphur and three aromatic sulphides namely, dibenzyl disulphide (DBDS), dibenzyl mono-sulphide (DBMS) and diphenyl disulphide (DPDS) each at various concentrations depending on the nature of the test. These additives were kindly provided by Thornton Research Centre (Shell Research Limited) in a crystalline form.

The structure of the aromatic sulphides are for:

i) Dibenzyl Disulphide (DBDS)

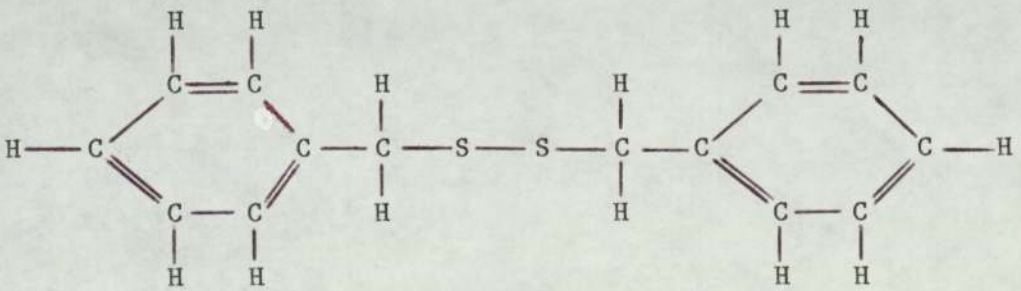

Chemical formula: $C_{14}H_{14}S_2$

Molecular weight: 246.395

Property	Temperature	
	30°C	100°C
Dynamic viscosity ($\times 10^{-3}$ Nsm^{-2})	62.37	5.09
Pressure Coefficient ($\times 10^{-9}$ m^2N^{-1})	28.50	18.50
Viscosity Index	89	

Table 2.1: Physical Properties of Risella 32 with Temperature.

ii) Dibenzyl Mono-sulphide (DBMS)

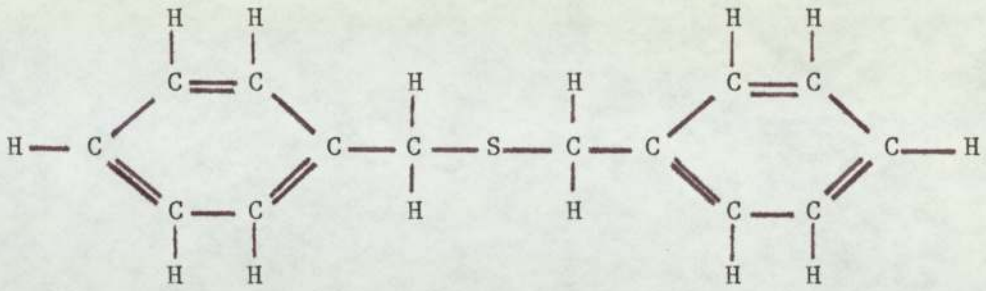

Chemical formula: $C_{14}\ H_{14}\ S$

Molecular weight: 214.331

iii) Diphenyl Disulphide (DPDS)

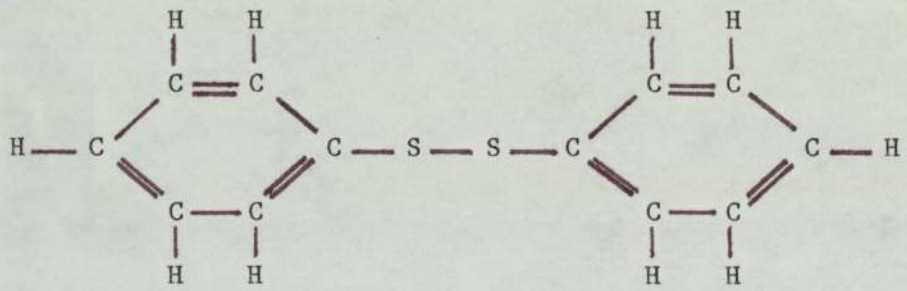

Chemical formula: $C_{12}\ H_{10}\ S_2$

Molecular weight: 218.341

2.3 X-ray Diffraction Technique

2.3.1 Production of Wear Debris

For some selected loads depending on the region (a.w. or e.p.) the time of the 4-ball test was extended to enable the formation of a

large quantity of debris in the oil blend under test. The wear debris collected from the test was washed by SPB2 then separated in the centrifuge. The precipitate was dried very gently on a hot plate to evaporate the remainder of the degreasing solution, leaving behind only the powder of the debris.

2.3.2 Powder Method

The powder method of X-ray diffraction was utilised to analyse the wear debris in order to identify the mechanism of a.w. and e.p. protection. More precisely the Debye-Scherrer method (37) was engaged to identify the elements which could form the surface layers of the scars.

The powder specimen was placed in a thin-walled glass container which was mounted on the axis of a powder camera (Figure 2.7) and a narrow strip of film was wrapped around the inside, as shown in Figure 2.8. A cobalt X-ray tube with an iron filter and a 0.5 mm collimator was employed to produce a fine monochromatic beam of CoK_{α} X-rays to irradiate the sample. The exposure time was set from 1 to 3 hours depending on the amount of the debris collected. The diffraction pattern was recorded on the film in the form of a series of lines in which their distance from the origin represented twice the value of the Bragg angle (θ). Using the Bragg relation (37) the interplanar spacing "d" for each line was calculated and then related to the possible compounds by referring to the American Society for Testing and Materials (A.S.T.M.) data file.

The Bragg relation is:

$$2d \sin\theta = \lambda \qquad \text{.....(2.1)}$$

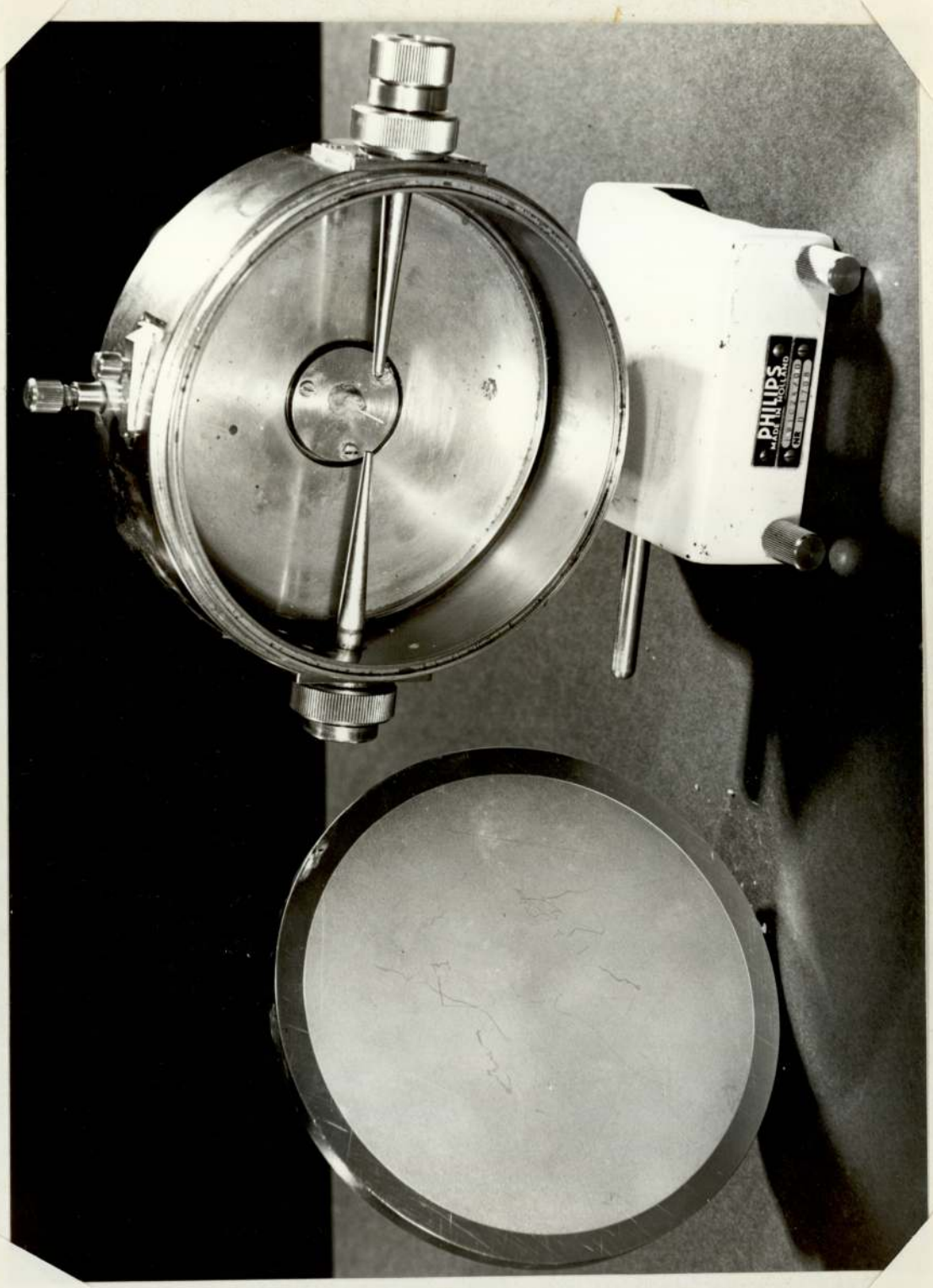

FIG. 2.7 DEBYE-SCHERRER CAMERA, WITH COVER PLATE REMOVED

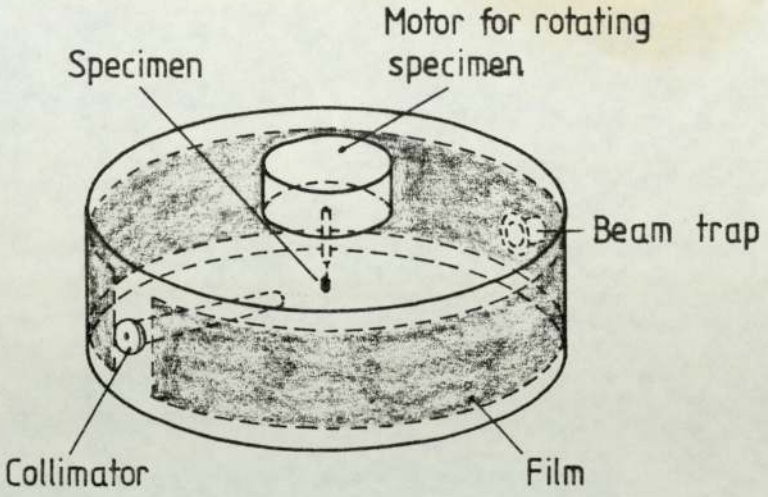

Fig 2:8 A typical arrangement for a powder photograph.

where $\begin{cases} d = \text{interplanar spacing} \\ \theta = \text{Bragg angle} \\ \lambda = \text{Wavelength of the X-ray beam} \end{cases}$

Mean $\lambda (K_{\alpha})$ for cobalt with an iron filter = 1.7909A°

2.3.3 X-ray Glancing Angle Method

In this analysis the scars were exposed to the X-ray beam using the same camera and technique described above. First the samples were half sectioned by means of a diamond belt then they were mounted in the camera by making sure that the incident X-ray beam hit the exposed edge without passing through the rest of the sample (Figure 2.9).

2.4 Analysis of the Worn Surfaces by using Scanning Electron Microscopy Coupled with Energy Dispersive X-ray Analyser

One of the main advantages of using the Scanning Electron Microscope (S.E.M.) is the ability of having micrograph images of surfaces of specimens with a good depth of focus. Also during the scan of the electron beam over the surface there is a production of X-rays. The emitted X-rays are characteristic of the chemical elements present on the area studied. The measure of their energies or their wavelengths provides a complete analysis and this is achieved by coupling the S.E.M. with an X-ray detector. The detector used in these experiments is commercially known as the KEVEX attachment.

2.4.1 Characteristic of the System used

A Cambridge Stereoscan S150 coupled with an energy dispersive

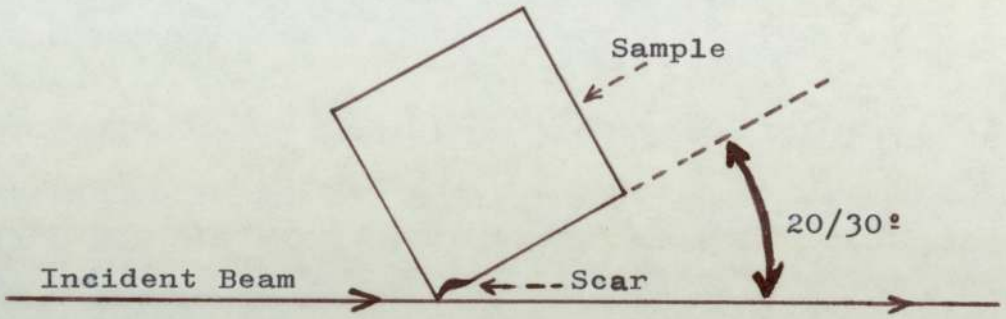

a) Half-roller

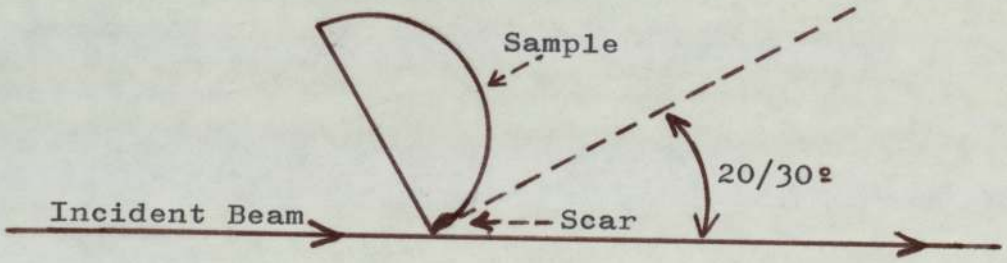

b) Half-ball

FIG. 2.9 SCHEMATIC REPRESENTATION OF THE ARRANGEMENT OF THE SAMPLE INSIDE THE POWDER CAMERA WHEN THE X-RAY GLANCING ANGLE METHOD WAS USED.

X-ray analyser (KEVEX) was used to identify the elements present on the worn surfaces and also to study the topography of these areas. The diameter of the electron beam utilised was 70 A°. A lithium-drifted silicon detector collected the X-rays which were produced simultaneously over the scanned area, and then a chart of the complete results was displayed on a video screen.

2.4.2 Analysis

During the analysis of samples from different tests, micrographs of the scars were taken at low and high magnification. X-ray charts covering these areas at low scale were plotted and also simultaneously photographs showing the X-rays distribution of sulphur and iron were recorded.

2.5 Analysis of the Worn Surfaces by using Electron-Probe Microanalysis (E.P.M.A.)

2.5.1 General Function of E.P.M.A.

The principle of Electron Probe Microanalysis (E.P.M.A.) is quite simple and is a logical extension of the pioneering experiments of Moseley (38, 39) on the wavelength of characteristic X-ray radiation excited by electron bombardment. The microvolume of a particular point at the surface of a metallographically polished sample is excited by a focused electron beam. The beam about 1μm in diameter is accelerated by a voltage of 3 to 50 kV. The excited volume emits a complex X-ray spectrum which is selectively analysed by one or more X-ray spectrometers. Comparisions between the intensities of characteristic X-rays, emitted under identical experimental conditions

by the sample "I_A" and by a calibration standard "$I_{[A]}$" (usually the pure element), permits the determination of the respective elementary mass concentration "C_A", to a first approximation.

2.5.2 Characteristics of the System used

A Cambridge Microscan 5 was used to analyse wear scars formed on the surfaces of the rollers. Due to the thinness of these films formed, the accelerating voltage for the electron beam was always set to 15 kV because this value was found to be suitable for analysing the depth of these layers. The maximum resolution achieved was 0.3 A°. The X-rays generated by the sample were collected by two ordinary fully spectrometers mounted on each side of the specimen stage at a take-off angle of 75°. Throughout the analysis the two crystals used were Pentaerythontal (P.E.T.) for the 1st spectrometer and Lithium Fluoride (LiF) for the second. Table 2.2 gives some properties of the crystals available in the system used.

2.5.3 Operating Mode

Roller samples and the plate bearing the standards were mounted in a holder then the latter was placed inside the specimen chamber of the probe.

At completion of the procedure involved in the preparation of the apparatus for use, the area of interest was observed in the optical microscope which is coaxial with the electron beam. Once ready for the analysis, the crystals inside the spectrometers were rotated to the relevant Bragg angle of a particular element of

CRYSTAL	d-spacing (A°)	λ_{min} (A°) (*)	λ_{max} (A°) (**)	Elements (Z)
LiF	2.015	1.04	3.79	Ra(88)-K(19)
P.E.T.	4.37	2.26	8.21	Cr(23)-Al(13)

Table 2.2: Some properties of crystals available on the Cambridge Microscan 5.

1) (*): Calculated from $\lambda_{min} = 2d \sin \theta_{min}$ where θ_{min} is taken as equal to 15°

2) (**): Calculated from $\lambda_{max} = 2d \sin \theta_{max}$ where θ_{max} is taken as equal to 70°

interest. Hence the P.E.T. crystal was rotated to the angle 75°49' whilst the LiF was set to the angle 57°29' which correspond to the theoretical Bragg angles of the sulphur and the iron elements respectively.

2.5.4 Analysis

For each scar the investigation was carried out over several points and the intensity of the X-rays was recorded, resulting in at least three separate counts of 10 seconds being produced. The experimental Bragg angle for each element was obtained by rotating the crystals by $\pm$ 2° until the ratemeter indicated maximum counts. The background count rate was recorded by switching off the peak. After the analysis of the sample under test was completed the same conditions were used to observe the count rates for the standard. Sulphur from iron disulphide (FeS_2) was used as the standard element for the sulphur analysis whilst the pure iron was used as the second standard.

The net count per second was obtained by taking into account the background count rates and the dead time. Therefore the concentration of the element of interest in the sample was found by taking the ratio of the net counts per second of this element and its respective standard. In other words the concentration of the element A for each scan was:

$$K_A = \frac{I_A}{I_{[A]}} = \frac{(\text{Peak c/s} - \text{Background c/s} + \text{Dead Time c/s})_{\text{element A}}}{(\text{Peak c/s} - \text{Background c/s} + \text{Dead Time c/s})_{\text{standard [A]}}}$$

Then the result for each wear scar studied was presented in the form of an average value for the concentration.

At the end the corrected concentration (C_A) was obtained by taking into consideration the atomic number (that is the backscattering effect and the stopping power), the absorption effect and the fluorescence correction factors (40, 41, 42). This is given by:

$$C_A = K_A \left[\frac{R_{[A]} \cdot S_A}{R_A \cdot S_{[A]}}\right] \cdot \left[\frac{f(X)_{[A]}}{f(X)_A}\right] \cdot \left[\frac{1}{1 + \gamma}\right]$$

where:

C_A = corrected concentration of element A on the surface of the sample.

K_A = measured concentration of element A on the surface of the sample.

$R_{[A]}$ = backscattering effect of the standard A

R_A = backscattering effect of the element A

$S_{[A]}$ = stopping power of the standard

S_A = stopping power of the element

$f(X)_{[A]}$ = absorption effect of the standard

$f(X)_A$ = absorption effect of the element

γ = fluorescence effect

The calculations for C_A have been obtained by using a computer programme.

2.6 Analysis by X-ray Photoelectron Spectroscopy (X.P.S.)

2.6.1 Principle of the Technique

If an X-ray photon falls on a free atom, an electron could be

possibly ejected from an orbital shell in which, therefore, a "hole" (0) is left. the photoemitted electron has a kinetic energy, KE, given by the following expression:

$$KE = h\gamma - BE \qquad \text{.....(2.2)}$$

where h = Plank's constant, γ = frequency of the incident X-ray photon and BE = binding energy of the atomic orbital from which the electron originates.

Figure 2.10 shows a simple diagram of the photoemission process when the X-ray photon falls on an electron from the level K (ie the core state). For this typical example equation 2.2 could be written as follows:

$$KE = h\gamma - (BE)_K \qquad \text{.....(2.3)}$$

Now, if $h\gamma$ is known and KE can be measured, then BE can be determined. Consequently the relevant atom could be determined and the basis of this technique is known as X-ray Photoelectron Spectroscopy (X.P.S.). The method consists of irradiating a sample with monoenergetic soft X-rays and measuring the energies of the electrons emitted. In the practical case, the spectrometer work function, ϕ_s, must be taken into consideration in the expression of the kinetic energy of the electron ejected. Thus equation (2.2) becomes:

$$KE = h\gamma - BE - \phi_s \qquad \text{.....(2.4)}$$

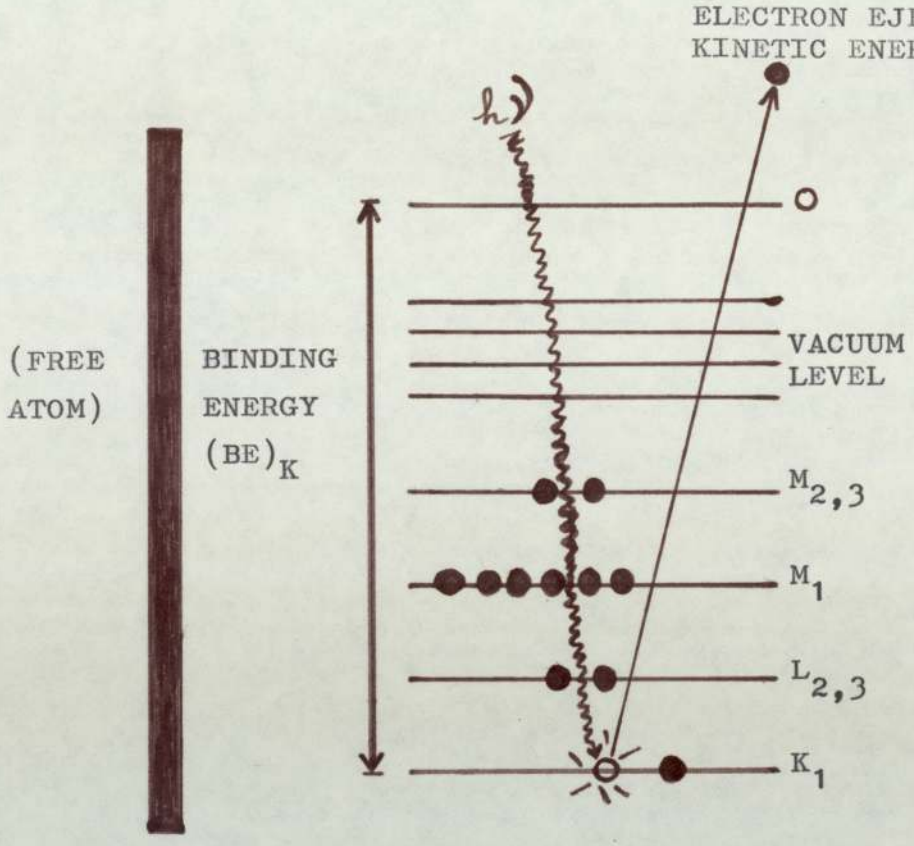

FIGURE 2.10 TYPICAL X-RAY PHOTOEMISSION DIAGRAM.

2.6.2 Characteristics of the System used

A number of rollers were taken to Thornton Research Centre (Shell Research Limited) to be analysed on the AEI ES 200 Electron Spectroscopy using an AlK_{α} exciting radiation with an energy of 1.4 KeV. As the depth of analysis is only a few nanometres therefore an extra cleaning was necessary to be sure that the test oil was removed completely from the wear scar. the analysis and the interpretation of the results were conducted by Mr R. J. Bird.

2.7 Analysis Using High Energy Charged Particles

Interest in surfaces over the past decade has stimulated the development of many techniques of surface anslysis. Of these, nuclear analyses using high energy charged particles as an analytical probe are well developed. Nevertheless, such methods are not widely used in tribological research. Hence a study of the suitability of using these new techniques for investigating the structure and formation of extreme-pressure surface films was carried out. The two main analytical techniques retained were Rutherford Backscattering (R.B.S.) using 2 MeV alpha particles and charged particle stripping reactions using deuterons [(d, p) reactions].

The particle beams were produced in the Dynamitron Accelerator at the Joint Radiation Facility operated by the University of Aston and the University of Birmingham (43).

A brief introduction to the theoretical point of view is given below.

2.7.1 Rutherford Backscattering (R.B.S.): General Principle

When a mono-energetic ion beam is incident upon a solid sample some of it will undergo elastic scattering resulting from its interation with the nuclei of the surface layers (44, 45). During this process the incident ions will transfer some of their energy to the target nuclei with respect to the conservation laws of energy and momentum. Therefore the final energy of the outgoing particles will be reduced from its original value and will be an identification of each individual mass of the struck atoms. Hence counting the backscattered ions and measuring their energies will provide a good qualitative and quantitative chart of the atoms forming the surface layers. This nuclear analysis is known as Rutherford Backscattering (R.B.S.). The ion beam employed in most practical cases (44, 45, 46) is either H or H_e with energies ranging between 1 and 4 MeV and the silicon surface barrier detector has been found very suitable for the purpose (precision 1%).

Furthermore the technique is also suitable for obtaining concentrations versus depth profiles of the elements of the analysed sample (44, 45, 46). This results from the energy loss due to the inelastic ionisation and excitation effects occurring as the incident beam enters deeper into the lower layers. This loss in energy is very small and is correlated to depth in the target at which the collision takes place.

It is essential to mention about the probability of backscattering (ie the reaction cross-section) which is proportional to the square of the atomic number (Z) of the target. This makes a small amount of a heavy element more easier to detect than the same amount of a light element. This is illustrated in Figure 2.11 (47).

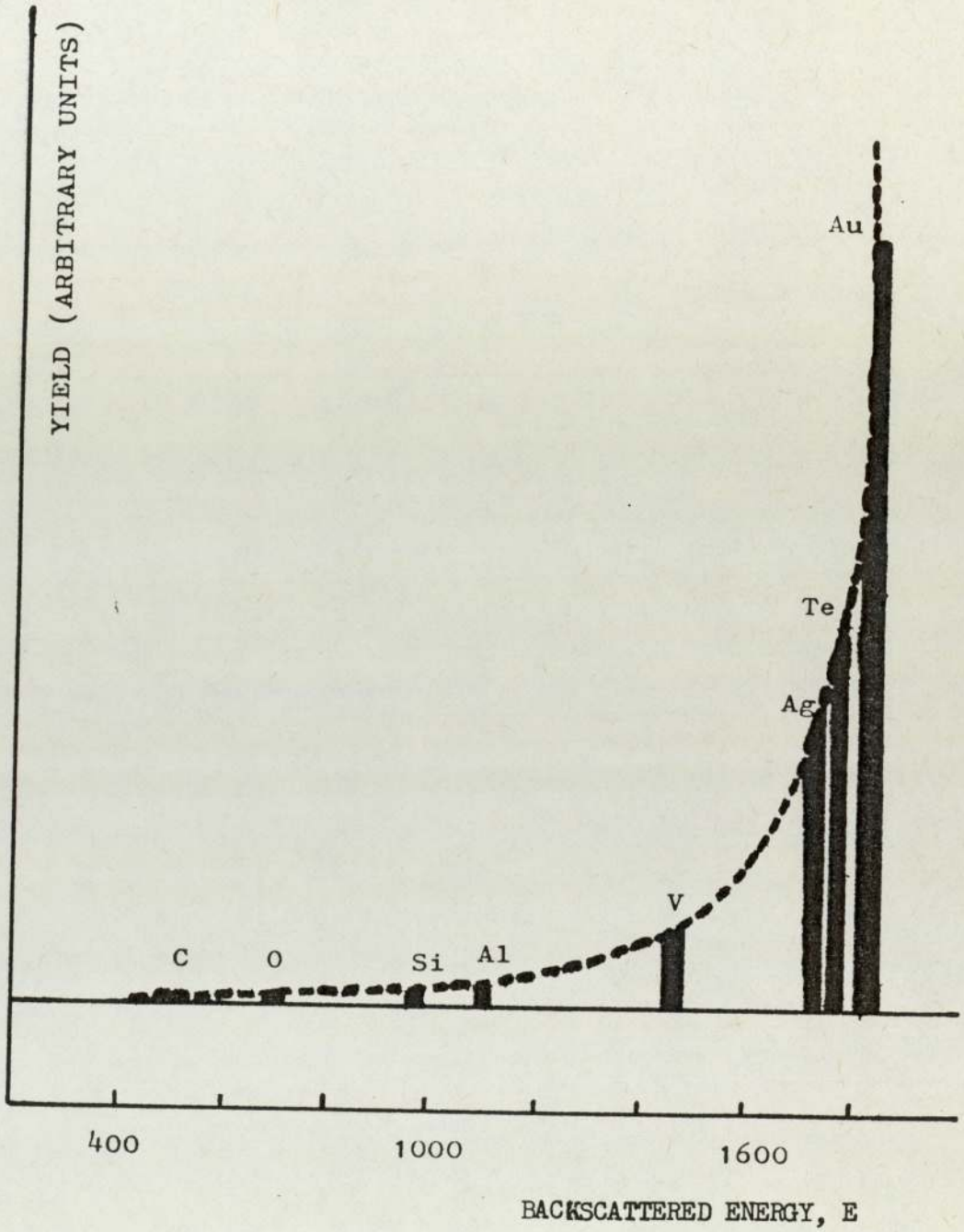

FIG. 2.11 IDEALISED SPECTRUM SHOWING YIELD VARIATION FOR EQUAL NUMBERS OF ATOMS OF EACH ELEMENT DUE TO SCATTERING CROSS-SECTION EFFECTS.

Figure 2.12 represents a schematic R.B.S. spectrum when alpha-particles of known energy E_o are used to bombard a film consisting of two types of element A and B on a substrate and where the atomic mass of the substrate, M, is greater than the atomic mass of element A, M_A, which in turn is greater than that of element B, M_B. Measurement of the energy of each step allows the elements A and B to be identified uniquely and the height of each step is a function of the number of atoms of each element, whilst the length of each step is a function of the film thickness.

2.7.2 Deuteron-proton Stripping Reactions

The technique consists of bombarding a solid sample with an energetic deuteron beam and measuring the energy spectrum of the protons produced by the induced nuclear reactions (44, 48, 49, 50). A schematic diagram of this kind of reaction is given in Figure 2.13. Such a reaction can be written symbolically as:

$$M_d + M_T \longrightarrow M_P + M_R + Q$$

so $$Q = (M_d + M_T)\,C^2 - (M_P + M_R)\,C^2 \qquad \text{.....(2.5)}$$

where M_d, M_T, M_P and M_R are the masses of the deuteron, the target nucleus, the proton and the residual nucleus respectively (measured in a.m.u.), Q represents the energy absorbed or released and "C" is the velocity of light.

The energy of the proton is given by the equation

$$E_P = \frac{E_d\, M_d\, M_p}{(M_P + M_R)}\left\{2\,\mathrm{Cos}^2\theta + \frac{M_R\,(M_P + M_R)}{M_d\;\;M_p}\left(\frac{Q}{E_d} + 1 - \frac{M_d}{M_R}\right) + \right.$$

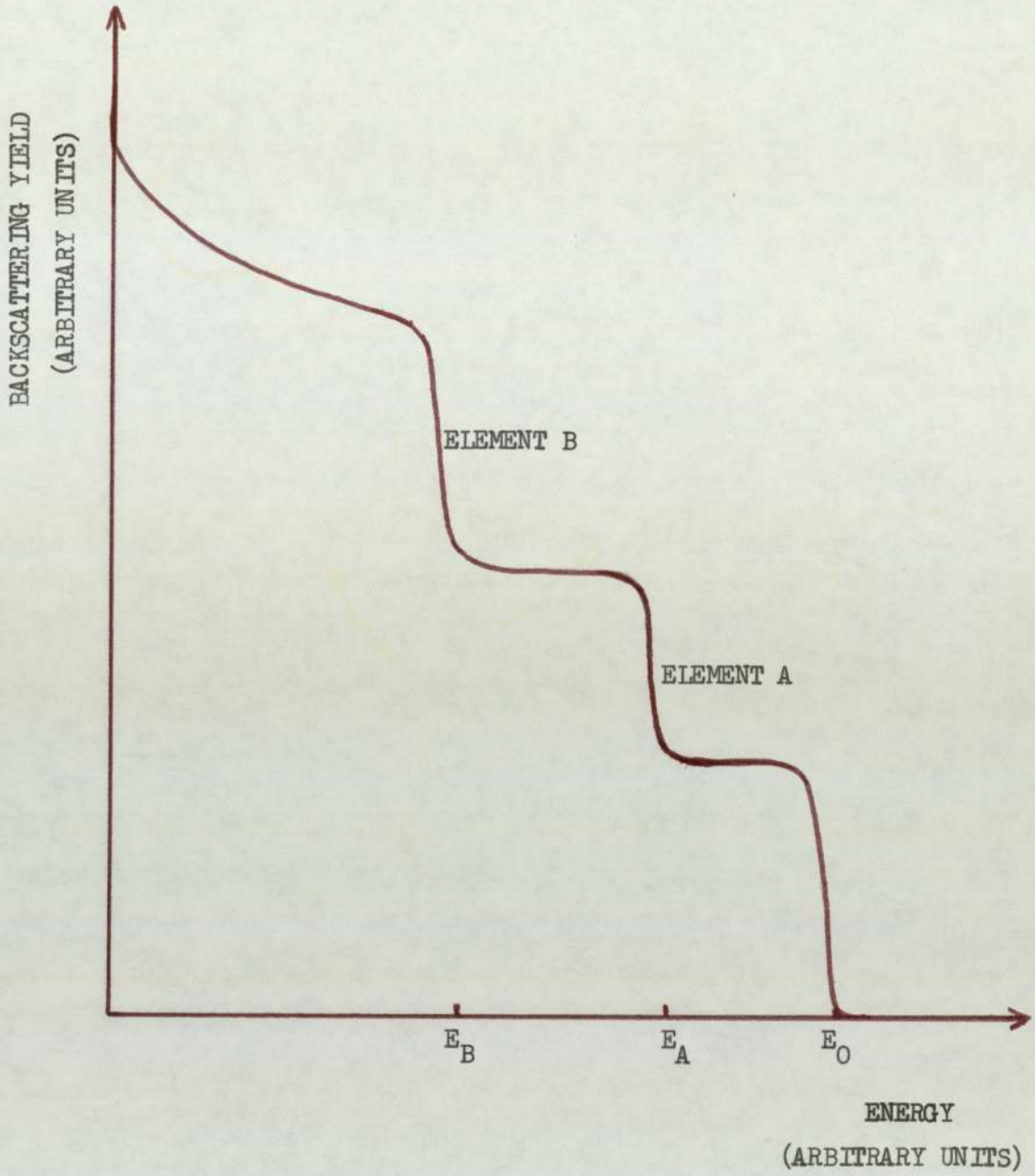

FIG. 2.12 SCHEMATIC R.B.S. SPECTRUM FROM A FILM CONSISTING OF TWO ELEMENTS ON A SUBSTRATE WHERE $M_A > M_B$.

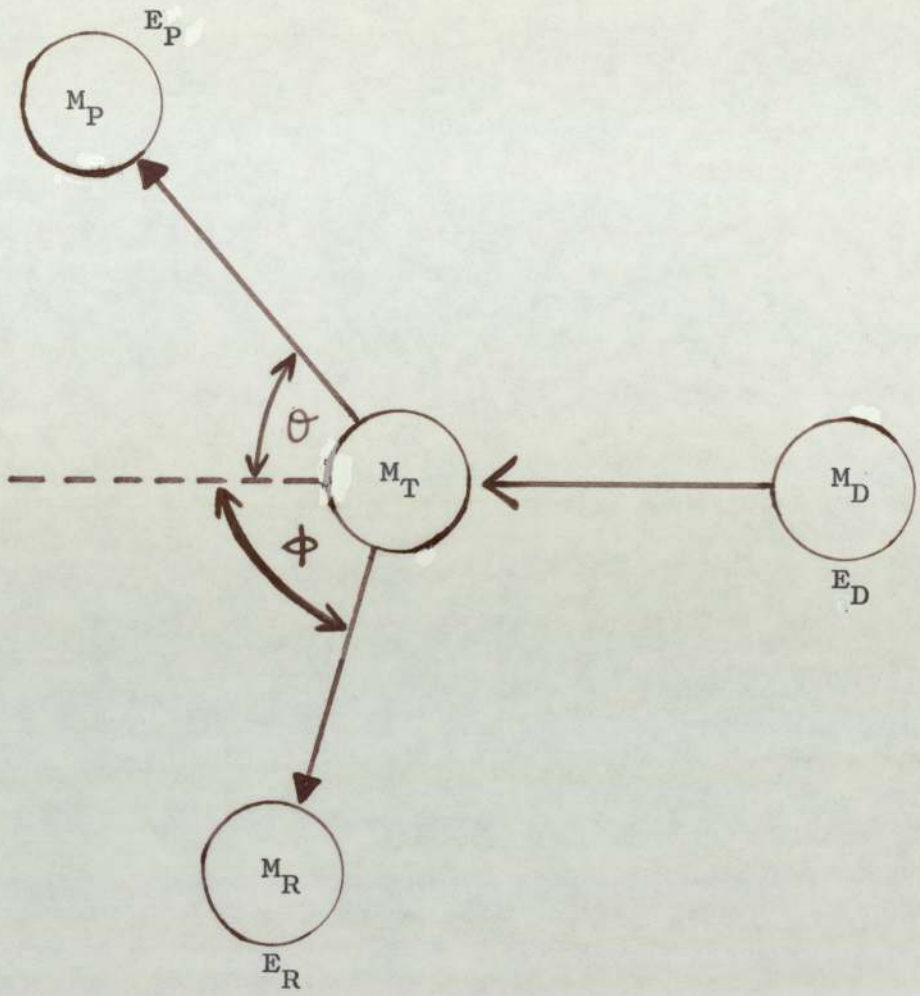

FIG. 2.13 SCHEMATIC DIAGRAM OF A (D,P) REACTION.

$$+ \quad 2\cos\theta \left[\cos^2\theta + \frac{M_R\,(M_P + M_R)}{M_d\ M_P} \left(\frac{Q}{E_d} + 1 - \frac{M_d}{M_R} \right) \right]^{\frac{1}{2}} \Bigg\} \qquad \ldots\ldots\ldots(2.6)$$

where E_d is the energy of the incident deuteron beam, and θ is the laboratory angle between the direction of the incident deuteron and the emitted proton as shown in Figure 2.13.

The reaction yield, Y, at the incident energy E_d, may be written as (46, 47):

$$Y_p(\theta) = n\,(N\,\triangle x)\,\sigma_{(\theta,\,E_d)}\,\Omega \qquad \ldots\ldots\ldots(2.7)$$

$$\text{so that} \quad (N\,\triangle x) = \frac{Y_p(\theta)}{n\,\Omega\sigma_{(\theta,\,E_d)}} \qquad \ldots\ldots\ldots(2.8)$$

where $(N\,\triangle x)$ is the number of target atoms per square centimetre; n is the number of incident deuterons; $\sigma_{(\theta,\,E_d)}$ is the differential cross-section (for the angle θ and at energy E_d) and Ω is the solid angle sampled by the detector.

Furthermore for a given E_d and θ, the energy spectrum of the emitted protons consists of discrete peaks which correspond to the energy levels of the excited residual nucleus. As an example the reaction "deuteron-sulphur" is considered and this gives:

$$d + S^{32} \longrightarrow p + S^{33} + Q$$

or this could be written in a condensed form:

$$S^{32}(d,\,p)\,S^{33}$$

The energy-level diagram of this nuclear reaction is represented below (Figure 2.14):

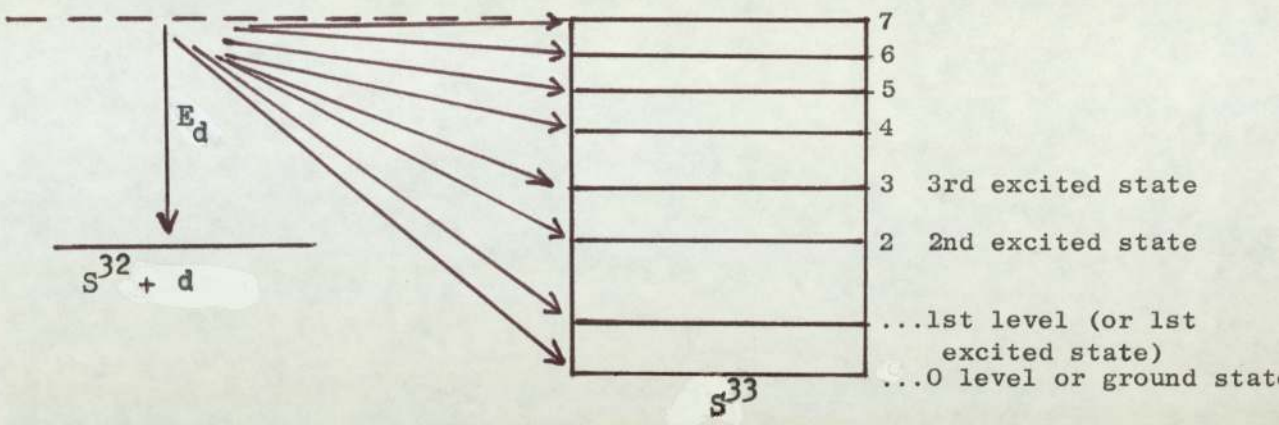

Figure 2.14

A typical spectrum of proton yield versus energy is shown in Figure 2.15. Seven proton groups appear at the energy spectrum of this particular case, and each one is related to a state level. Thus P_o corresponds to the ground state, P_1 to the 1st excited state and so on.

2.7.3 Experimental Procedure

Selected wear scars formed on the flat faces of the rollers were studied by both techniques, Rutherford Backscattering and Deuteron-proton stripping reactions, and the analyses were carried out at Birmingham Radiation Centre (43) already mentioned at the beginning of Section 2.7. As the additives used for preparing the samples were mainly organo-sulphur compounds, elemental sulphur was the main interest of the investigation.

Samples were placed on a stainless steel holder mounted inside the target chamber where a good vacuum was maintained during the experiments (cf. Figure 2.16). The measurements were acquired with a

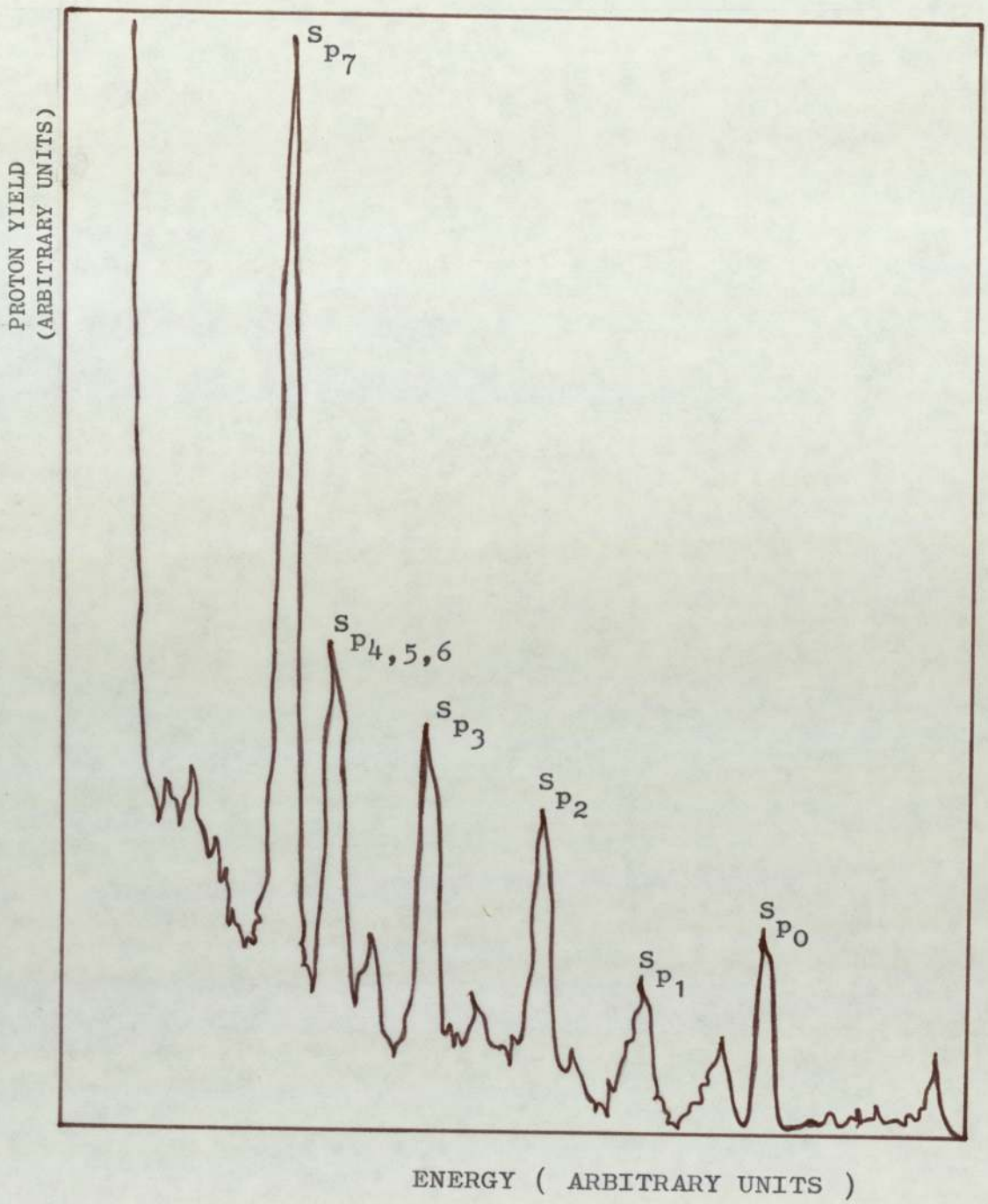

FIG. 2.15 PROTON GROUPS FROM THE REACTION $S^{32}(D,P)S^{33}$.

silicon barrier detector and the detection angle was between 170° and 176° with respect to the incident beam direction which was perpendicular to the area anlaysed.

During the examination by R.B.S. the worn surfaces were bombarded by an incident alpha-particle beam energy of 2 MeV then the recoil energy was measured and the number of scattered particles was counted for a range of time between 15 and 20 minutes.

The basic procedure used for Deuteron-stripping reactions was to bombard the specimens with a 2 MeV deuteron beam and to measure the energy spectrum of the particles produced by the induced nuclear reactions. Sulphur was identified by the energy positions of its seven proton groups resulting from the interaction between the projectile deuteron and the nuclei of the sulphur target. In this case a nickel foil was placed in front of the detector to stop the elastically scattered deuteron and alpha-particles from (d, α) reactions.

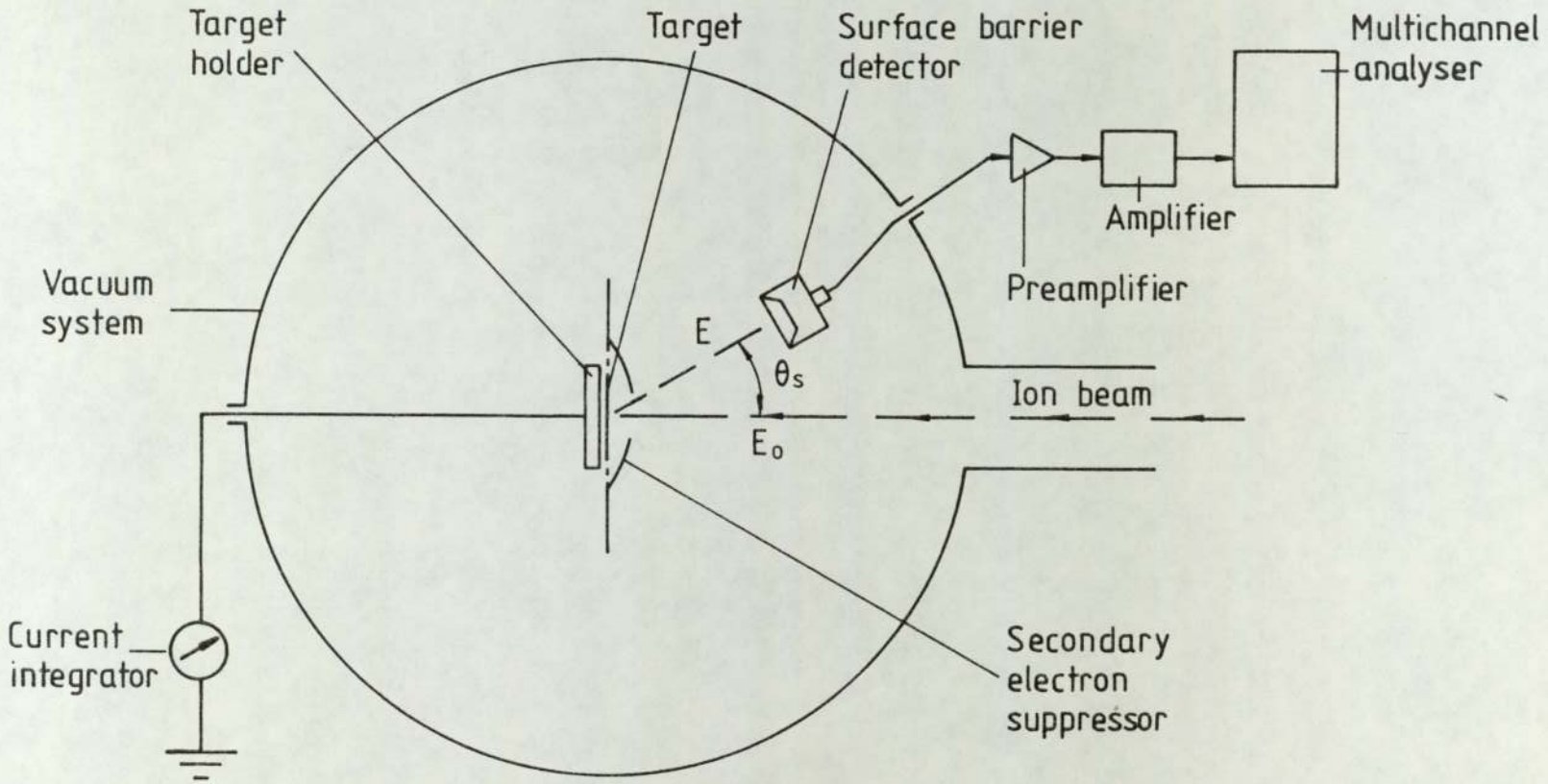

Fig 2.16 Schematic of Rutherford backscattering chamber and electronics for energy analysis of scattered particles

CHAPTER THREE

WEAR EXPERIMENTS AND X-RAY ANALYSIS OF THE WORN SURFACES

3.1 The Wear Experiments

3.1.1 Results of the Standard Tests

Before testing the additives, the performance of the base oil, ie Risella 32, was determined by proceeding the standard one minute tests on the 4-ball machine. Figure 3.1 shows the graph of the mean wear scar diameter versus the applied loads and this reveals that the intitial seizure occurred at a load of 50 kg, while the final seizure was at 70 kg. Beyond this load, the scoring of the surfaces in contact, was so high that no further run could be carried on. Alone, Risella 32, displays a mediocre a.w. performance and completely fails in the e.p. region.

The same standard test was used to determine the load-carrying performance of the four additives studied. During these experiments, the concentration per weight for the additives was chosen so that the same sulphur concentration was present in the lubricant plus additive. 0.25% by weight (wt) of elemental sulphur was blended with Risella 32, and 0.88% wt, 1.00% wt and 1.74% wt were respectively employed for DPDS, DBDS and DBMS. The test results are summarised in Tables 3.1 and 3.2, whilst the graphical representation of the scar diameter versus the applied loads obtained for these additives, are respectively shown in Figures 3.2, 3.3, 3.4 and 3.5.

LOAD (kg) / LUBRICANT USED	Mean Scar Diameter (mm)				
	Risella 32 (R)	R + elemental Sulphur	R + DPDS	R + DBDS	R + DBMS
30	0.30	0.325	0.35	0.28	0.31
40	0.33	0.36	0.37	0.32	0.36
50	0.376	0.40	0.38	0.35	0.39
60	I.S.	0.43	0.40	0.39	0.43
		I.S.			
70	0.64	0.68			
	Welding		I.S.	I.S.	I.S.
80		0.72	0.73		0.62
90		0.75	0.74	0.66	0.65
100		0.79	0.75	0.69	0.68
120		0.85	0.76	0.74	0.75
130		0.86	0.77	0.77	1.40
140		0.88	0.78	0.80	2.60
160		0.94	0.80	0.83	Welding
180		1.00	1.20	0.87	
200		1.05	1.75	0.91	
220		1.08	Welding	0.94	
240		1.15		0.98	
260		1.17		1.00	
280		1.20		1.05	
300		1.25		1.07	
320		1.25		1.10	
340		Welding		1.12	
360				1.15	
400				1.20	
500				1.32	
600				1.42	
700				1.50	
800				1.59	
900				1.65	
920				Welding	

Table 3.1: Four-ball Test Results.

ADDITIVES	LOAD RANGE (Kg)			Weld Load (Kg)
	A.W.	Initial Seizure	E.P.	
0.25% wt elemental sulphur	up to 60	60-70	70-300/320	340
0.88% wt DPDS	up to 60	60-80	80-200	220
1.00% wt DBDS	up to 60	60-90	90-900	220
1.74% wt DBMS	up to 60	60-80	80-140	160

Table 3.2: Anti-Wear, Initial seizure and Extreme-Pressure Load Range of the Additives used.

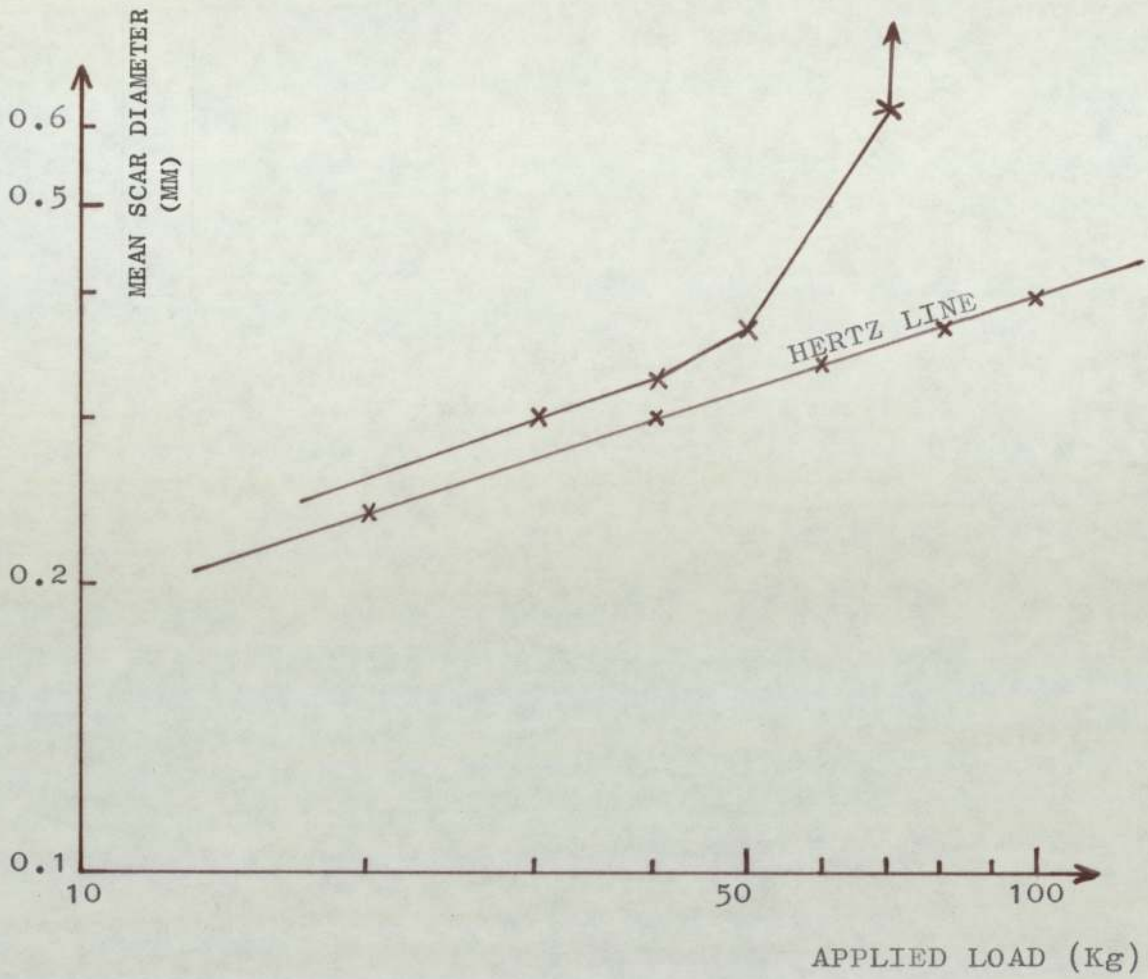

FIG.3.1 LOAD VERSUS MEAN WEAR SCAR DIAMETER.

LUBRICANT : RISELLA 32 OIL

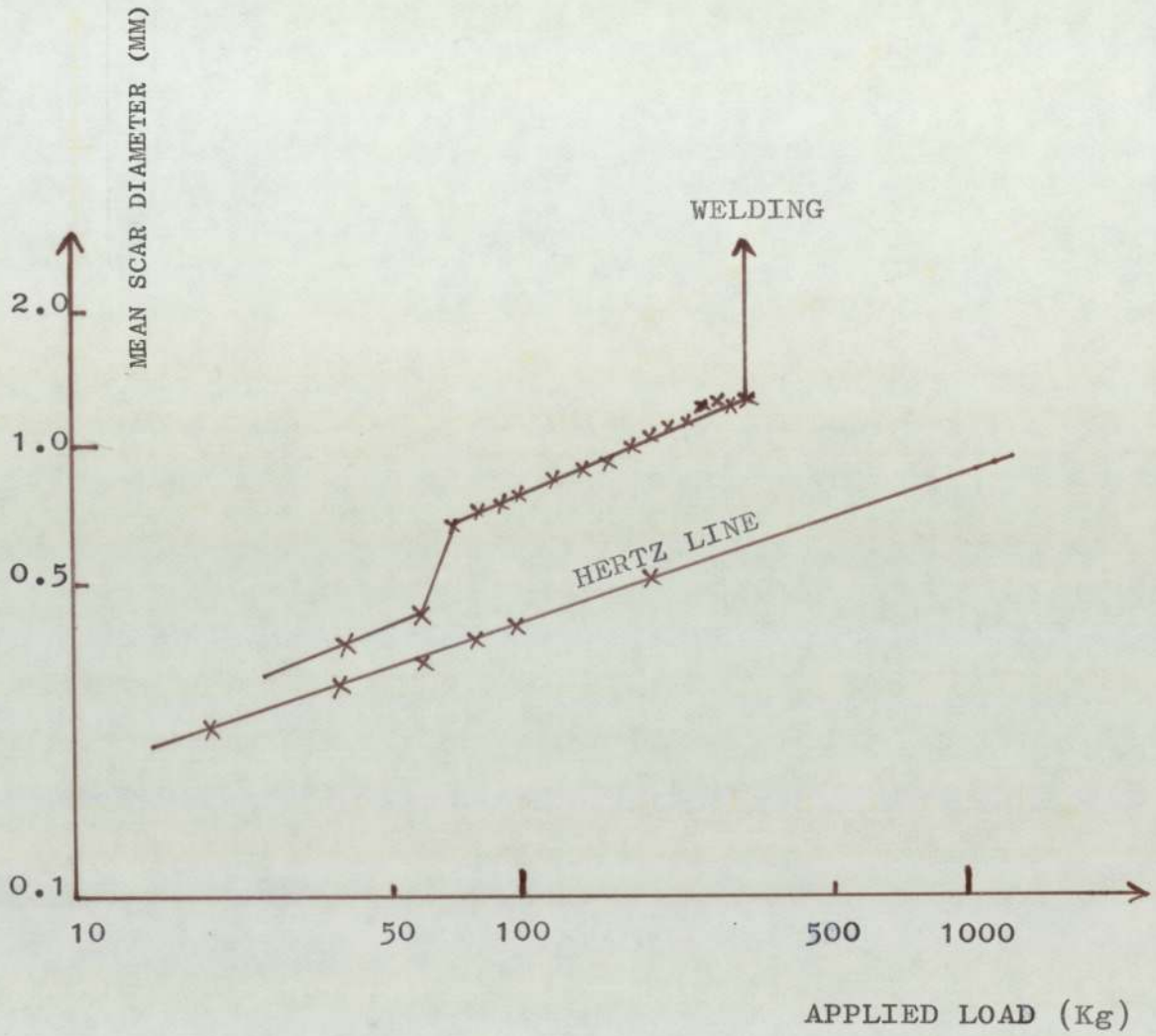

FIG. 3.2 LOAD VERSUS MEAN WEAR SCAR DIAMETER.

LUBRICANT : RISELLA 32 + 0.25 %wt ELEMENTAL SULPHUR

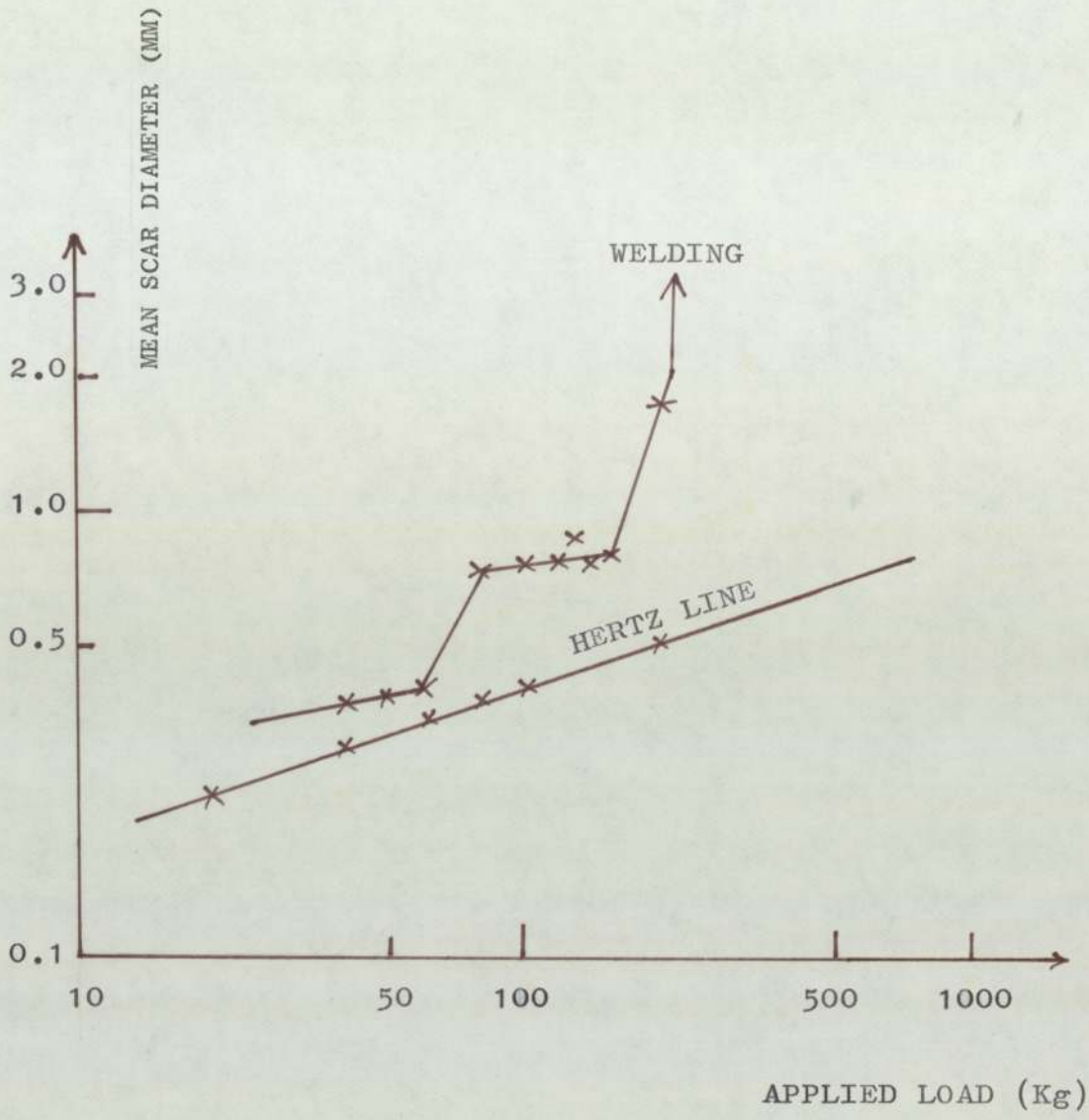

FIG. 3.3 LOAD VERSUS MEAN WEAR SCAR DIAMETER.

LUBRICANT : RISELLA 32 + 0.88 % wt DPDS

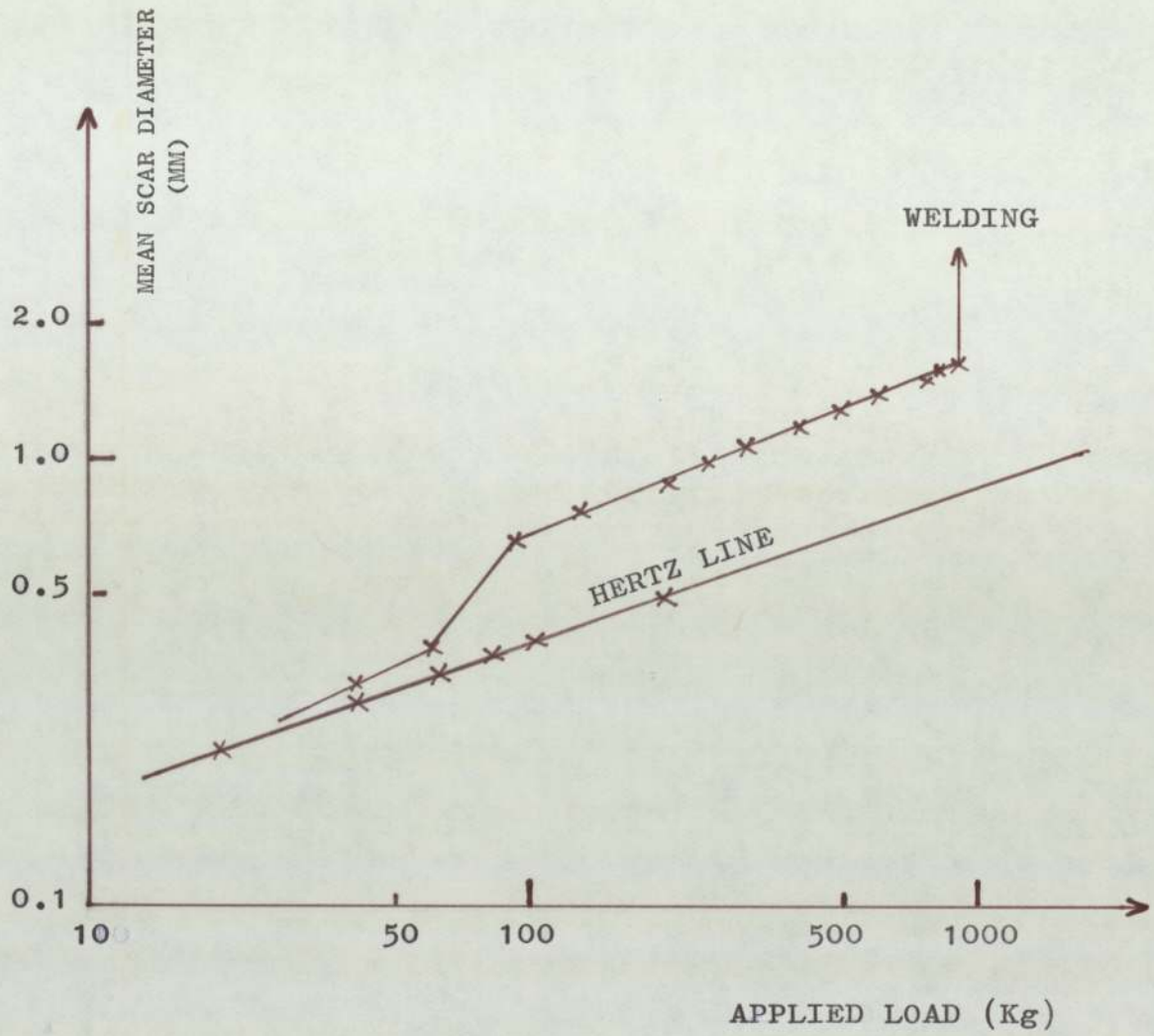

FIG. 3.4 LOAD VERSUS MEAN WEAR SCAR DIAMETER.

LUBRICANT : RISELLA 32 + 1.00 % wt DBDS

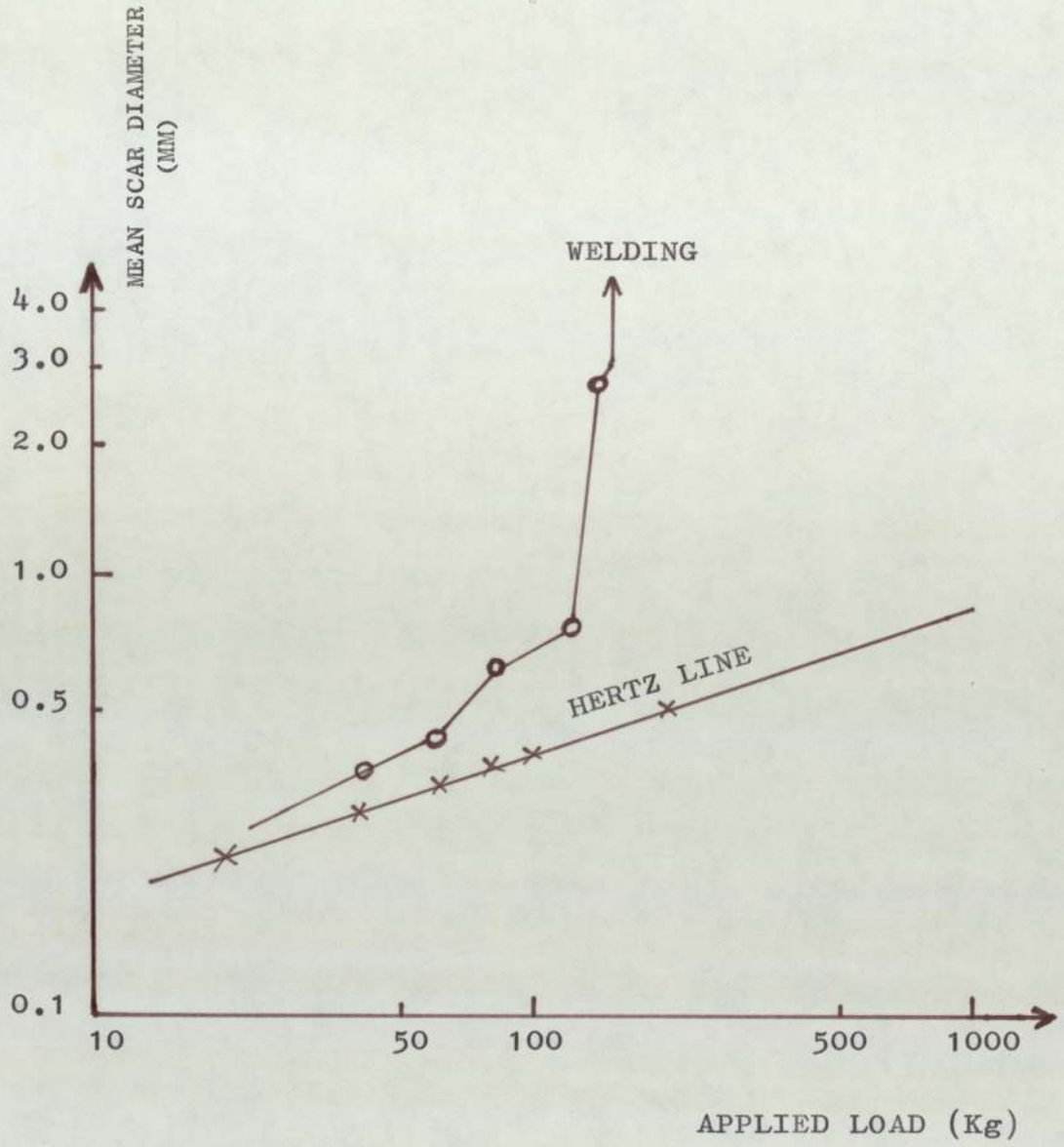

FIG 3.5 LOAD VERSUS MEAN WEAR SCAR DIAMETER.

LUBRICANT : RISELLA 32 + 1.74 %wt DBMS

The results indicate that during the a.w. regime, the additives contribute very little and to a certain extent show the same performance as Risella 32 when it is used on its own. Furthermore, the monosulphides (ie elemental sulphur and DBMS) manifest the same behaviour, whilst the disulphides (ie DBDS and DPDS) present more or less the same behaviour.

The contribution of the additives is quite substantial during the e.p. regime, but the performance seems to be affected by the environment of the sulphur atom in the molecule additive. The experiment shows that when sulphur atom is used on its own (ie the case of elemental sulphur additive), the load-carrying property of this additive is fairly good, but the test performance of the compounds changed according to the nature of the groups attached to the sulphur atom. The increasing order observed for the e.p. effectiveness is as follows:

DBMS $<$ DPDS $<$ elemental sulphur $<$ DBDS

3.1.2 The Effect of Temperature of the Lubricant on Standard Tests

The relation between the lubricant temperature and the applied load was investigated by recording the temperature simultaneously with the standard one minute wear test on the elemental sulphur additive (0.25% wt). The "temperature-load" chart obtained (Figure 3.6) shows the linear dependence between these two parameters.

To investigate the behaviour of each lubricant temperature during the a.w. and e.p. regimes, tests of recording temperature with

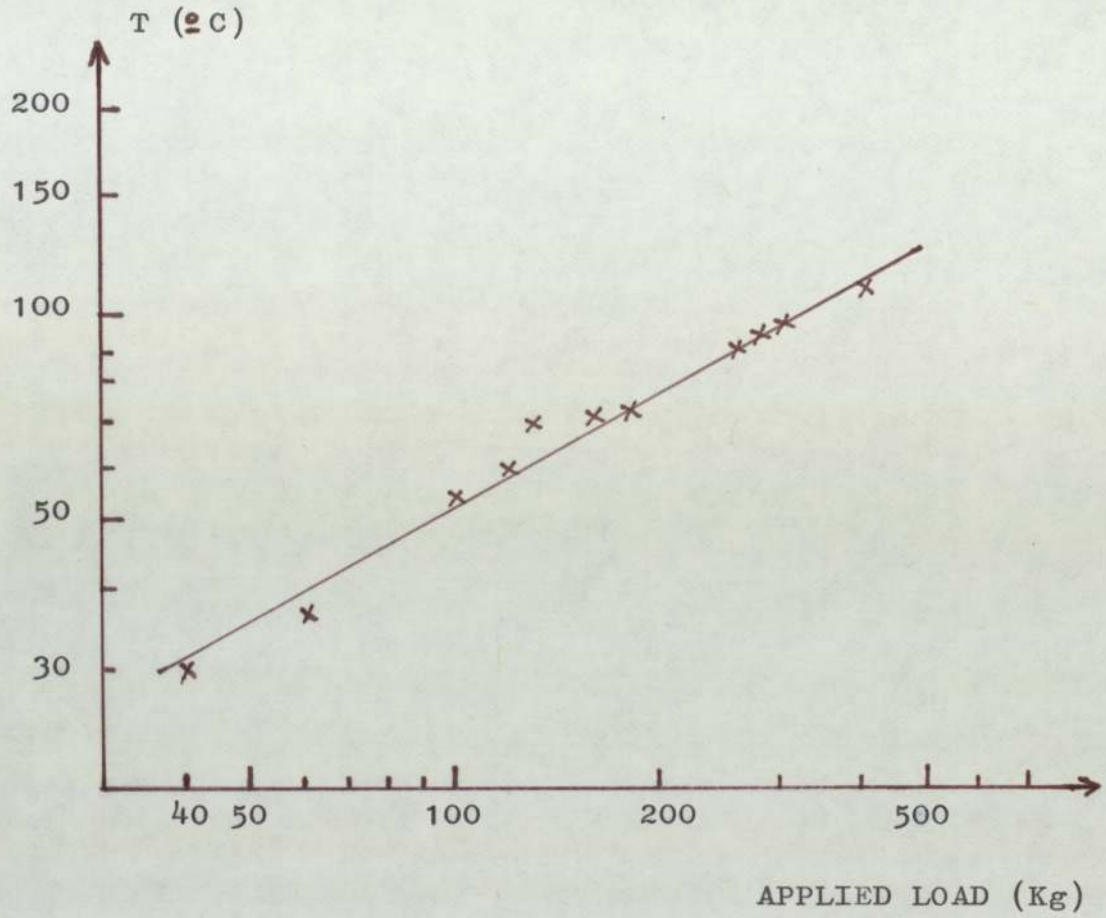

FIG. 3.6 TEMPERATURE VERSUS LOAD (ONE MINUTE RUNS).

LUBRICANT : RISELLA 32 + 0.25 % wt ELEMENTAL SULPHUR

time were carried out on two selected loads, 40 and 130 kg, corresponding respectively to the above mentioned regimes.

i) a.w. experiments:

During the a.w. regime, the results shown in Figures 3.7, 3.8, 3.9 and 3.10, reveal that, for all the additives used, the temperature rises rapidly but then approaches a maximum value for a certain time, and then stays constant for several hours. The maximum temperature value and its corresponding time vary for each compound additive employed. These values are presented in Table 3.3 and there is a distinction between those corresponding to the additive with a free sulphur atom (ie the case of elemental sulphur) and those where the sulphur atom is attached to a group of atoms (DPDS, DBDS and DBMS).

ii) e.p. experiments:

Figures 3.11, 3.12, 3.13 and 3.14 represent the results obtained during the e.p. experiments and the main observation is that the temperature rises linearly until reaching an equilibrium value at a specific time; a few minutes later, welding occurs. The equilibrium temperatuare value and its corresponding time, also, differ from one additive to another one. These values are given in Table 3.4 and they suggest the similarity of the e.p. performance, (already found in the previous test), between the elemental sulphur and DBDS on one hand and between DPDS and DBMS on the other hand.

Parameters Observed	Additive Used			
	Elemental Sulphur (0.25% wt)	DPDS (0.88% wt)	DBDS (1.00% wt)	DBMS (1.74% wt)
Maximum Temperature value (°C)	105	70	64	87
Time corresponding to the Maximum temperature (min)	55	35	40	40

Table 3.3: Temperature and time values observed during the a.w. experiments.

Parameters Observed	Additive Used			
	Elemental Sulphur (0.25% wt)	DPDS (0.88% wt)	DBDS (1.00% wt)	DBMS (1.74% wt)
Equilibrium Temperature value (°C)	160	152	172	142
Time corresponding to the Equilibrium Temperature "T_e" (min)	≏16	22	17	≏ 24
Interval of time between T_e and Welding Time (min)	3	2	3	5-7

Table 3.4: Temperature and time values observed during the e.p. experiments.

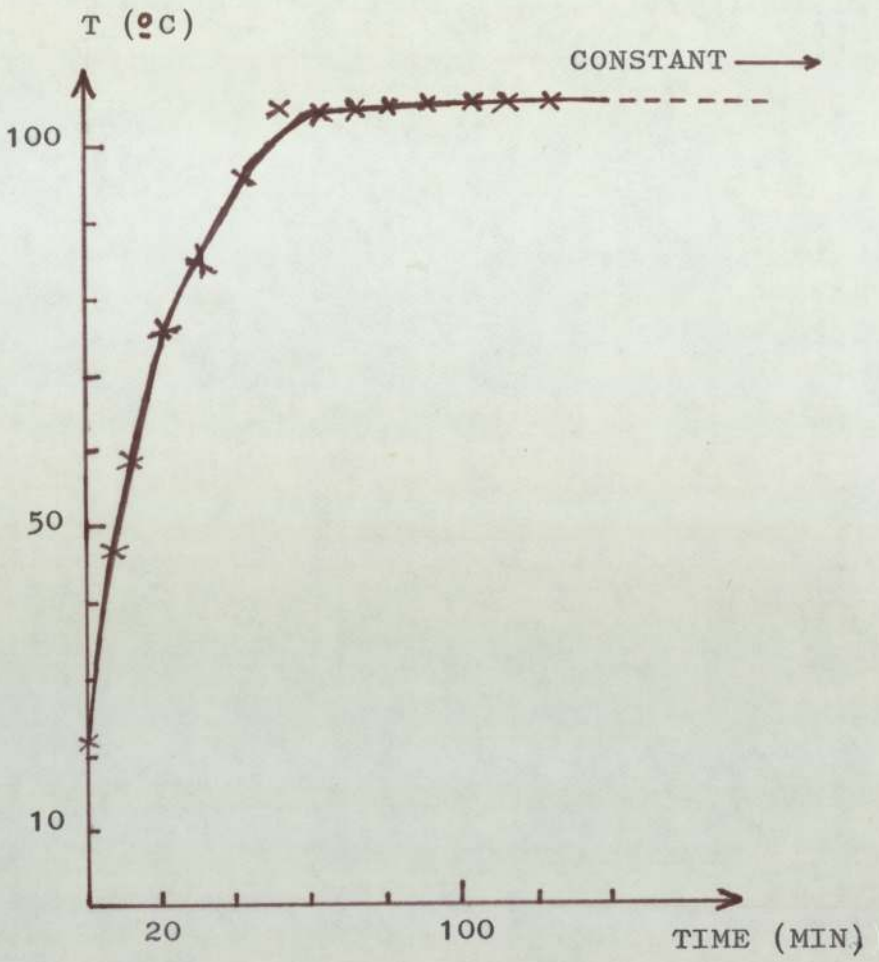

FIG. 3.7 TEMPERATURE VS. TIME OF AN A.W. LOAD (40 KG).

LUBRICANT : RISELLA 32 + 0.25 % wt ELEMENTAL SULPHUR

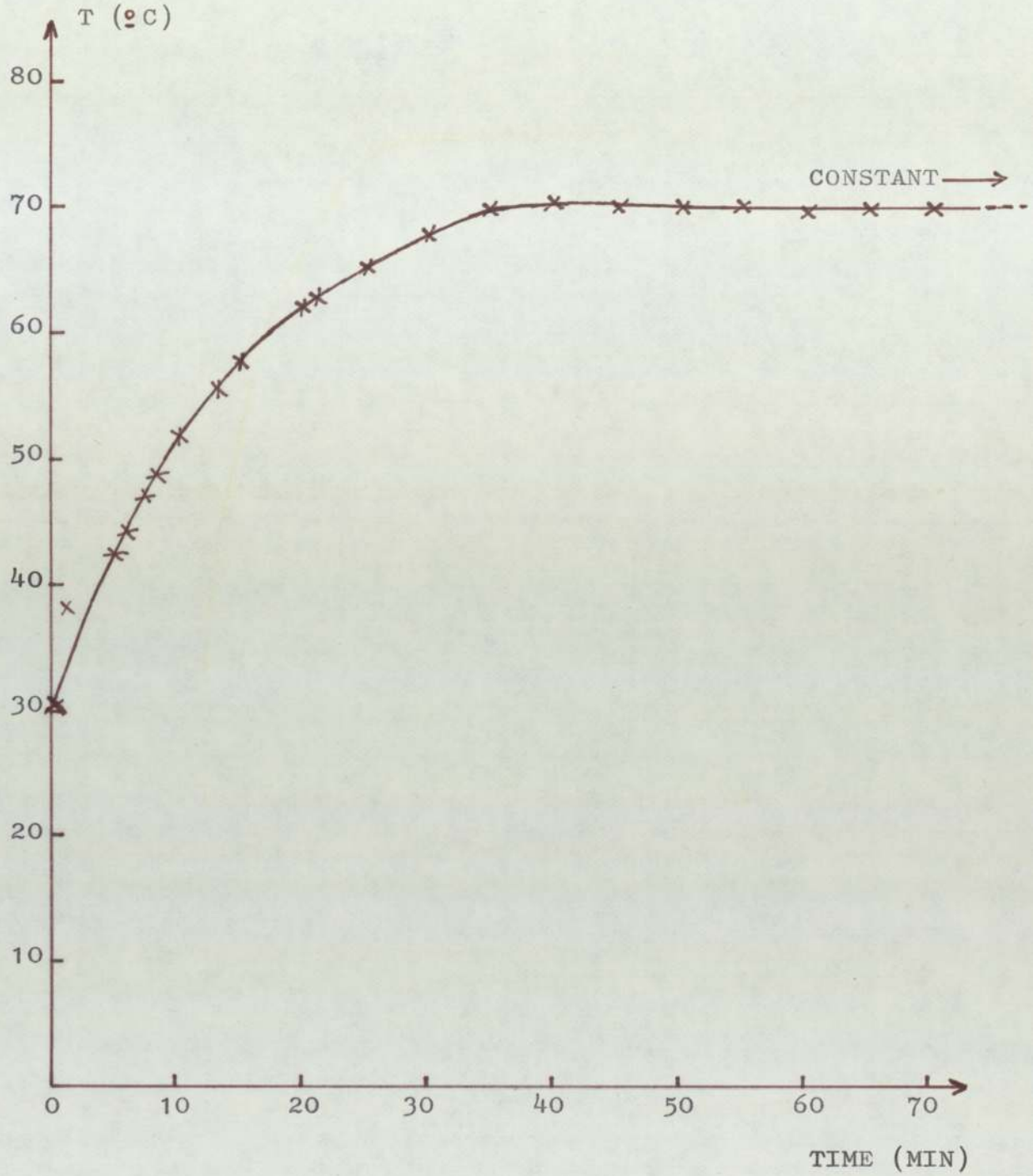

FIG. 3.8 TEMPERATURE VS. TIME OF AN A.W. LOAD (40 KG).

LUBRICANT : RISELLA 32 + 0.88 % wt DPDS

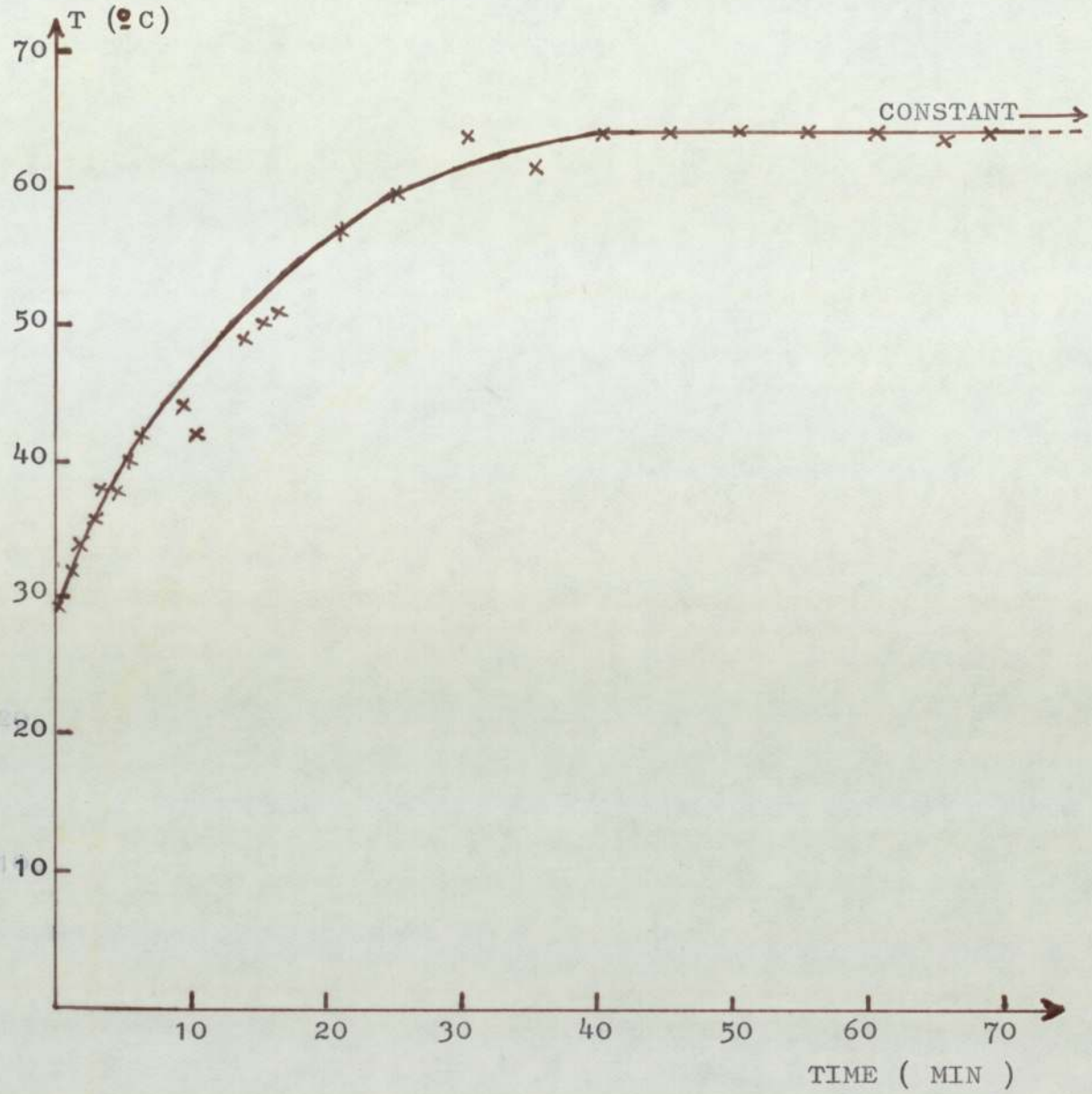

FIG.3.9 TEMPERATURE VS. TIME OF AN A.W. LOAD (40 KG).

LUBRICANT : RISELLA 32 + 1.00 %wt DBDS

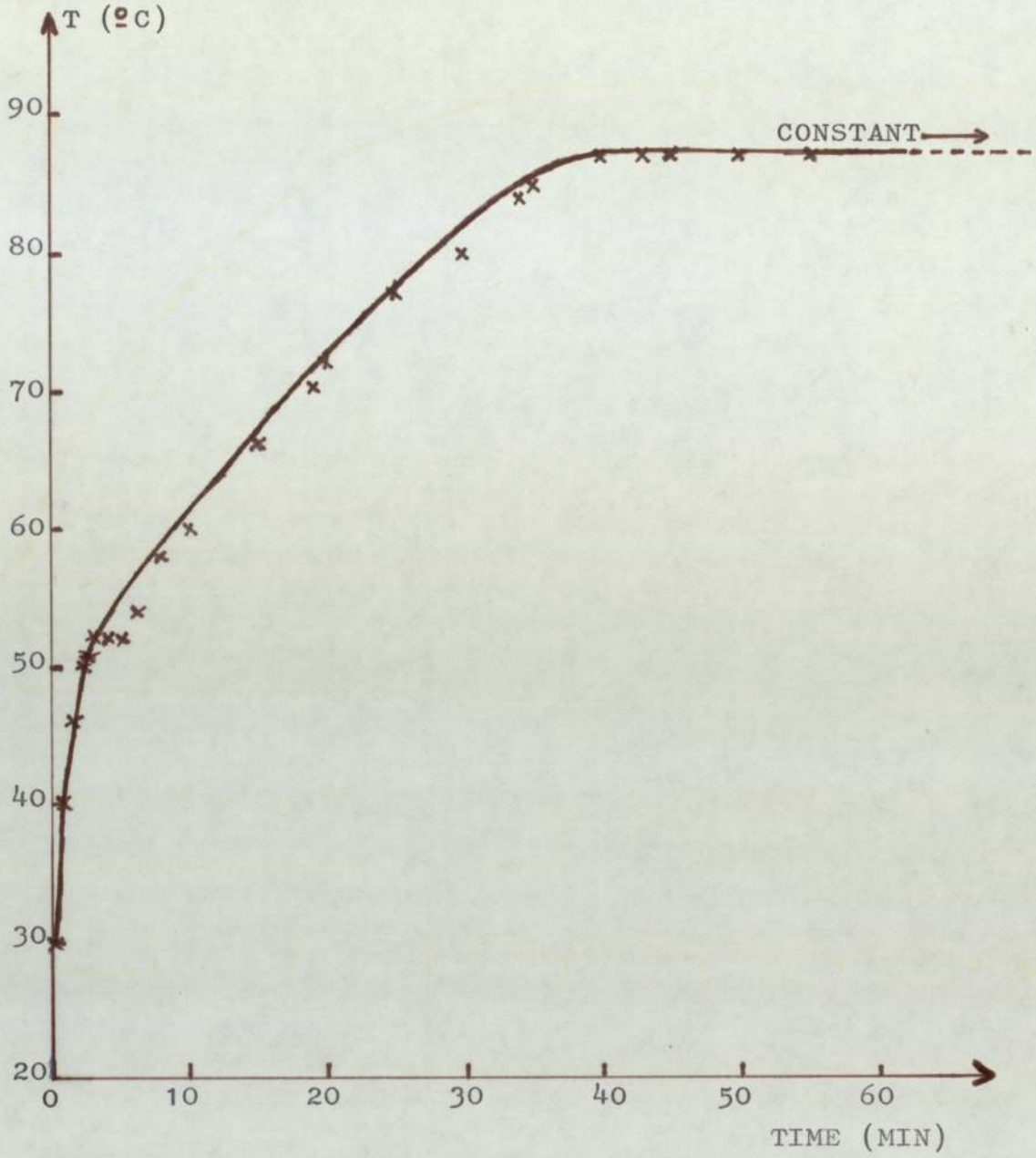

FIG.3.10 TEMPERATURE VS. TIME OF AN A.W. LOAD (40 KG).

LUBRICANT : RISELLA 32 + 1.74 %wt DBMS

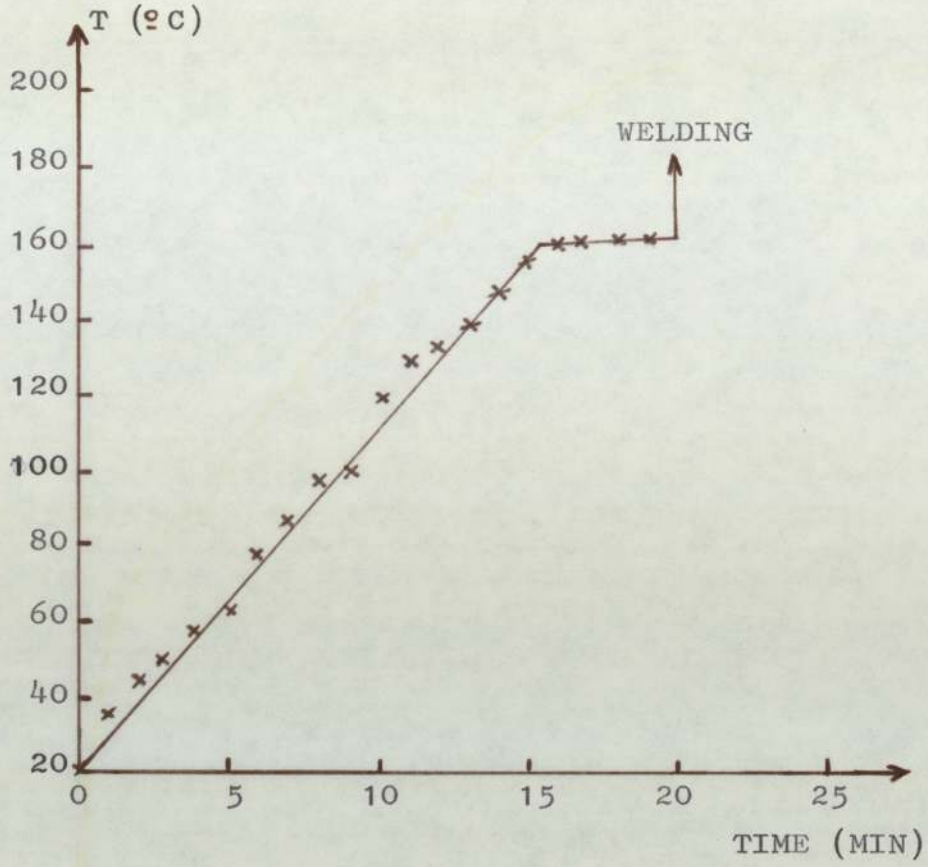

FIG.3.11 TEMPERATURE VS. TIME OF AN E.P. LOAD (130 KG).

LUBRICANT : RISELLA 32 + 0.25 %wt ELEMENTAL SULPHUR

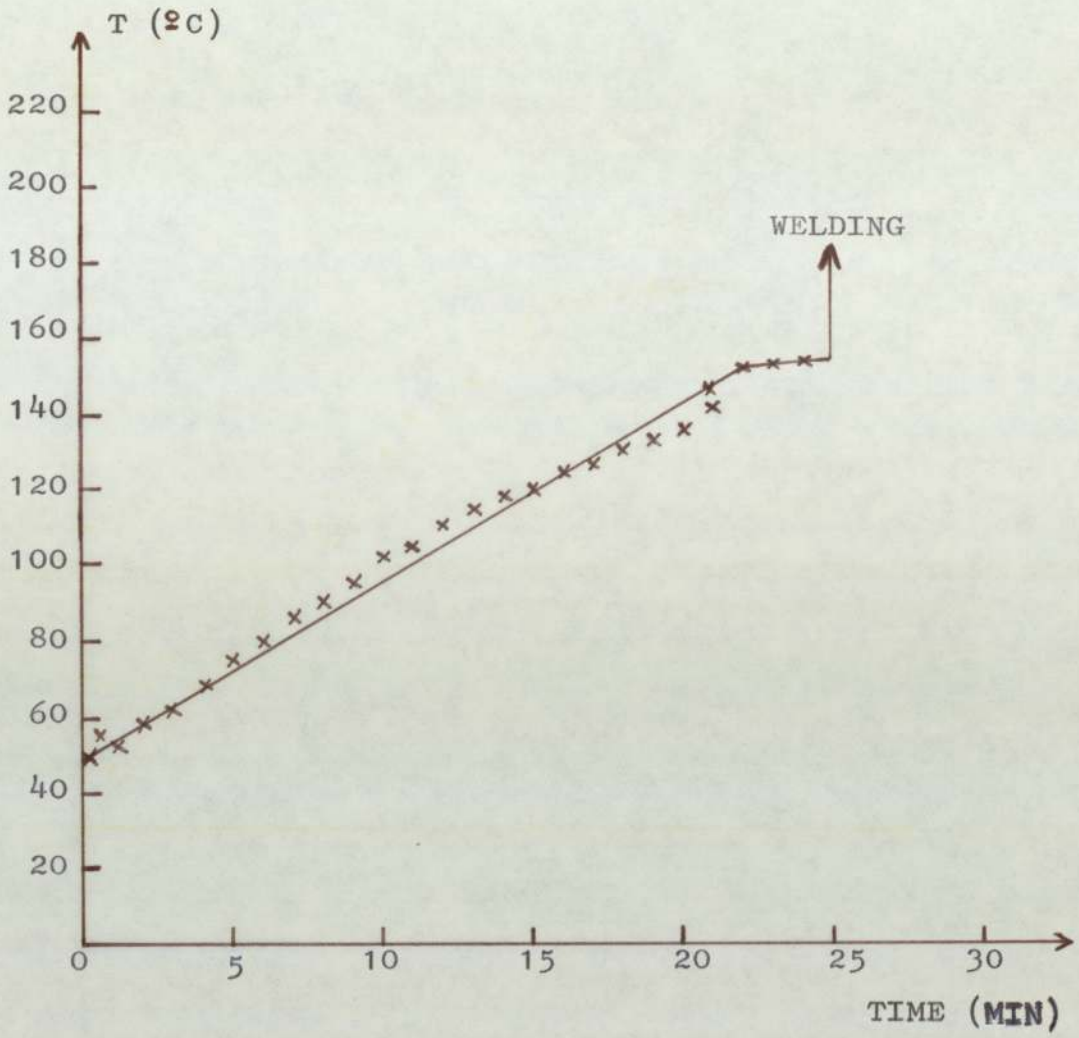

FIG.3.12 TEMPERATURE VS. TIME OF AN E.P. LOAD (130 KG).

LUBRICANT : RISELLA 32 + 0.88 %wt DPDS

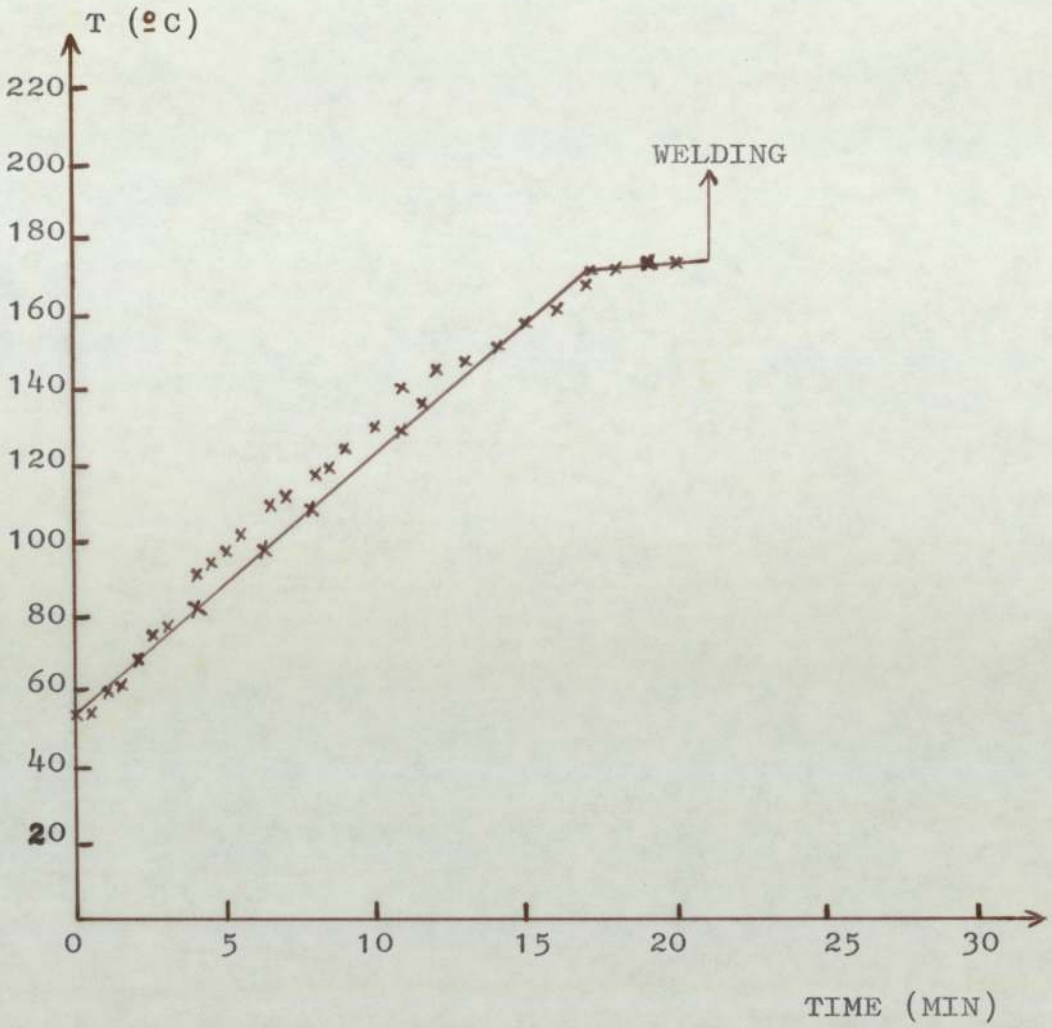

FIG.3.13 TEMPERATURE VS. TIME OF AN E.P. LOAD (130 KG).

LUBRICANT : RISELLA 32 + 1.00 %wt DBDS

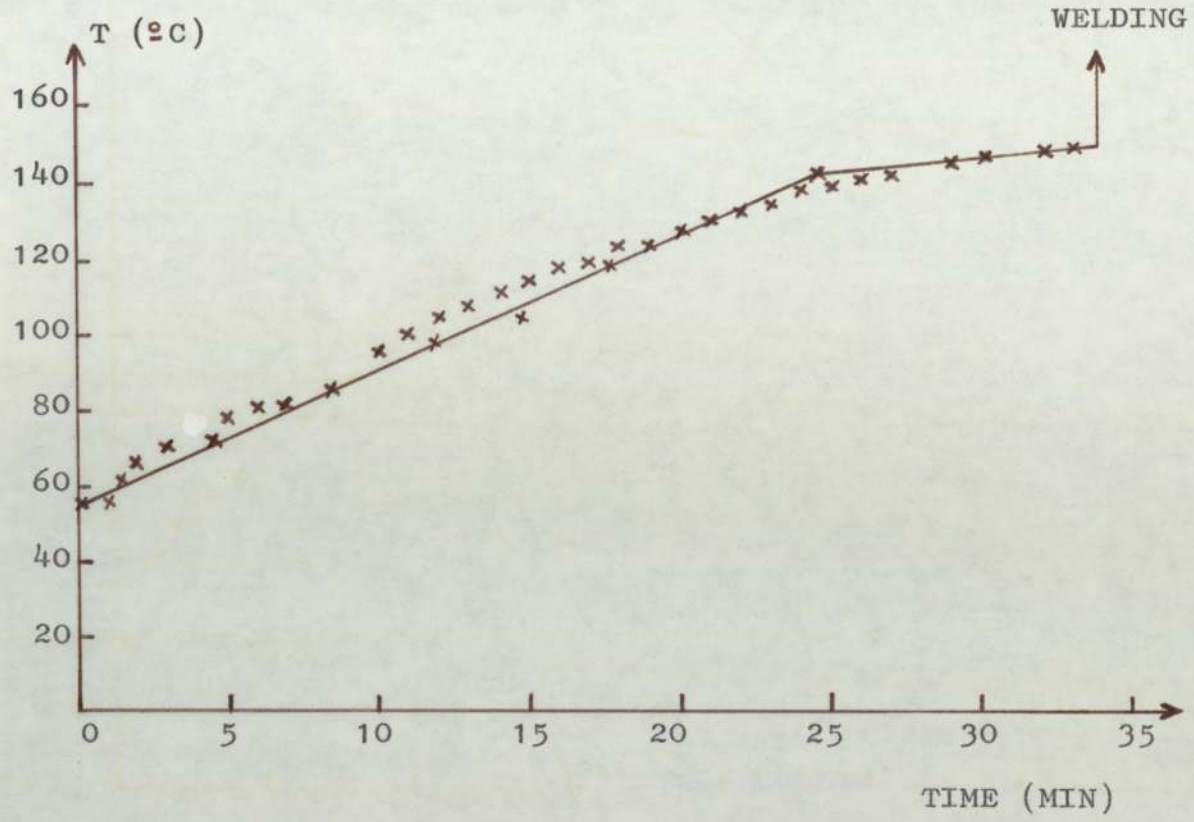

FIG.3.14 TEMPERATURE VS. TIME OF AN E.P. LOAD (130 KG).

LUBRICANT : RISELLA 32 + 1.74 %wt DBMS

Furthermore, the first conclusion drawn from these experiments, is that they could be taken as a single reference for explaining the differences between the a.w. and e.p. film formations. The a.w. film tends to build up smoothly until reaching its maximum value, then stays constant for several hours. On the other hand, the e.p. film build up is not uniform and this is due to the chemical reaction taking place between the oil film and the surface. To support these suggestions, tests of measuring scar diameters with time, under a.w. and e.p. conditions, were carried out using elemental sulphur as the additive. The results are shown in Figures 3.15 and 3.16 and they confirm the proposals put above.

3.2 X-ray Diffraction Analysis of Specimens

In order to identify the main components which constitute the a.w. and e.p. films, an indirect examination was attempted through the use of x-ray diffraction analysis of the wear debris collected during the 4-ball tests.

3.2.1 Identification of the Wear Debris for the A.W. Region

To produce sufficient quantity of wear debris, a period of time between 6 hours and 8 hours was found to be necessary for the load of 40 kg used for this test. The long running time did not result in the balls becoming too hot which could affect the properties of the surface. The debris collected from experiments using elemental sulphur (0.25% wt) and DBDS (1.00% wt) as the additives was exposed to the X-rays for nearly two hours. The interpretation of the films is shown in Tables 3.5 and 3.6. The main component found to be present

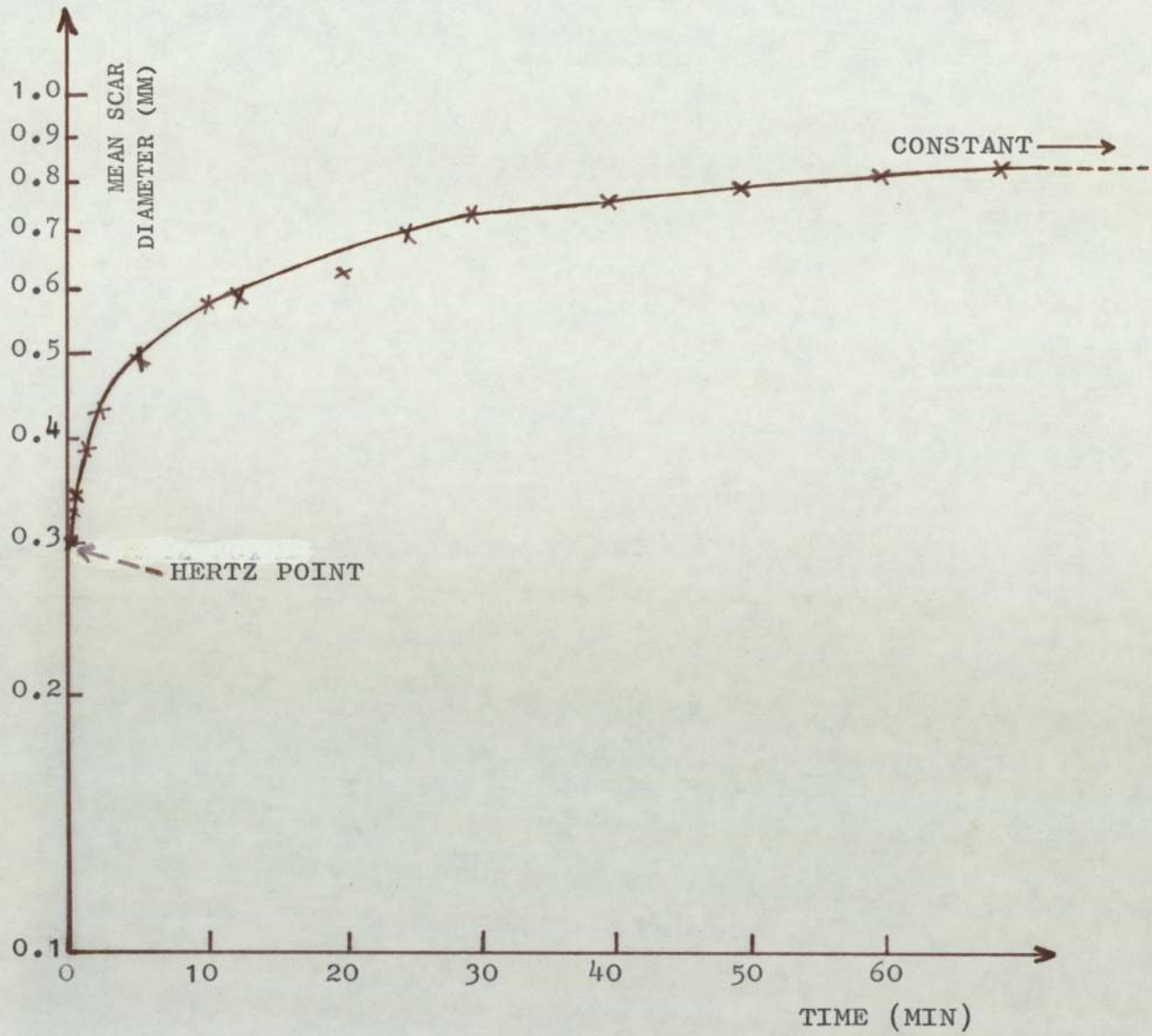

FIG. 3.15 FOUR-BALL ANTI-WEAR RESULTS.

LUBRICANT : RISELLA 32 + 0.25 %wt ELEMENTAL SULPHUR

LOAD USED : 40 KG

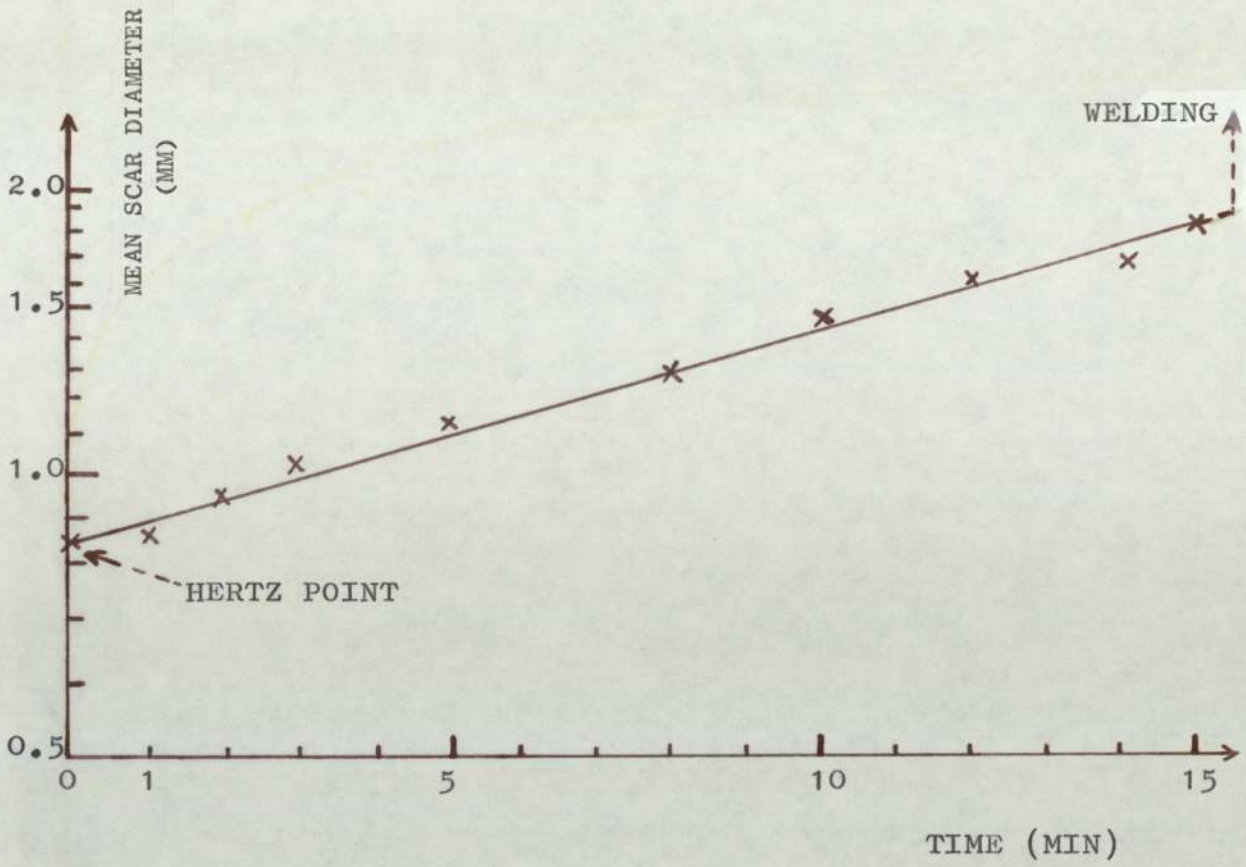

FIG. 3.16 FOUR-BALL EXTREME PRESSURE RESULTS.

LUBRICANT : RISELLA 32 + 0.25 %wt ELEMENTAL SULPHUR

LOAD USED : 130 KG

Line N°	Distance (mm)	2θ (°)	d (A°)	Possible compounds or elements
1/S	35.00	35.00	2.977	FeS (2.980)
2/F	43.00	43.00	2.4432	FeS (2.524)?//Fe_2O_3 (2.519)
3	47.50	47.50	2.223	Fe_2O_3 (2.210)?
4/V.S	52.00	52.00	2.043	FeS (2.092)
5	57.50	57.50	1.862	Fe_2O_3 (1.840)?
6	58.50	58.50	1.833	αFe_2O_3 (1.838)
7	68.00(?)	68.00	1.601	FeS (1.640)?//Fe_3O_4 (1.614)??

Table 3.5: X-ray diffraction pattern of wear debris obtained in the a.w. region when elemental sulphur was used as the additive.

Line N°	Distance (mm)	2θ (°)	d (A°)	Possible compounds or elements
1/F	37.00	37.00	2.820	?
2/F	40.00	40.00	2.618	FeS (2.660)
3/F	42.00	42.00	2.499	Fe_2O_3 (2.520)?
4/S	51.50	51.50	2.061	FeS (2.090)
5	67.00	67.00	1.622	FeS (1.640)//Fe_3O_4(1.614)??

Table 3.6: X-ray diffraction pattern of wear debris obtained in the a.w. region when DBDS was used as the additive.

N.B: 1) F = Faint
S = Strong
V.S = Very Strong

2) The figures between brackets represent the "d" values for the corresponding compounds taken from the A.S.T.M. data file.

in the wear debris is FeS with some lines which could have been attributed to αFe_2O_3 and/or Fe_3O_4.

3.2.2 Identification of the Wear Debris for the E.P. Region

A load of 130 kg, with running time up to 20 minutes, was used for producing wear debris from tests using elemental sulphur, DPDS, DBDS and DBMS. The measurements and interpretation of the X-ray films are summarized in Tables 3.7 to 3.10. FeS is present in all the wear debris analysed but also αFe_2O_3 and $FeSO_4$ seem to be present.

3.2.3 X-ray glancing Angle Method

To verify that the results found during the analysis of the wear debris correspond to the compounds which could be formed on the scars, the latter were examined by the X-ray glancing angle method. As the scars from the a.w. region were too small to be useful for a good analysis (cf. Chapter 2 section 3.3), the experiments were concentrated on the wear scars developed under the e.p. regime. The results obtained for the elemental sulphur, DBDS and DPDS are shown in Tables 3.11, 3.12 and 3.13 respectively. The main compound is FeS, but there is an indication of the presence of $FeSO_4$ and αFe_2O_3. It is worth noting that during the experiments, the angle was chosen so that the X-ray beam will not penetrate into the substrate to detect the Fe and perhaps the Cr.

3.2.4 Discussion

The results from the two tests show there is no trace of FeS_2. This might suggest that the sulphur containing in the lubricant in

Line N°	Distance (mm)	2θ (°)	d (A°)	Possible compounds or elements
1/S	35.00	35.00	2.978	FeS (2.98)
2	37.50	37.50	2.786	Fe_2O_3 (2.70)?
3/S	39.50	39.50	2.650	FeS (2.660)?//$FeSO_4$ (2.618)
4	42.00	52.00	2.499	Fe_2O_3 (2.52)??
5/V.S	51.50	51.50	2.061	FeS (2.09)
6	63.00	63.00	1.714	Fe_2O_3 (1.704)?//$FeSO_4$ (1.706)
7	67.50	67.50	1.612	FeS (1.64)//Fe_3O_4 (1.614)??//
8	78.00	78.00	1.423	FeS (1.423)// α Fe (1.433)?
9	85.50	85.50	1.319	FeS (1.317)
10	100.00	100.00	1.169	FeS (1.18)
11	109.50	109.50	1.097	FeS (1.092)
12	119.00	119.00	1.039	FeS (1.030)
13	129.00	129.00	0.990	FeS (0.999)// α Fe (0.906)?

Table 3.7: X-ray diffraction pattern of wear debris obtained in the e.p. region when elemental sulphur was used as the additive.

N.B.: 1) S = Strong
V.S = Very Strong

2) The figures between brackets represent the "d" values for the corresponding compounds taken from the A.S.T.M. data file.

Line N°	Distance (mm)	2θ (°)	d (A°)	Possible compounds or elements
1	29.00	29.00	3.580	Fe_2O_3 (3.69)??
2	35.00	35.00	2.978	FeS (2.98)
3/V.S	40.00	40.00	2.618	FeS (2.660)?//$FeSO_4$ (2.618)
4/V.S	52.00	52.00	2.043	FeS (2.09)
5/S	63.00	63.00	1.714	Fe_2O_3 (1.704)?//$FeSO_4$ (1.706)
6	67.00	67.00	1.622	FeS (1.64)//Fe_3O_4 (1.614)??
7	77.00	77.00	1.438	FeS (1.423)//α Fe (1.433)?
8	85.00	85.00	1.325	FeS (1.33)
9	100.00	100.00	1.169	FeS (1.18)
10	108/109	108/109	1.107	FeS (1.108)

Table 3.8: X-ray diffraction pattern of wear debris obtained in the e.p. region when DBDS was used as the additive.

N.B.: 1) S = Strong
V.S = Very Strong

2) The figures between brackets represent the "d" values for the corresponding compounds taken from the A.S.T.M. data file.

Line N°	Distance (mm)	2θ (°)	d (A°)	Possible compounds or elements
1/S	35.00	35.00	2.978	FeS (2.980)
2/V.S	40.00	40.00	2.618	FeS (2.660)?//$FeSO_4$ (2.618)
3/V.S	51.50	51.50	2.061	FeS (2.090)
4/V.S	63.50	63.50	1.702	Fe_2O_3 (1.704)//$FeSO_4$ (1.706)
5	68.00	68.00	1.601	FeS (1.64)//Fe_3O_4 (1.614)??
6	77.50	77.50	1.431	FeS (1.423)// α Fe (1.433)?
7	85.50	85.50	1.319	FeS (1.317)
8	100.00	100.00	1.169	FeS (1.180)
9	108/109	108/109	1.103	FeS (1.108)?
10	116.00	116.00	1.056	FeS (1.053)

Table 3.9: X-ray diffraction pattern of wear debris obtained in the e.p. region when DPDS was used as the additive.

N.B.: 1) S = Strong
V.S = Very Strong

2) The figures between brackets represent the "d" values for the corresponding compounds taken from the A.S.T.M. data file.

Line N°	Distance (mm)	2θ (°)	d (A°)	Possible compounds or elements
1/F	35.00	35.00	2.978	FeS (2.980)
2/V.F	37.00	37.00	2.822	Fe_2O_3 (2.703)??
3/S	39.50	39.50	2.650	FeS (2.660)//$FeSO_4$ (2.618)?
4/V.S	51.50	51.50	2.061	FeS (2.090)
5/F	63.00	63.00	1.714	Fe_2O_3 (1.704)?//$FeSO_4$ (1.706)
6	67.00	67.00	1.622	FeS (1.640)//Fe_3O_4 (1.614)??
7	110.00	110.00	1.093	FeS (1.092)
8	119.00	119.00	1.039	FeS (1.030)

Table 3.10: X-ray diffraction pattern of wear debris obtained in the e.p. region when DBMS was used as the additive.

N.B.: 1) F = Feint
V.F = Very Feint
S = Strong
V.S = Very Strong

2) The figures between brackets represent the "d" values for the corresponding compounds taken from the A.S.T.M. data file.

Line N°	Distance (mm)	2 θ (°)	d (A°)	Possible compounds or elements
1	30.00	30.00	3.460	Fe_2O_3 (3.690)?//$FeSO_4$ (3.410)
2/V.F	34.00	34.00	3.063	FeS (2.980)?
3	43.00	43.00	2.443	FeS (2.520)?//$FeSO_4$ (2.519)
4/V.S	52.00	52.00	2.043	FeS (2.090)
5/V.S	76.00	76.00	1.454	FeS (1.446)
6/V.S	99/100	99/100	1.174	FeS (1.180)
7/V.S	124.00	124.00	1.014	FeS (1.030)

Table 3.11: X-ray glancing angle diffraction pattern obtained in the e.p. region when elemental sulphur was used as the additive.

Line N°	Distance (mm)	2 θ (°)	d (A°)	Possible compounds or elements
1/S	34.00	34.00	3.063	FeS (2.980)
2	42.00	42.00	2.500	FeS (2.524)//Fe_2O_3 (2.519)?// $FeSO_4$ (2.618)
3/V.S	52.00	52.00	2.042	FeS (2.090)
4/F	77.00	77.00	1.438	FeS (1.423)// αFe (1.433)?
5/S	100.00	100.00	1.169	FeS (1.180)

Table 3.12: X-ray glancing angle diffraction pattern obtained in the e.p. region when DBDS was used as the additive.

N.B.: 1) S = Strong
V.S = Very Strong
F = Faint
V.F = Very Feint

2) The figures between brackets represent the "d" values for the corresponding compounds taken from the A.S.T.M. data file.

Line N°	Distance (mm)	2θ (°)	d (A°)	Possible compounds or elements
1	42.00	42.00	2.50	FeS (2.524)//Fe_2O_3 (2.519)?// $FeSO_4$ (2.618)
2/V.S	52.00	52.00	2.043	FeS (2.090)
3	76.00	76.00	1.454	FeS (1.446)?//Fe_2O_3 (1.454)
4	100.00	100.00	1.169	FeS (1.180)

Table 3.13: X-ray glancing angle diffraction pattern obtained in the e.p. region when DPDS was used as the additive.

N.B.: 1) V.S = Strong

2) The figures between brackets represent the "d" values for the corresponding compounds taken from the A.S.T.M. data file.

the form of disulphide could facilitate the formation of a surface layer of FeS in both regions (a.w. and e.p.).

3.3 Analysis of Selected Specimens by the Means of X-ray Photoelectron Spectroscopy

Six worn roller bearings were examined by X-ray Photoelectron Spectroscopy (X.P.S.) at Thornton Research Centre (Shell Limited). Elemental sulphur and DBDS were the additives used during the wear tests for preparing the selected scars (ie specimens). The specimens were as follows:

	Additive	Load (kg)	Test time (s)	Area
Specimen 1	0.25% wt elemental sulphur	40	60	a.w.
Specimen 2	"	130	60	e.p.
Specimen 3	"	130	1100	e.p.
Specimen 4	"	300	60	e.p.
Specimen 5	1.00% wt DBDS	130	1110	e.p.

Specimen N° 6 is referred to a thick iron sulphate film prepared on one of the base of an unworn roller bearing. This sample was used as a reference.

The detection of the S_{2p} peaks obtained for each sample are illustrated from Figures 3.17 to 3.22. Table 3.14 shows the interpretation of the spectra produced from the whole analysis, ie including the detection of Fe, O and C. The results indicate that when using sulphur

	Elements or compounds detected with their measured binding energies in eV.					
	Fe_{2p}	Fe_{3p}	O_{1s}	FeS	Sulphate	Sulphur or Organic sulphide
Sp. No. 1	x	v (55.40)	v (532.20) and (530.30)	x	v (168.70)	x
Sp. No. 2	x	v (55.60)	v (531.50) and (530.15)	v (161.75)	v (168.75)	x
Sp. No. 3	x	v (55.90)	v (532.05) and (531.05)	v (162.80)	v (169.15)	v (164.15)
Sp. No. 4	x	v (56.05)	v (532.55) and (530.25)	v (162.00)	v (169.20)	v (163.80)
Sp. No. 5	x	v (56.10)	v (532.20) and (530.60)	x	v (168.90)	x
Sp. No. 6	x	v (57.50) (55.40)	v (532.00)	x	v (168.80)	x

Table 3.14: Results of the X.P.S. examination.

N.B.: x = indicates no detection v = indicates detection

as the additive the product is iron sulphate and sulphide in the e.p. region, whereas when DBDS was used as the additive the product was iron sulphate in the e.p. region.

3.4 Summarising Remarks

It is worth noting that, although X.P.S. is a very sensitive surface analyser, it failed to detect FeS in the a.w. region or more important in the e.p. region when DBDS was used as the additive. However, this compound has been detected by both methods, namely X-ray diffraction and X-ray glancing angle. There is a good agreement between the three methods with the respect to the detection of $FeSO_4$ for both regions (a.w. and e.p.). The earlier suggestion about the presence of $FeSO_4$, is that this compound could be the result of the contribution mainly from the un-rubbed surface adjacent to the wear scar.

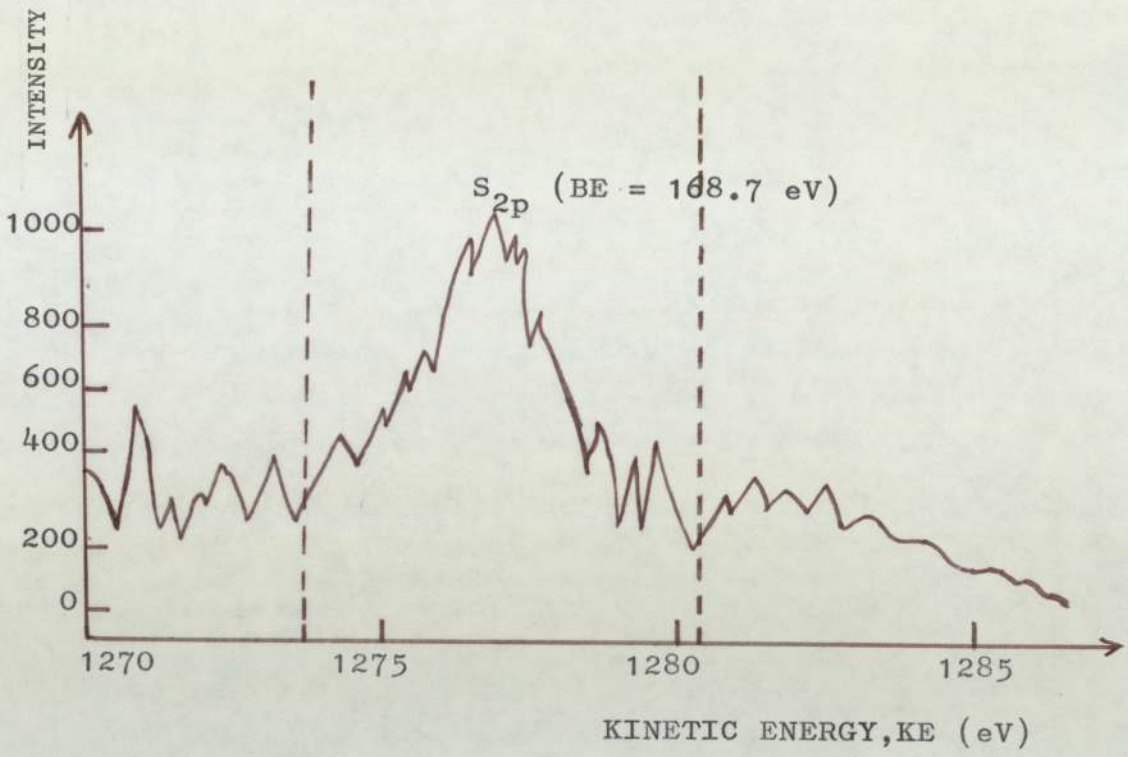

FIG. 3.17 S_{2p} SPECTRUM FROM X.P.S. ANALYSIS OF SAMPLE 1 :

(ADDITIVE : 0.25 %wt ELEMENTAL SULPHUR
APPLIED LOAD : 40 KG
TEST TIME : 60 SECONDS.)

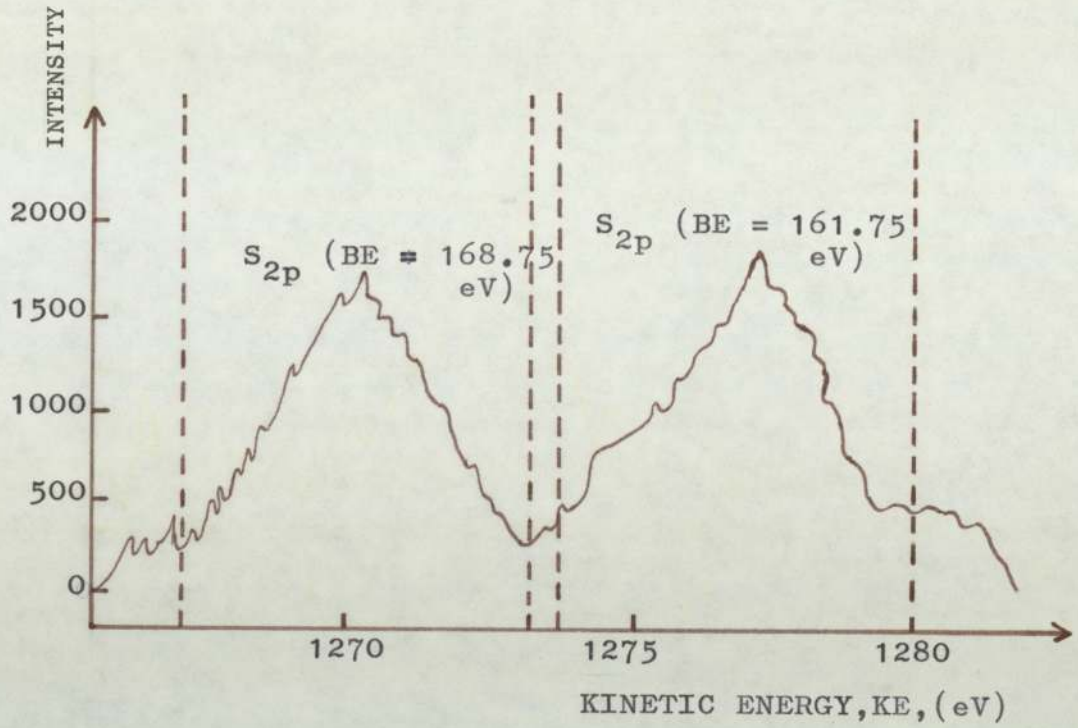

FIG. 3.18 S_{2p} SPECTRUM FROM X.P.S. ANALYSIS OF SAMPLE 2 :
(ADDITIVE : 0.25 %wt ELEMENTAL SULPHUR
APPLIED LOAD : 130 KG
TEST TIME : 60 SECONDS.)

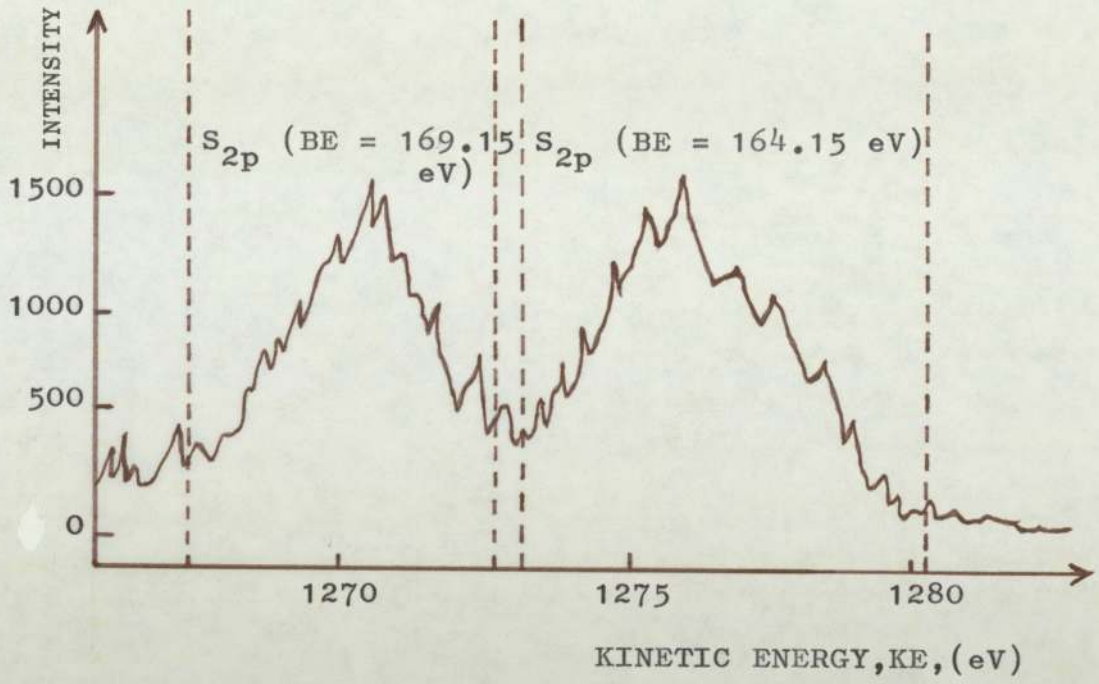

FIG. 3.19 S_{2p} SPECTRUM FROM X.P.S. ANALYSIS OF SAMPLE 3 :
(ADDITIVE : 0.25 %wt ELEMENTAL SULPHUR
APPLIED LOAD : 130 KG
TEST TIME : 1100 SECONDS.)

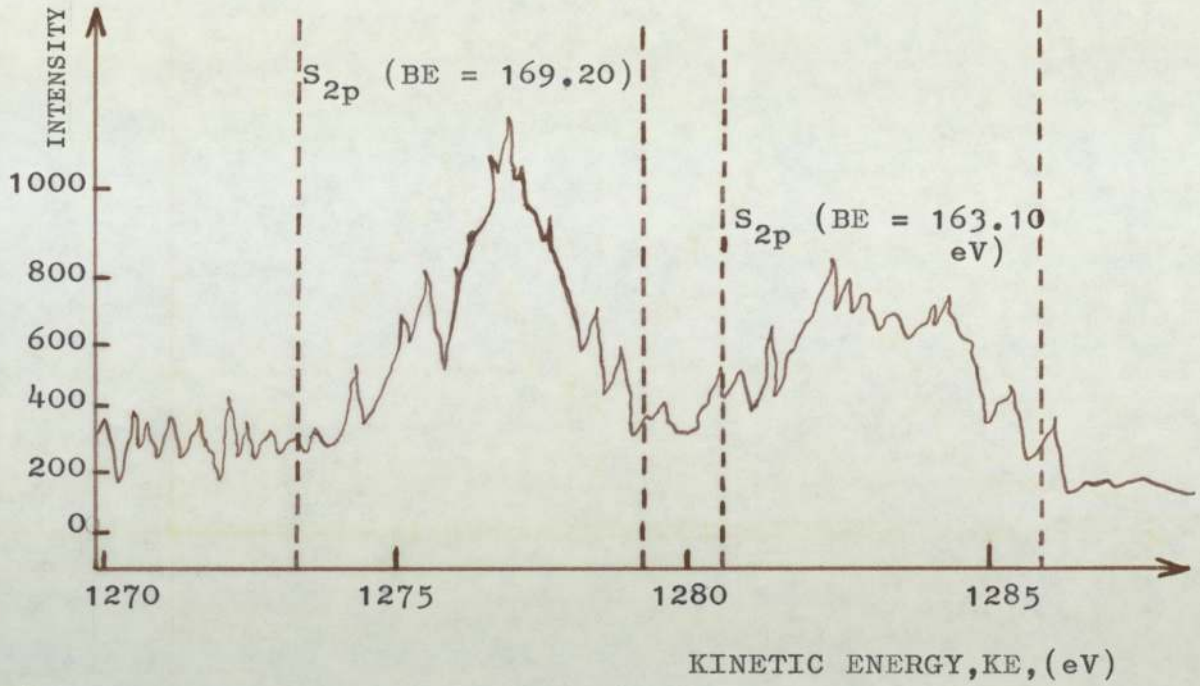

FIG. 3.20 S_{2p} SPECTRUM FROM X.P.S. ANALYSIS OF SAMPLE 4 :
(ADDITIVE : 0.25 %wt ELEMENTAL SULPHUR
APPLIED LOAD : 300 KG
TEST TIME : 60 SECONDS.)

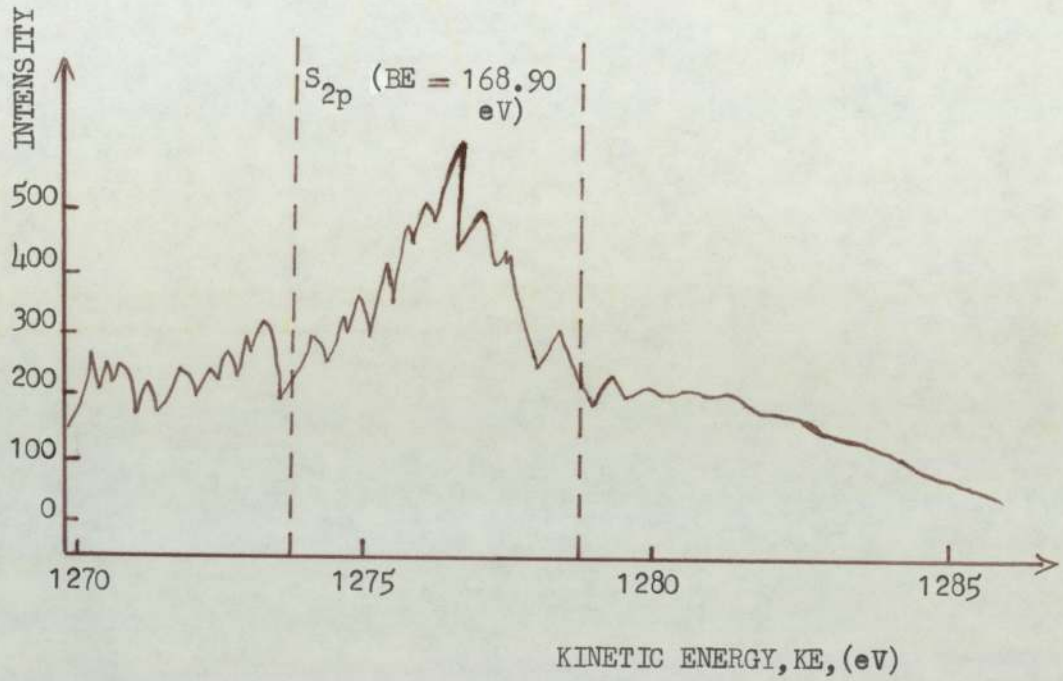

FIG. 3.21 S_{2p} SPECTRUM FROM X.P.S. ANALYSIS OF SAMPLE 5 :
(ADDITIVE : 1.00 %wt DBDS
APPLIED LOAD : 130 KG
TEST TIME : 1100 SECONDS).

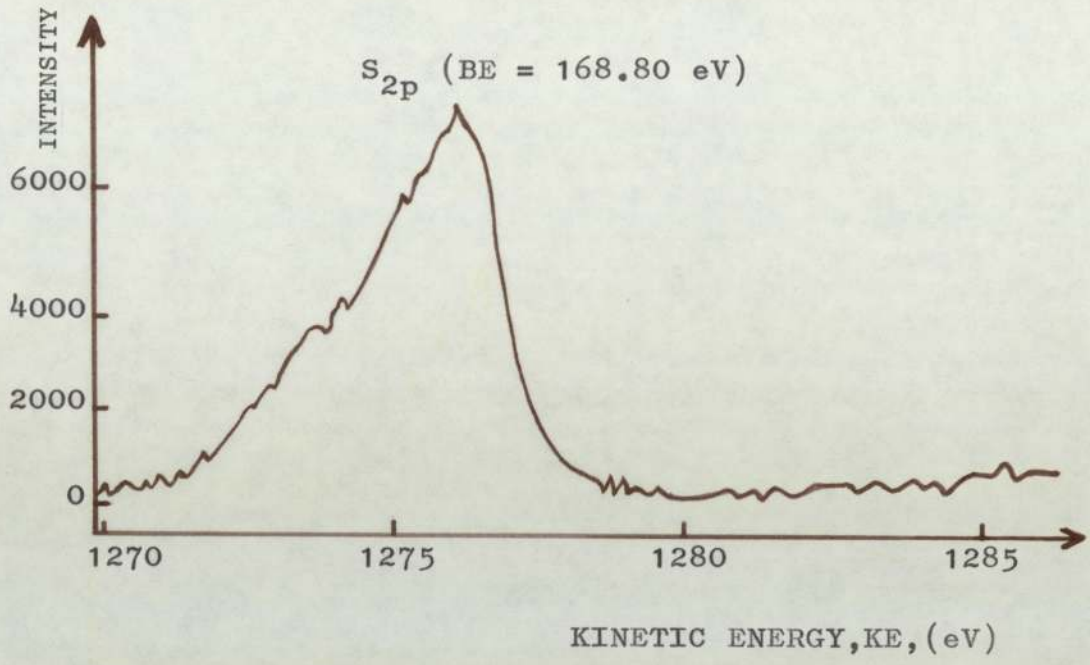

FIG. 3.22 S_{2p} SPECTRUM FROM X.P.S. ANALYSIS OF SAMPLE 6 : (THICK IRON SULPHATE FILM).

CHAPTER FOUR

ANALYSIS OF THE WORN SURFACES BY USING S.E.M. AND E.P.M.A.

4.1 Analysis using S.E.M. Coupled with an Energy Dispersive X-ray Analyser (KEVEX).

The difference between the formation of the a.w. and e.p. films was studied from the micrographs of the wear scars and also from the X-ray distribution of the main elements of interest (ie sulphur and iron) covering the scars. Thus surface topographies were obtained with the use of a Scanning Electron Microscope (S.E.M.), and alongside X-ray maps of the areas were recorded by using an X-ray detector. The accelerating voltage for the electron beam was set to 20 kV for all the analyses carried out on the S.E.M.

Before studying the different specimens prepared under specific conditions, an unworn EN31 steel ball was analysed and the electron picture of the surface together with the iron X-ray image are shown in Figure 4.1, whilst Figure 4.2 displays the X-ray chart obtained for that area. There is no sign of sulphur peak and the main peak belongs to iron, which is the major constituent of EN31 steel (95.90% to 97.50%). There was also evidence of very small peaks of Si, Cr, and Mn, which also are part of the original composition of the steel, but in a very low concentration (0.10% to 0.35% for Si, 1.00% to 1.60% for Cr and 0.30% to 0.75% for Mn).

4.1.1 Anti-Wear Analysis

To study the dependence of a.w. film formation on time, four worn surfaces obtained using the same additive (0.25% wt elemental

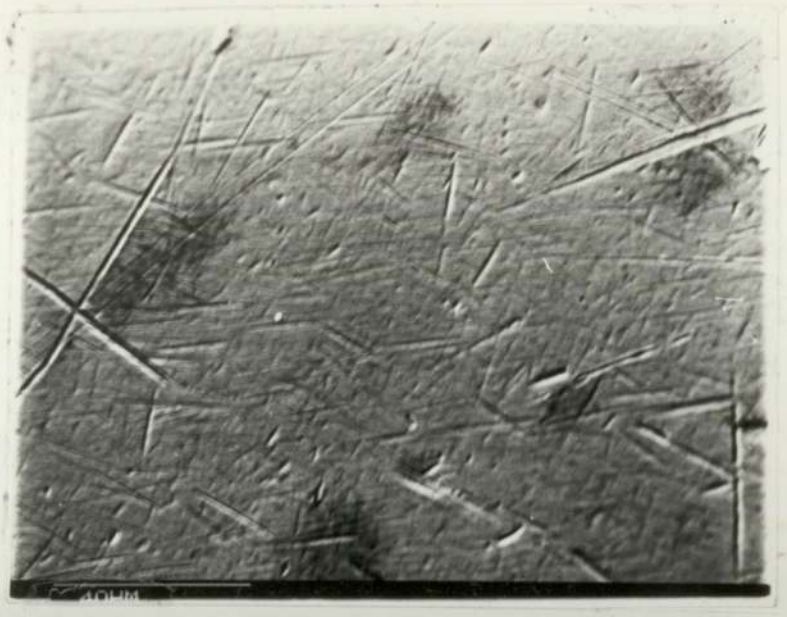

(a)

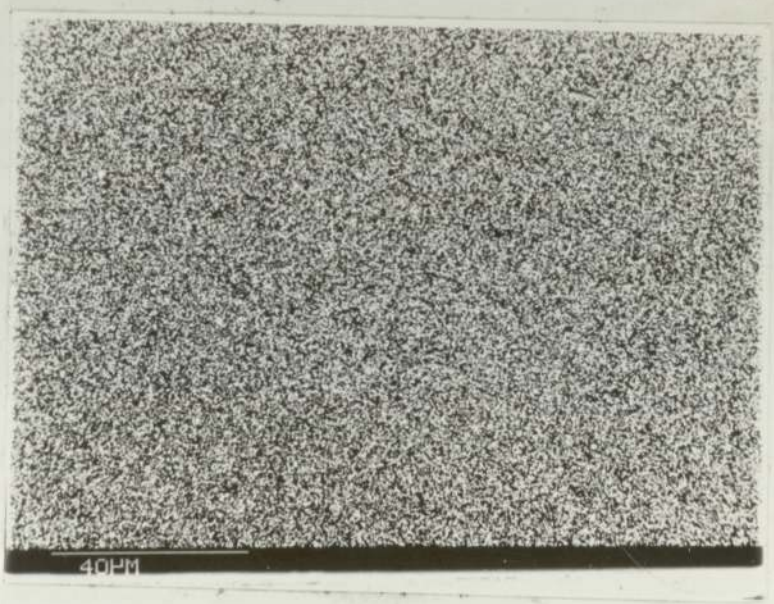

(b)

FIG 4.1. ELECTRON PICTURE AND X-RAY IMAGE DISTRIBUTION OF THE UNWORN SURFACE.

a) Micrograph of the surface.

b) Iron X-ray image.

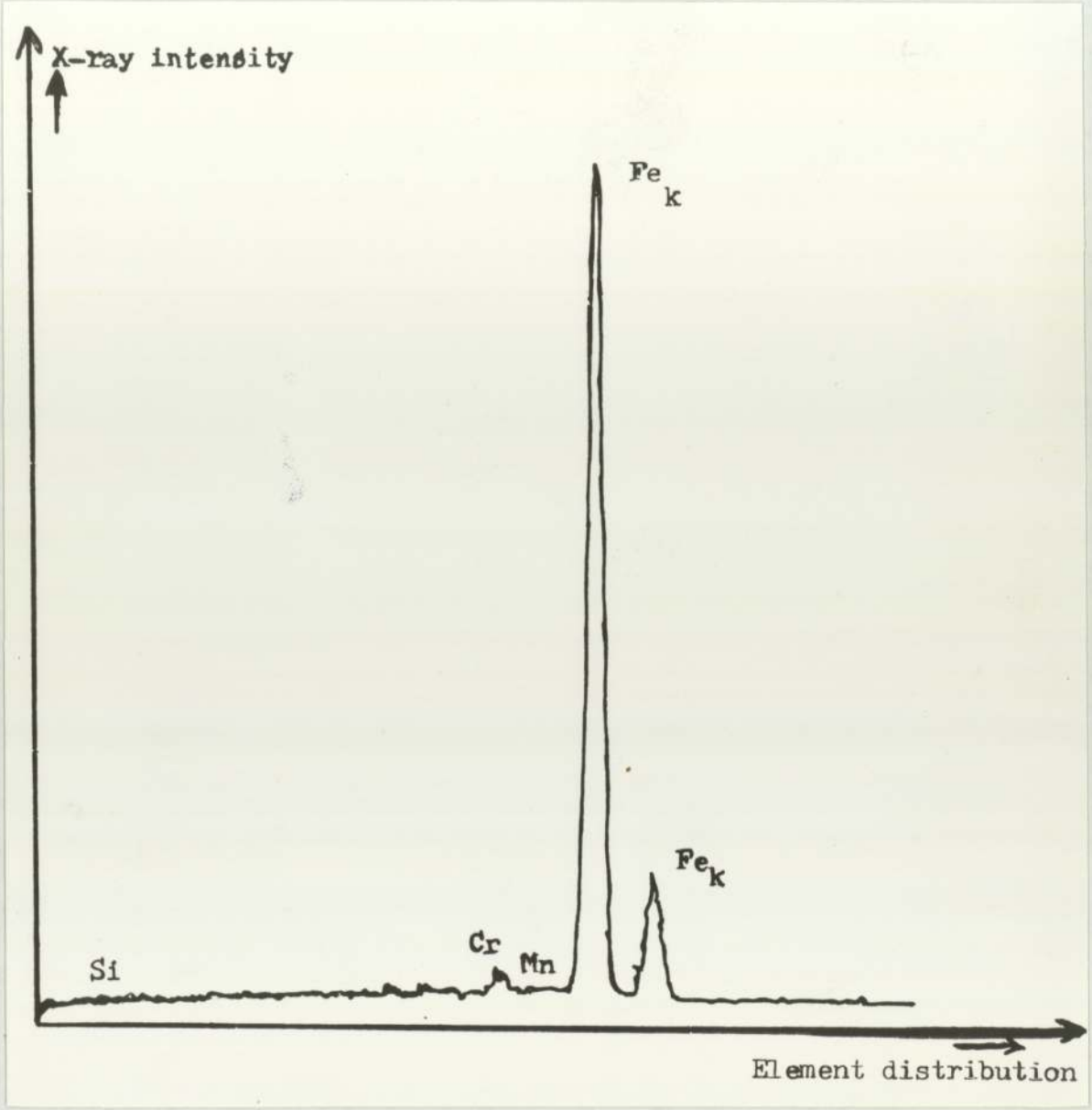

FIG. 4.2 X-RAY CHART OF THE UNWORN SURFACE

sulphur), but prepared at different times, were investigated. The selected load was 40 kg for each case.

i) Sample No. 1.

Running Time: Standard One Minute

The worn area forms an indistinct circle [Figure 4.3(a)]. At higher magnification [Figure 4.3(b)], the worn surface is rough and the central part is dark. The photograph reveals a lot of scratches but no indication of a visible film. Figures 4.3(c) and (d) show the X-ray distribution for iron and sulphur respectively. The distribution of sulphur is uniform which suggests that it could be from the original steel. The iron covers all the damaged surface. The X-ray chart (Figure 4.4) displays the elements detected over the scar and the results confirm the above remark that there is no visible film and all the detected substances are originally part of the material.

ii) Specimen No. 2.

Running Time: One Hour

With an increase in time the improved protectives, characteristics of the lubricant, becomes more evident. This can be seen in Figure 4.5(a), which shows the perfect circular form of the scar. At higher magnification, the photograph in Figure 4.5(b) indicates that the worn area is formed by a series of layers adjacent to each other. Furthermore, it can be seen that the reacted film is smooth and the fine tracks on

FIG. 4.3 ELECTRON PICTURES AND X-RAY IMAGE DISTRIBUTIONS OF THE A.W. REGION FOR THE FOLLOWING SAMPLE :

ADDITIVE : 0.25 % wt ELEMENTAL SULPHUR
APPLIED LOAD : 40 KG
TEST TIME : STANDARD ONE MINUTE

a) Micrograph of the worn surface (Mag. X 200)
b) Micrograph of the worn surface (Mag. X 500)
c) Iron X-ray image
d) Sulphur X-ray image

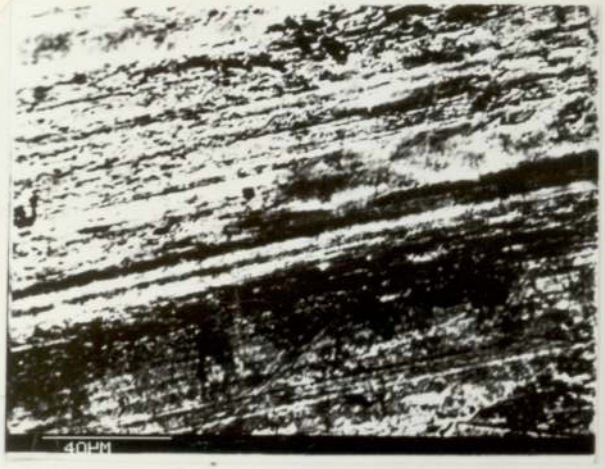

(b)

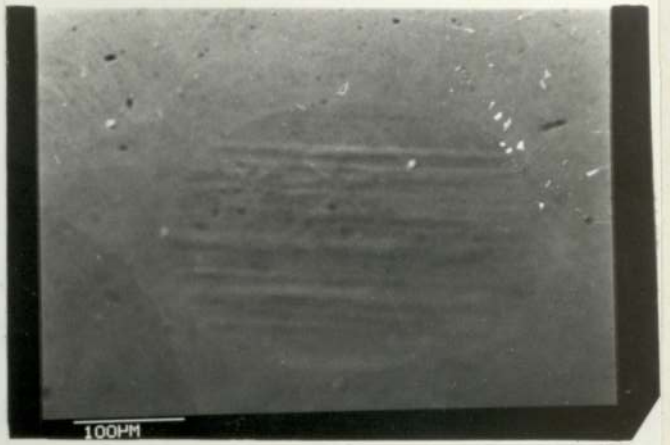

(a)

(c)

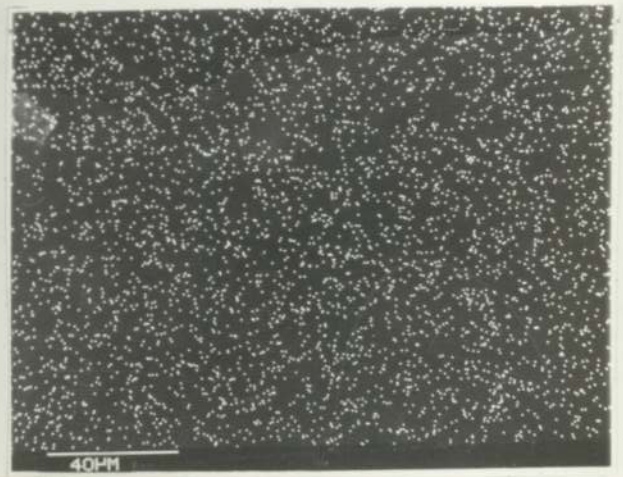

(d)

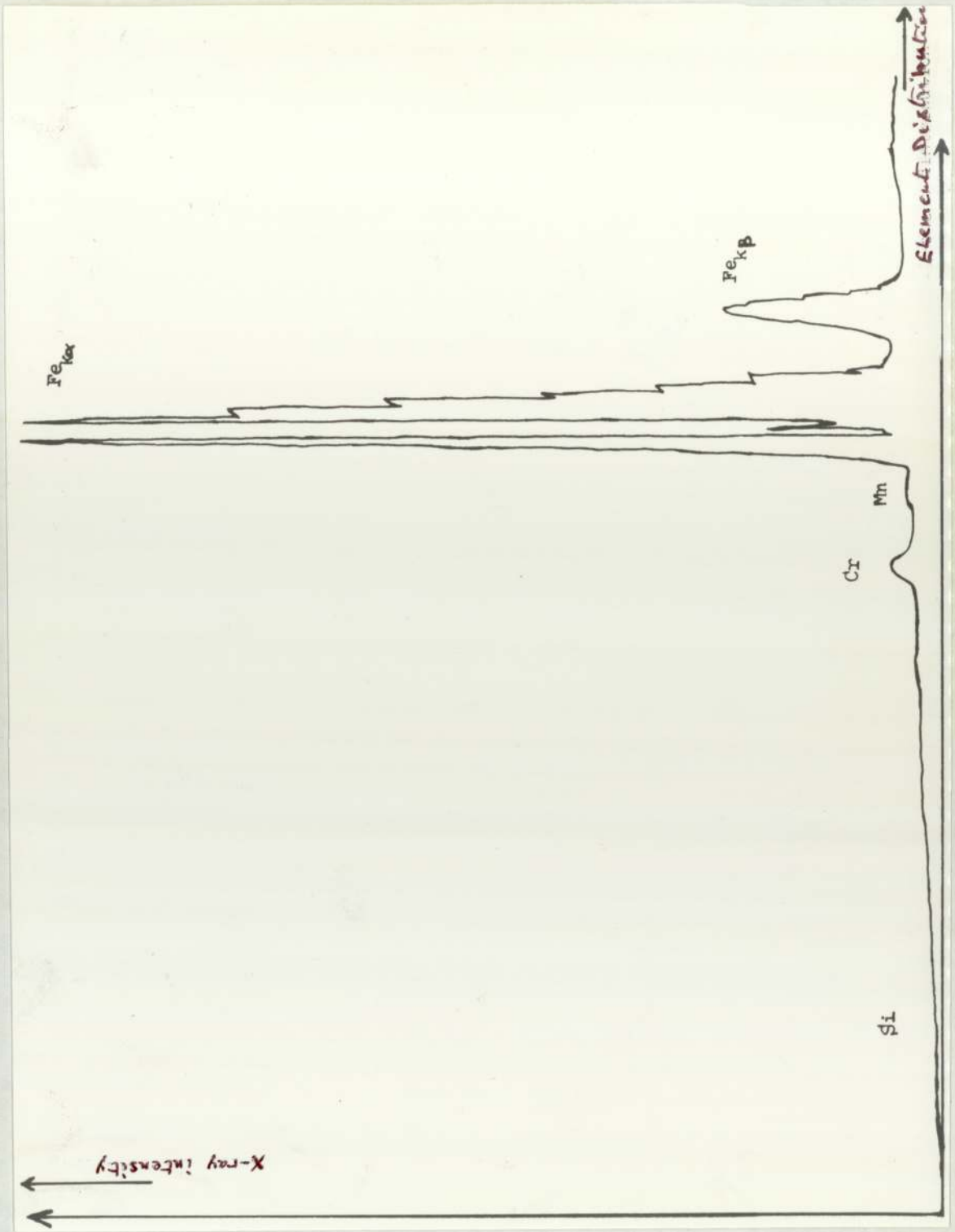

FIG. 4.4 X-RAY CHART OF AN A.W. REGION

ADDITIVE : 0.25 % wt ELEMENTAL SULPHUR

APPLIED LOAD : 40 KG

TEST TIME : STANDARD ONE MINUTE

FIG. 4.5 ELECTRON PICTURES AND X-RAY IMAGE DISTRIBUTIONS OF THE A.W. REGION FOR THE FOLLOWING SAMPLE :

ADDITIVE : 0.25 % wt ELEMENTAL SULPHUR
APPLIED LOAD : 40 KG
TEST TIME : ONE HOUR

a) General view of the scar (Mag. X 50)
b) Micrograph of the worn surface (Mag. X 500)
c) Iron X-ray image
d) Sulphur X-ray image

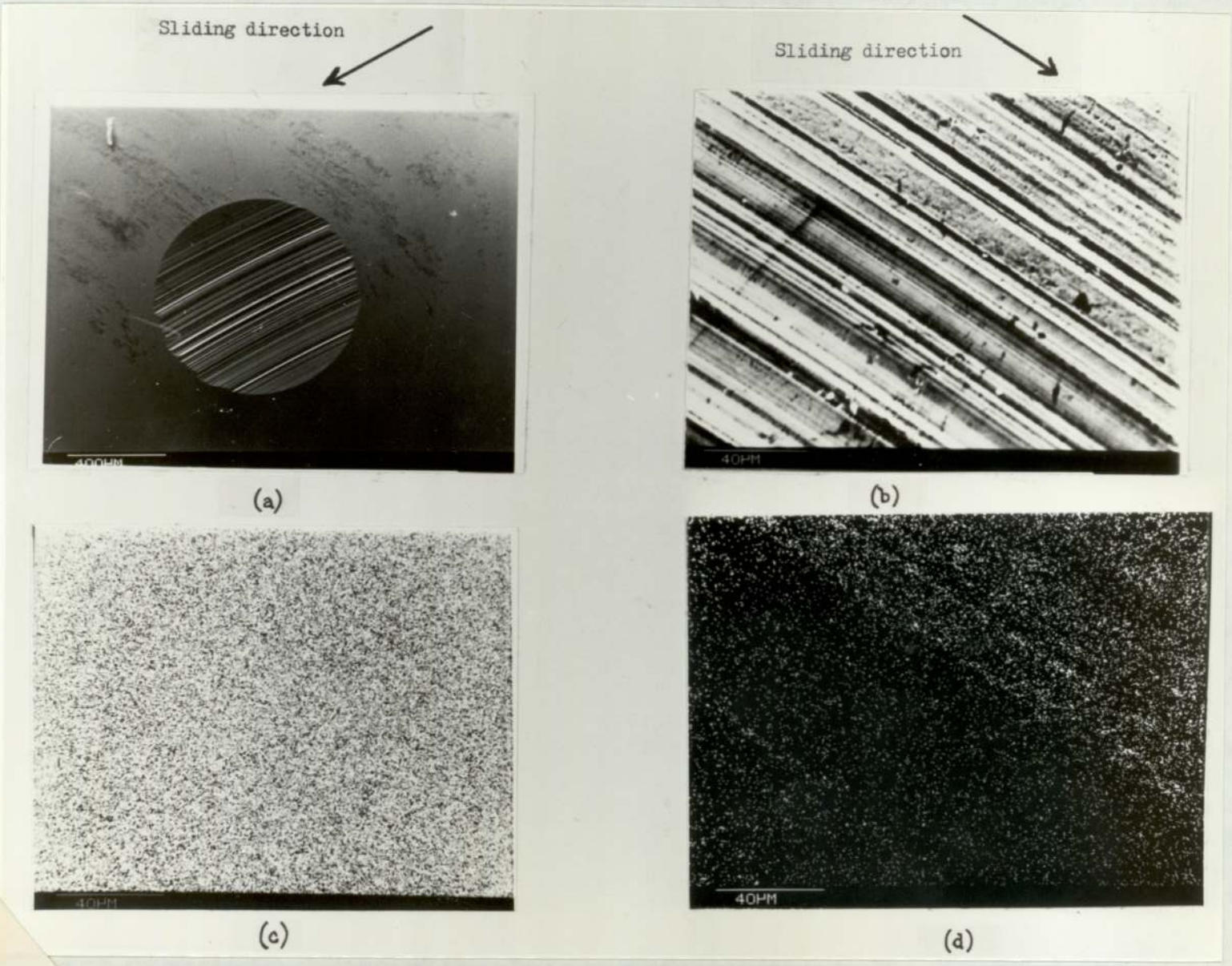

(a) (b)

(c) (d)

the scar are parallel to the direction of sliding. Some tracks are darker than others and this suggests that a thin film of sulphur or iron sulphide is formed on these layers. Figures 4.5(c) and (d) represent the X-ray image distributions of the iron and sulphur respectively. The picture for the Fe is more or less darker on the right part, meanwhile for the S, it shows white spots all over the area. But in addition there are concentrated spots in the shape of tracks on the right top of the picture. The corresponding X-ray distribution (Figure 4.6) indicates a presence of an amount of sulphur beside the iron.

iii) Specimen No. 3.

Running Time: 3 Hours

It seems that the time factor has improved the tracks and this can be seen in Figure 4.7(a), where the distinction of the tracks is more clearly marked. The film is smoother than the previous one. From Figure 4.7(b), which shows the X-ray image distribution of the iron over the worn area, it is clearly seen that there are dark stripes in almost all the picture. This means the presence of another element along with the Fe. Meanwhile Figure 4.7(c) indicates the distribution of the sulphur. The spots are concentrated and form tracks with one greatest concentration in the middle. This suggests an increase of sulphur film with the increase of running time. The orientation of the film is parallel to the sliding direction. The corresponding X-ray distribution (Figure 4.8) confirms the increase of the sulphur.

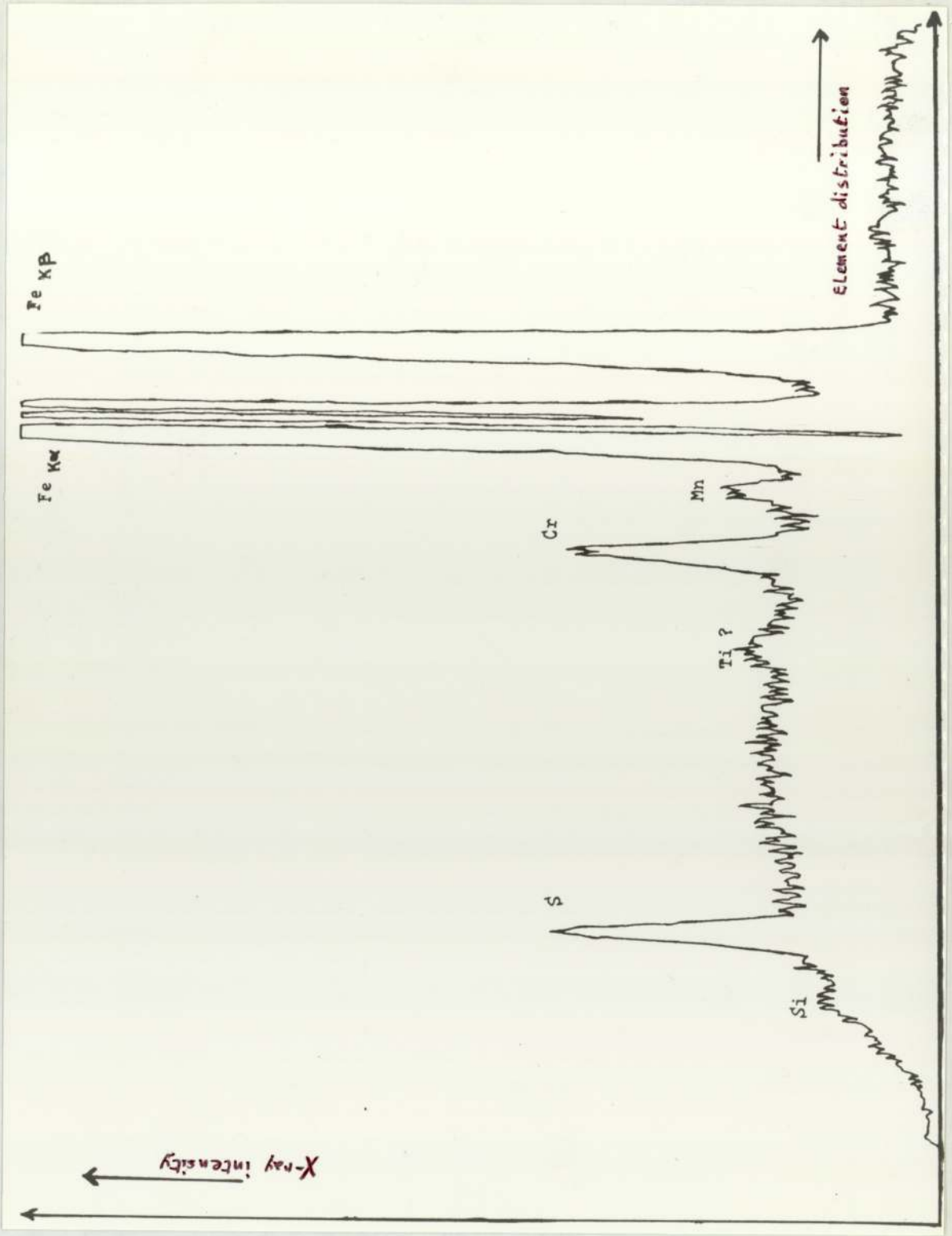

FIG. 4.6 X-RAY CHART OF AN A.W. REGION

ADDITIVE : 0.25 % wt ELEMENTAL SULPHUR

APPLIED LOAD : 40 KG

TEST TIME : ONE HOUR

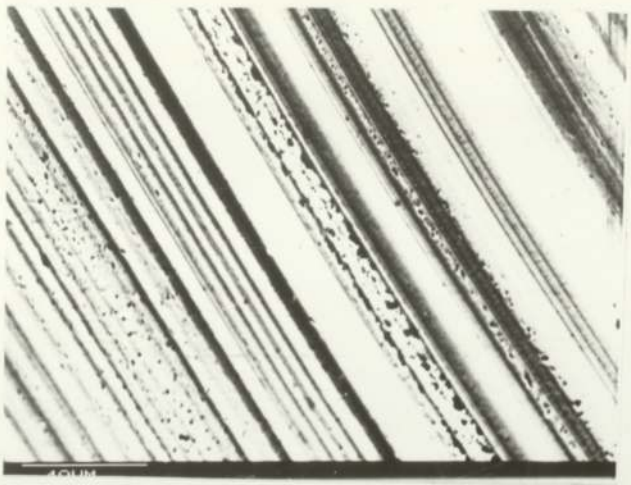

a) Micrograph of the worn surface (Magn. X 500).

Sliding direction

b) Iron X-ray image.

c) Sulphur X-ray image.

FIG. 4.7 ELECTRON PICTURE AND X-RAY IMAGE DISTRIBUTIONS OF THE A.W. REGION FOR THE FOLLOWING SAMPLE :

ADDITIVE : 0.25 % wt ELEMENTAL SULPHUR

APPLIED LOAD : 40 KG

TEST TIME : 3 HOURS

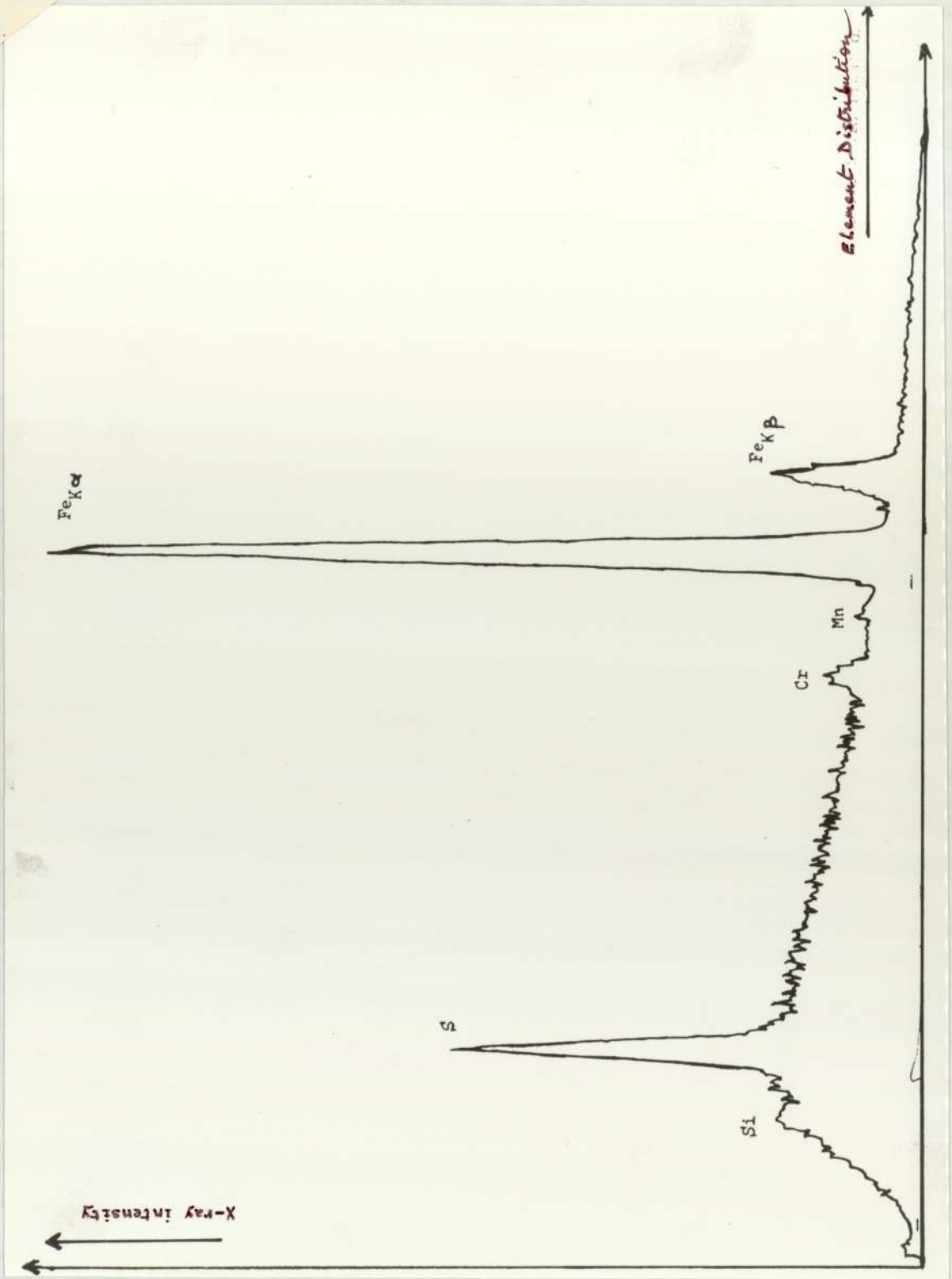

FIG. 4.8 X-RAY CHART OF AN A.W. REGION

ADDITIVE : 0.25 % wt ELEMENTAL SULPHUR

APPLIED LOAD : 40 KG

TEST TIME : THREE HOURS

iv) Specimen No. 4.

Running Time: 6 Hours

This sample was prepared during the experiments of determining the effect of the temperature of the lubricant on standard 4-ball tests (see Chapter 3 Section 1.2). From Figure 4.9(a) which shows a general view of the scar obtained after a long running time (6 hours), it appears that the perfect circular form of the scar is still preserved. The resulting micrograph of the area [Figure 4.9(b)] puts in evidence the presence of the fine tracks but much wider than the ones already obtained for the previous damaged areas. Figure 4.9(c), which represents the X-ray image distribution of the sulphur, indicates the presence of concentrated white spots in the shape of large tracks over most of the area except in the right bottom of the picture. The uniform striations of the film are still observed and this means that whenever elemental sulphur is used as the additive, the long running time during the a.w. regime, does not affect the tribo-chemical effect on the adjacent layers formed by sulphur and iron.

When 1.00% wt DBDS was used as the additive during the a.w. regime, more or less the same phenomenon described above, was observed. Figure 4.10 represents the results obtained for analysis of the scar formed at a load of 40 kg for the standard one minute run. The photograph No. 4.10(a) shows the scar at higher magnification, and it can be seen that the area is formed by a series of layers (white and dark) adjacent to each other. The X-ray maps of the Fe [Figure 4.10(b)]

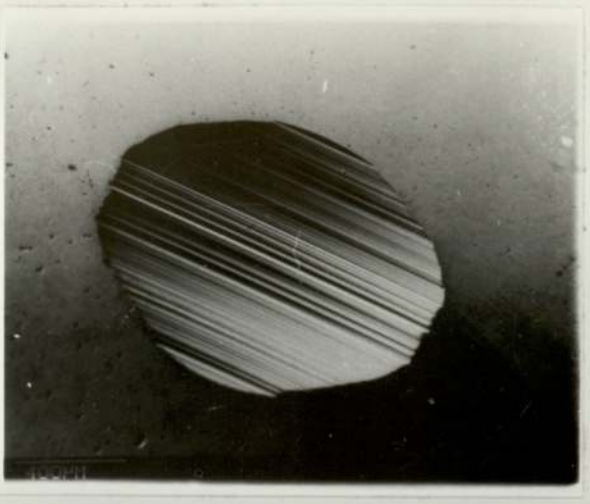

a) General view of the scar (Magn. X 50).

Sliding direction

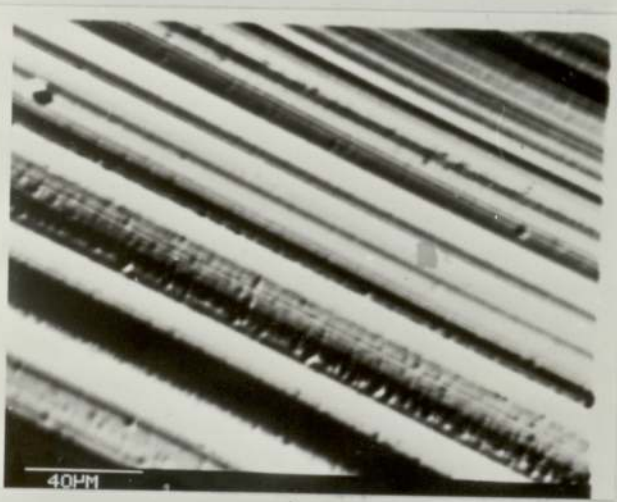

b) Micrograph of the worn surface (Magn. X 500).

Sliding direction

c) Sulphur X-ray image.

FIG. 4.9 ELECTRON PICTURES AND X-RAY IMAGE DISTRIBUTION OF THE A.W. REGION FOR THE FOLLOWING SAMPLE :

ADDITIVE : 0.25 % wt ELEMENTAL SULPHUR

APPLIED LOAD : 40 KG

TEST TIME : 6 HOURS

a) Micrograph of the worn surface (Magn. X 2000).

Sliding direction

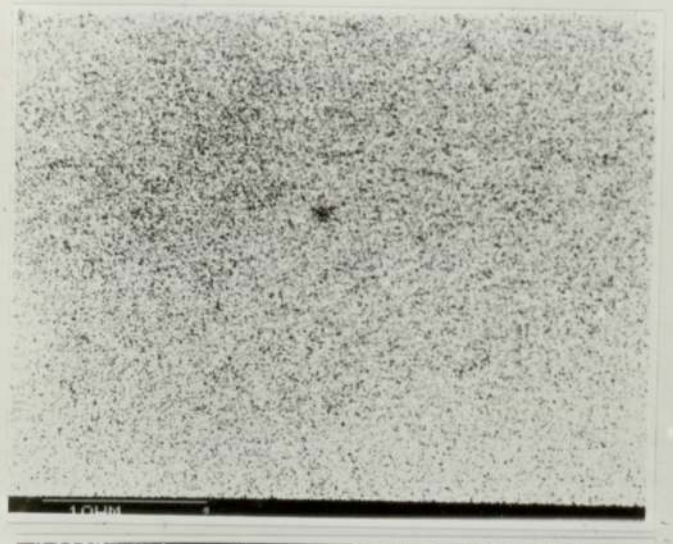

b) Iron X-ray image.

c) Sulphur X-ray image.

FIG. 4.10 ELECTRON PICTURE AND X-RAY IMAGE DISTRIBUTIONS OF THE A.W. REGION FOR THE FOLLOWING SAMPLE :

ADDITIVE : 1.00 % wt DBDS

APPLIED LOAD : 40 KG

TEST TIME : STANDARD ONE MINUTE

and of the S [Figure 4.10(c)] reveal that the first element is distributed all over the area, whilst the second element is concentrated in the form of tracks, right in the middle of the damaged area. The relevant X-ray chart (Figure 4.11) corroborates the presence of the sulphur.

4.1.2 Extreme-Pressure Analysis

Wear scars prepared under e.p. conditions, were obtained for each additive studied in this research. The selected load was 130 kg for each case.

When sulphur was used as the additive, the scar has an oval shape and this is illustrated in Figure 4.12(a). To the naked eye, the edge of the scar is coloured and this suggests that the temperature is high at this point. Figure 4.12(b) represents the micrograph of one part of the damaged area and it is clear that a thick and rough film covers the worn area. Looking at this and also at Figures 4.12(c) and (d), which represent the distributions for the iron and sulphur respectively, one sees that there are no regularities (as in the a.w. film). The sulphur is scattered over the area, whilst Fe covers most of the surface except in small places. This means that the region is mainly iron and a strong presence of sulphur scattered all over the scar. The considerable amount of sulphur is represented by the height of its peak on the corresponding X-ray chart (Figure 4.13).

When using 1.00% wt DBDS, the form of the wear scar obtained is similar to the one described above. This is shown in Figure 4.14(a). The surface has broken up in some places and around the edge. The

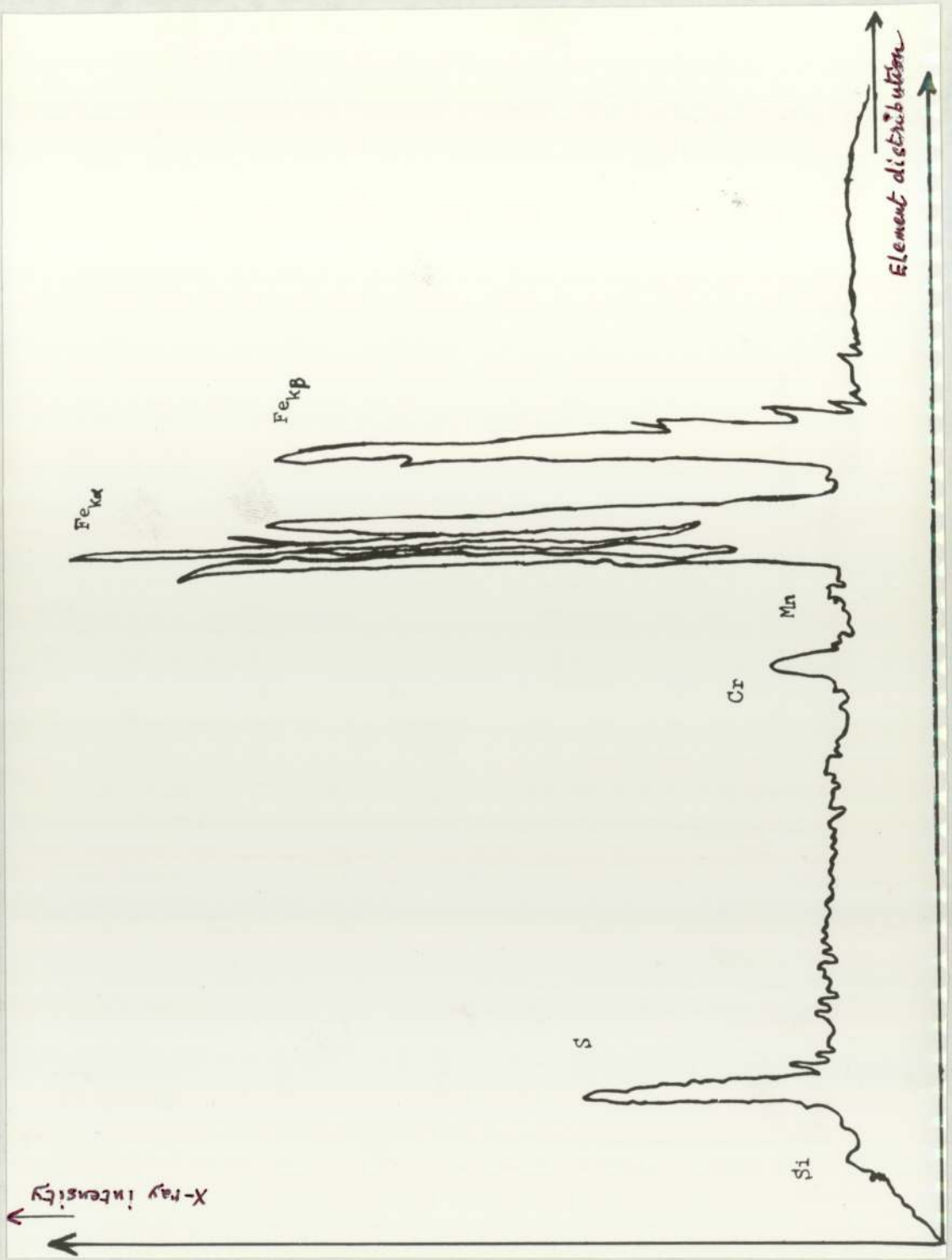

FIG. 4.11 X-RAY CHART OF AN A.W. REGION

ADDITIVE : 1.00 % wt DBDS

APPLIED LOAD : 40 KG

TEST TIME : STANDARD ONE MINUTE

FIG. 4.12 ELECTRON PICTURES AND X-RAY IMAGE DISTRIBUTIONS OF THE E.P. REGION FOR THE FOLLOWING SAMPLE :

ADDITIVE : 0.25 % wt ELEMENTAL SULPHUR
APPLIED LOAD : 130 KG
TEST TIME : 1100 SECONDS

a) General view of the scar (Mag. X 50)
b) Micrograph of the worn surface (Mag. X 500)
c) Iron X-ray image
d) Sulphur X-ray image

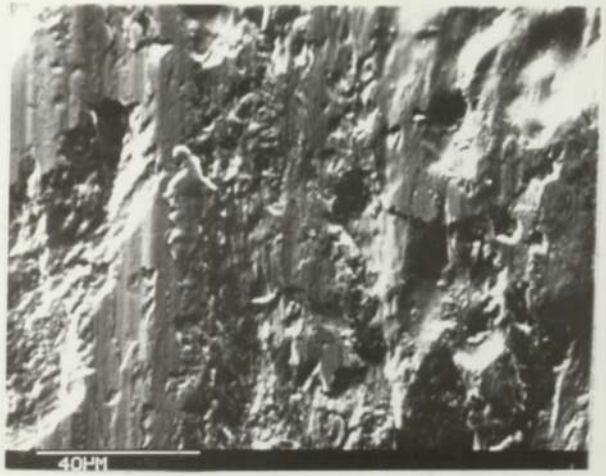

(b)

Sliding direction

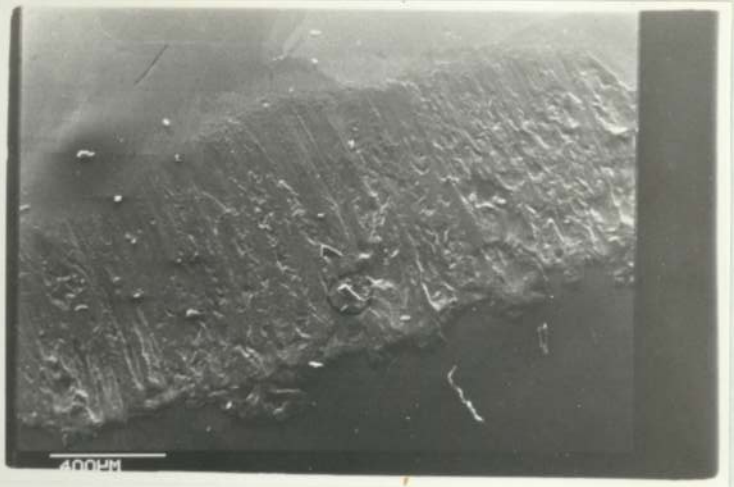

(a)

Sliding direction

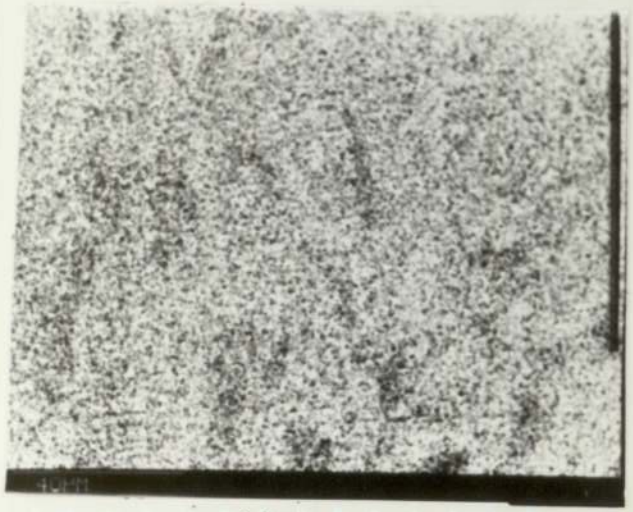

(c)

(d)

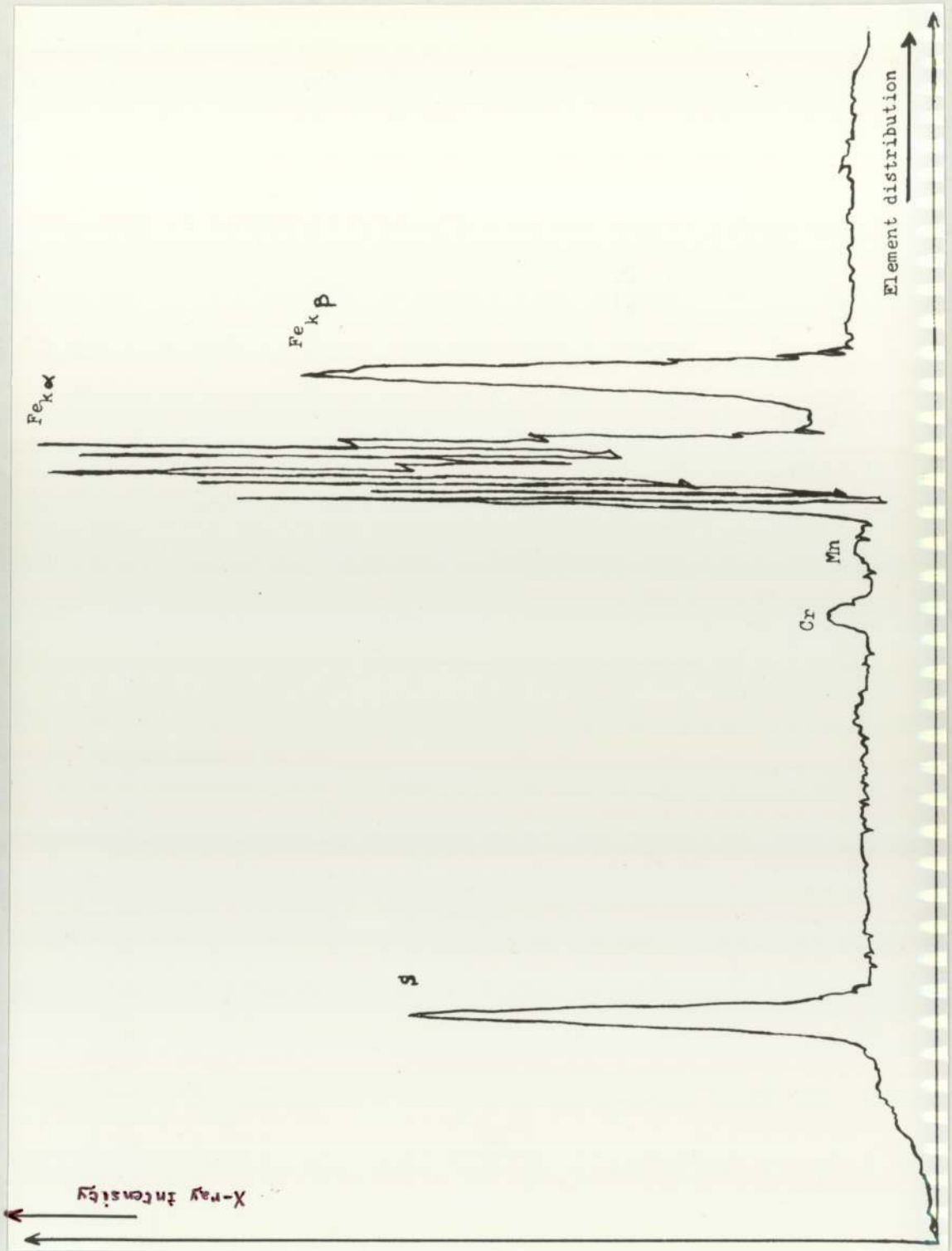

FIG. 4. 13 X-RAY CHART OF AN E.P. REGION

ADDITIVE : 0.25 % wt ELEMENTAL SULPHUR

APPLIED LOAD : 130 KG

TEST TIME : 1100 SECONDS

representation of one part of the damaged area taken at very high magnification [Figure 4.14(b)] shows evidence of the slit on the surface occurring parallel to the sliding direction and this results in the formation of islands alongside the propagation of the cracks. Figure 4.14(c) indicates that Fe is distributed over most of the worn surface except in two clearly defined areas along the scar. High concentration of sulphur lays on these areas and this is confirmed by the observation of the X-ray results displayed in Figure 4.14(d) and 4.15.

In the case of applying 0.88% wt DPDS, the scar produced consists of tracks parallel to the sliding direction irregularly pock-marked by craters where material has been torn out of the surface. This is shown in Figure 4.16 (a). A study of the corresponding X-ray photographs [Figure 4.16 (b) and (c)] and also the diagram (Figure 4.17) suggests that the tracks are mainly iron whilst the craters are a mixture of iron and sulphur.

A micrograph of a region of the scar obtained in the case of using 1.74% wt DBMS [Figure 4.18(a)] reveals that the surface was partially pulled out leaving large craters. The largest crater stands right across the middle of the picture. The examination of the corresponding X-ray elemental surface maps [Figure 4.18(b) and (c)] leads to the conclusion that the sulphur lays in the craters whilst the iron is distributed all over the area but with less density inside the craters. Figure 4.19, which represents the X-ray graph, shows the presence of the sulphur beside the iron.

FIG. 4.14 ELECTRON PICTURES AND X-RAY IMAGE DISTRIBUTIONS OF THE E.P. REGION FOR THE FOLLOWING SAMPLE :

ADDITIVE : 1.00 % wt DBDS
APPLIED LOAD : 130 KG
TEST TIME : STANDARD ONE MINUTE

a) General view of the scar (Mag. X 1)
b) Micrograph of the worn surface (Mag. X 2000)
c) Iron X-ray image
d) Sulphur X-ray image

(b) / Sliding direction

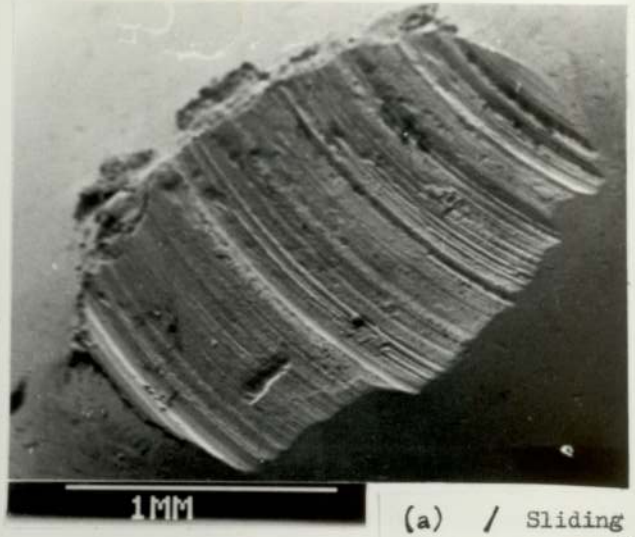

(a) / Sliding direction

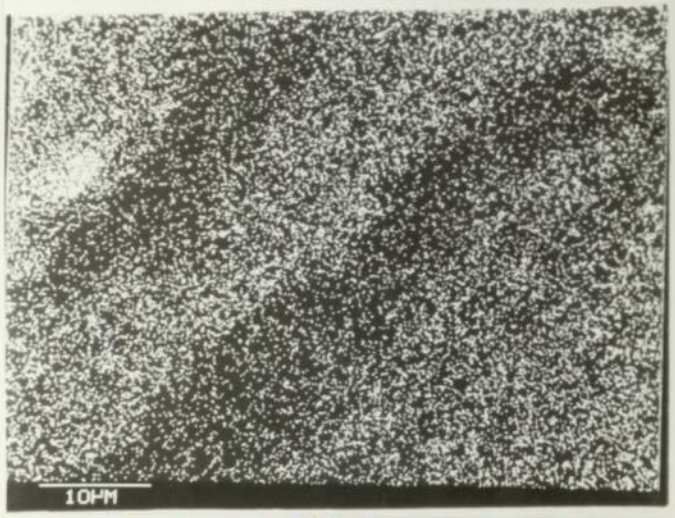

(c)

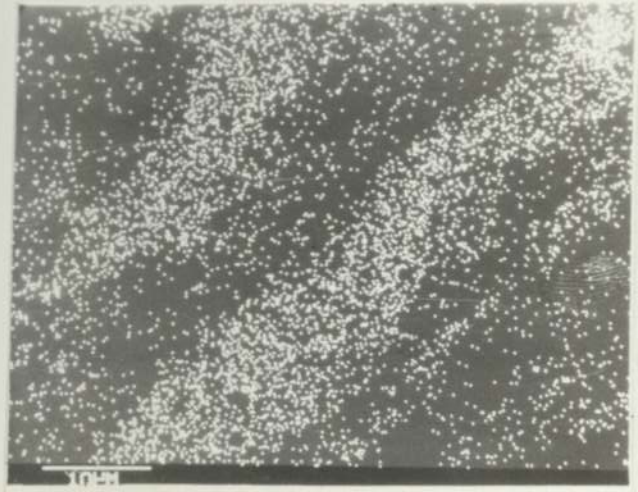

(d)

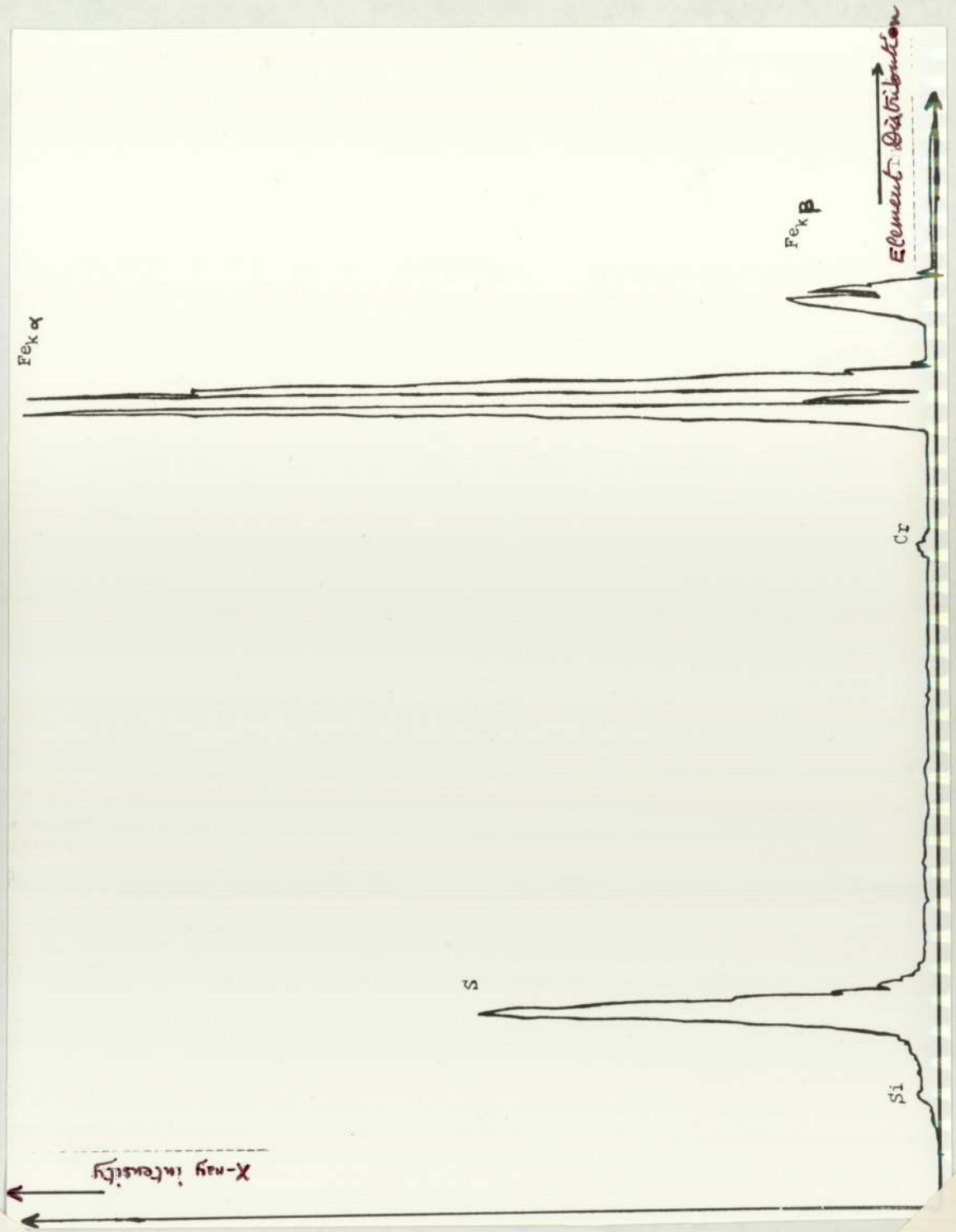

FIG. 4.15 X-RAY CHART OF AN E.P. REGION

ADDITIVE : 1.00 % wt DBDS

APPLIED LOAD : 130 KG

TEST TIME : STANDARD ONE MINUTE

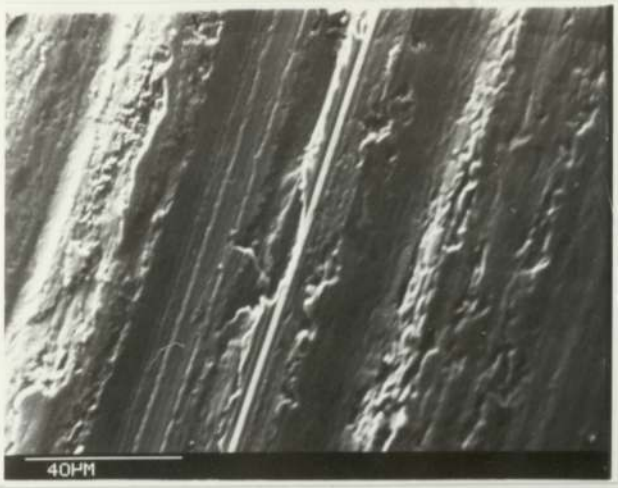

a) Micrograph of the worn surface (Magn. X 500).

Sliding direction

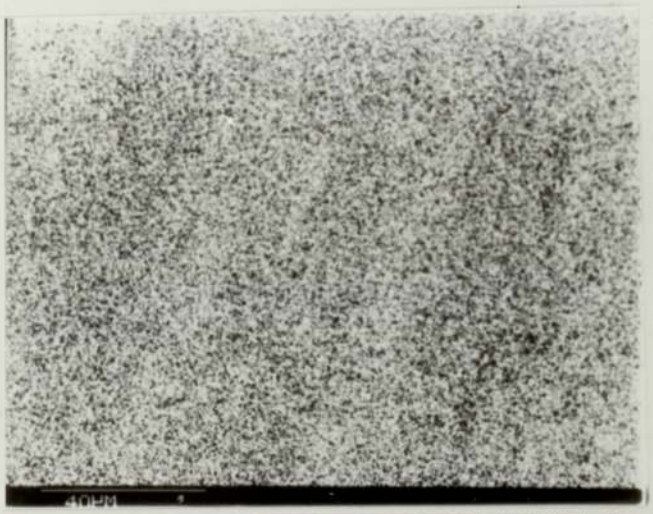

b) Iron X-ray image.

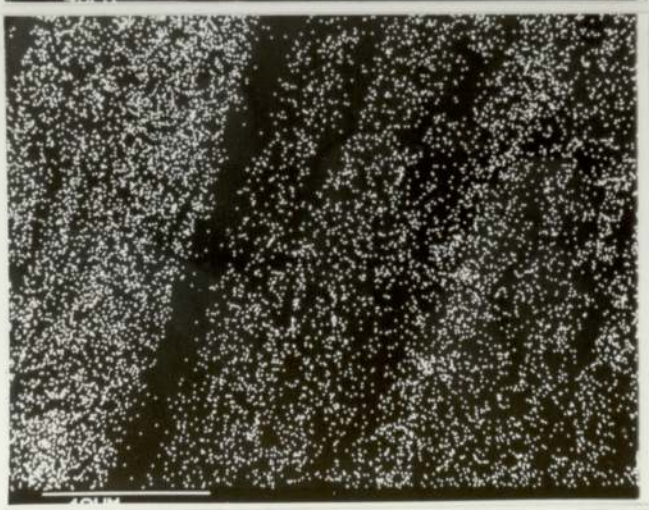

c) Sulphur X-ray image.

40μm

FIG. 4.16 ELECTRON PICTURE AND X-RAY IMAGE DISTRIBUTIONS OF THE E.P. REGION FOR THE FOLLOWING SAMPLE :

ADDITIVE : 0.88 % wt DPDS

APPLIED LOAD : 130 KG

TEST TIME : 1100 SECONDS

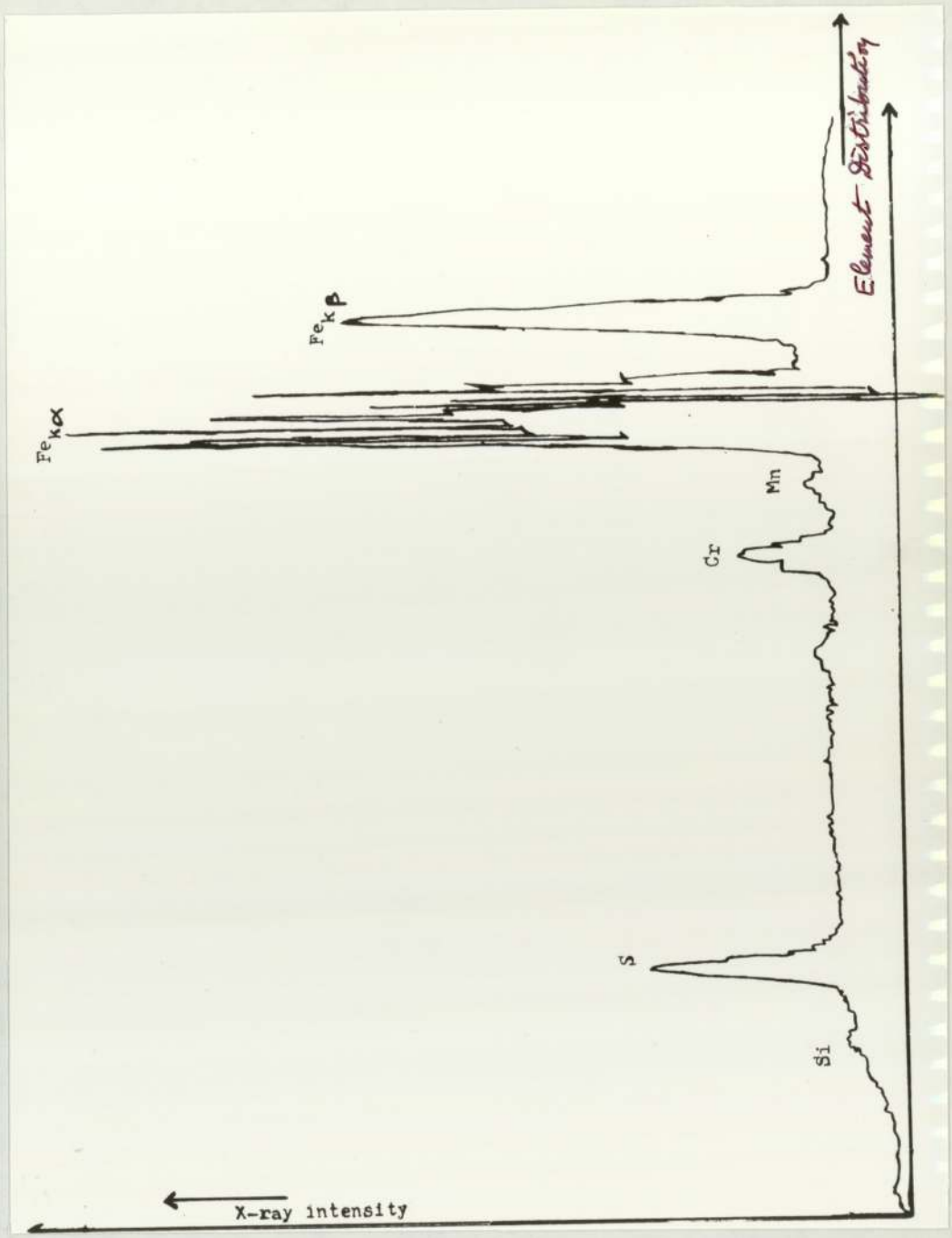

FIG. 4.17 X-RAY CHART OF AN E.P. REGION

ADDITIVE : 0.88 % wt DPDS

APPLIED LOAD : 130 KG

TEST TIME : 1100 SECONDS

a) Micrograph of the worn surface (Magn. X 500).

Sliding direction

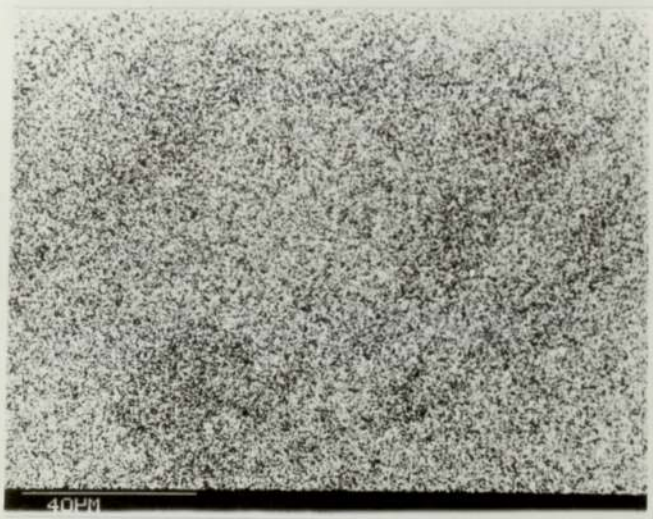

b) Iron X-ray image.

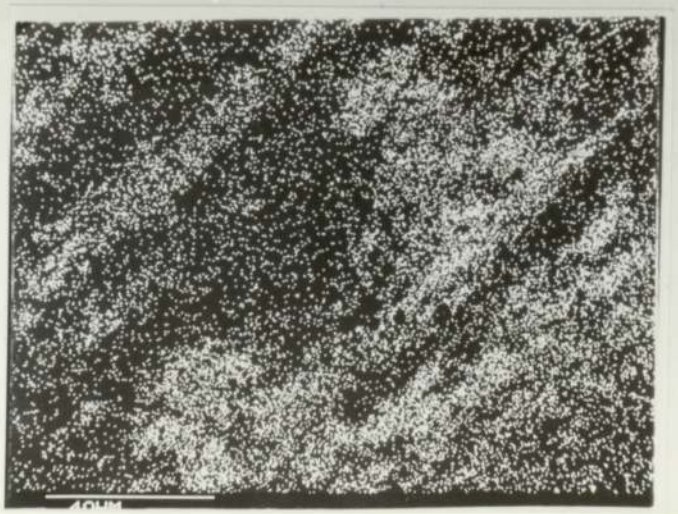

c) Sulphur X-ray image.

FIG. 4.18 ELECTRON PICTURE AND X-RAY IMAGE DISTRIBUTIONS OF THE E.P. REGION FOR THE FOLLOWING SAMPLE :

ADDITIVE : 1.74 % wt DBMS
APPLIED LOAD : 130 KG
TEST TIME : 1100 SECONDS

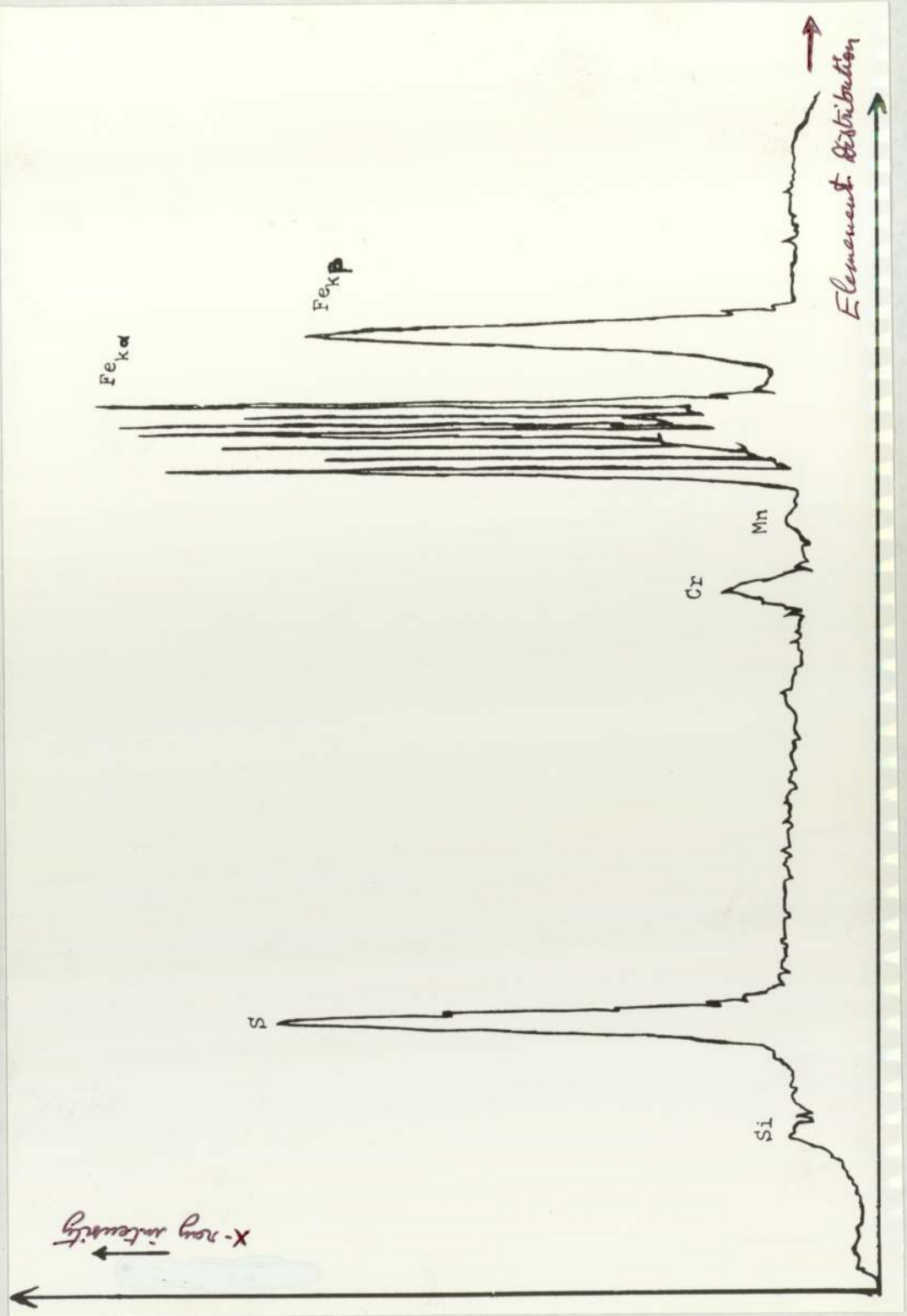

FIG. 4.19 X-RAY CHART OF AN E.P. REGION

ADDITIVE : 1.74 % wt DBMS

APPLIED LOAD : 130 KG

TEST TIME : 1100 SECONDS

4.2 Analysis using E.P.M.A.

An Electron Probe Microanalysis (E.P.M.A.) was employed for determining the sulphur and iron content of some selected wear scars. For each worn surface, the analysis was carried out over several small areas, then the average value of the concentration for each element was estimated. At the end, taking into consideration the effects from the mass atomic number, the absorption and the fluorescence, the corrected concentration for each element was obtained by using a computer programme.

Table 4.1 displays the results of the examination of scars formed at various loads and at different running times when 0.25% wt elemental sulphur was used as the additive. The first observation made from these results are as expected when engaging the standard one minute tests, the sulphur amount increases with the increase of the applied load whilst the iron amount decreases. In the a.w. region, the sulphur content is very low (0.10% - 0.14%). This demonstrates the lack of reactivity between the additives and the metal asperities in order to form a protective film for reducing the intermetallic contact. Thus this could explain the initial seizure phenomenon which happens at very low load (cf. Table 3.1 and Figure 3.2).

The results found in the case of examining films formed with 1.00% wt DBDS as the additive, are shown in Table 4.2. The increasing of the sulphur concentration with the applied load is still observed. Furthermore, it is worth noting that at the vicinity of the welding point, and although DBDS presents a very high e.p. load range, the amount of sulphur is found to be similar to the one connected to the elemental sulphur additive.

Load (kg)	Test Time (s)	S (% wt)	Fe (% wt)	Other Elements (oxides etc.) (% wt)	Remarks
40	60	0.10	96.84	3.06	—
←repeat→		0.14	95.03	4.83	Another Analysis
130	60	10.71	86.58	2.71	—
130	1100	2.96	88.70	8.34	—
←repeat→		7.46	49.43	43.11	Another Analysis
130	1400	19.63	71.07	9.30	—
200	60	17.31	74.32	8.37	—
300	60	19.89	81.92	-1.81(?)	Total of F_e and S >100?
←repeat→		13.53	75.82	10.65	Another Analysis
300	300	22.50	70.67	6.83	—

Table 4.1: Results of the E.P.M.A. examination of selected specimens when elemental sulphur was used as the additive.

Percentage of DBDS	Load (kg)	Test Time (s)	S (% wt)	Fe (% wt)	Other Elements (oxides etc...) (% wt)	Remarks
1.00% wt	130	60	3.61	90.70	5.69	—
	130	1100	7.30	87.80	4.90	—
	140	60	9.97	89.50	0.53	—
	200	60	20.58	74.19	5.23	—
	300	60	10.06	72.63	17.31	—
	← repeat →		17.09	72.40	10.51	Another Analysis
	400	60	13.60	91.40	-5.00(?)	Total of Fe and S > 100
	← repeat →		15.41	76.11	8.48	—
	2nd repeat →		18.36	68.27	13.37	—
	720	weld (starting)	15.34	41.33	43.34	Roller + Weld debris
	870	weld (very high)	1.14	95.17	3.69	
0.26% wt	130	60	3.60	88.70	7.70	
	130	1100	3.60	95.50	0.90	

Table 4.2: Results of the E.P.M.A. examination of selected specimens when DBDS was used as the additive.

The standard one minute test and the extended test (just before welding) were carried out on all the additives in order to compare the mass composition of the main elements, (ie sulphur and iron), present in the films formed during the e.p. regime. The results obtained are summarised in Table 4.3, in which are also included the ones obtained for some reference samples. This indicates that the time has an influence on the rate of the reaction according to the environment of the sulphur in the molecule additive. For the standard test, additive with a free sulphur atom reacts faster, by forming a sulphide layer, than those where the sulphur atom is attached to a group of atoms. As the test time increases towards reached the value corresponding to the equilibrium temperature, DBDS and elemental sulphur additives present the same amount of sulphur and iron. This confirms the suggestion put forward in the previous chapter concerning the same behaviour manifested by these two additives when used under e.p. conditions. The low rate of reaction shown by DPDS and DBMS does not favour the formation of the sulphide protective film. This explains their low e.p. performance already mentioned previously.

4.3 Summarizing Remarks

The interpretation of the S.E.M. results obtained for all the four additives leads to the following conclusion:

- There is a distinct difference between the formation of the a.w. and e.p. films.

- The film formed under a.w. regime is smooth and composed of fine tracks mainly formed by sulphur and iron adjacent to each other.

Additive	Load (kg)	Test Time (s)	S (% wt)	Fe (% wt)	Ag (% wt)	Other Elements (oxides etc.) (% wt)	Remarks
0.25% wt Elemental Sulphur	130	60	10.71	86.58	–	2.71	
	130	1100	2.96	88.70	–	8.34	
	← repeat →		7.46	49.43	–	43.11	Good Values
	130	1400	19.63	71.07	—	9.30	
1.00% wt DBDS	130	60	3.61	90.70	–	5.69	
	130	1100	7.30	87.80	—	4.90	
0.26% wt DEDS	130	60	3.60	88.70	—	7.70	
	130	1100	3.60	95.50	—	0.90	
0.88% wt DPDS	130	60	5.32	71.13	—	23.55	
	130	1100	5.78	22.09	—	72.13	
0.26% wt DPDS	130	60	4.10	91.96	—	3.94	
	← repeat →		5.96	90.60	—	3.44	2nd Analysis
	130	1100	3.26	84.20	—	12.54	
	200 welding (≃10 s)		0.48	85.95	—	13.57	
1.74% wt DBMS	130	1100	6.11	54.46	—	39.43	
1 Medium film of $FeSO_4$	Reference samples only		14.00	56.00	—	30.00	
2 Thick film of $FeSO_4$			24.16	28.06	—	47.78	
3 Thin film of S on Ag			6.25	—	87.00	6.75	
4 Medium film of S on Ag			13.70	—	80.00	6.30	
5 Pure standard FeS_2			not measured	47.31	—	52.69	

Table 4.3: Results of the E.P.M.A. examination of some selected e.p. specimens and some reference samples.

- Under e.p. regime, the film formation is irregular. The worn surfaces is composed by scattered "lumps" of material, (ie in the case of sulphur and DBDS additives), or by a number of craters (as in the case of DPDS and DBMS). The presence of sulphur located near to the iron suggests the formation of "islands" and craters on the surface depending on the additive.

The E.P.M.A. data could be used as a "gauge" for explaining the mechanism of the formation of the film. The very low percentage of the sulphur obtained in the a.w. region indicates that the film must be thin and this is the consequence of the very slow reaction between the additive and the metal asperities. For the elemental sulphur and DBDS additives, the results show that a fast chemical reaction is taking place between the additive and the surface metals. This explains the presence of "islands" made from a mixture of iron and sulphur. In the case of DPDS and DBMS, the slow rate of reaction gives rise to a very thin protective sulphide film and as the pressure gets higher, this accentuates the breakdown of the protective film very easily, which, in turn favours the destruction and the removal of the material in contact. Thus this could be the answer of the presence of the craters and the low e.p. performance displayed by both additives.

CHAPTER FIVE

ANALYSIS OF THE WORN SURFACES BY MEANS OF HIGH ENERGY CHARGED PARTICLES

The need for additional information about the composition of the films formed by organo-sulphur additives during wear tests using the four-ball machine has stimulated the search for new analytical methods capable of identifying and measuring the amount of sulphur in the surface layers constituting these films. One possible technique is the nuclear microprobe. In this investigation, only two high energy charged particle reactions were found to be suitable for the aim of the work. These were (i) charged particle stripping reactions using deuterons [(d,p) reactions], with the sensitivity of the technique being shown to be such that it was suitable for the identification of sulphur in thin films, and (ii) Rutherford Backscattering (R.B.S.), using 2 MeV alpha particles which had the complementary advantage of providing mass and depth analysis of surface constituents.

5.1 Results from (d,p) reactions

For a uniform film of pure sulphur deposited on a substrate of pure silver, the typical spectrum from the reaction $s^{32}(d,p)S^{33}$ would appear as in Figure 5.1. To provide reference samples, three uniform films (thin, medium and thick) of pure sulphur deposited on pure silver were studied, and the resulting spectra are shown in Figures 5.2, 5.3 and 5.4 respectively. Also, three calibration specimens consisting of thin, medium and thick films of $FeSO_4$ were prepared by reacting one of the base of a clean unworn roller bearing into a solution of sulphuric acid for a time of 0.5, 1 and 5 minutes respectively. As it can be seen from the spectra obtained for these

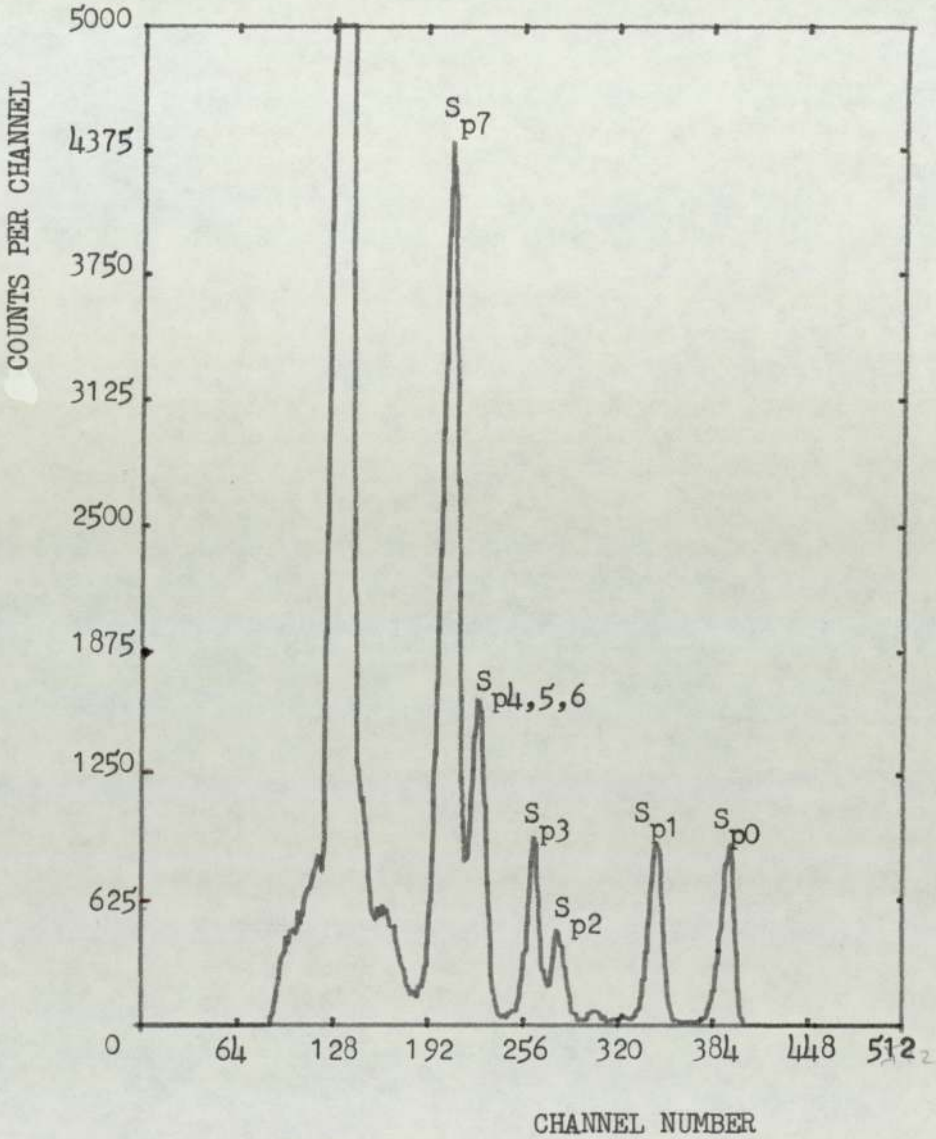

FIG. 5.1 TYPICAL PROTON SPECTRUM FROM THE (D,P) REACTION ON S^{32}.

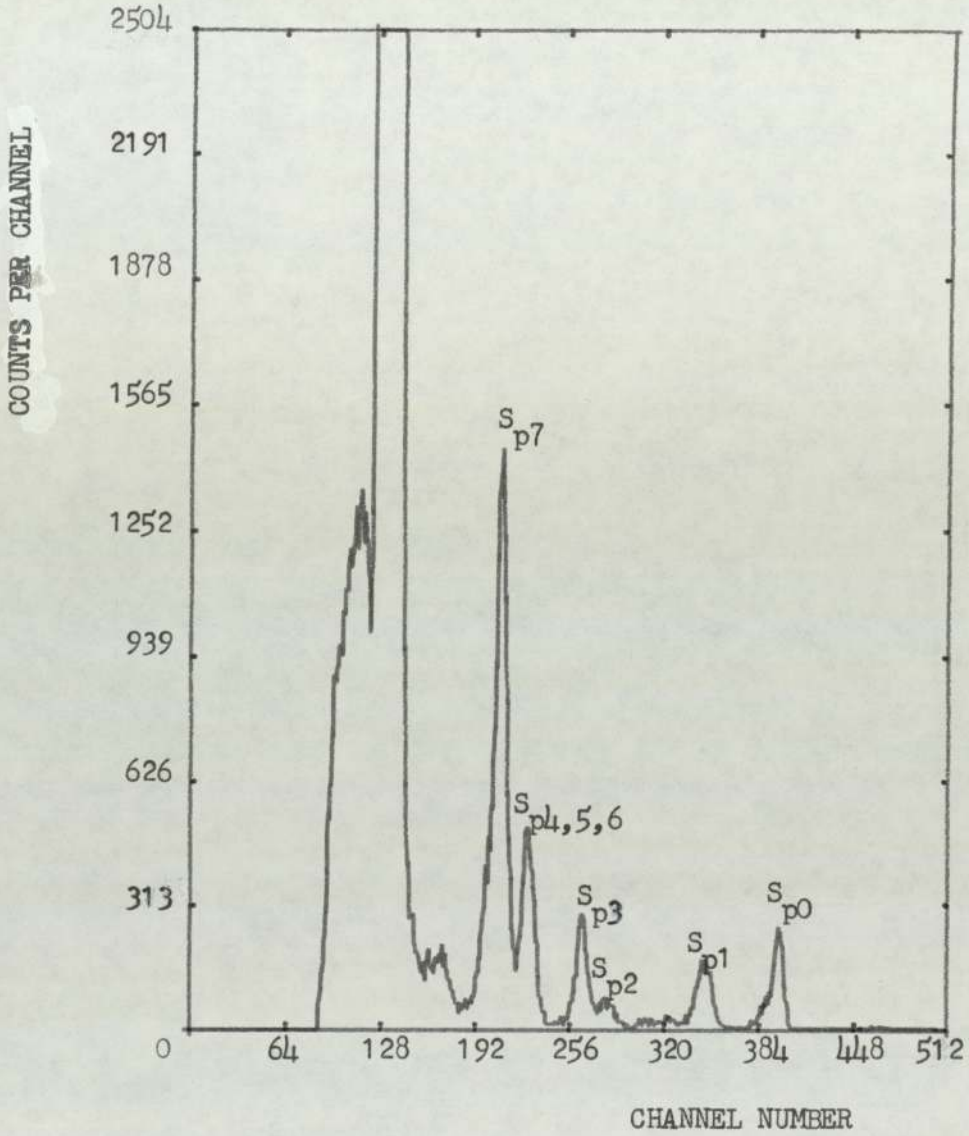

FIG. 5.2 PROTON SPECTRUM OBTAINED BY BOMBARDING A THIN LAYER OF SULPHUR ON SILVER SUBSTRATE WITH A 2 MeV DEUTERON BEAM. (SAMPLE : "REFERENCE THIN LAYER").

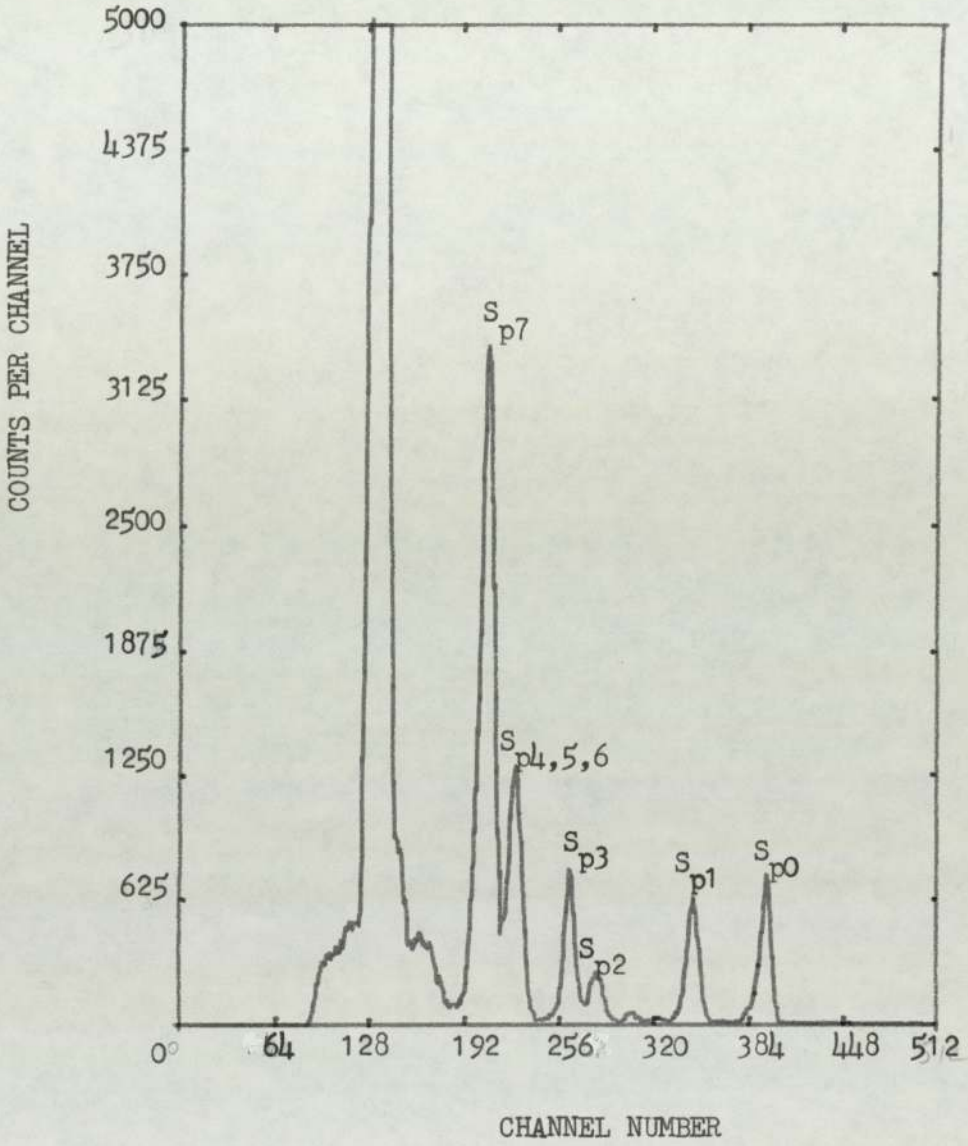

FIG. 5.3 PROTON SPECTRUM OBTAINED BY BOMBARDING A MEDIUM LAYER OF SULPHUR ON SILVER SUBSTRATE WITH A 2 MeV DEUTERON BEAM : (SAMPLE : "REFERENCE MEDIUM LAYER").

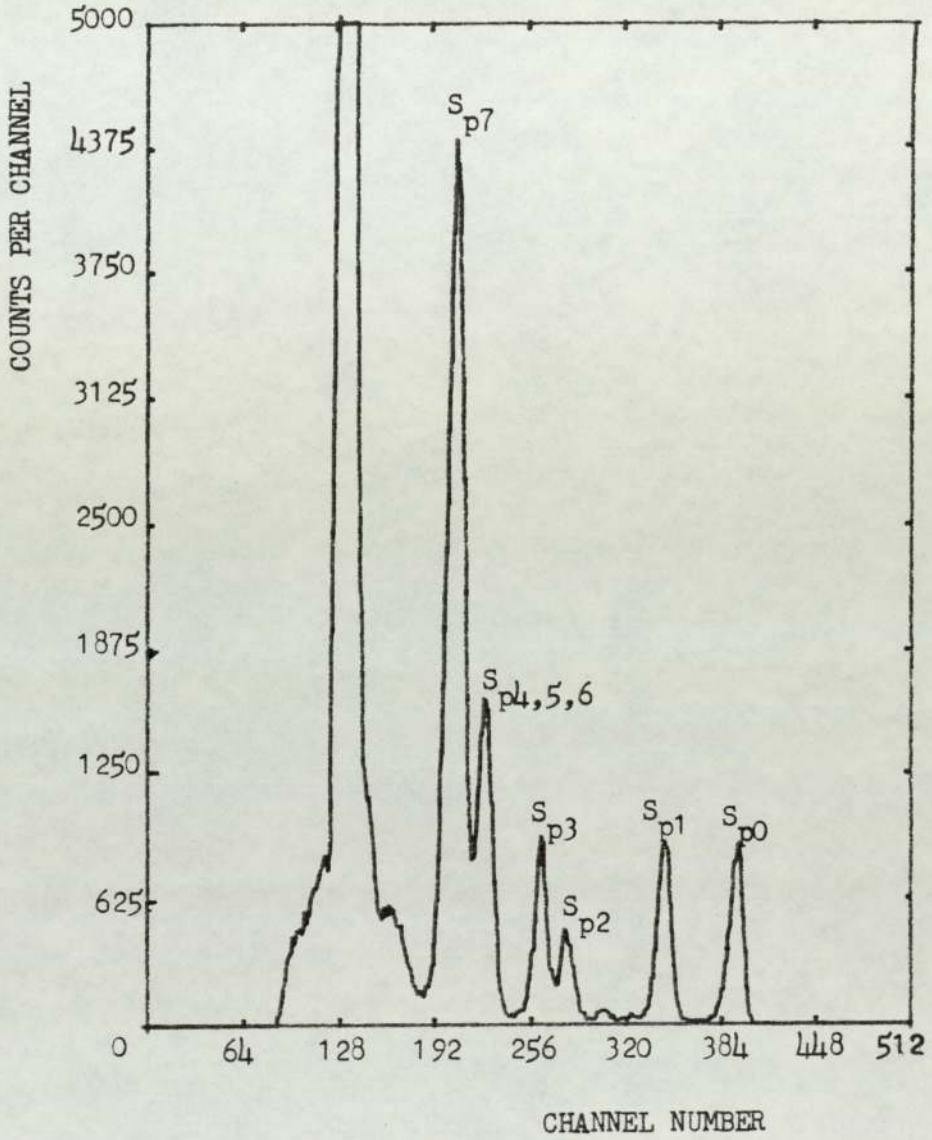

FIG. 5.4 PROTON SPECTRUM OBTAINED BY BOMBARDING A THICK LAYER OF SULPHUR ON SILVER SUBSTRATE WITH A 2 MeV DEUTERON BEAM (SAMPLE : "REFERENCE THICK LAYER").

calibration specimens (Figures 5.5, 5.6 and 5.7), the sulphur peaks appear clearly on their own for the case of the medium and thick films of $FeSO_4$, whilst for the thin film (Figure 5.5), silicon peaks appear alongside with the sulphur peaks. This means that the sulphur layer must be very thin to allow the silicon from the substrate surface to be detected. The spectrum from an unworn roller bearing (Figure 5.8), which shows only the presence of silicon peaks, confirms the absence of sulphur layer and, also, indicates that the silicon detected is part of the original material. As an indication, a typical spectrum of a pure silicon is shown in Figure 5.9.

For the analytical purpose which will follow throughout the (d,p) experiments, the reaction yield, $Y_p(\theta)$, for the detected sulphur, was obtained by taking the proton counts of the proton groups P_0 and P_7. These proton groups were selected because they are characteristic of the reaction S^{32} (d,p) S^{33}. The net count-rate of each group was provided by summing all the counts belonging to the area under the peak of interest and substracting the count-rate of the relevant background. Then the number of sulphur atoms per square centimetre of surface for each peak [ie $(N \triangle x)_p$] was calculated by using equation (2.8) (cf. Chapter 2 section 8). Theoretically, the value of $(N \triangle x)_p$ must be the same for each group of protons pertaining to the same atom. But, in most practical cases, there will be some variations and this is due to the presence of proton groups from other elements (eg. carbon contaminant from the vacuum and silicon from the substrate). As a result of this, the number of sulphur atoms per square centimetre $(N \triangle x)$ for each analysis was found by taking the average between the value calculated for the groups P_o [ie $(N \triangle x)P_o$] and the groups P_7 [ie $(N \triangle x)P_7$].

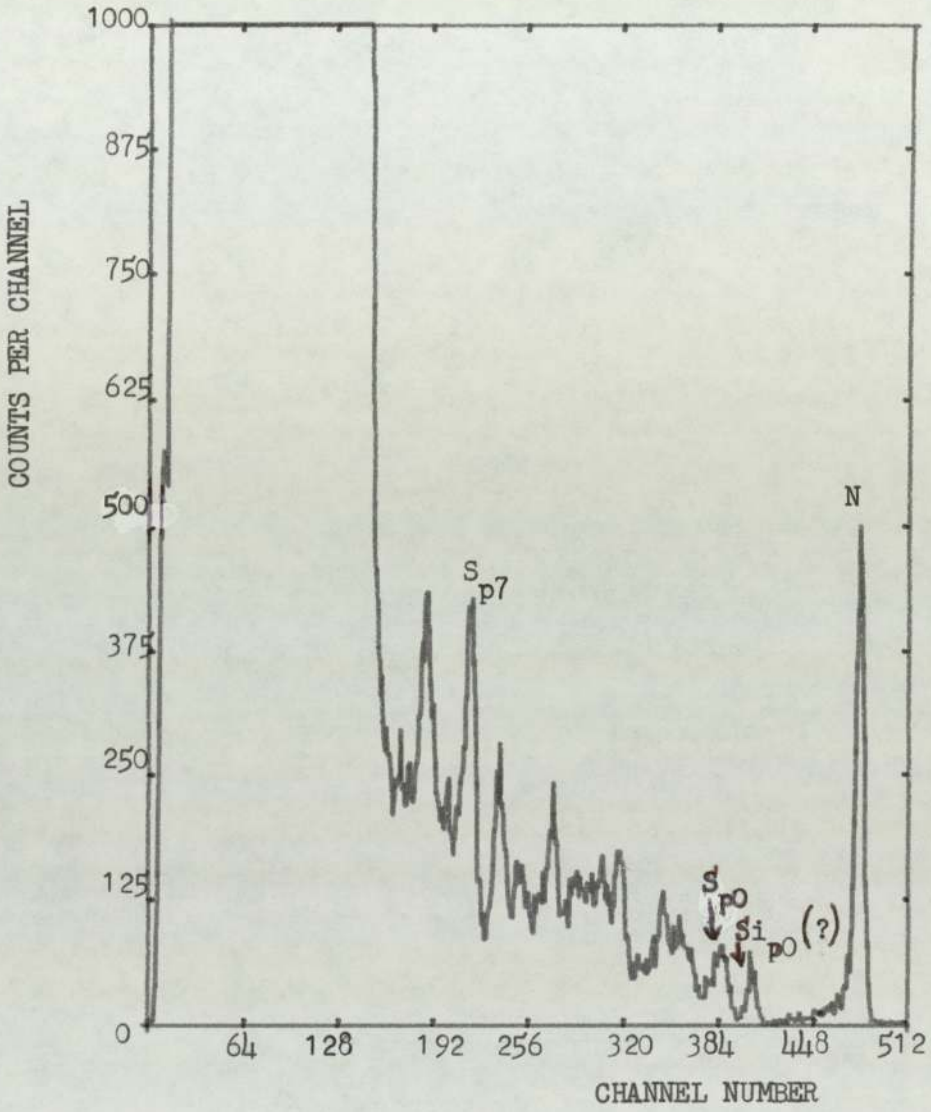

FIG. 5.5 REACTION YIELD SPECTRUM INDUCED BY DEUTERON BEAM PROBING ON A THIN FILM OF $FeSO_4$ DEPOSITED ON A ROLLER BEARING (CALIBRATION SPECIMEN).

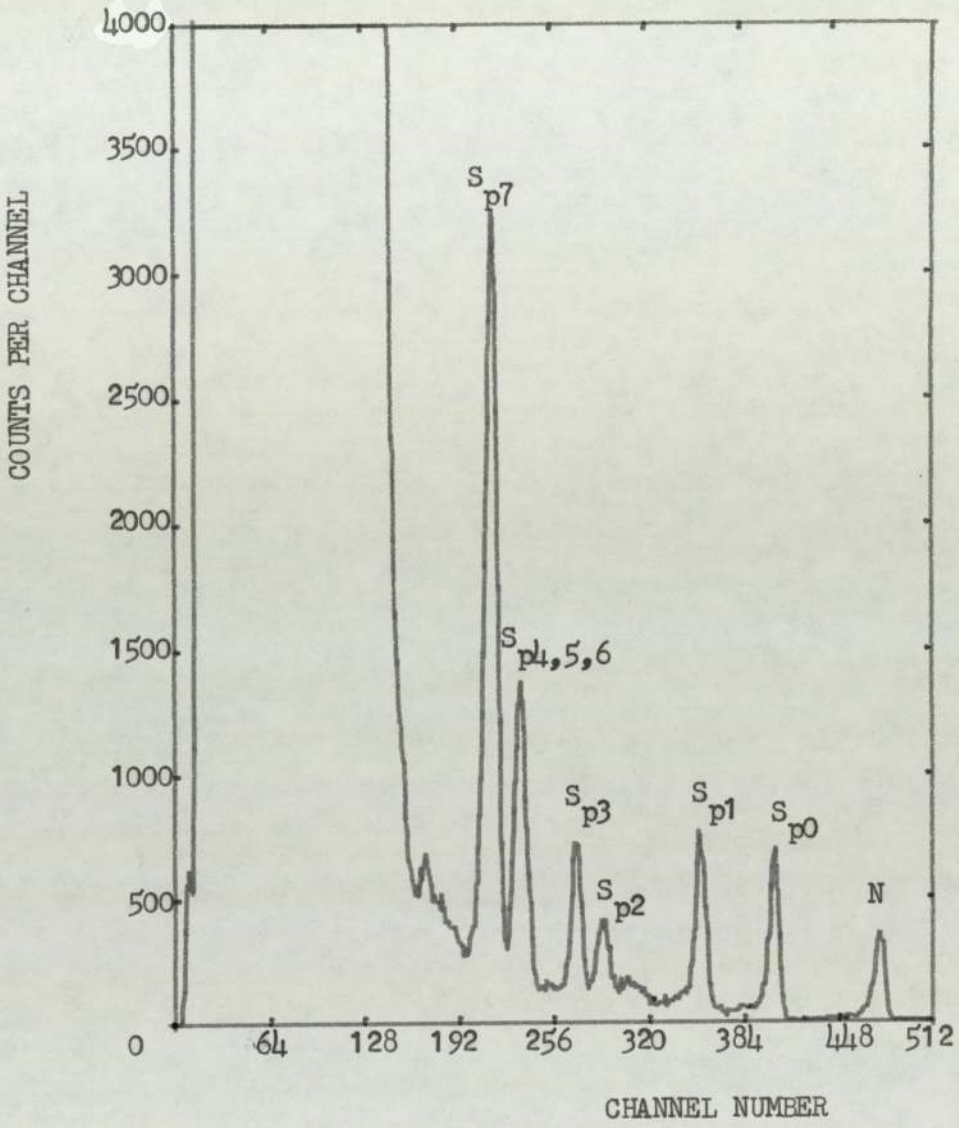

FIG. 5.6 -REACTION YIELD SPECTRUM INDUCED BY DEUTERON PROBING ON A MEDIUM FILM OF $FeSO_4$ DEPOSITED ON A ROLLER BEARING (CALIBRATION SPECIMEN).

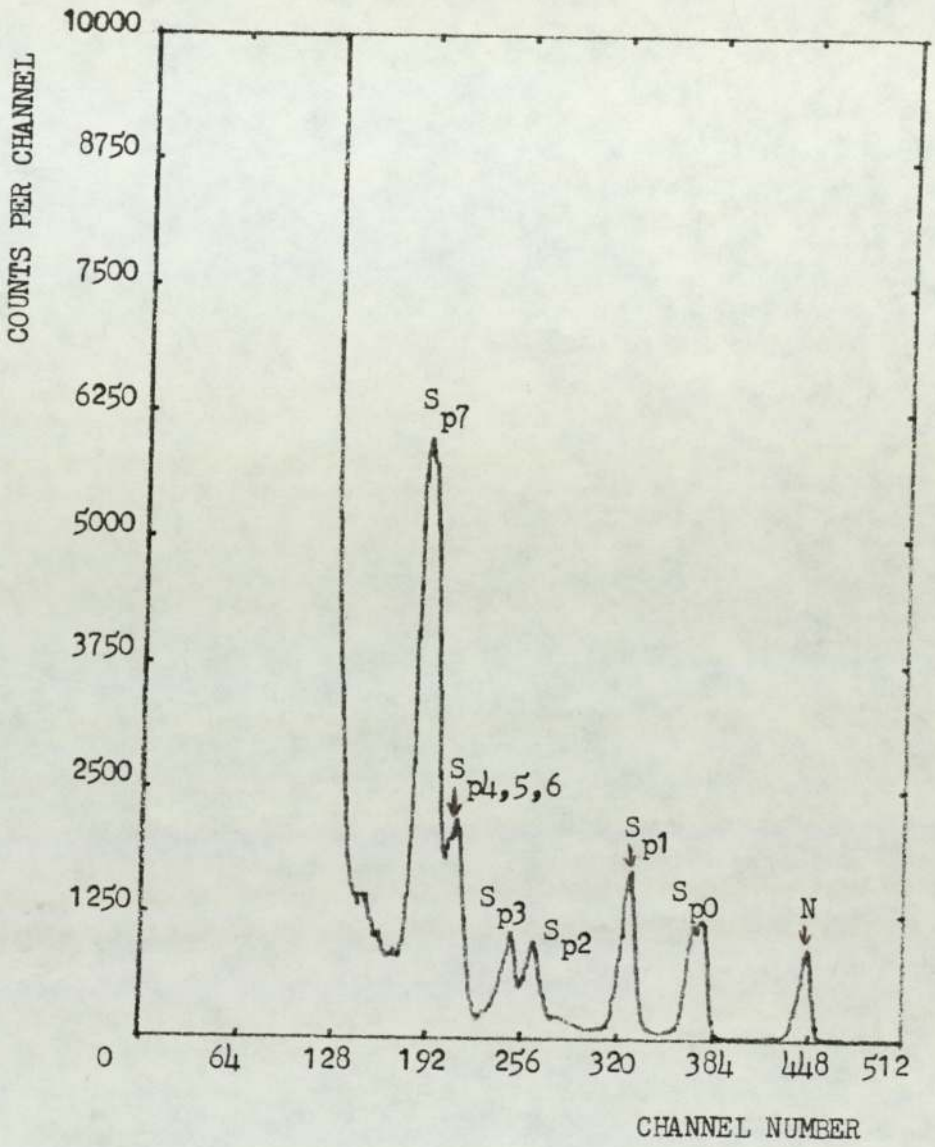

FIG. 5.7 REACTION YIELD SPECTRUM INDUCED BY DEUTERON BEAM PROBING ON A THICK FILM OF $FeSO_4$ DEPOSITED ON A ROLLER BEARING (CALIBRATION SPECIMEN).

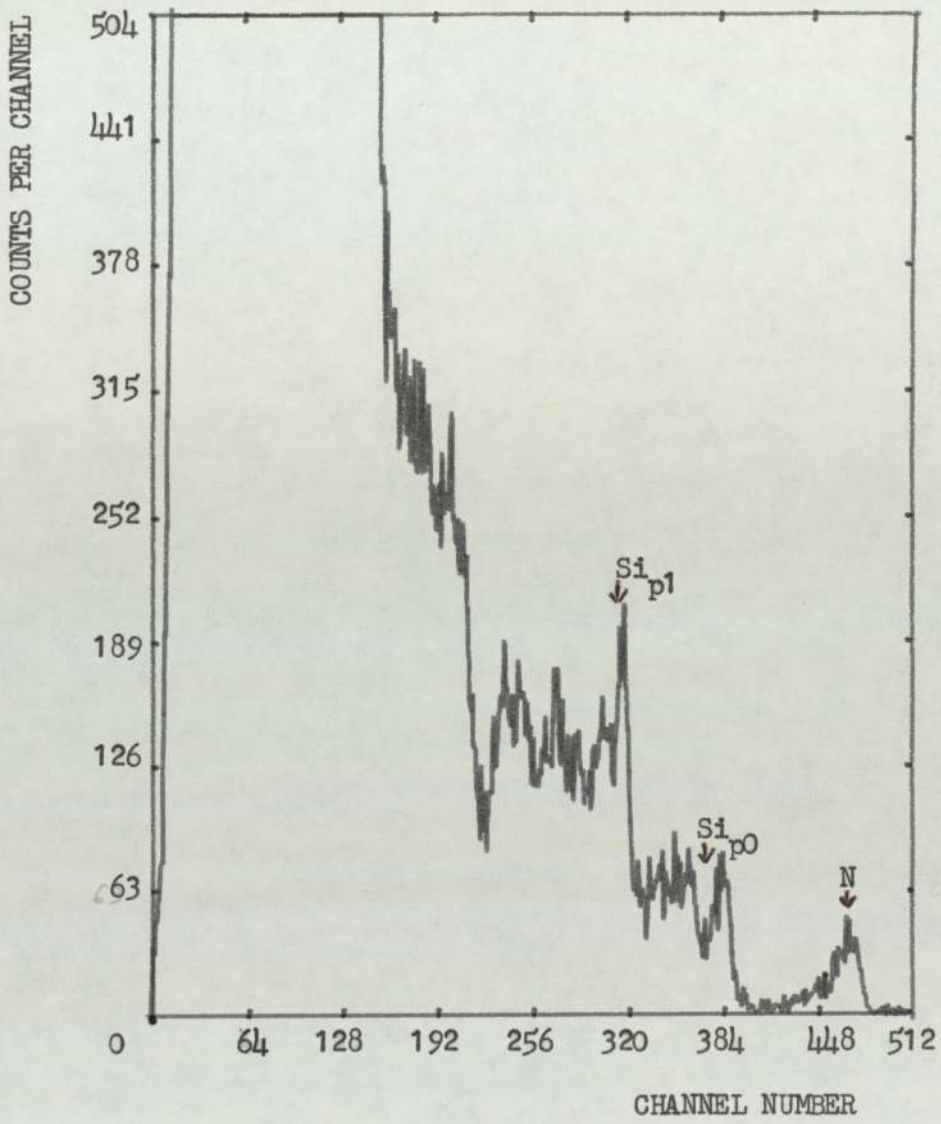

FIG. 5.8 REACTION YIELD SPECTRUM OBTAINED BY BOMBARDING AN UNWORN EN 31 SAMPLE WITH 2 MeV DEUTERON BEAM.

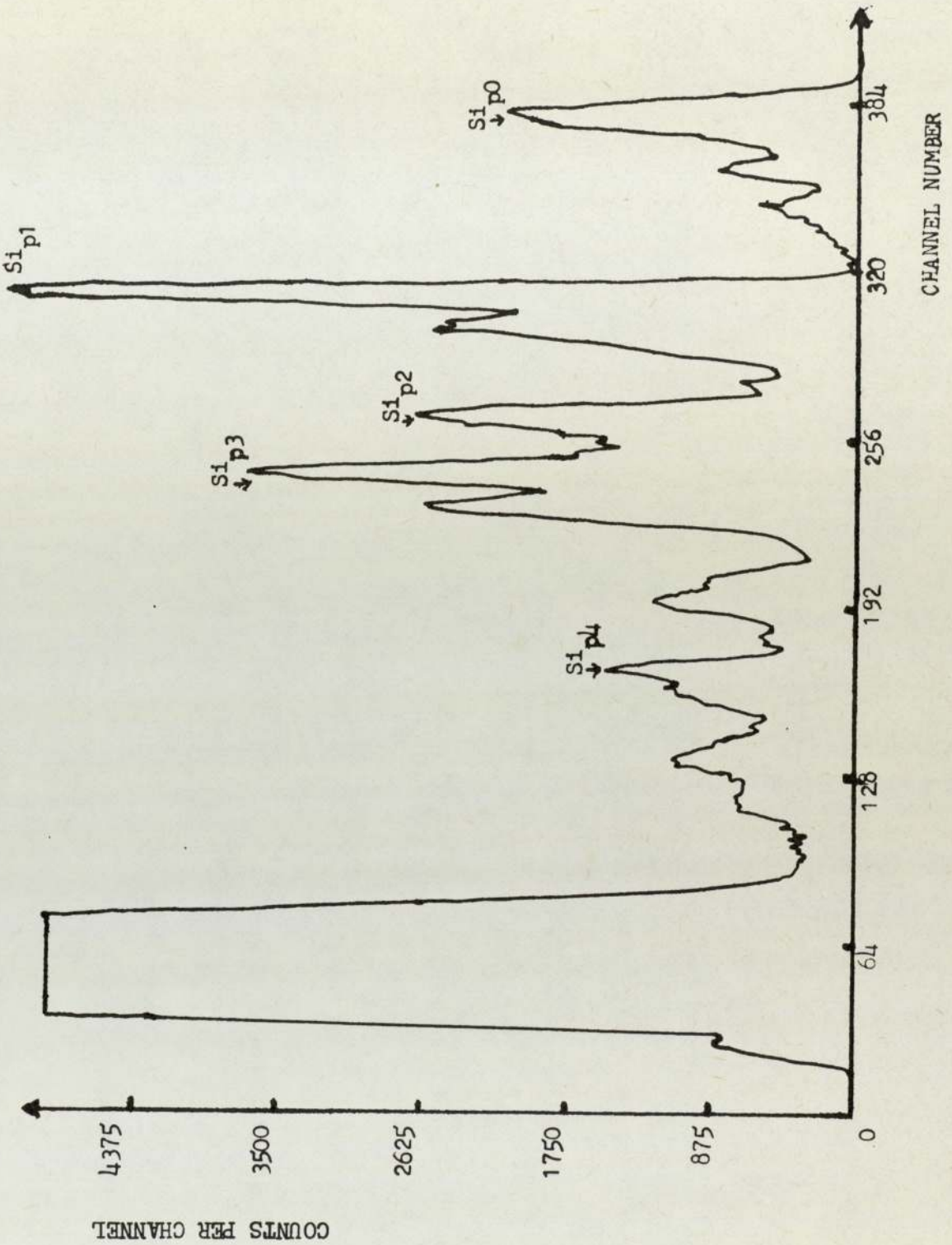

FIG. 5.9 TYPICAL SPECTRUM FROM THE (D,P) REACTION OBTAINED FOR A PURE SILICON (DEUTERON ENERGY : 2 MeV).

The results obtained for the reference and the calibration specimens, and also for the unworn EN31 sample, are presented in Table 5.1.

5.1.1 Anti-Wear Film Analysis

Wear scars formed under the a.w. regime by the use of the four additives, namely elemental sulphur, DPDS, DBDS and DBMS, were examined by means of the deuteron-proton stripping reaction technique. The results show that the utilisation of the S^{32} (d,p) S^{33} reaction to detect the sulphur generated in the wear films formed under the a.w. conditions was unsatisfactory. Silicon was the main element detected as it can be seen in Figure 5.10, which represents one of the typical spectrum obtained from the analysis of these films. Since the silicon spectrum seems to be characteristic of the unworn metal, this means that the a.w. films are too thin to be detected by the deuteron-proton stripping reaction technique.

5.1.2 Extreme-Pressure Film Analysis

For the investigation of the films formed when 0.25% wt elemental sulphur was used as the additive, the same samples analysed previously by the E.P.M.A. (cf. Table 4.1), were scanned with the 2 MeV deuteron beam. The spectra of the reactions induced by the deuteron beam for these e.p. films are shown from Figure 5.11 to Figure 5.15, whilst the reaction yield and the average value of the sulphur atoms per square centimetre obtained for these samples are displayed in Table 5.2. The spectra indicate that, for the standard wear test, the probability of detecting sulphur gets higher with the increase of the

Samples	Reaction yield, Y_p (ie count number)		$(N \triangle x)_p$ for Proton Group (S atoms.cm^{-2})		Average $(N \triangle x)$ (S atoms.cm^{-2})
	P_7	P_0	P_7	P_0	
Thin film of S on Ag	12934.00	2247.26	$5.06\ 10^{17}$	$4.79\ 10^{17}$	$4.93\ 10^{17}$
Medium film of S on Ag	32051.60	6396.08	$1.25\ 10^{18}$	$1.36\ 10^{18}$	$1.31\ 10^{18}$
Thick film of S on Ag	45737.40	9322.07	$1.79\ 10^{18}$	$1.99\ 10^{18}$	$1.89\ 10^{18}$
Thin film of $FeSO_4$	2337.61	477.38	$1.37\ 10^{17}$	$1.53\ 10^{17}$	$1.45\ 10^{17}$
Medium film of $FeSO_4$	28501.50	4994.83	$1.67\ 10^{18}$	$1.60\ 10^{18}$	$1.64\ 10^{18}$
Thick film of $FeSO_4$	66436.20	17518.60	$2.60\ 10^{18}$	$3.74\ 10^{18}$	$3.17\ 10^{18}$
Unworn EN31 sample	← No Sulphur detected →				

Table 5.1: Results of the $S^{32}(d,p)S^{33}$ examination of the reference and calibration samples.

Load (kg)	Test Time (s)	Reaction yield, Y_p (ie. count number) for proton groups		$(N \triangle x)_p$ for Proton Groups (S atoms.cm^{-2})		Average $(N \triangle x)$ (S atoms.cm^{-2})
		P_7	P_0	P_7	P_0	
130	60	4464.03	285.63	$1.75\ 10^{17}$	$6.09\ 10^{16}$	$1.18\ 10^{17}$
130	1100	24295.30	2215.91	$1.43\ 10^{18}$	$7.09\ 10^{17}$	$1.07\ 10^{18}$
200	60	120018.00	7994.01	$4.69\ 10^{18}$	$1.71\ 10^{18}$	$3.20\ 10^{18}$
300	60	19927.10	3200.56	$7.79\ 10^{17}$	$6.83\ 10^{17}$	$7.31\ 10^{17}$
300	300	91056.10	9983.67	$3.56\ 10^{18}$	$2.13\ 10^{18}$	$2.85\ 10^{18}$

Table 5.2: Results of the $S^{32}(d,p)S^{33}$ examination obtained for the e.p. films when elemental sulphur was used as the additive.

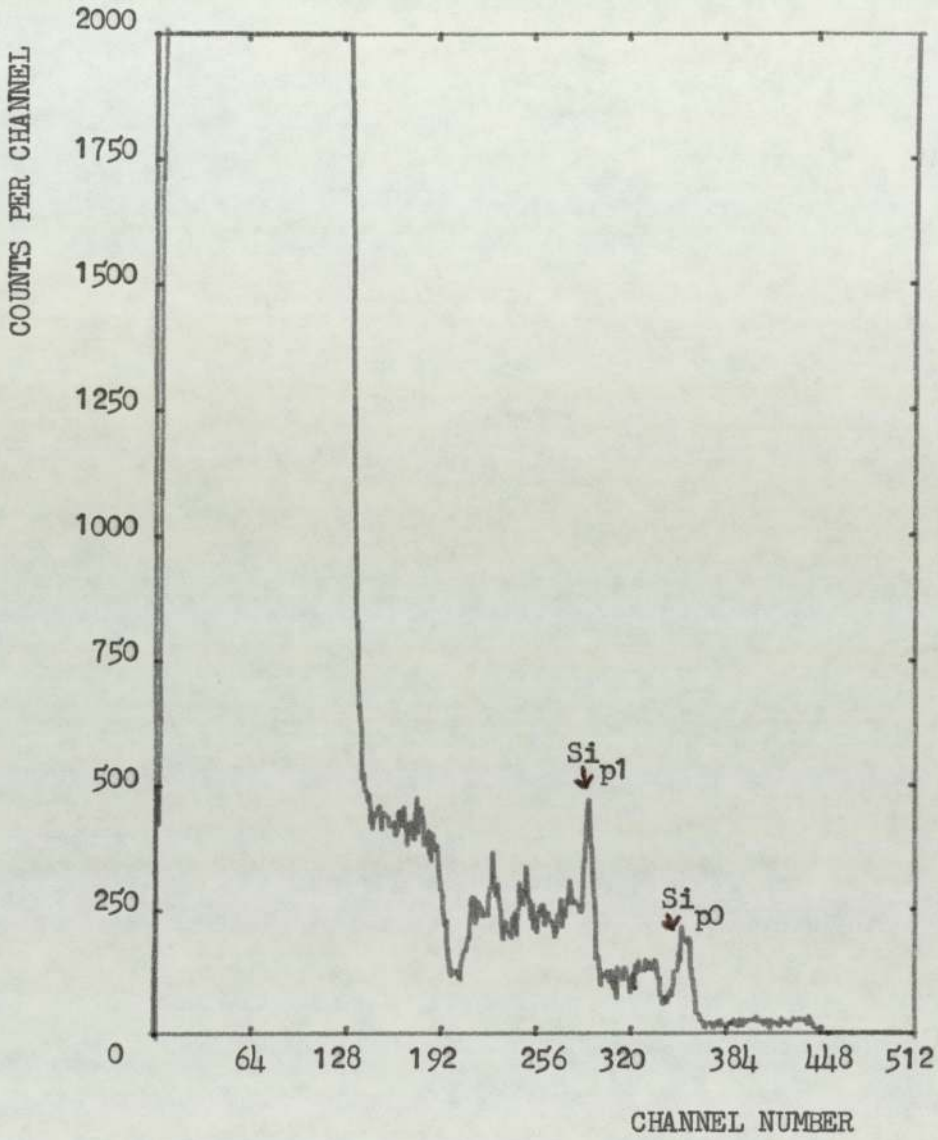

FIG. 5.10 TYPICAL SPECTRUM FROM (D,P) REACTION OBTAINED FOR A.W. FILMS.

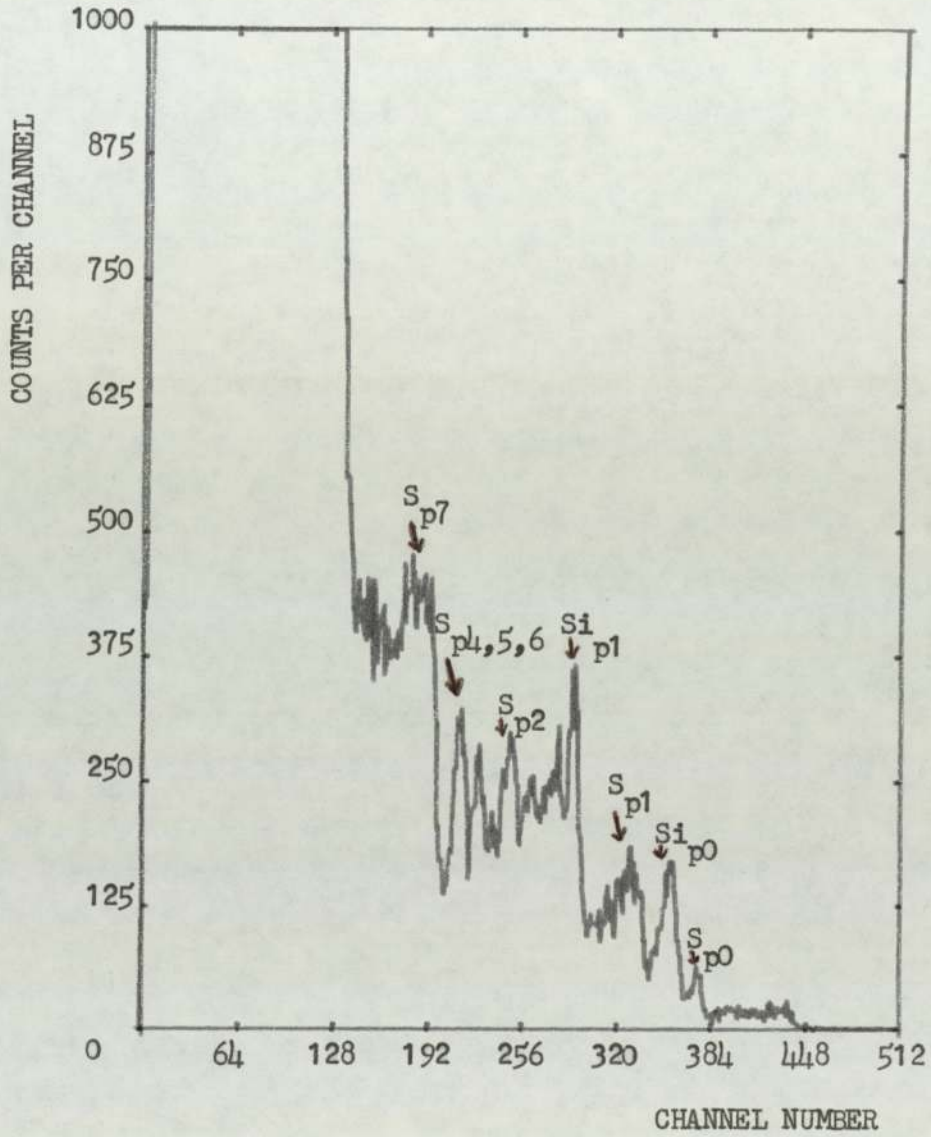

FIG. 5.11 REACTION YIELD SPECTRUM INDUCED BY DEUTERON BEAM PROBING ON AN E.P. FILM FROM THE FOLLOWING SAMPLE :

ADDITIVE : 0.25 % wt ELEMENTAL SULPHUR

APPLIED LOAD : 130 KG

TEST TIME : STANDARD ONE MINUTE

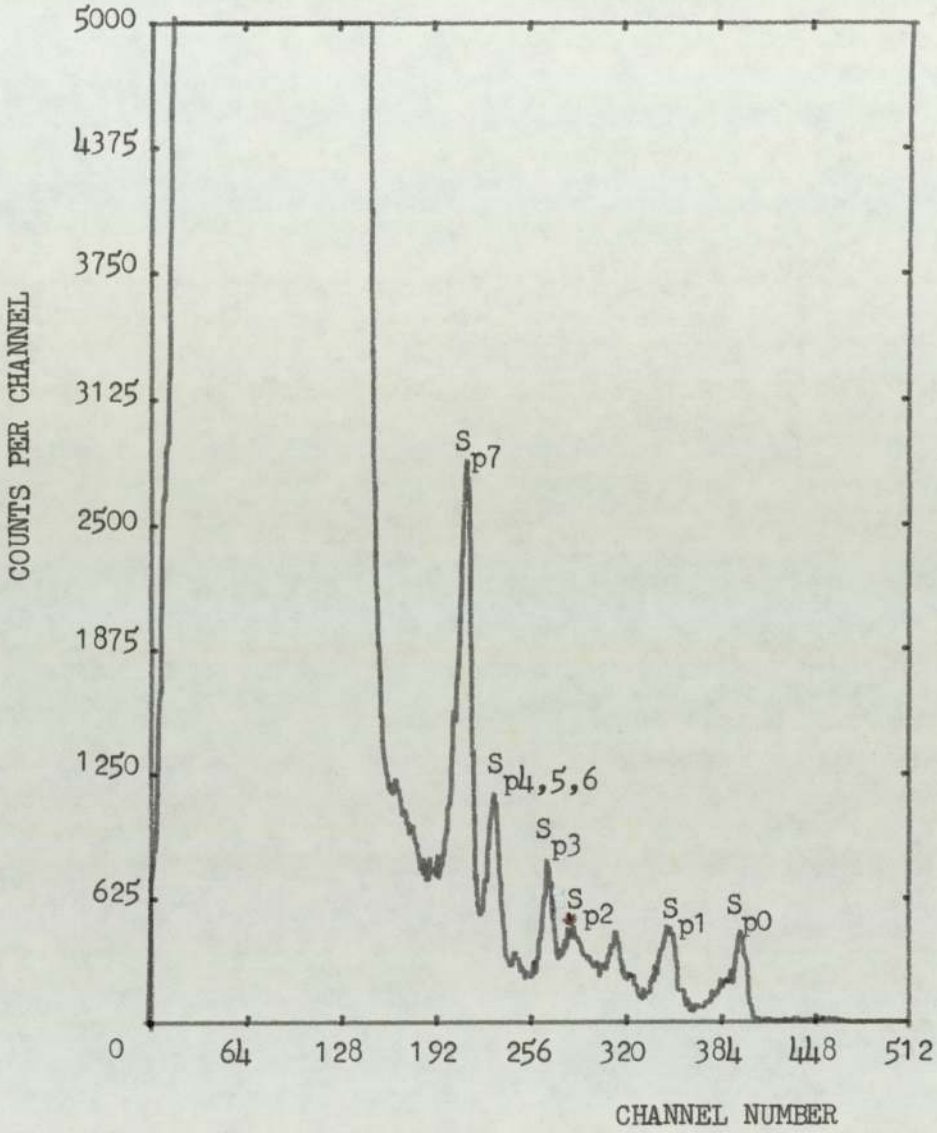

FIG. 5.12 REACTION YIELD SPECTRUM INDUCED BY DEUTERON BEAM PROBING ON AN E.P. FILM FROM THE FOLLOWING SAMPLE :

ADDITIVE : 0.25 % wt ELEMENTAL SULPHUR

APPLIED LOAD : 130 KG

TEST TIME : 1100 SECONDS

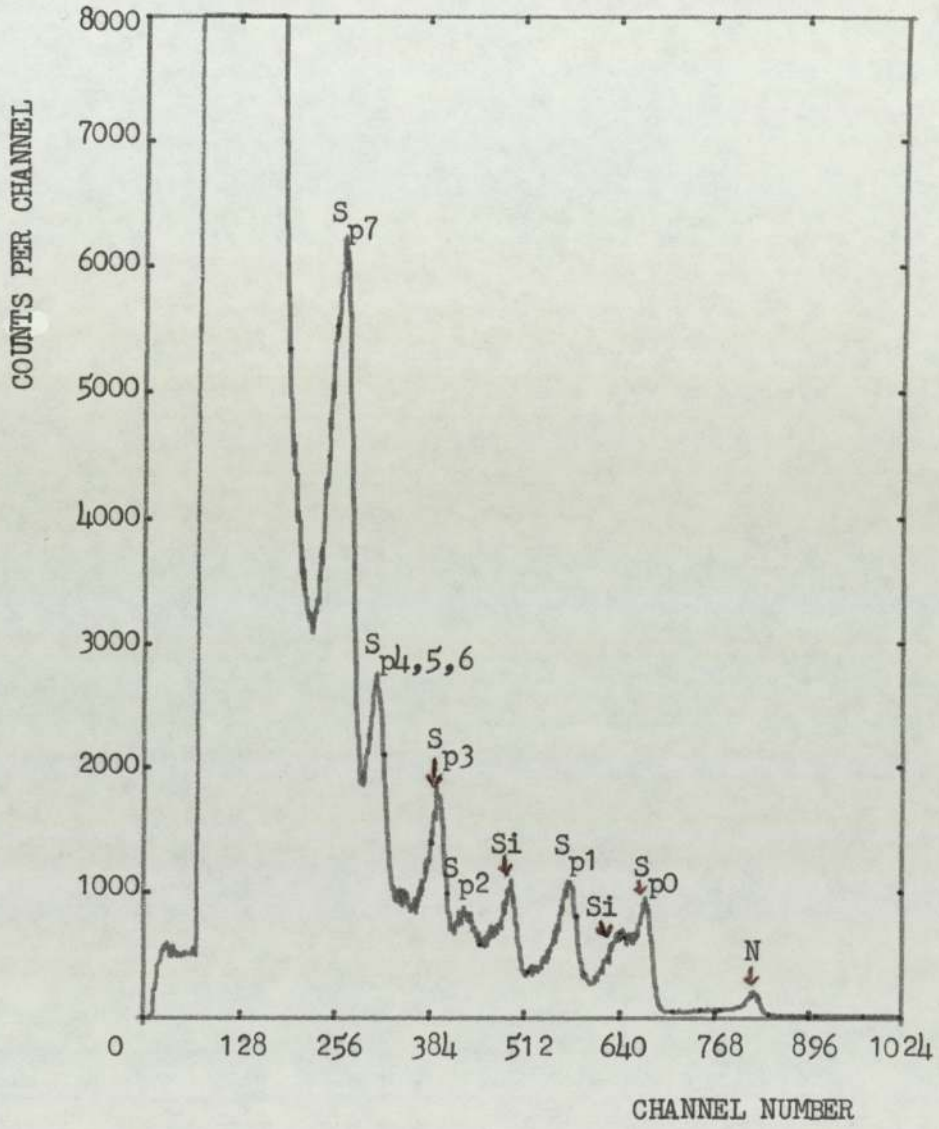

FIG. 5.13 REACTION YIELD SPECTRUM INDUCED BY DEUTERON BEAM PROBING ON AN E.P. FILM FROM THE FOLLOWING SAMPLE :

ADDITIVE : 0.25 % wt ELEMENTAL SULPHUR

LOAD : 200 KG

TEST TIME : STANDARD ONE MINUTE

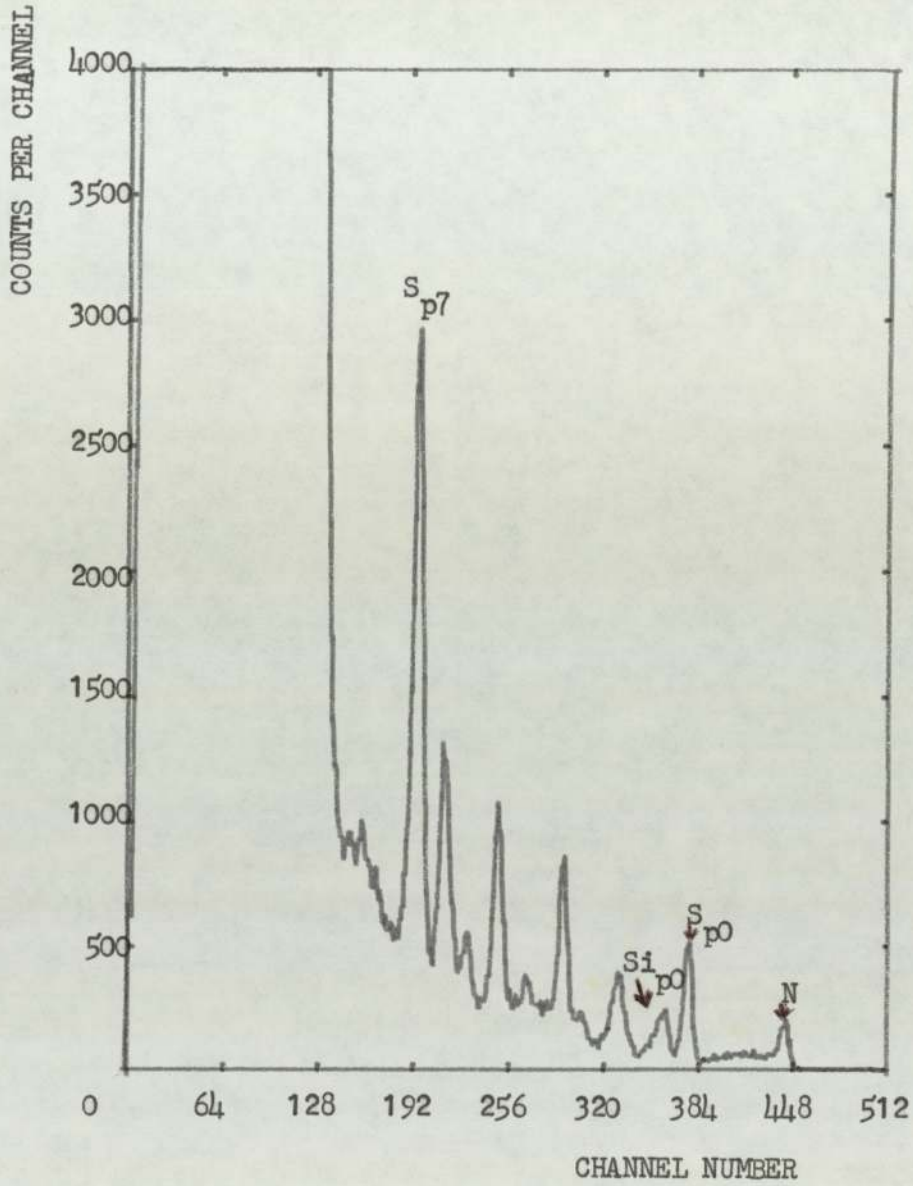

FIG. 5.14 REACTION YIELD SPECTRUM INDUCED BY DEUTERON BEAM PROBING ON AN E.P. FILM FROM THE FOLLOWING SAMPLE :

ADDITIVE : 0.25 % wt ELEMENTAL SULPHUR

APPLIED LOAD : 300 KG

TEST TIME : STANDARD ONE MINUTE

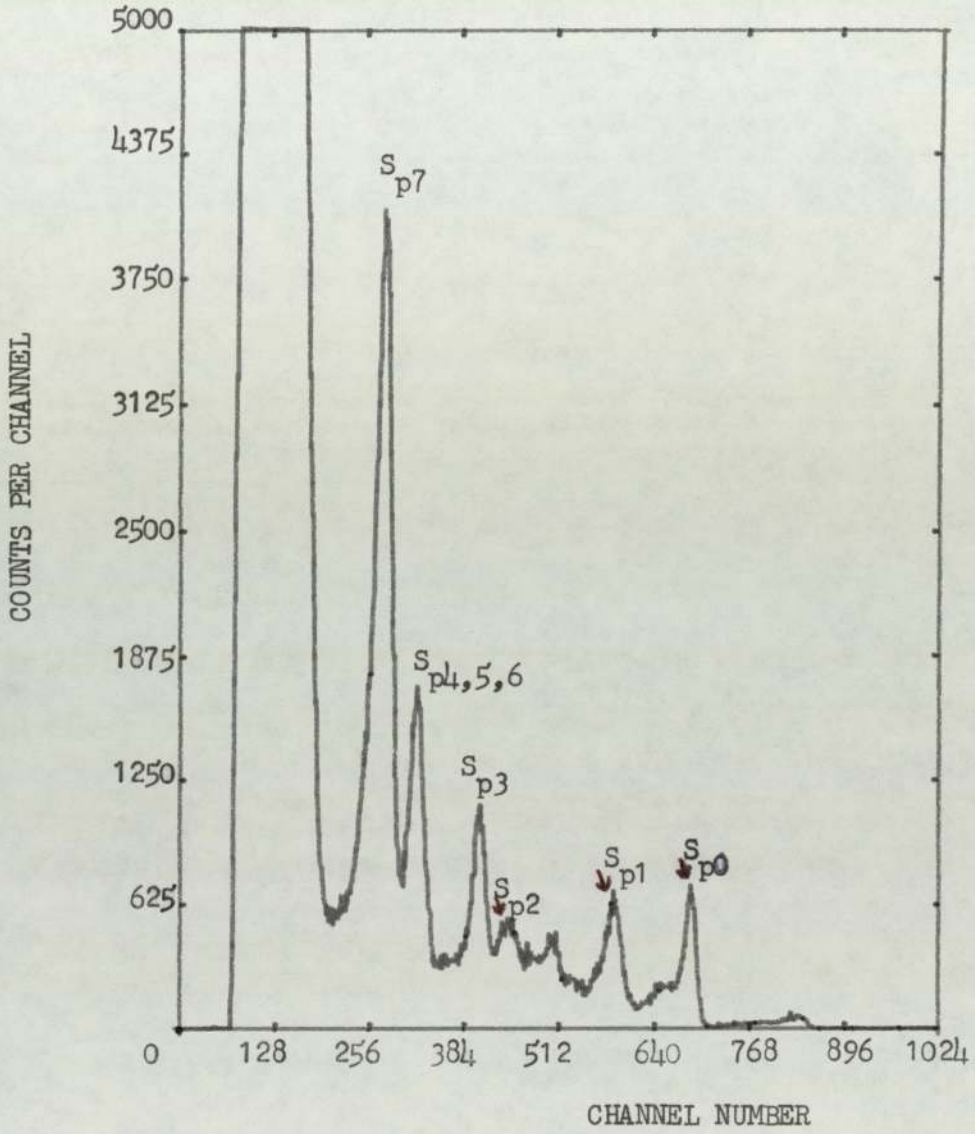

FIG. 5.15 REACTION YIELD SPECTRUM INDUCED BY DEUTERON BEAM PROBING ON AN E.P. FILM FROM THE FOLLOWING SAMPLE :

ADDITIVE : 0.25 % wt ELEMENTAL SULPHUR

APPLIED LOAD : 300 KG

TEST TIME : 300 SECONDS

applied load, as expected. The interference from the silicon element is less prominent at high loads. The strength of the two characteristic sulphur peaks (P_0 and P_7) increases with load. This is apparent from their tendency to gain in height and, also, to separate from the silicon peaks (cf Figures 5.11, 5.13 and 5.15). Even though the distinction between the peaks of these elements (ie S and Si) is very clear in the region near the welding point (Figure 5.15), the film is thinner than the one belonging to the middle of the e.p. area (Figure 5.13). The extension of the test time, which augments the rate of the film formation, tends to favour the detection of the sulphur. For the low e.p. load (ie 100 kg), the sulphur layer produced after 1100 seconds, is very thin and this is deduced from the gaussian shape of the S peaks (very narrow) and, also from the Si peaks which are still observable (Figure 5.12). On the other hand, for a very high load (ie just before the welding), and even for the test in where the time has only been prolonged for a short period (300 s), the resulting film is much thicker. This is concluded from the width of the S peaks (very broad) and the total absence of the Si peaks (Figure 5.15). The results obtained for ($N \triangle x$) are comparable to those found for the medium-to-thick calibration films of $FeSO_4$.

The spectra found for the e.p. films formed with 1.00% wt DBDS as the additive, are shown from Figure 5.16 to Figure 5.21, whilst their corresponding measures of the count-rate and calculations of the number of sulphur atoms are presented in Table 5.3. The analyses show that the use of the (d,p) reaction for detecting sulphur films produced during the standard one-minute wear test, is satisfactory. The value of the number of sulphur atoms per cm^2 increases with the applied load and, on the whole, it is included within the range of the one found for

Percentage of DBDS	Load (kg)	Test Time	Reaction Yield, Y_p, (ie count number) for Proton Groups		$(N \Delta x)_p$ for Proton Groups (S atoms.cm^{-2})		Average $(N \Delta x)$ (S atoms.cm^{-2})
			P_7	P_0	P_7	P_0	
1.00% wt	130	15	2273.97	2178.80	$8.89\ 10^{16}$	$4.65\ 10^{17}$	$2.77\ 10^{17}$
	130	60	← No sulphur detected (??) →				(**)
	130	1100	10376.10	1139.98	$6.09\ 10^{17}$	$3.65\ 10^{17}$	$4.87\ 10^{17}$
	140	60	7526.35	913.50	$4.42\ 10^{17}$	$2.92\ 10^{17}$	$3.67\ 10^{17}$
	200	60	18872.00	2292.00	$7.38\ 10^{17}$	$4.29\ 10^{17}$	$5.84\ 10^{17}$
	300	60	24539.00	3160.00	$9.60\ 10^{17}$	$6.74\ 10^{17}$	$8.17\ 10^{17}$
	400	60	18131.00	3465.50	$7.09\ 10^{17}$	$7.39\ 10^{17}$	$7.24\ 10^{17}$
	720	60	33259.90	4793.03	$1.30\ 10^{18}$	$1.02\ 10^{18}$	$1.16\ 10^{17}$
	820	60	15600.00	2030.70	$6.10\ 10^{17}$	$4.33\ 10^{17}$	$5.22\ 10^{17}$
	870	Starting of welding	← No sulphur detected, only Si →				
0.26% wt	130	60	← No sulphur detected, only Si →				
	130	1100	(*)	1264.00	(*)	$2.70\ 10^{17}$	$2.70\ 10^{17}$
	300	Weld at 11 sec.	← No sulphur detected, only Si →				

(*): Tremendous background.

(**): Scar might have been missed during the scan.

Table 5.3: Results of the S^{32} (d,p) S^{33} examination obtained for the e.p. films when DBDS was used as the additive.

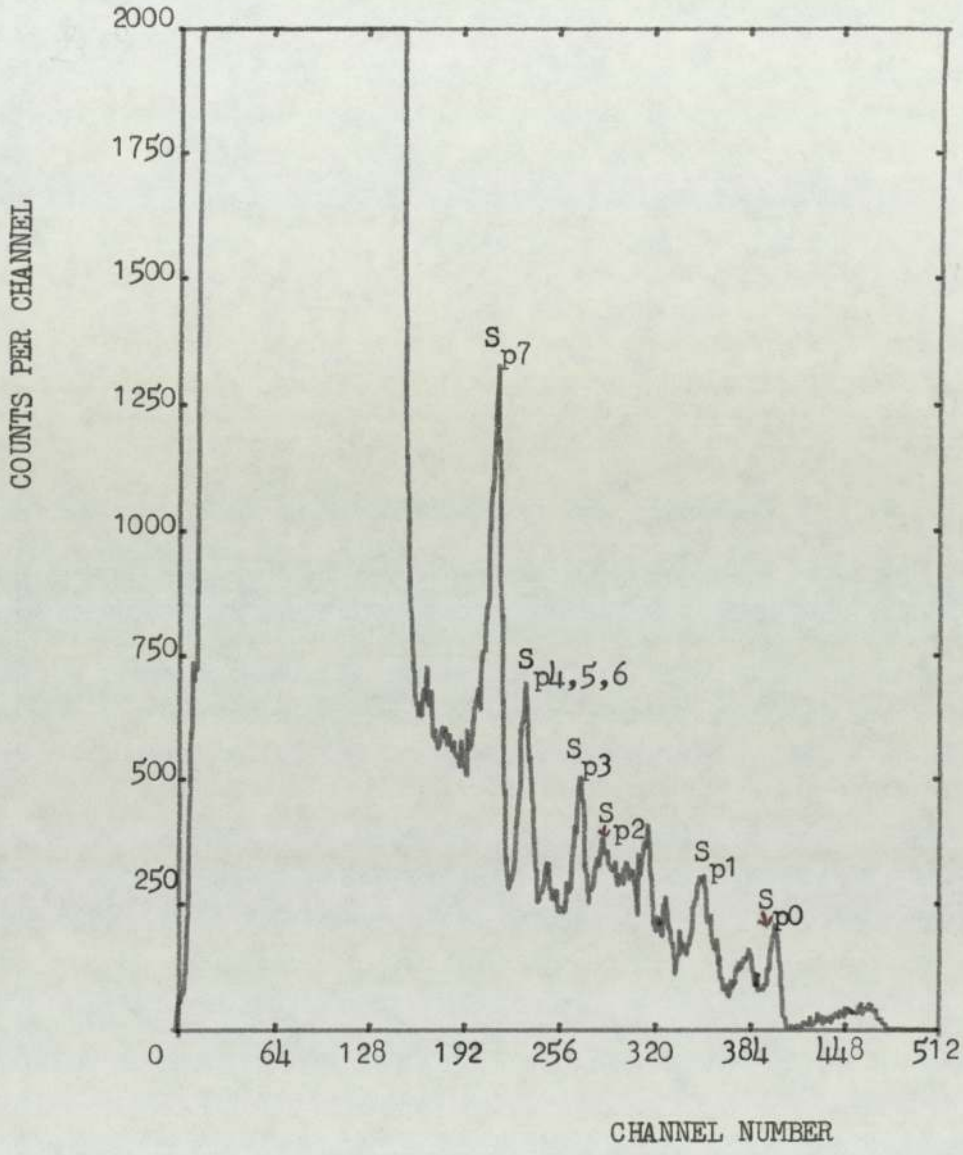

FIG. 5.16 REACTION YIELD SPECTRUM INDUCED BY DEUTERON BEAM PROBING ON AN E.P. FILM FROM THE FOLLOWING SAMPLE :

ADDITIVE : 1.00 % wt DBDS

APPLIED LOAD : 130 KG

TEST TIME : 1100 SECONDS

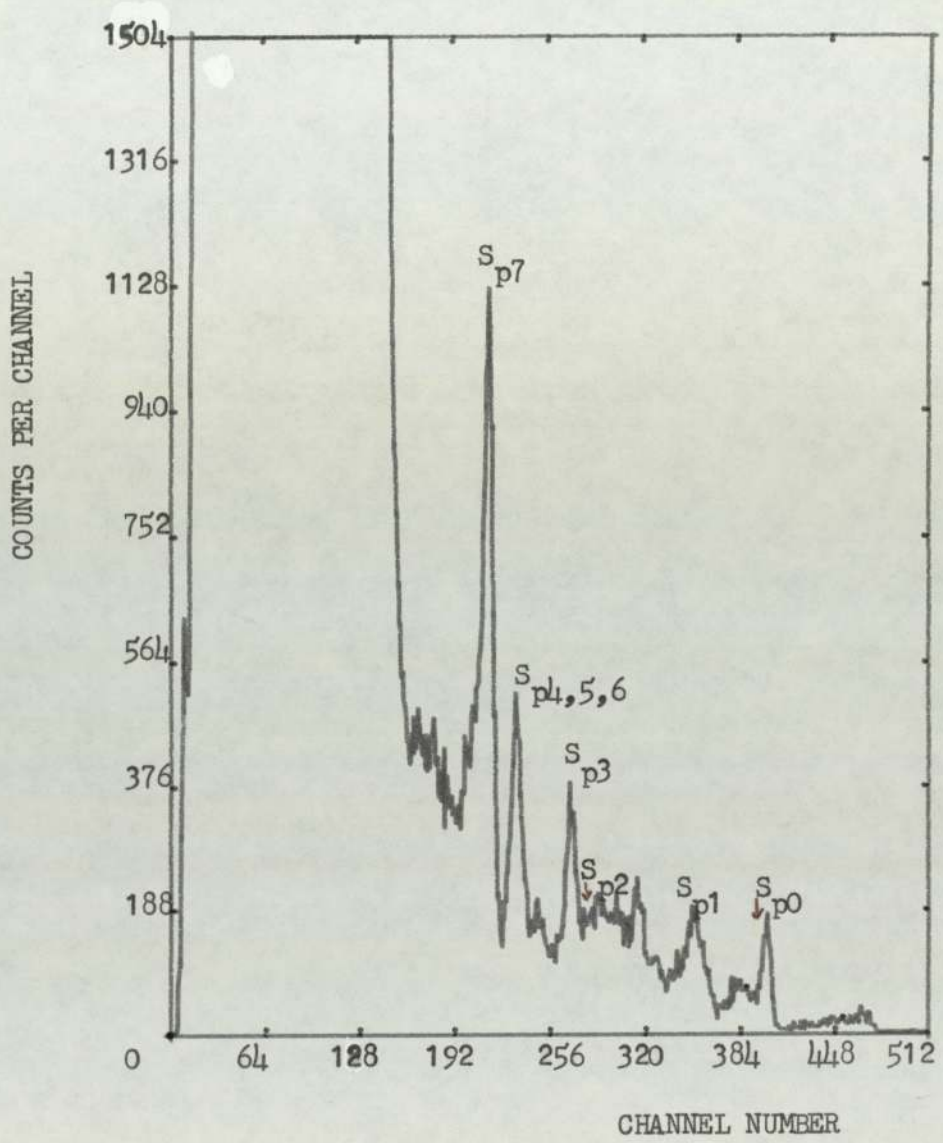

FIG. 5.17 REACTION YIELD SPECTRUM INDUCED BY DEUTERON BEAM PROBING ON AN E.P. FILM FROM THE FOLLOWING SAMPLE :

ADDITIVE : 1.00 % wt DBDS
APPLIED LOAD : 140 KG
TEST TIME : 60 SECONDS

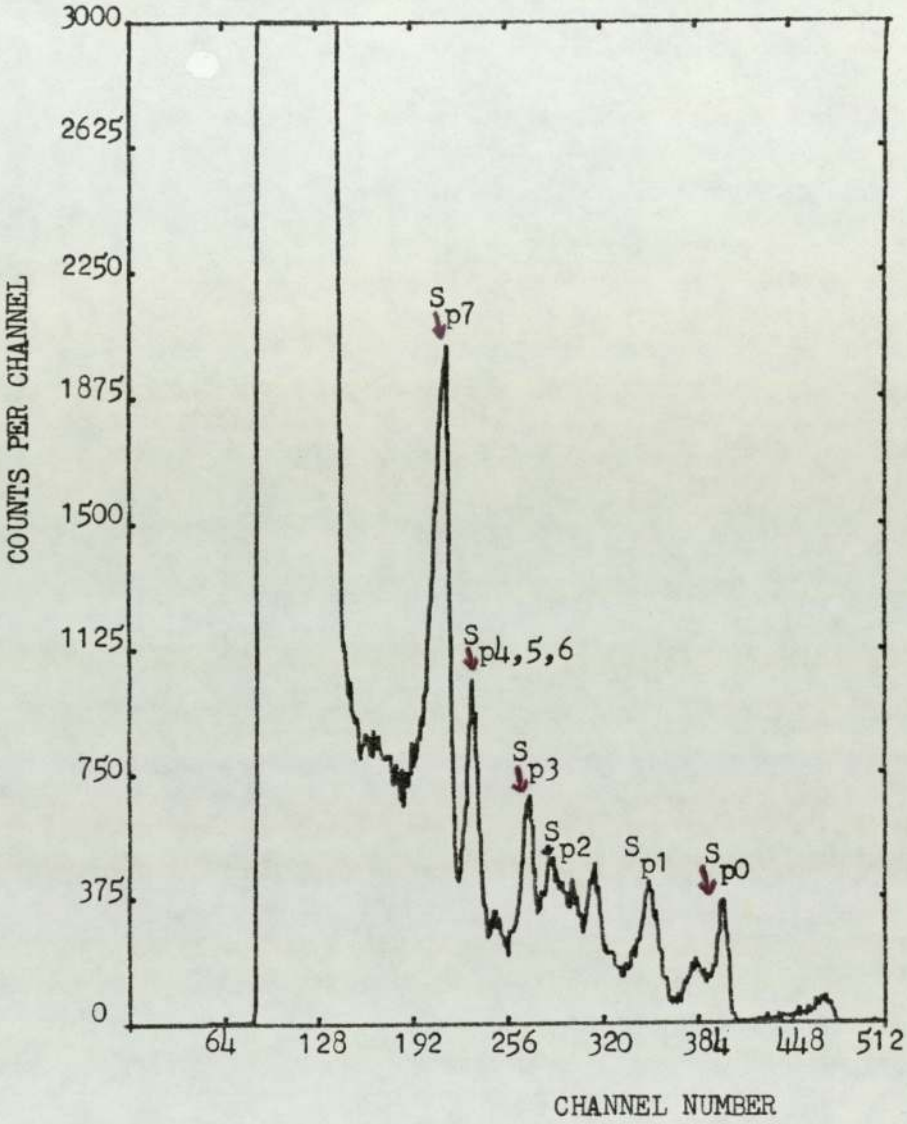

FIG. 5.17 REACTION YIELD SPECTRUM INDUCED BY DEUTERON BEAM PROBING ON AN E.P. FILM FROM THE FOLLOWING SAMPLE :

ADDITIVE : 1.00 % wt DBDS

APPLIED LOAD : 200 KG

TEST TIME : 60 SECONDS

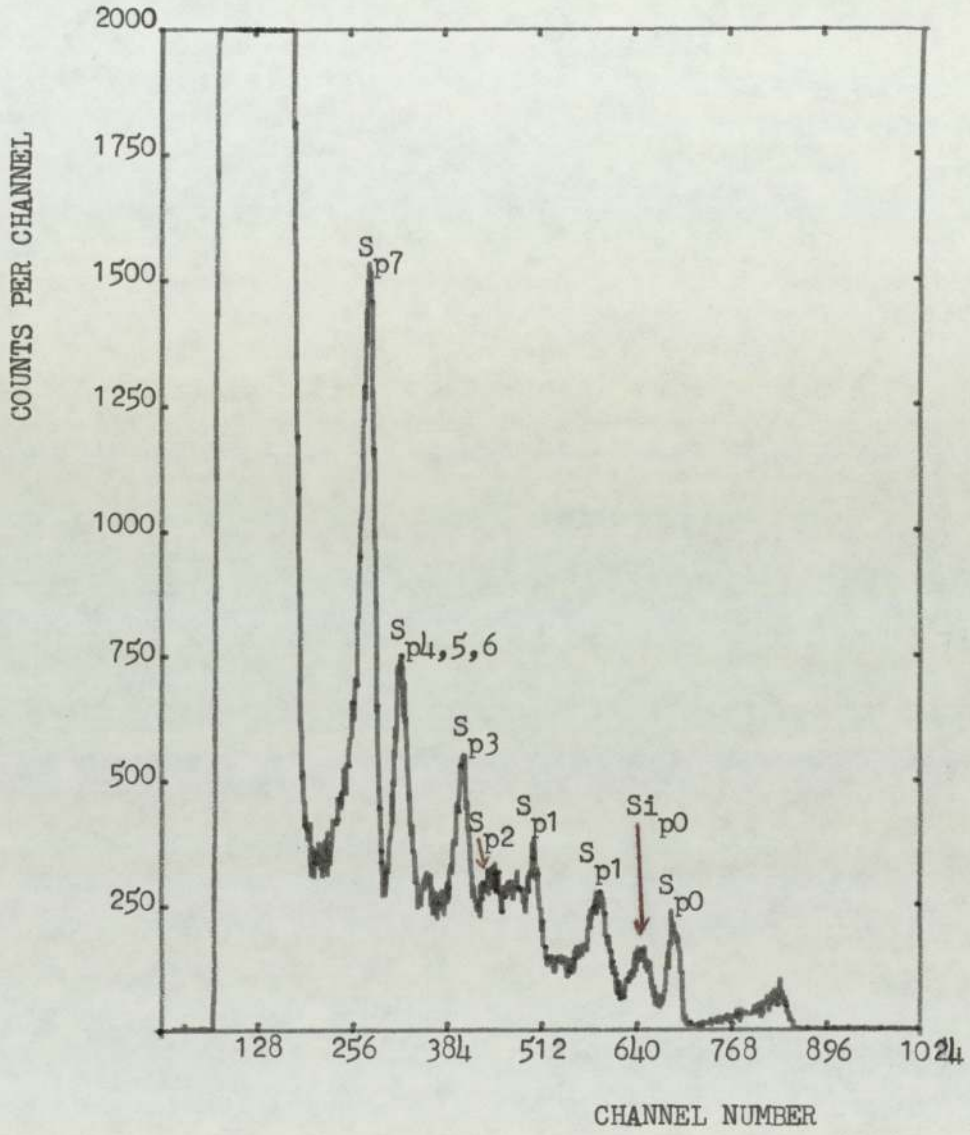

FIG. 5.18 REACTION YIELD SPECTRUM INDUCED BY DEUTERON BEAM PROBING ON AN E.P. FILM FROM THE FOLLOWING SAMPLE :

ADDITIVE : 1.00 % wt DBDS

APPLIED LOAD : 300 KG

TEST TIME : 60 SECONDS

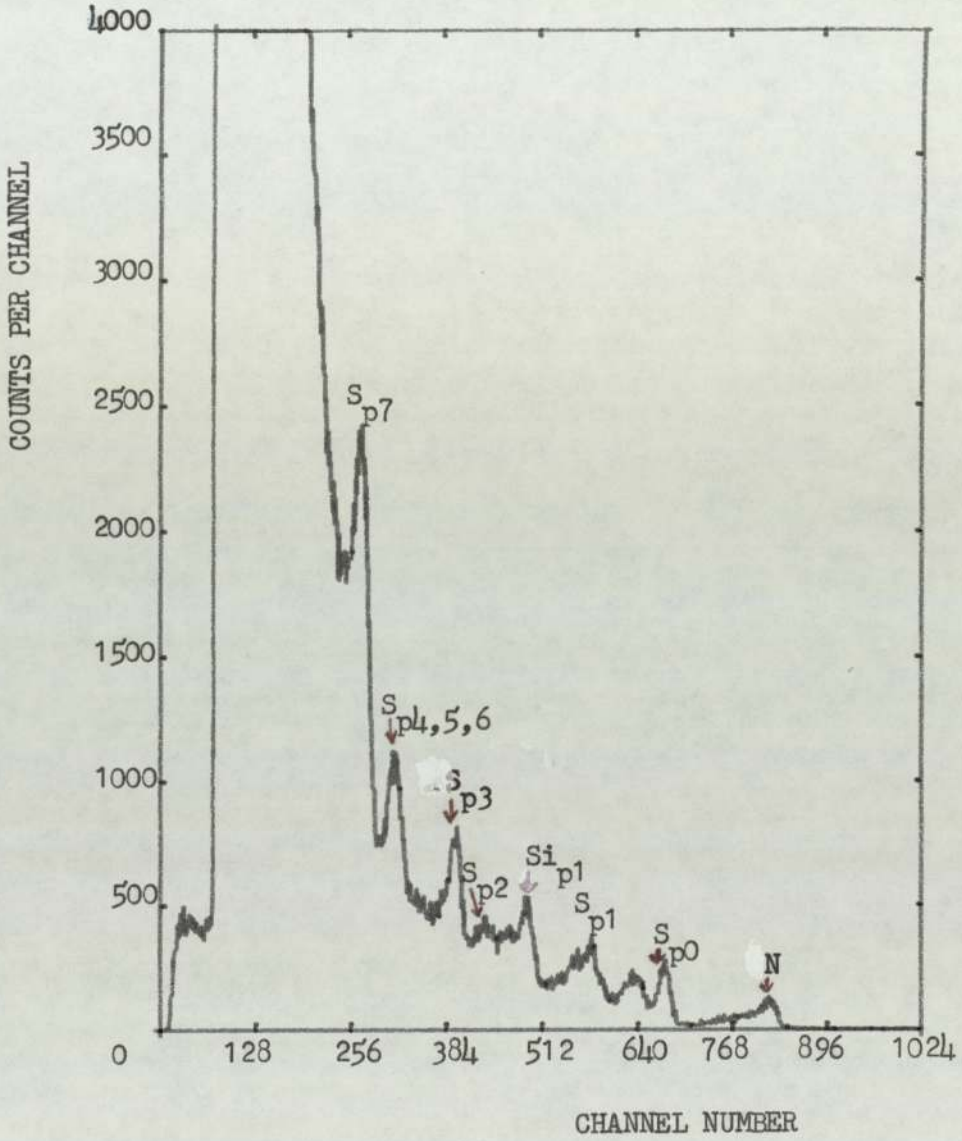

FIG. 5.19 REACTION YIELD SPECTRUM INDUCED BY DEUTERON BEAM PROBING ON AN E.P. FILM FROM THE FOLLOWING SAMPLE :

ADDITIVE : 1.00 % wt DBDS

APPLIED LOAD : 400 KG

TEST TIME : 60 SECONDS

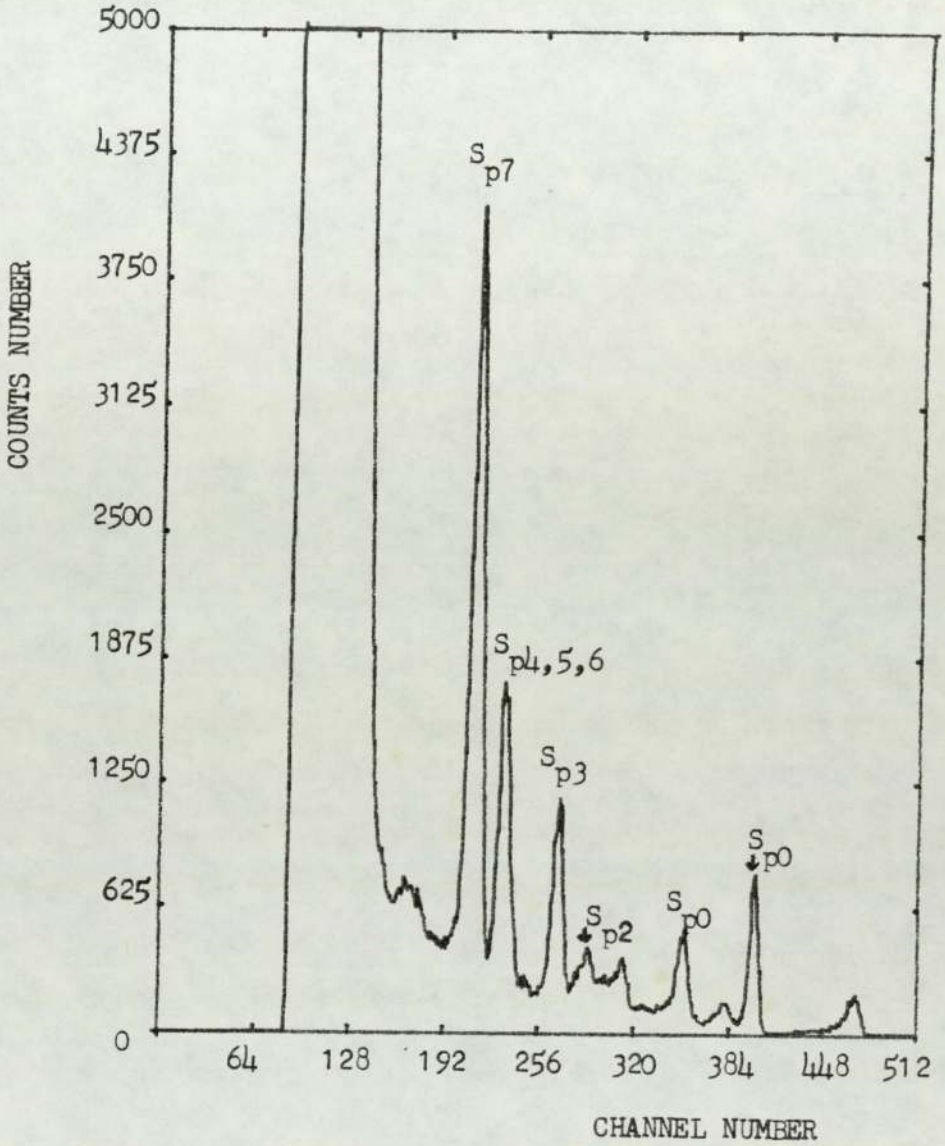

FIG. 5.20 REACTION YIELD SPECTRUM INDUCED BY DEUTERON BEAM PROBING ON AN E.P. FILM FROM THE FOLLOWING SAMPLE :

ADDITIVE : 1.00 % wt DBDS
APPLIED LOAD : 720 KG
TEST TIME : 60 SECONDS

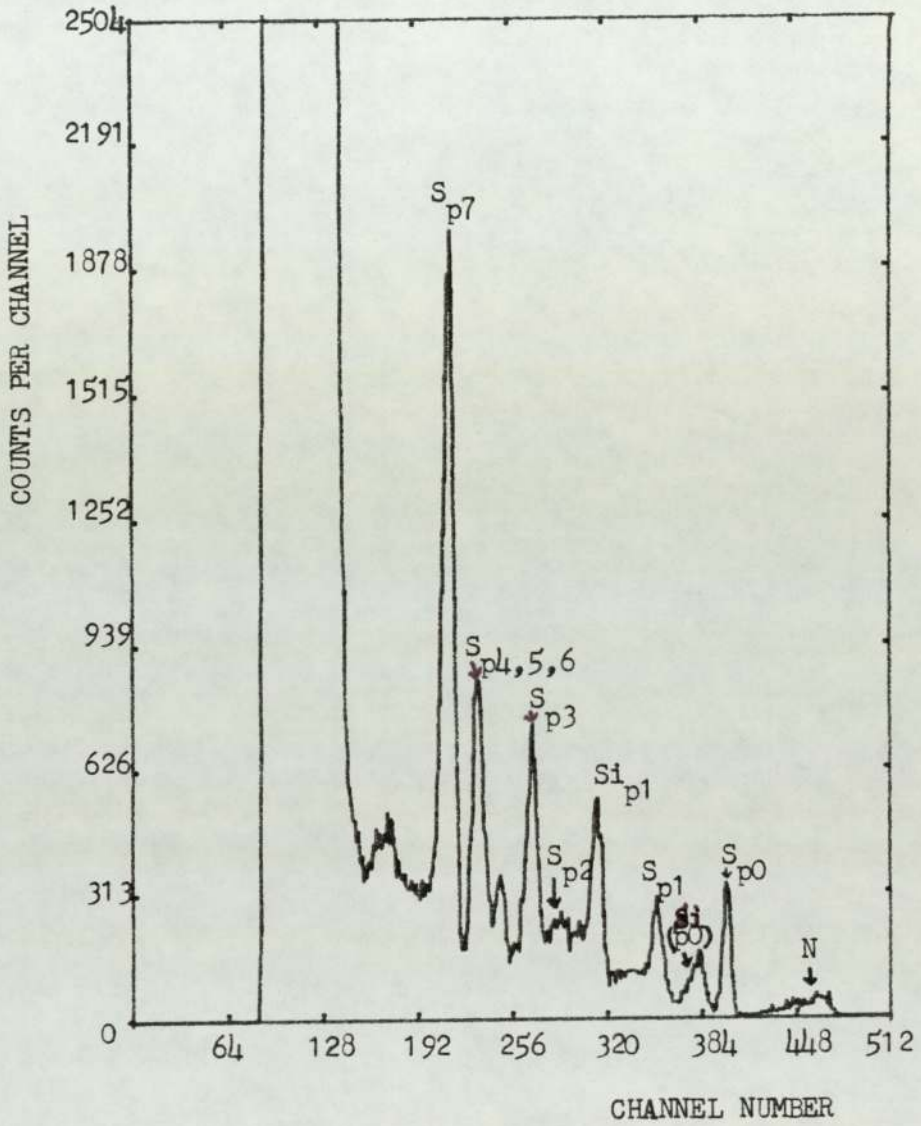

FIG. 5.21 REACTION YIELD SPECTRUM INDUCED BY DEUTERON BEAM PROBING ON AN E.P. FILM FROM THE FOLLOWING SAMPLE :

ADDITIVE : 1.00 % wt DBDS

APPLIED LOAD : 820 KG

TEST TIME : 60 SECONDS

the thin-to-medium calibration films of $FeSO_4$. Furthermore, the shape of the S peaks are gaussian (narrow) and the presence of the Si peaks confirm the thinness of the film. It is worth noting that as in the previous case (for the elemental sulphur additive), the film seems to be thicker in the middle of the e.p. area than the one near to the welding point. In addition, an analysis of a sample representing the welding process did not show any trace of sulphur, but on the contrary indicates the detection of silicon. This means that there is no sulphur in the wear layer connected with the welding event (Figure 5.22) (or may be a very small amount of it compared to the iron).

To see the effect on the reacted layer by reducing the amount of sulphur in the oil solution, three samples were prepared by lessening the concentration of DBDS to 0.26% wt. The examination reveals that the sulphur layer is too thin to be detected, with the exception of the one related to the extended test time. The spectra corresponding to this part of the investigation are shown in Figures 5.23, 5.24 and 5.25. The comparison between the statistics obtained for the two films formed under the same conditions (ie 130 kg and 1100 seconds) but with the two different percentage of DBDS, leads to the observation that while the sulphur concentration in the oil solution is nearly reduced to a quarter (0.26% to 0.068%), the number of sulphur atoms/cm^2 is only halved in the actual reacted films.

Due to the slow-rate of film formation shown by DPDS and DBMS additives, only specimens related to the load of 130 kg, were examined through the use of the $S^{32}(d,p)S^{33}$ reaction. However, even though the technique seems satisfactory for anlaysing these samples,

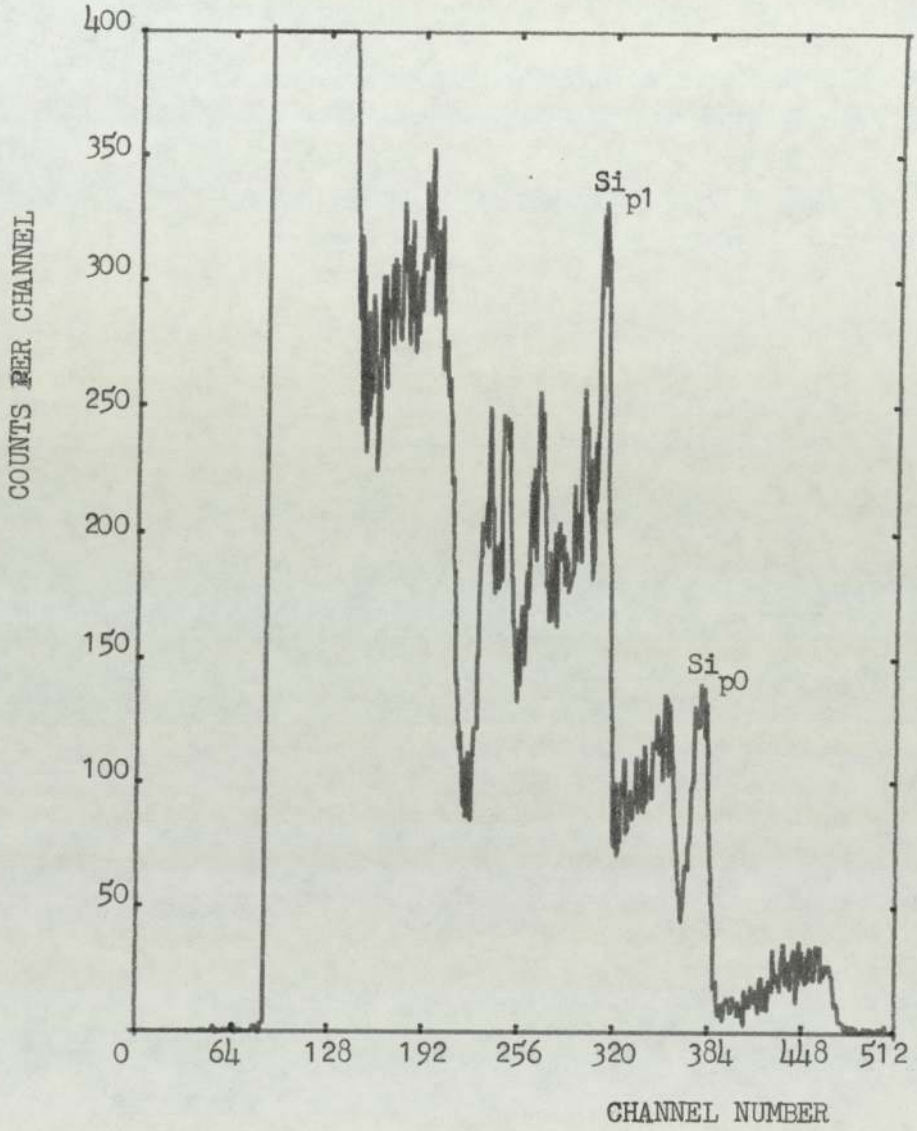

FIG. 5.22 REACTION YIELD SPECTRUM INDUCED BY DEUTERON BEAM PROBING ON A WELDED SURFACE :

ADDITIVE : 1.00 % wt DBDS

APPLIED LOAD : 870 KG

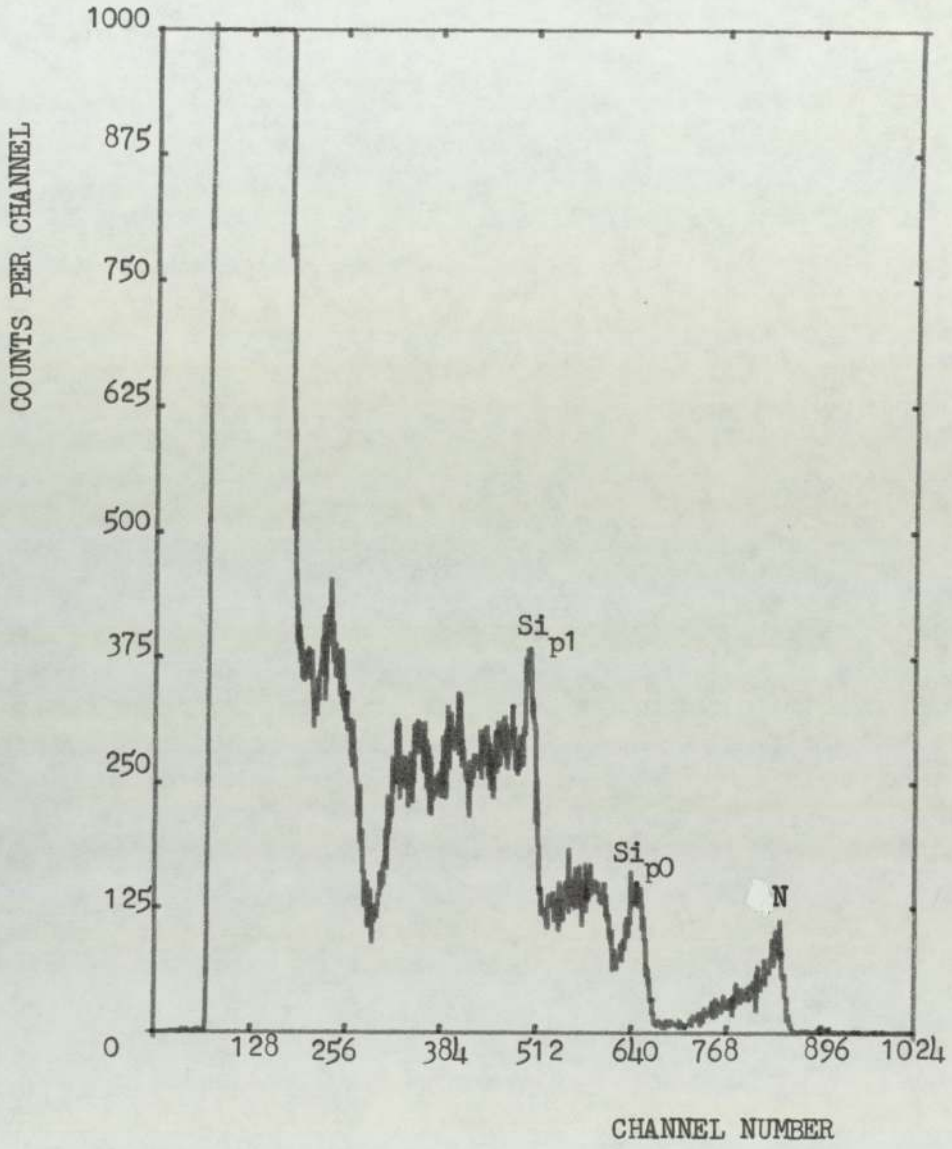

FIG. 5.23 REACTION YIELD SPECTRUM INDUCED BY DEUTERON BEAM PROBING ON AN E.P. FILM FROM THE FOLLOWING SAMPLE :

ADDITIVE : 0.26 % wt DBDS

APPLIED LOAD : 130 KG

TEST TIME : 60 SECONDS

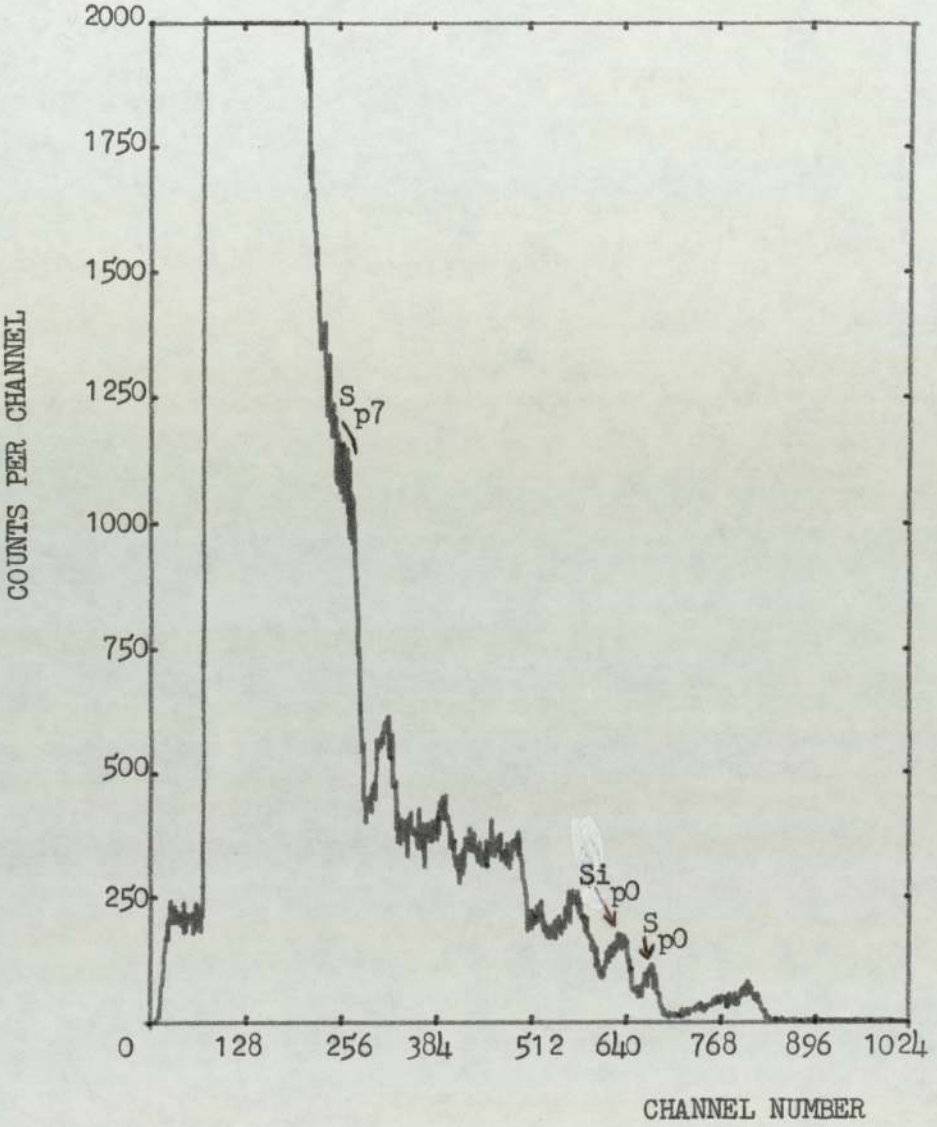

FIG. 5.24 REACTION YIELD SPECTRUM INDUCED BY DEUTERON BEAM PROBING ON AN E.P. FILM FROM THE FOLLOWING SAMPLE :

ADDITIVE : 0.26 % wt DBDS

APPLIED LOAD : 130 KG

TEST TIME : 1100 SECONDS

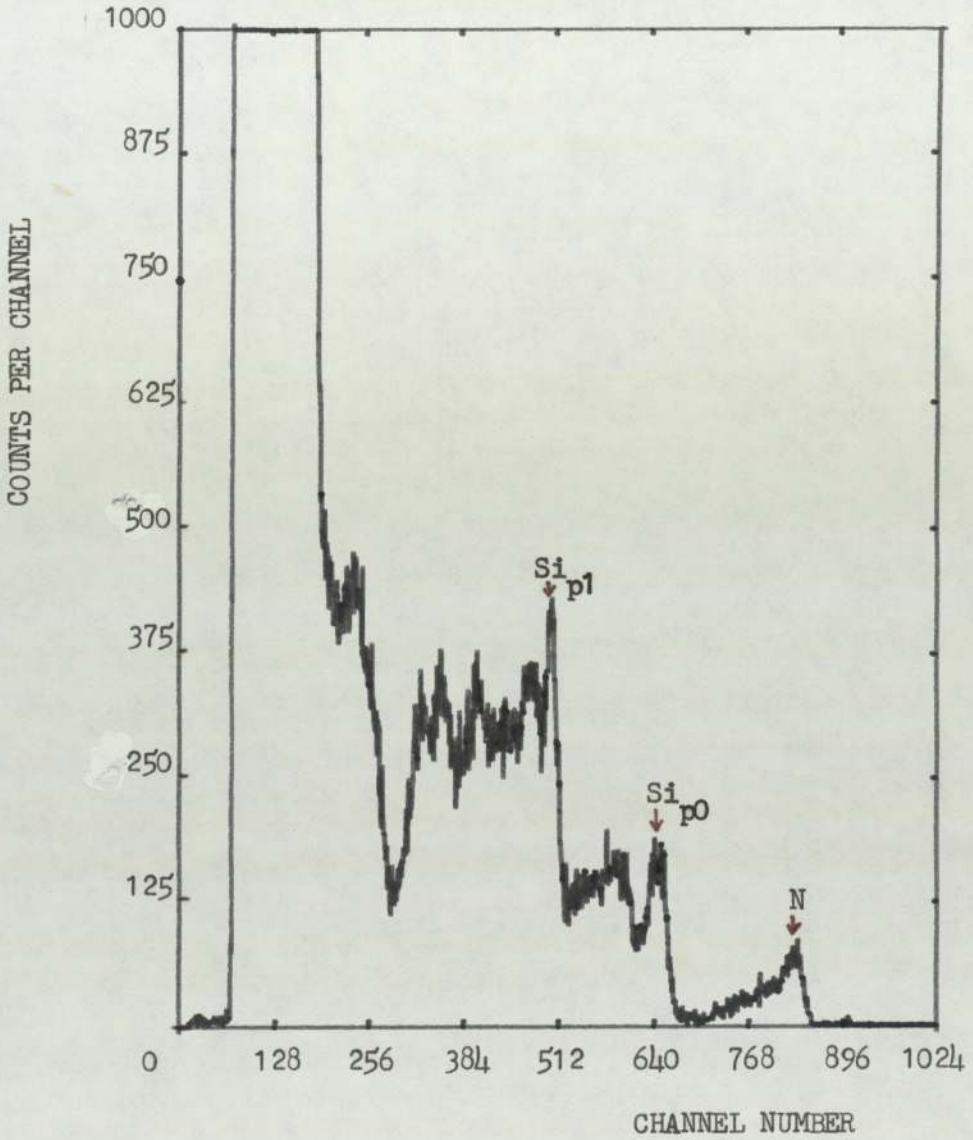

FIG. 5.25 REACTION YIELD SPECTRUM INDUCED BY DEUTERON BEAM PROBING ON A WELDED SURFACE :

ADDITIVE : 0.26 % wt DBDS

APPLIED LOAD : 300 KG

TEST TIME : 11 SECONDS

the corresponding spectra (Figures 5.26 to 5.32) reveal that the sulphur peak P_7 produced on each diagram is dwarfed by the highly interference from the silicon presence. This indicates that the reacted film is very thin and, in fact, it is much thinner than the calibration thin film of $FeSO_4$. Tables 5.4 and 5.5 present the results obtained for DPDS and DBMS additives respectively.

Figure 5.33 shows the spectrum obtained for the sample representing the welding process (ie load of 180 kg) demonstrated during the use of 0.88% wt DPDS as the additive. As seen before, no sulphur is detected. The main element is silicon and this corroborates the previous statement made about the non-existence or the small amount of sulphur in the wear-welding process.

5.2 Results from Rutherford Backscattering (R.B.S.) Analysis

The energy spectrum of the backscattered α-particles obtained from the analysis of an unworn sample by the R.B.S. technique, is shown in Figure 5.34. It can be seen that the spectrum is distinguished by a sloping plateau terminated by a sharp edge. The sharp edge represents the characteristic energy of the iron obtained by scattering from the surface layers. The counts recorded at lower energies are derived from the particles scattered from progressively greater depths. The slope of the spectrum edge is due to the finite resolution of the detector involved. The value of the energy (E) of the backscattered particles from the iron in the surface layers, is calculated through the following equation:

$$E = k^2 E_o \qquad \text{.....(5.1)}$$

Percentage of DPDS	Load (kg)	Test Time (s)	Reaction Yield, Y_p, (ie count number) for Proton Groups		$(N \Delta x)_p$ for Proton Groups (S atoms.cm^{-2})		Average $(N \Delta x)$ (S atoms.cm^{-2})
			P_7	P_0	P_7	P_0	
0.88% wt	130	60	1004.67	166.83	$1.70\ 10^{16}$	$1.54\ 10^{16}$	$1.62\ 10^{16}$
	130	1100	1183.33	255.00	$2.00\ 10^{16}$	$2.35\ 10^{16}$	$2.18\ 10^{16}$
	180	start weld	← No sulphur detected, only Si →				
0.26% wt	130	60	← No sulphur detected, only Si →				
	130	1100	(*)	1654.00	(*)	$3.53\ 10^{17}$	$3.53\ 10^{17}$
	200	10 sec	Welding; No sulphur detected, only Si →				
	300	Welding	← No sulphur detected, only Si →				

(*): Tremendous background.

Table 5.4: Results of the S^{32} (d,p) S^{33} examination obtained for the e.p. films when DPDS was used as the additive.

Percentage of DBMS	Load (kg)	Test Time (s)	Reaction Yield, Y_p, (ie count number) for Proton Groups		$(N \triangle x)_p$ for Proton Groups (S atoms.cm^{-2})		Average $(N \triangle x)$ (S atoms.cm^{-2})
			P_7	P_0	P_7	P_0	
1.74% wt	130	60	2233.17	383.50	$3.80\ 10^{16}$	$3.54\ 10^{16}$	$3.67\ 10^{16}$
	130	1100	4900.00	629.33	$8.29\ 10^{16}$	$5.81\ 10^{16}$	$7.05\ 10^{16}$
	140	60	907.00(*)	132.26	$1.54\ 10^{16}$	$1.22\ 10^{16}$	$1.38\ 10^{16}$
1.00% wt	130	9	← Welding →				
0.26% wt	130	<60	← Welding →				

(*): Area not quite clearly defined.

Table 5.5: Results of the S^{32} (d,p) S^{33} examination obtained for the e.p. films when DBMS was used as the additive.

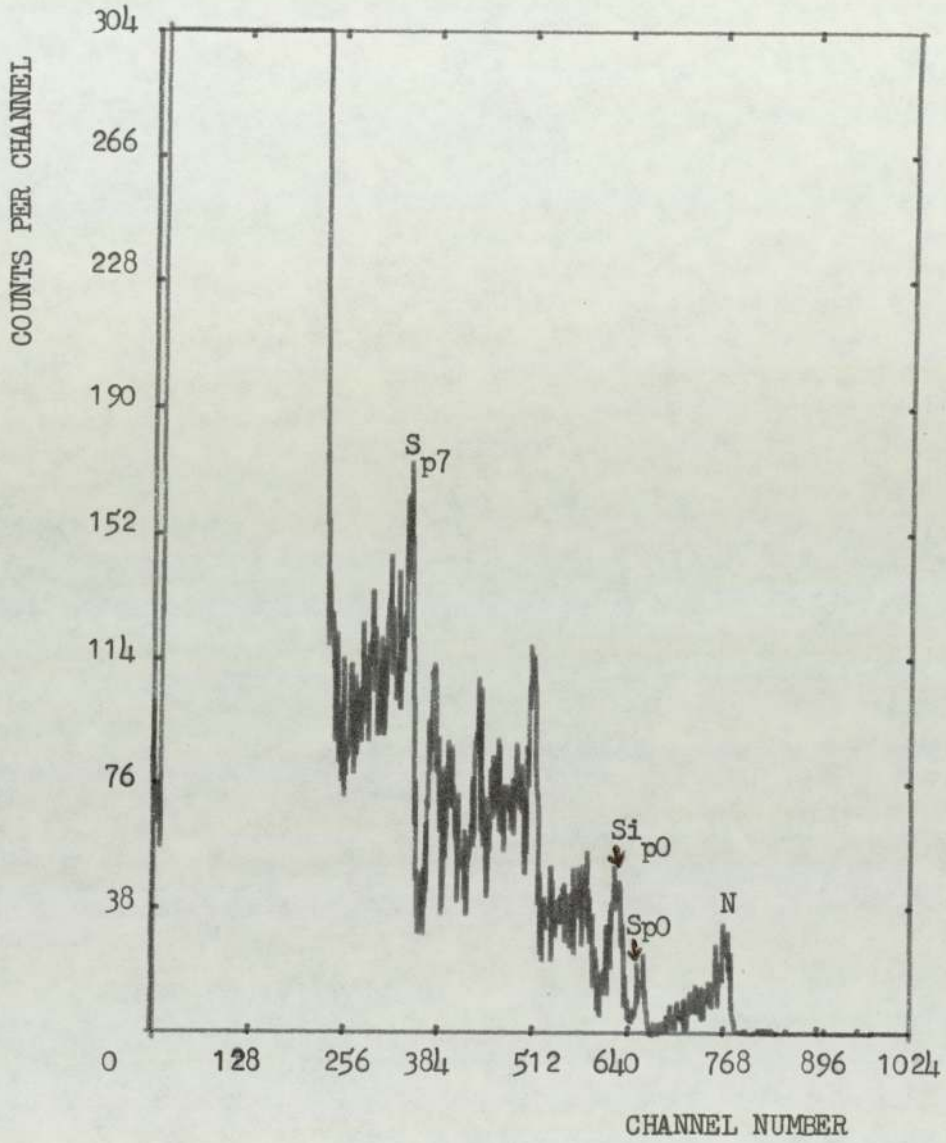

FIG. 5.26 REACTION YIELD SPECTRUM INDUCED BY DEUTERON BEAM PROBING ON AN E.P. FILM FROM THE FOLLOWING SAMPLE :

ADDITIVE : 0.88 % wt DPDS

APPLIED LOAD : 130 KG

TEST TIME : 60 SECONDS

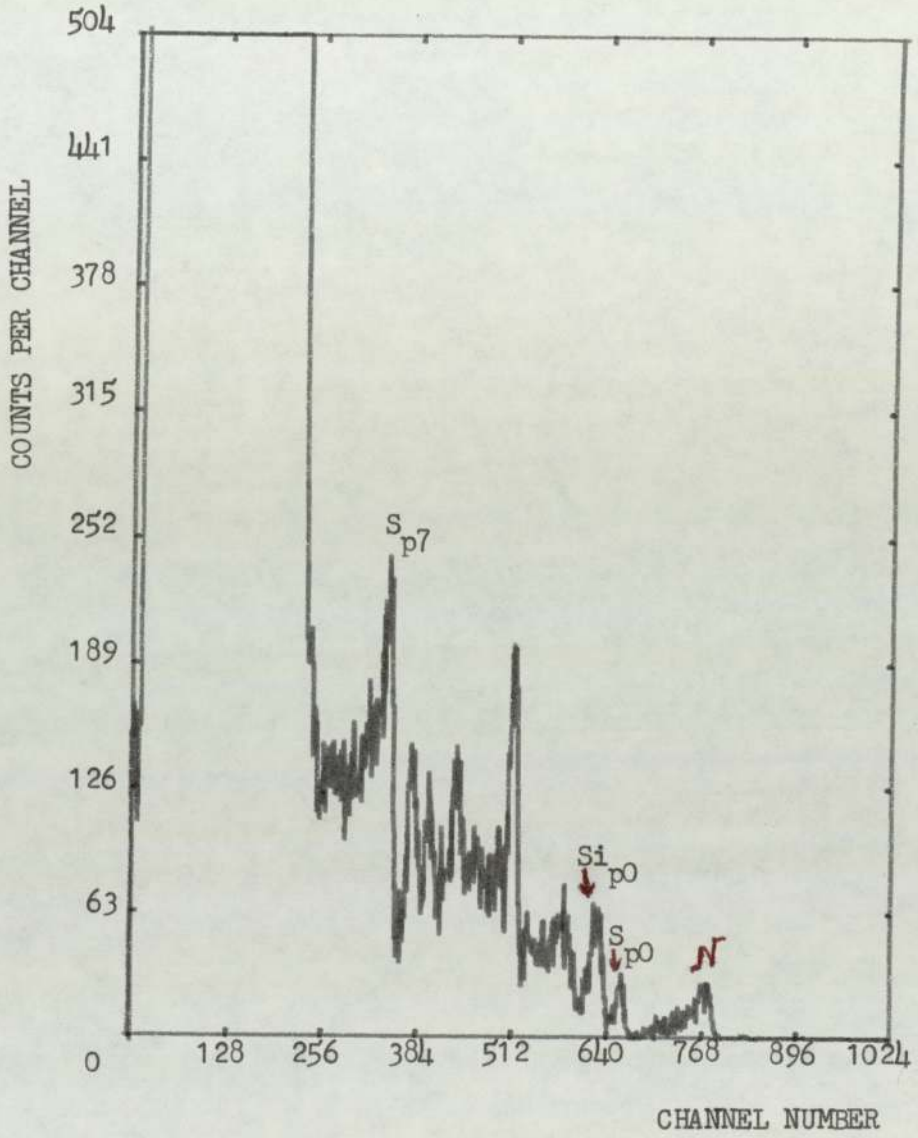

FIG. 5.27 REACTION YIELD SPECTRUM INDUCED BY DEUTERON BEAM PROBING ON AN E.P. FILM FROM THE FOLLOWING SAMPLE :

ADDITIVE : 0.88 % wt DPDS
APPLIED LOAD : 130 KG
TEST TIME : 1100 SECONDS

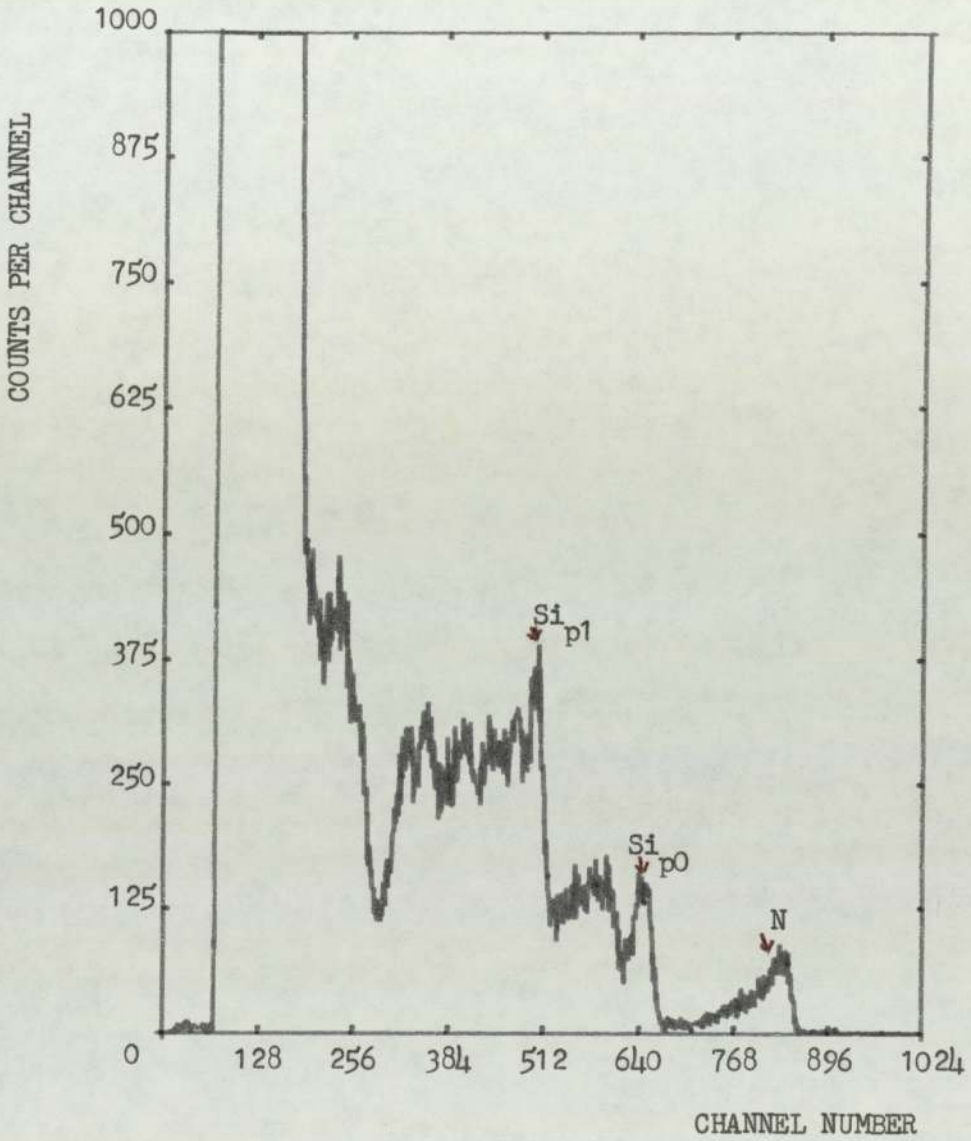

FIG. 5.28 REACTION YIELD SPECTRUM INDUCED BY DEUTERON BEAM PROBING ON AN E.P. FILM FROM THE FOLLOWING SAMPLE :

ADDITIVE : 0.26 % wt DPDS

APPLIED LOAD : 130 KG

TEST TIME : 60 SECONDS

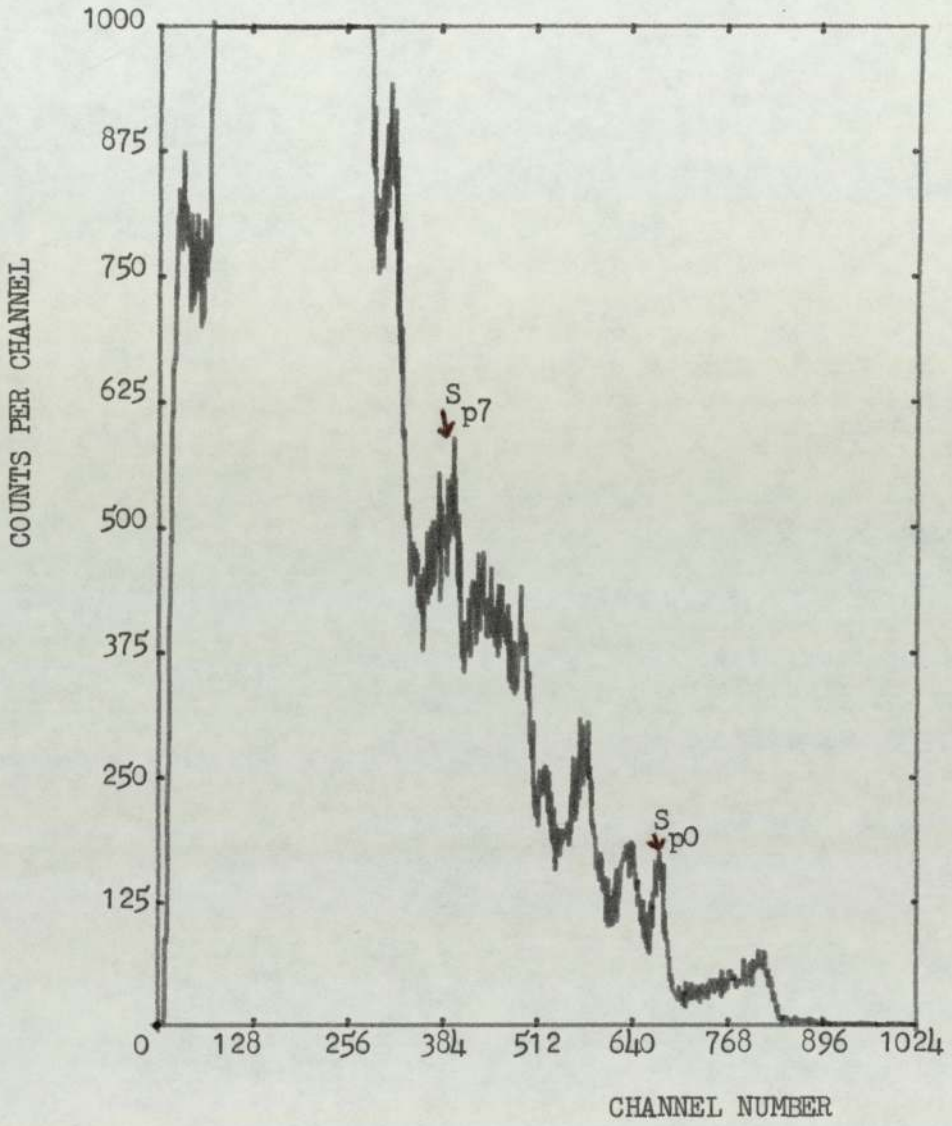

FIG. 5.29 REACTION YIELD SPECTRUM INDUCED BY DEUTERON BEAM PROBING ON AN E.P. FILM FROM THE FOLLOWING SAMPLE :

ADDITIVE : 0.26 % wt DPDS

APPLIED LOAD : 130 KG

TEST TIME : 1100 SECONDS

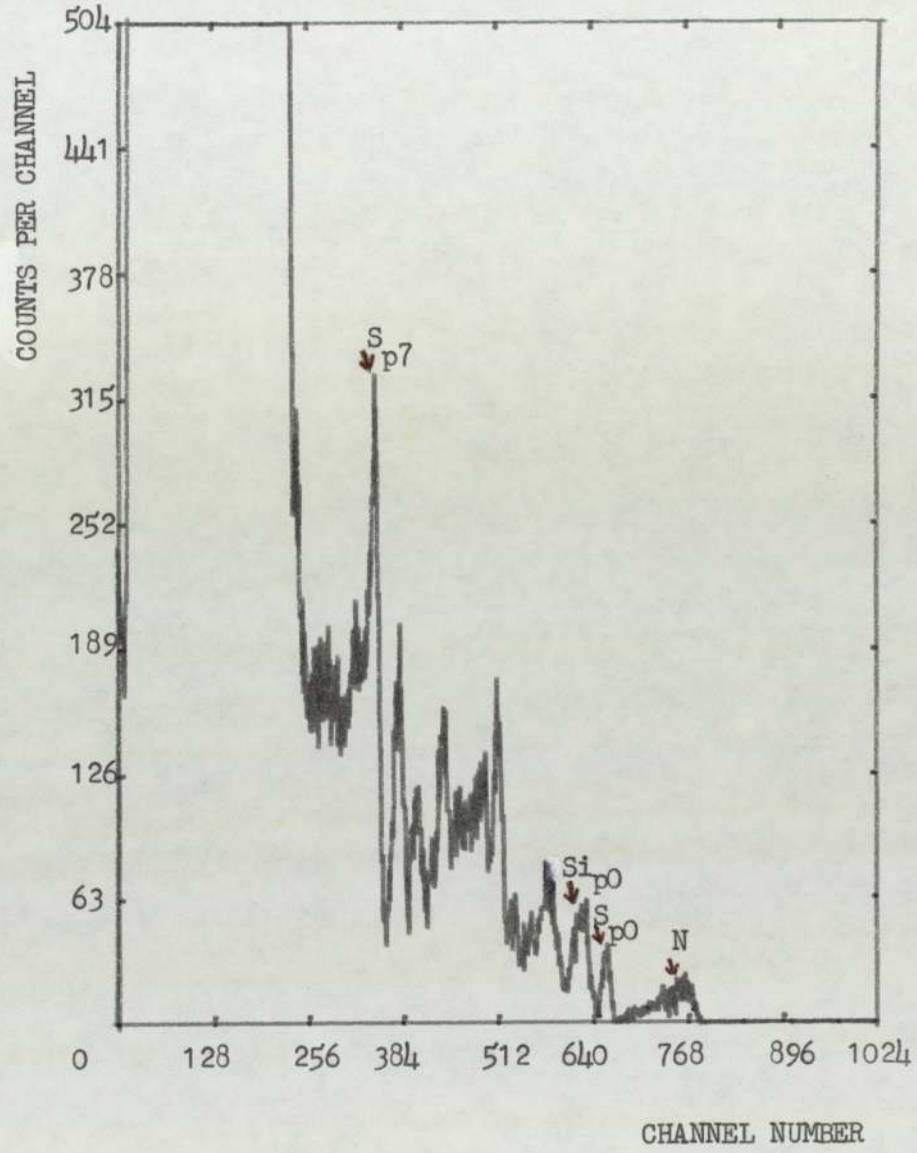

FIG. 5.30 REACTION YIELD SPECTRUM INDUCED BY DEUTERON BEAM PROBING ON AN E.P. FILM FROM THE FOLLOWING SAMPLE :

ADDITIVE : 1.74 % wt DBMS
APPLIED LOAD : 130 KG
TEST TIME : 60 SECONDS

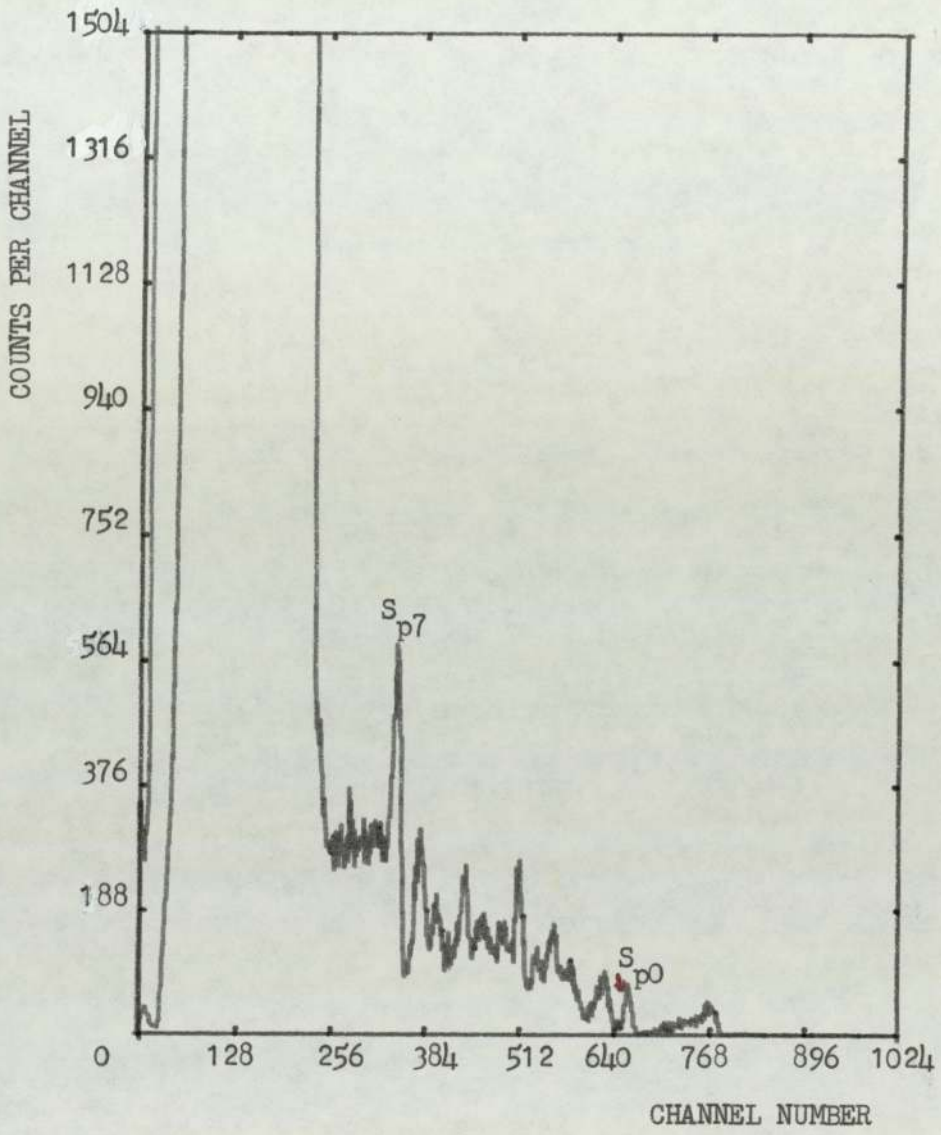

FIG. 5.31 REACTION YIELD SPECTRUM INDUCED BY DEUTERON BEAM PROBING ON AN E.P. FILM FROM THE FOLLOWING SAMPLE :

ADDITIVE : 1.74 % wt DBMS
APPLIED LOAD : 130 KG
TEST TIME : 1100 SECONDS

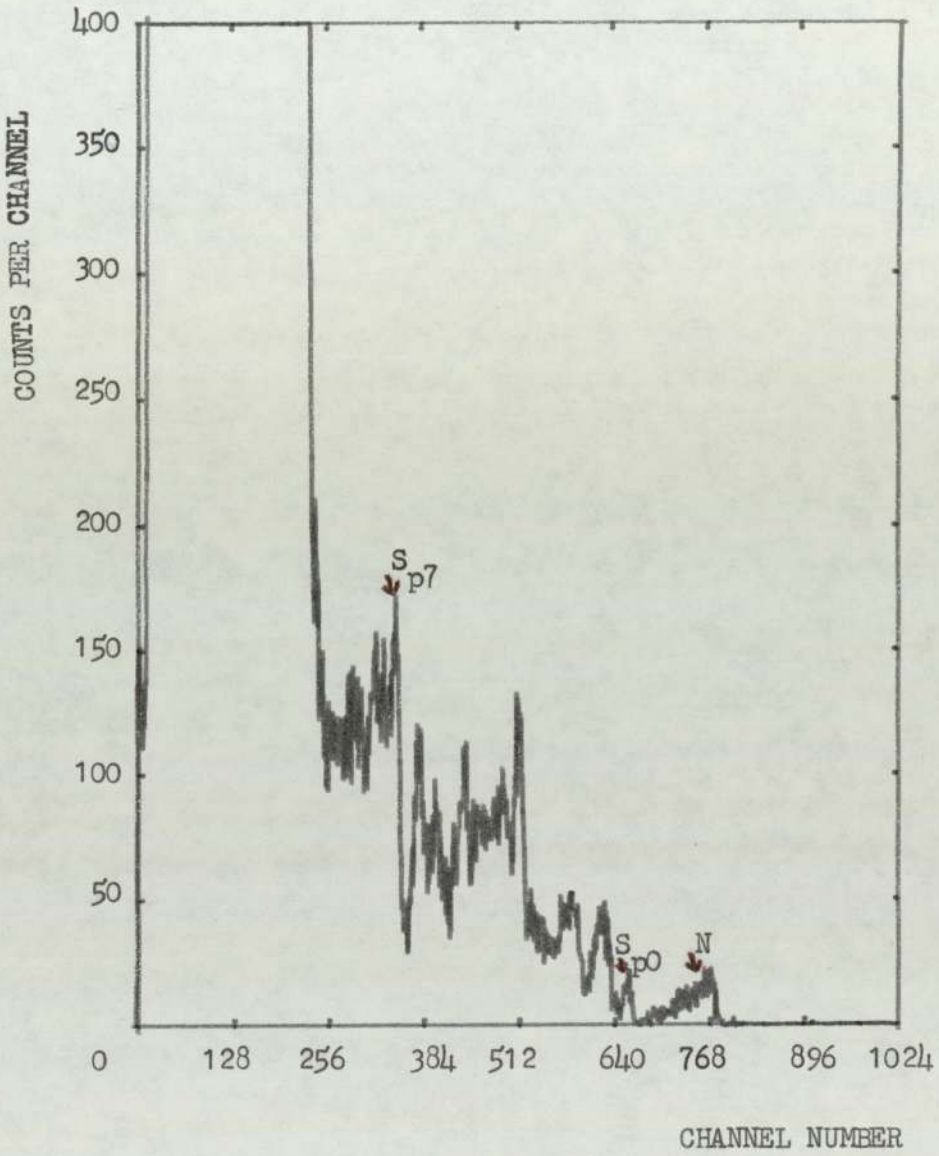

FIG. 5.32 REACTION YIELD SPECTRUM INDUCED BY DEUTERON BEAM PROBING ON AN E.P. FILM FROM THE FOLLOWING SAMPLE :

ADDITIVE : 1.74 % wt DBMS
APPLIED LOAD : 140 KG
TEST TIME : 60 SECONDS

where $k = \frac{M_\alpha \cos\theta_s + M_{Fe}}{M_\alpha + M_{Fe}}$ and E_0 = incident energy = 2.00 MeV;

[M_α = mass of the incident alpha-particle = 4.0026 a.m.u.

M_{Fe} = mass of the struck iron atom = 55.847 a.m.u.

θ_s = laboratory scattering angle (set between 170° to 176° during the experimental procedure)].

The energy related to the iron in the surface layers is evaluated at 1.50_2 MeV for the experimental conditions.

According to the theory of the R.B.S. technique, the examination of a solid surface covered with a uniform film formed by elements whose masses are less than those of the substrate, the resulting energy spectrum would display peaks superimposed on the plateau. These peaks represent the energy distributions of those elements.

As a result of this, the experimental spectra of the three calibration films of $FeSO_4$ (thin, medium and thick) are expected to appear in a shape similar to the one decribed above. The respective Figures 5.35, 5.36 and 5.37 show the expected behaviour. Furthermore, it can be clearly seen that the height of each "step" representing the sulphur and oxygen peaks, is proportional to the amount of the elements constituent in the $FeSO_4$ film. Also, it can be noticed that the size of the peaks increases from Figure 5.35 to Figure 5.37, following the order of magnitude of the thickness of the $FeSO_4$ surface layer.

5.2.1 Anti-Wear Films

The use of Rutherford Backscattering technique to detect the sulphur formed in the wear films generated under the anti-wear regime,

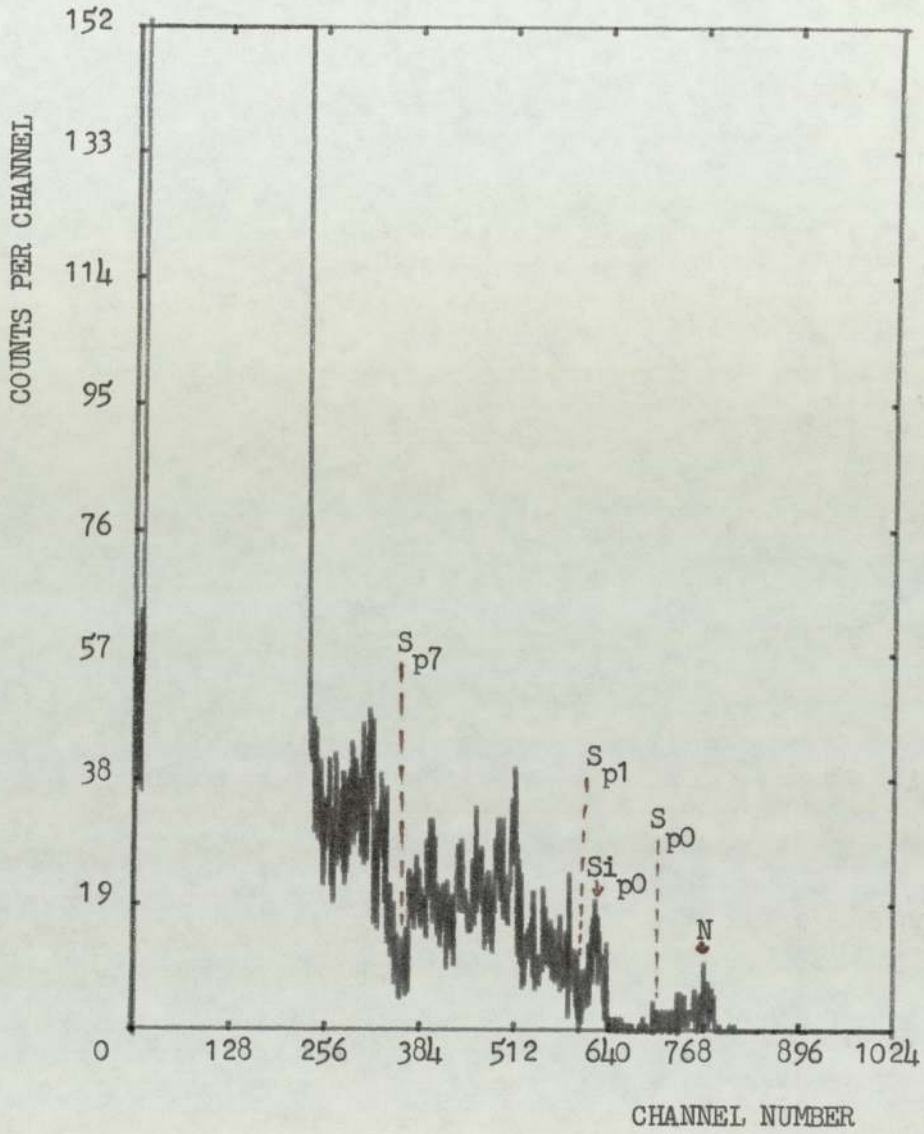

FIG. 5.33 REACTION YIELD SPECTRUM INDUCED BY DEUTERON BEAM PROBING ON A WELDED SURFACE :

ADDITIVE : 0.88 % wt DPDS

APPLIED LOAD : 180 KG

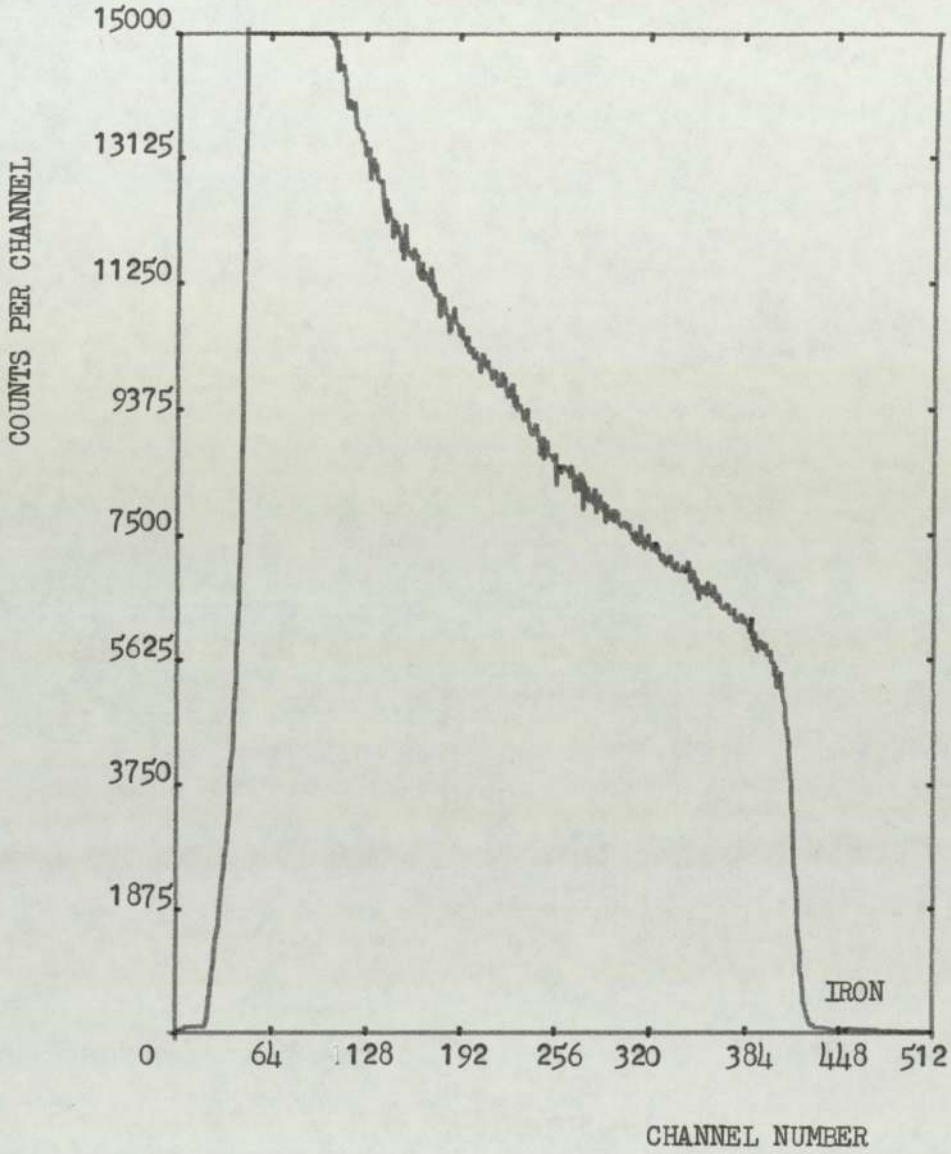

FIG. 5.34 R.B.S. SPECTRUM OBTAINED FOR AN UNWORN SAMPLE.

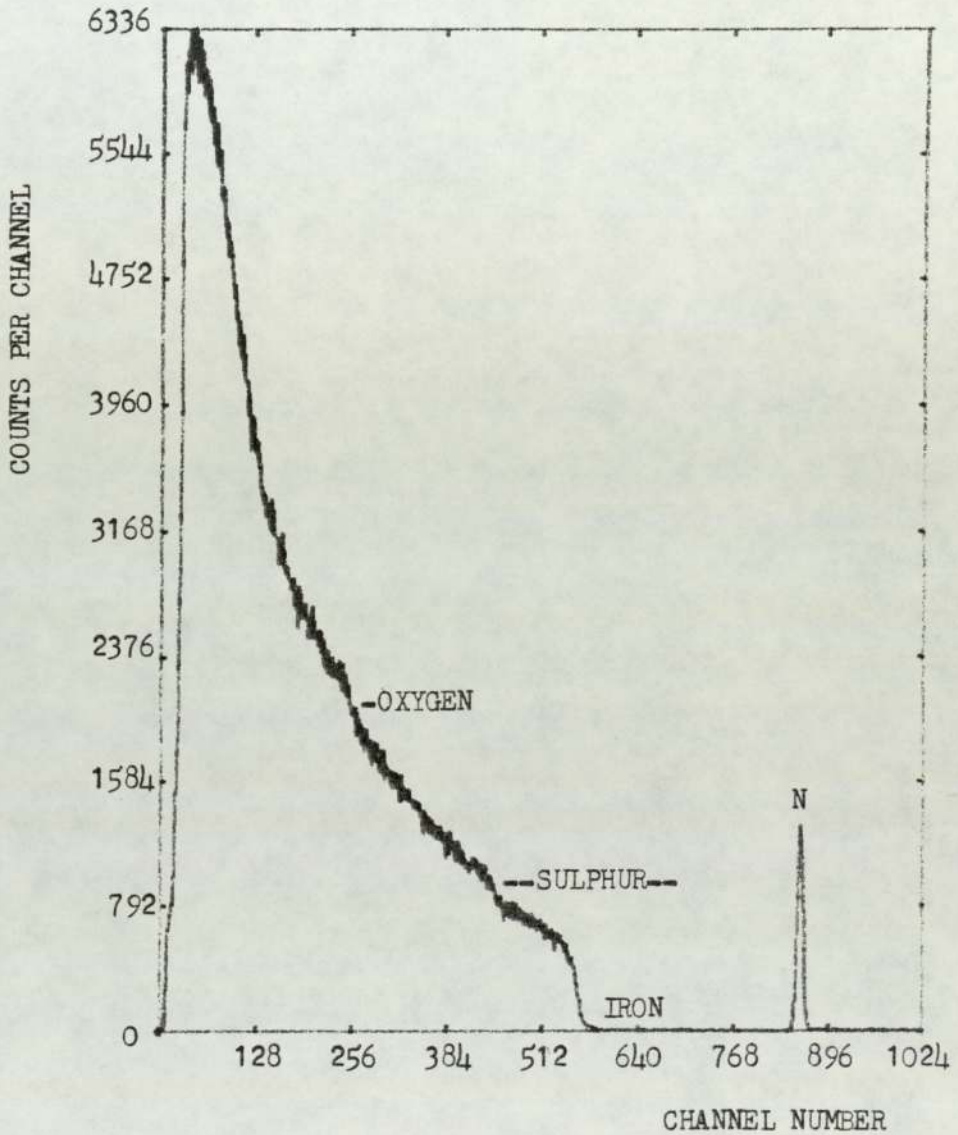

FIG. 5.35 R.B.S. SPECTRUM OBTAINED FOR THE THIN CALIBRATION FILM OF $FeSO_4$.

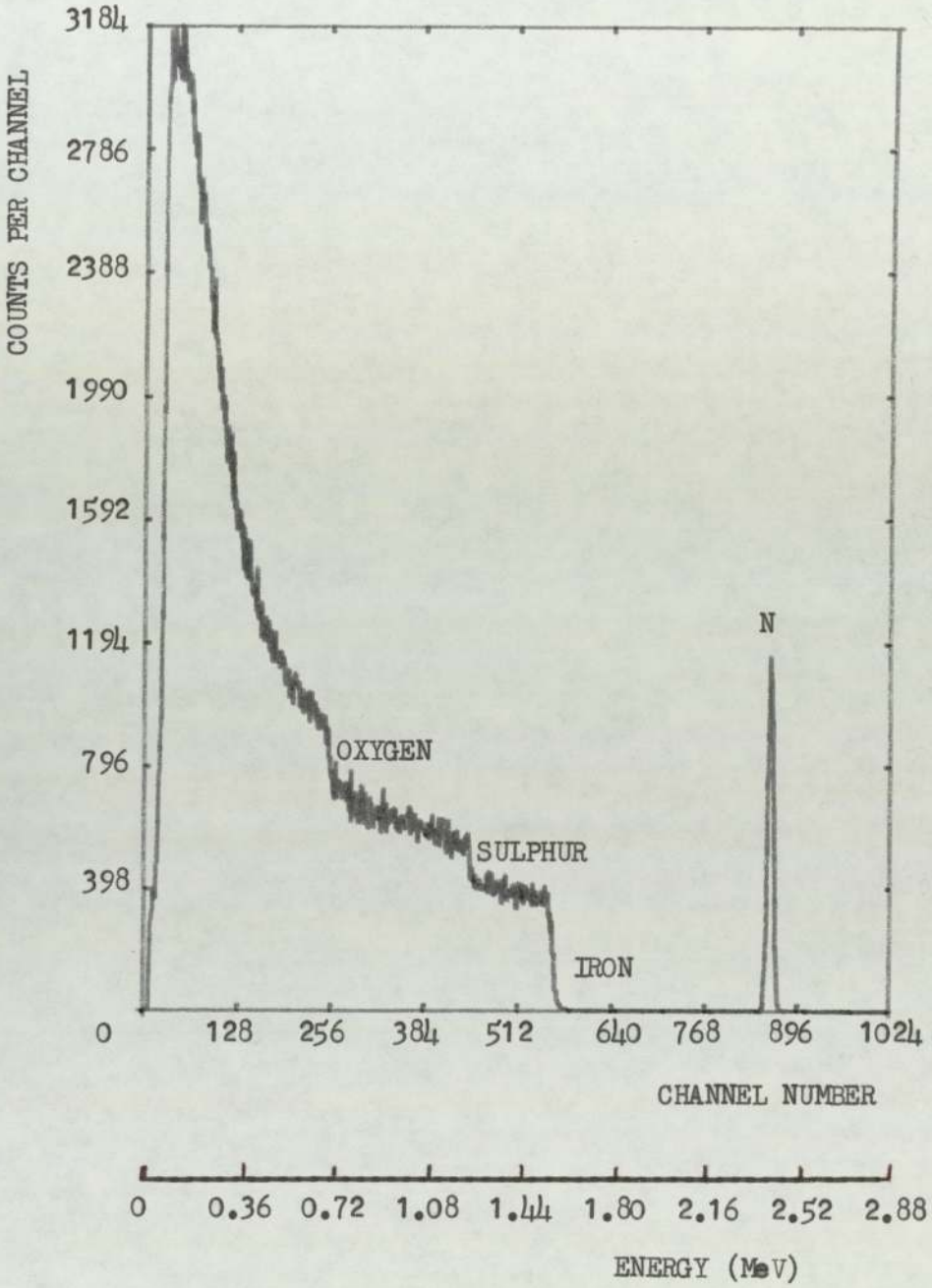

FIG. 5.36 R.B.S. SPECTRUM OBTAINED FOR THE MEDIUM CALIBRATION FILM OF $FeSO_4$.

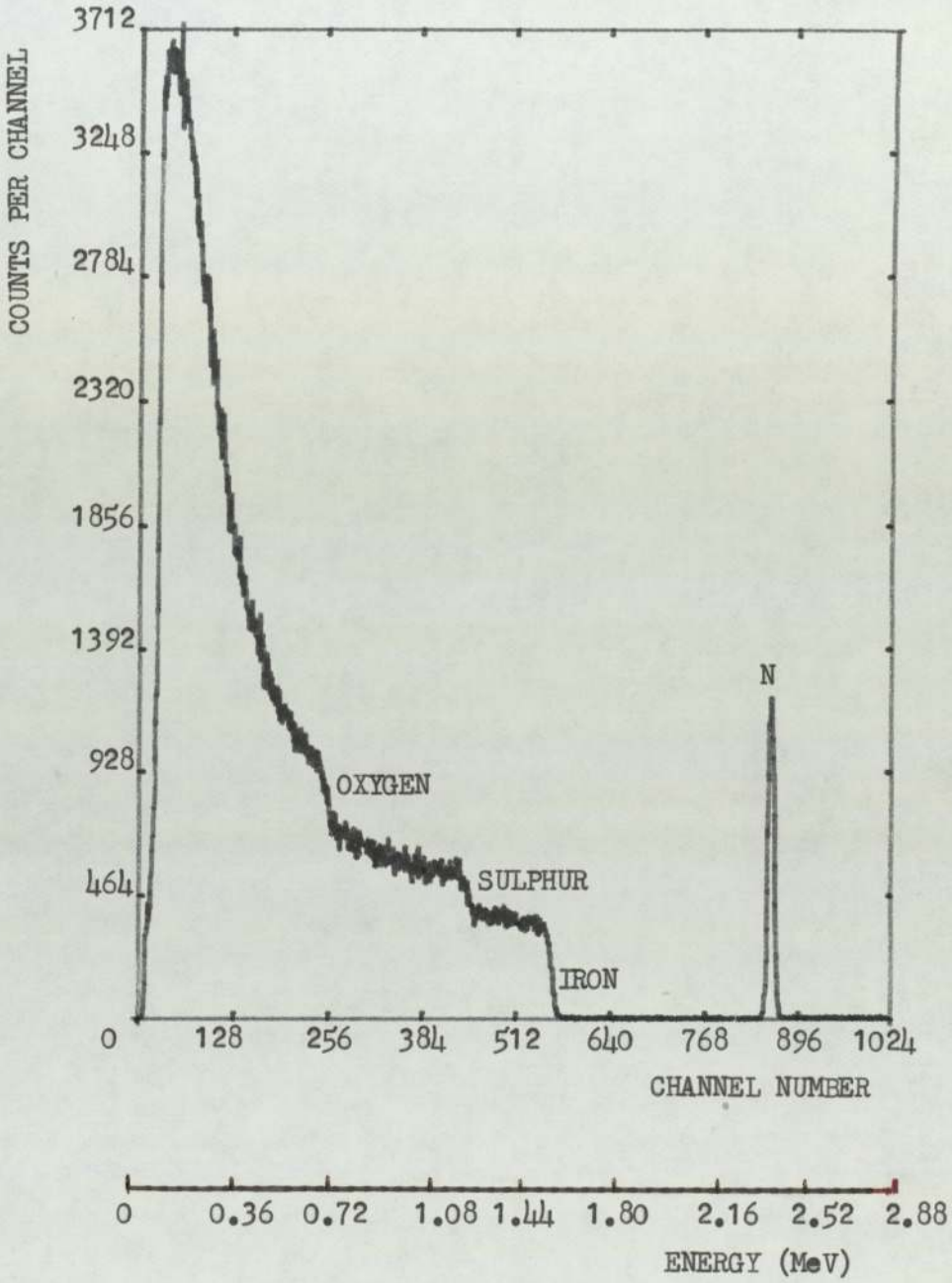

FIG. 5.37 R.B.S. SPECTRUM OBTAINED FOR THE THICK CALIBRATION FILM OF $FeSO_4$.

was not effective. In general, the energy spectrum (Figure 5.38) obtained for each additive, appears to be similar to the one produced for the unworn sample (cf. Figure 5.34), indicating that this nuclear probe technique is also unable to detect the a.w. films known to be present from other techniques.

5.2.2 Extreme-Pressure Films

The results of the investigation conducted by R.B.S. of some selected e.p. films formed with each additive, are summarized in Table 5.6. The latter displays the probability of detecting sulphur on the scars. The sulphur presence starts to show off in films generated under heavy loads (>200 kg) when 0.25% wt elemental sulphur or 1.00% wt DBDS were used as the additive (Figure 5.39 to 5.45). Also the results show that no other element (e.g. oxygen) is detected in the e.p. films by this technique.

In the case of 0.26% wt DBDS, DPDS and DBMS additives, neither sulphur nor other elements were detected during the investigation.

5.3 Summarizing Remark

The experiments discussed in this chapter were designed to demonstrate the limit of employing high energy charged particles as a means for investigating the films generated when elemental and organo sulphur additives were tested on the 4-ball machine.

In the case of films formed under the a.w. regime, the investigation shows that the nuclear techniques are not recommended for use.

Additive	Load (kg)	Test Time (s)	Possible detection of sulphur
0.25% wt Elemental Sulphur	130	60	No
	130	1100	No
	200	60	Yes (small)
	300	60	No (??)
	300	300	Yes
1.00% wt DBDS	130	15	No
	130	60	No
	130	1100	No
	140	60	No
	200	60	Yes (very small)
	300	60	No (??)
	400	60	Yes (Good)
	720	60	Yes (High)
	820	60	Yes (High)
	870	Starting of Welding	No
0.26% wt DBDS	130	60	No
	130	1100	No
	300	11, Welding	No
0.88% wt DPDS	130	60	No
	130	1100	No
	180	Welding	No
0.26% wt DPDS	130	60	No
	130	1100	No
1.74% wt DBMS	130	60	No
	130	1100	No
	140	60	No

Table 5.6: Results of the R.B.S. examination of selected specimens (extreme pressure films).

For the examination carried out on e.p. films, the study demonstrates the possibility of employing (d,p) reactions and R.B.S. techniques as a means for identifying the structure of the layers of these films. However, factors such as the percentage of the additive, the test time and the load used seem to have significant effects on the effectiveness of each method. This point will be discussed in great detail in the General Discussion Chapter. Nevertheless, in general, it can be said that the deuteron-proton stripping reactions are more appropriate in this field than the R.B.S., and this is especially true for films produced by the sulphur and DBDS additives.

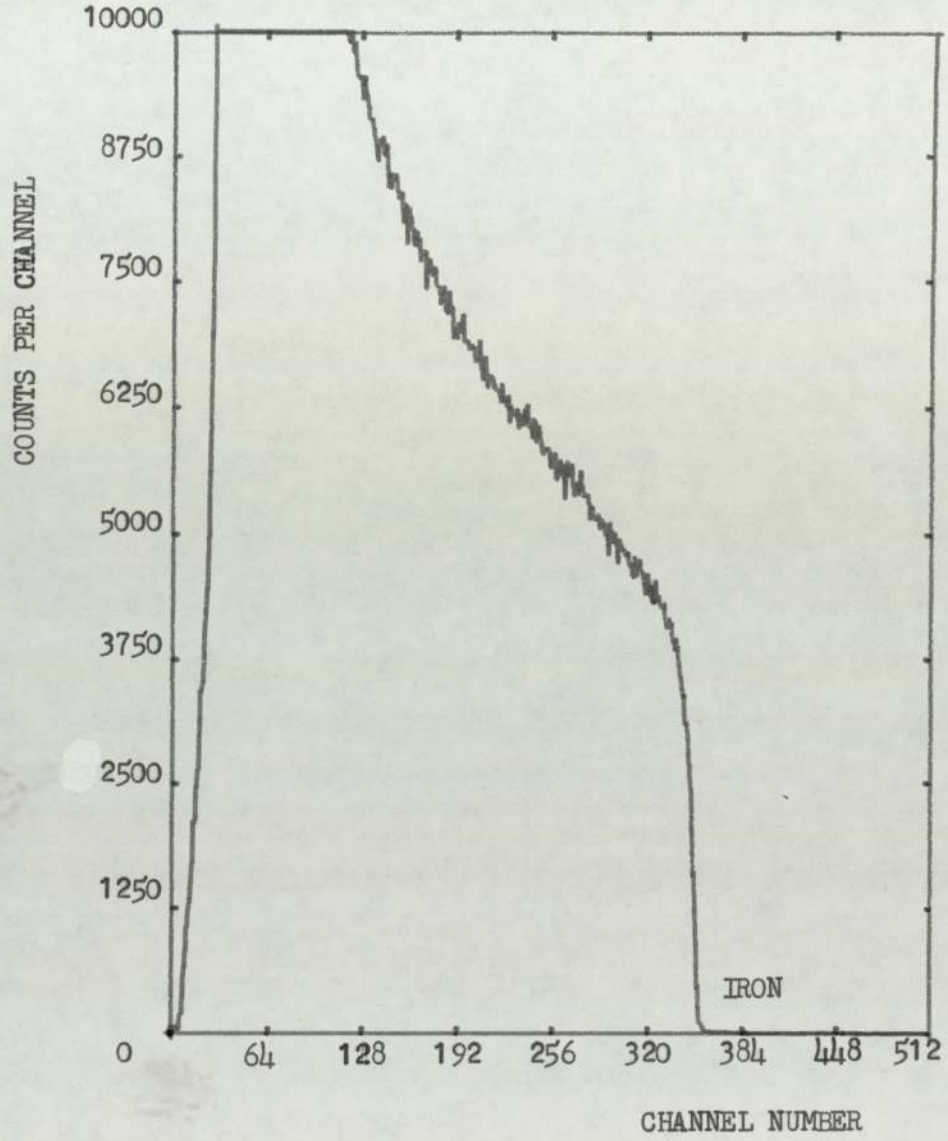

FIG. 5.38 TYPICAL R.B.S. SPECTRUM OBTAINED FOR A.W. FILMS.

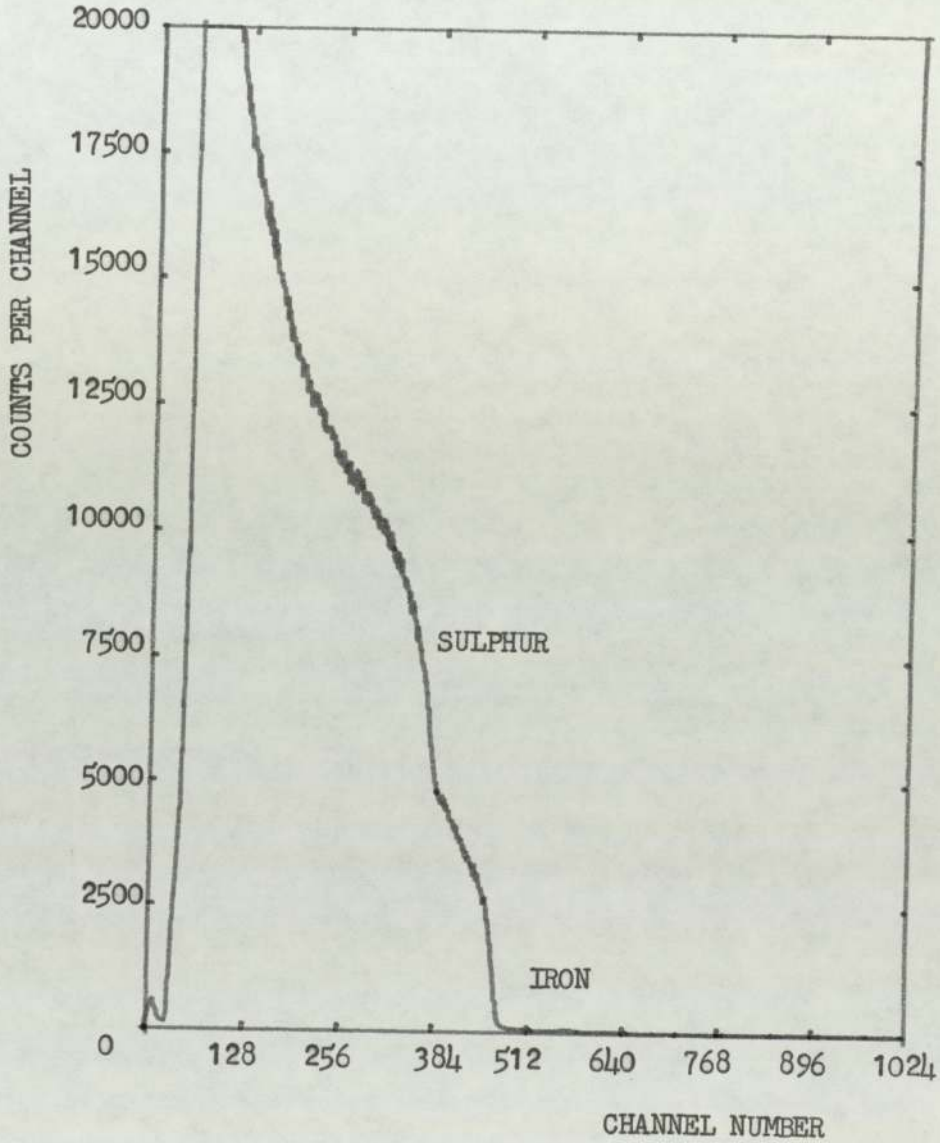

FIG. 5. 39 R.B.S. SPECTRUM OBTAINED FOR THE FOLLOWING SAMPLE :

ADDITIVE : 0.25 % wt ELEMENTAL SULPHUR

APPLIED LOAD : 200 KG

TEST TIME : 60 SECONDS

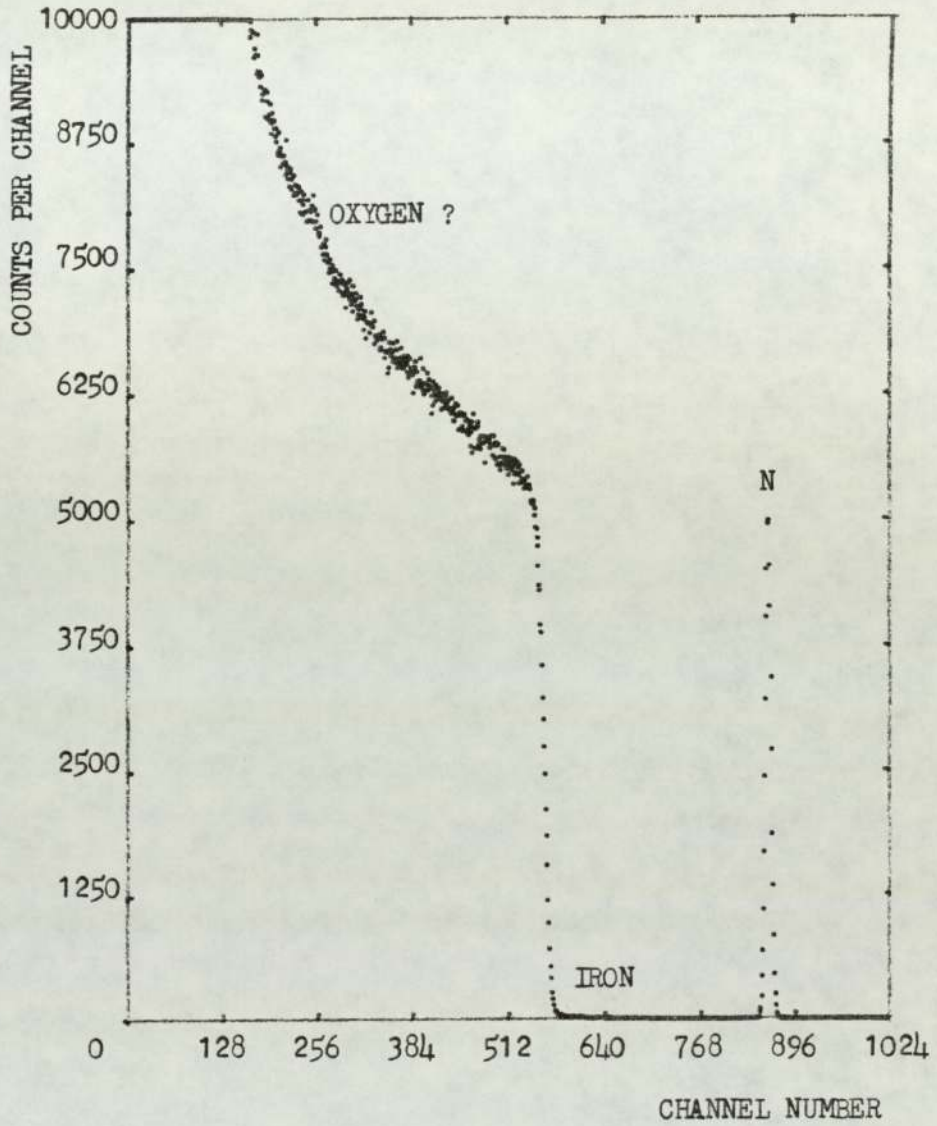

FIG. 5.40 R.B.S. SPECTRUM OBTAINED FOR THE FOLLOWING SAMPLE :

ADDITIVE : 0.25 % wt ELEMENTAL SULPHUR

APPLIED LOAD : 300 KG

TEST TIME : 60 SECONDS

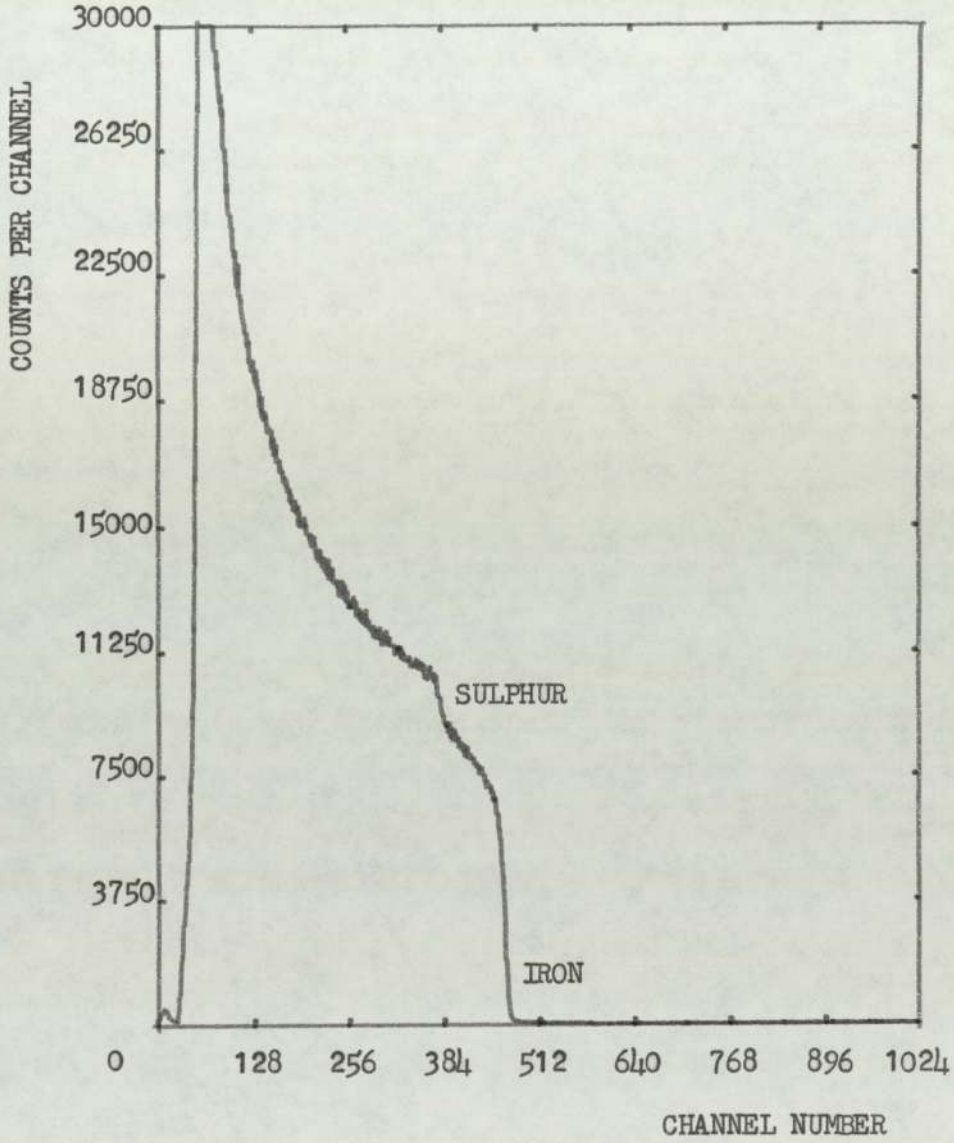

FIG. 5.41 R.B.S. SPECTRUM OBTAINED FOR THE FOLLOWING SAMPLE :

ADDITIVE : 0.25 % wt ELEMENTAL SULPHUR

APPLIED LOAD : 300 KG

TEST TIME : 300 SECONDS

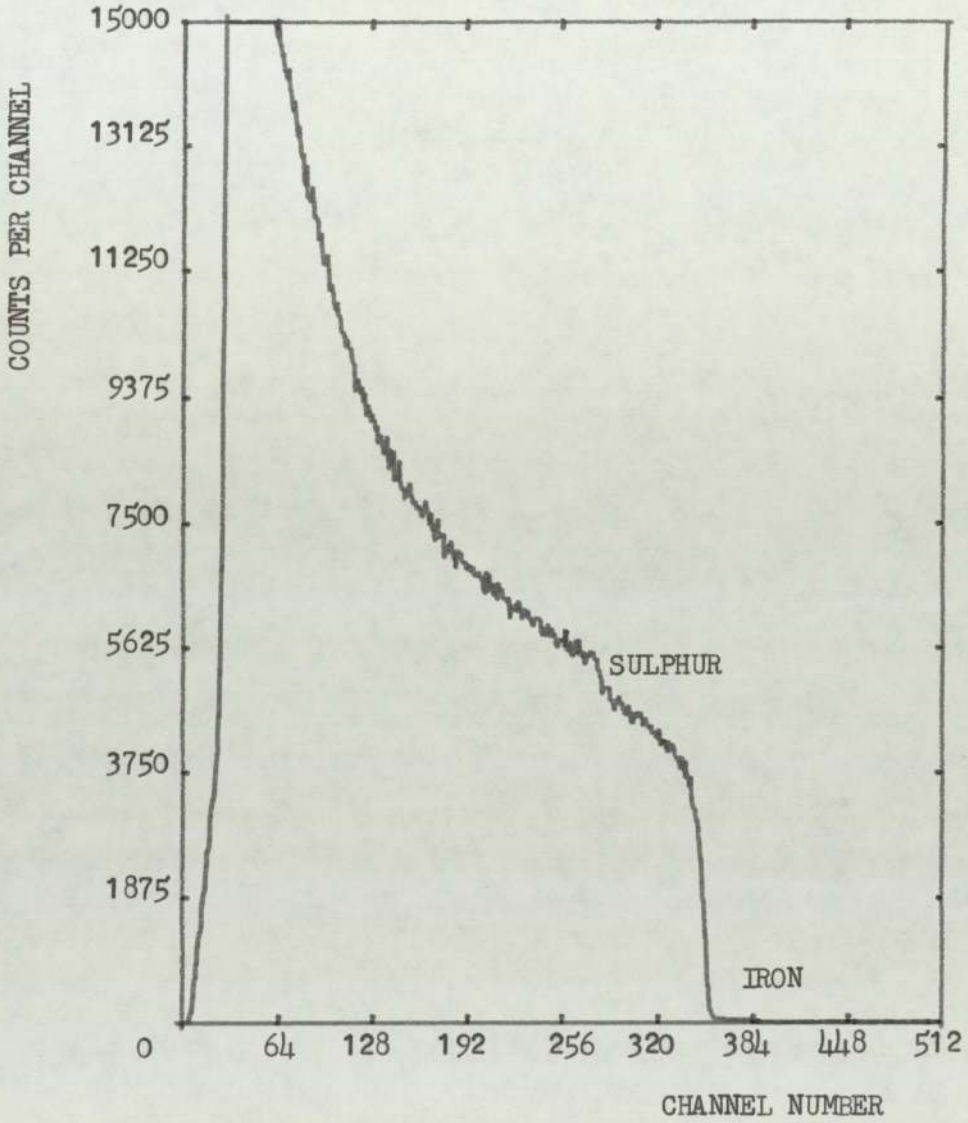

FIG. 5.42 R.B.S. SPECTRUM OBTAINED FOR THE FOLLOWING SAMPLE :

ADDITIVE : 1.00 % wt DBDS

APPLIED LOAD : 200 KG

TEST TIME : 60 SECONDS

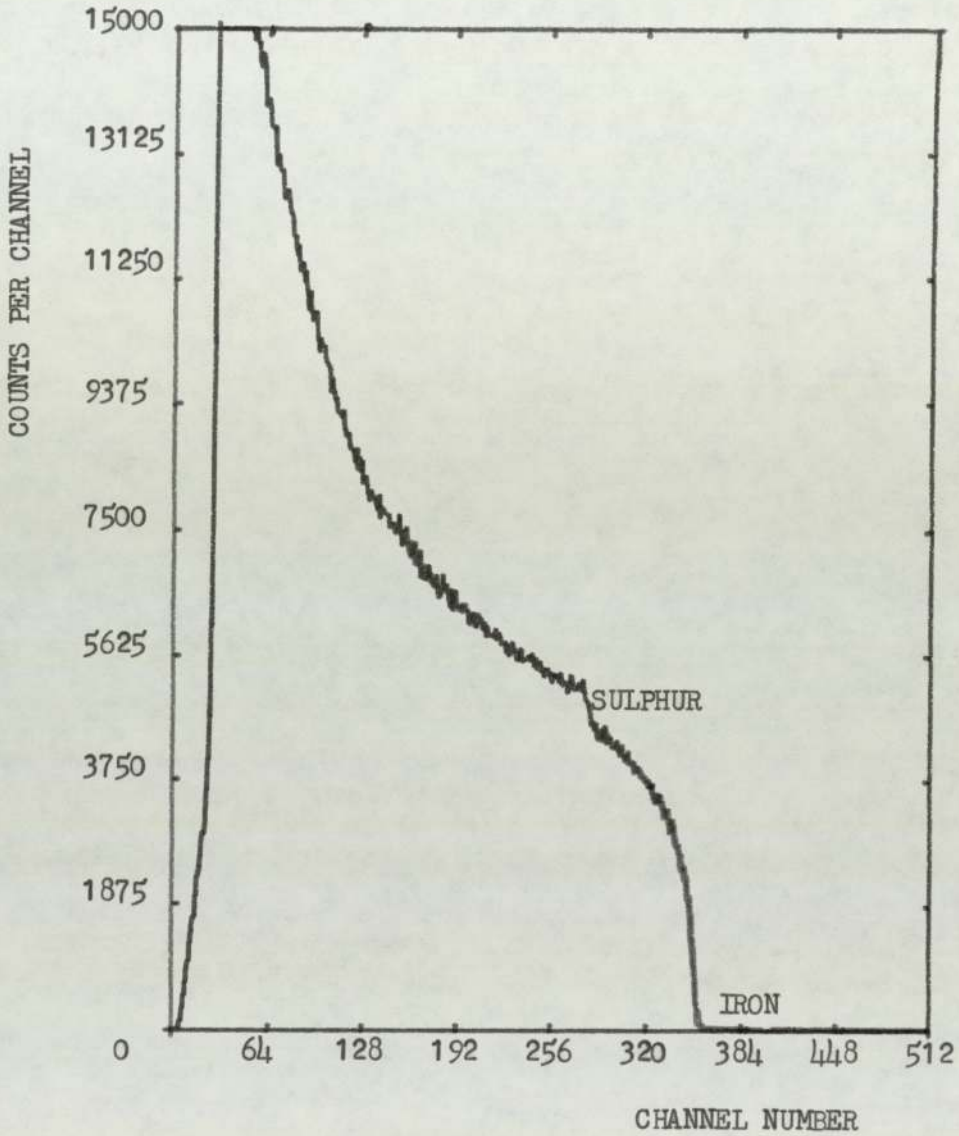

FIG. 5.43 R.B.S. SPECTRUM OBTAINED FOR THE FOLLOWING SAMPLE :

ADDITIVE : 1.00 % wt DBDS

APPLIED LOAD : 400 KG

TEST TIME : 60 SECONDS

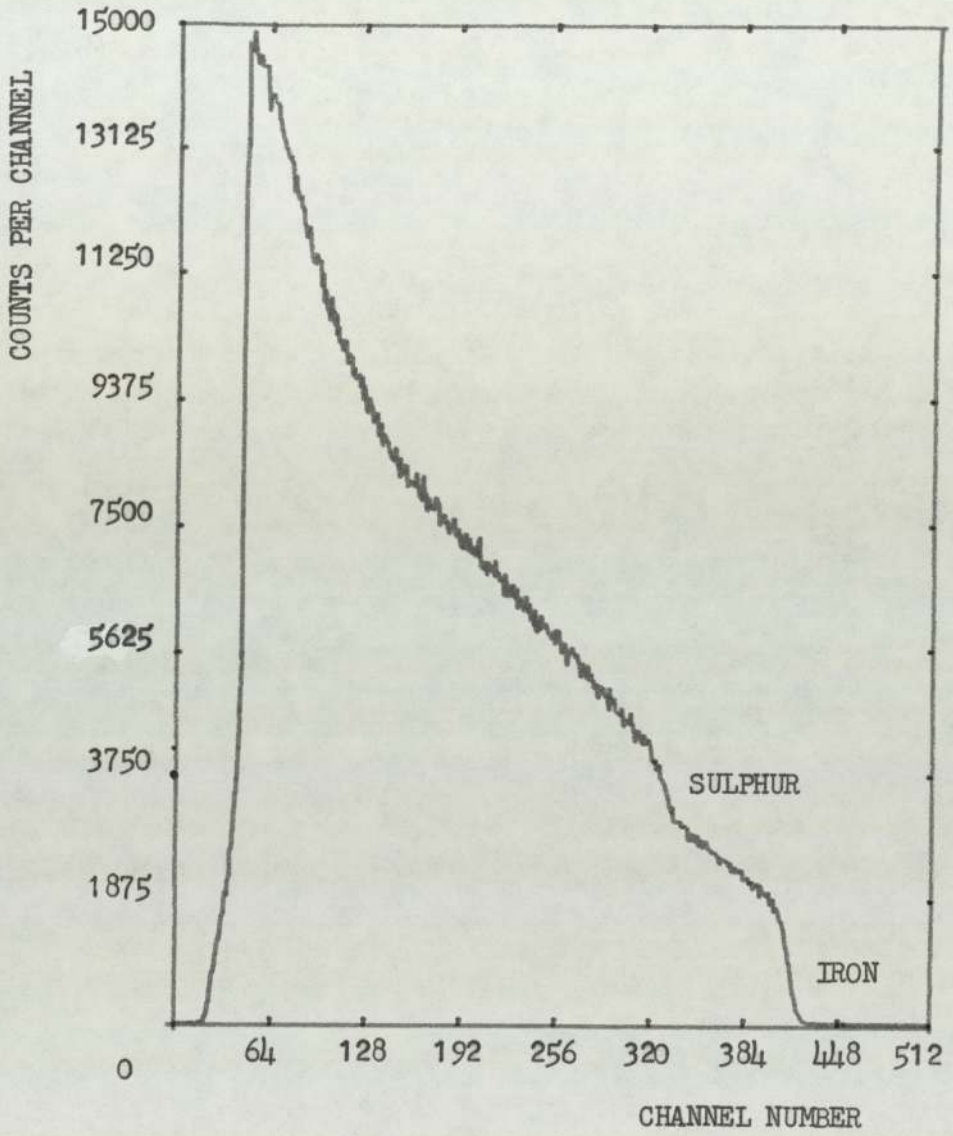

FIG. 5.44 R.B.S. SPECTRUM OBTAINED FOR THE FOLLOWING SAMPLE :

ADDITIVE : 1.00 % wt DBDS

APPLIED LOAD : 720 KG

TEST TIME : 60 SECONDS

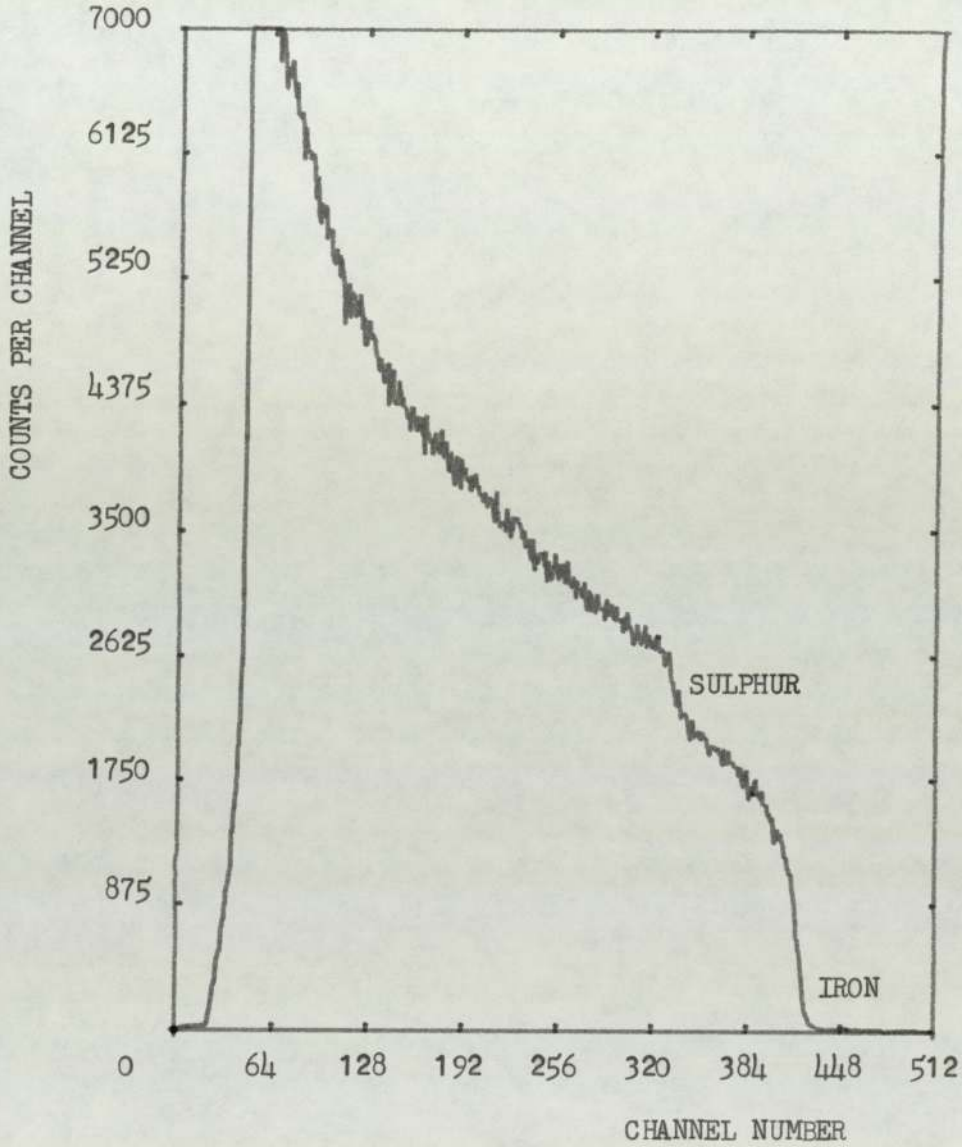

FIG. 5.45 R.B.S. SPECTRUM OBTAINED FOR THE FOLLOWING SAMPLE :

ADDITIVE : 1.00 % wt DBDS

APPLIED LOAD : 820 KG

TEST TIME : 60 SECONDS

CHAPTER SIX

GENERAL DISCUSSION

The literature survey shows that one of the unknown parameters in the study of wear scars produced by organo-sulphur additives, when tested on the 4-ball machine, is still the thickness of the surface layers forming the scar. The previous attempts to apply direct measurement by various techniques, already used in this field, were limited by the geometry of the scar on a spherical steel ball and, above all, by the low thickness of the film.

It is important to point out that much of the discussion is carried out using the C.g.s. units and this is due to the fact that this system is still widely used in Nuclear Physics. However, whenever the S.I. units are used, it will be made clear in the text.

6.1 Calculation of the Film Thickness

The different analyses carried out in this research show that the sulphur is present on the scar and, furthermore, the combination of the results demonstrated that the surface layers are mainly a mixture of inorganic compounds such as FeS, $FeSO_4$ and αFe_2O_3. These findings corroborate the structure of the films and, together with the interpretation of the (d,p) results led to the calculation of the thickness of the surface layers for each sample analysed. Thus the thickness of the sulphur layer alongside with the one corresponding to the above mentioned compounds, was deduced by using the following equation:

$$t = \frac{[N \triangle x] \text{ mol.weight}}{N_A \rho} 10^{-2} \text{ (m)} \qquad \ldots\ldots\ldots(6.1)$$

where $[N \Delta x]$ = average number of sulphur atoms per square centimetre (cf. equation 2.8)

ρ = density of the relevant structure ($g.cm^{-3}$)

N_A = Avogadro's number

Consequently the results found for each examined sample are presented from Table 6.1 to Table 6.5.

6.2 The Relevance of Stopping Power for Protons for Measuring the Thickness of the Surface Reacted Films

During the analysis of the scars by the deuteron-proton stripping reactions, the energy of the incident deuteron will be reduced as the beam penetrates into the lower layers. This slowing-down process is known as the stopping power "S", and its value will depend on the target material and also on the incident energy used. For a given element, "S" is defined as (51):

$$"S" = \frac{dE}{d(\rho x)} \quad (MeV.cm^2/g) \qquad \ldots\ldots\ldots\ldots (6.2)$$

where ρ = density of the considered element

x = thickness of the maximum depth of penetration for the incident beam

E = Energy

However the stopping power for a chemical compound and a mixture can be found from:

$$"S" = \frac{dE}{d(\rho x)} = \frac{\sum_{1}^{n} A_i \left[\frac{dE}{d(\rho x)_i}\right]}{\sum_{1}^{n} A_i} \quad (MeV.cm^2/g) \qquad \ldots\ldots\ldots (6.3)$$

where A_i = (Atomic weight). (number of atoms of that type in the molecule).

Once "S" is found, the result is multiplied by the density of either the element or the chemical compound (according to the case studied), and the product will give the rate of energy loss with the penetrated thickness. The results obtained from these calculations, are summarised in Table 6.6. Thus taking the values of the thickness found for the reference and calibration samples (cf Table 6.1), the energy loss suffered by the incident beam going through the layers of the two main films is deduced for each case. These calculations together with the values of the energy of the deuteron beam leaving the films, are presented in Table 6.7. This indicates that for a beam having energies between 2.00 and 1.80 MeV, the energy loss is comprised between 4 to 145 keV, which gives the value of the final energy between 1.996 to 1.855 MeV. The investigation of the reaction S^{32} (d,p) S^{33} published up to now (52, 53) shows that the cross-section $\sigma(E)$ does not change markedly in the range of 2.00 to 1.88 MeV for either the P_0 or the P_7 peaks (ie for an energy loss of about 120 keV). This energy loss corresponds to the values of 3.50 μm and 2.36 μm in thickness for a sulphur and $FeSO_4$ films respectively. This implies that the sulphur layer on the reference samples should be less than 3.50 μm in thickness, while the $FeSO_4$ film should be less than 2.40 μm in thickness so that equation 2.8 could be applied to the (d,p) results in order to calculate the number of sulphur atoms per square centimetre ($N \triangle x$) in the films. The deduction of the thickness for the reference and calibration samples presented earlier in Table 6.1 indicates that the maximum value found for the film of sulphur on pure silver (reference specimen) is 0.49 μm, whilst the thick $FeSO_4$ film (calibration sample) gives a film thickness of 2.69 μm.

Samples	Average [N Δx] (S atoms.cm^{-2})	"t" calculated film thickness (μm) assuming structure	
		S	$FeSO_4$
Thin film of S on Ag	$4.9\ 10^{17}$	0.13	-
Medium film of S on Ag *	$1.3\ 10^{18}$	0.34	-
Thick film of S on Ag	$1.9\ 10^{18}$	0.49	-
Thin film of $FeSO_4$	$1.5\ 10^{17}$	-	0.12
Medium film of $FeSO_4$ **	$1.6\ 10^{18}$	-	1.32
Thick film of $FeSO_4$	$3.2\ 10^{18}$	-	2.69
Unworn EN31 sample	← No sulphur detected →		

Table 6.1: Calculated film thickness (in μm) for the reference and calibration samples.

(*): Reference samples

(**): Calibration samples

Load (kg)	Test Time (s)	Average [N Δx] (S atoms.cm^{-2})	"t" = calculated film thickness (μm) assuming structure			
			S	FeS	$FeSO_4$	α Fe_2O_3
130	60	$1.2\ 10^{17}$	0.03	0.04	0.10	0.06
130	1100	$1.1\ 10^{18}$	0.28	0.33	0.93	0.54
200	60	$3.2\ 10^{18}$	0.83	0.96	2.71	1.62
300	60	$7.3\ 10^{17}$	0.19	0.23	0.62	0.37
300	300	$2.8\ 10^{18}$	0.73	0.85	2.41	1.44

Table 6.2: Calculated film thickness (in μ m) for the e.p. films when elemental sulphur was used as the additive.

Percentage of DBDS	Load (kg)	Test Time (s)	Average [N Δx] (S atoms.cm^{-2})	"t" = calculated film thickness (μm) assuming structure			
				S	FeS	$FeSO_4$	αFe_2O_3
1.00% wt	130	15	$2.8\ 10^{17}$	0.07	0.09	0.24	0.14
	130	60	← No sulphur detected (??) →				
	130	1100	$4.9\ 10^{17}$	0.13	0.15	0.41	0.25
	140	60	$3.7\ 10^{17}$	0.10	0.11	0.31	0.19
	200	60	$5.8\ 10^{17}$	0.16	0.18	0.52	0.31
	300	60	$8.2\ 10^{17}$	0.21	0.24	0.69	0.41
	400	60	$7.2\ 10^{17}$	0.19	0.22	0.62	0.37
	720	60	$1.2\ 10^{18}$	0.30	0.35	0.98	0.59
	820	60	$5.2\ 10^{17}$	0.13	0.16	0.44	0.26
	870	Starting of welding	← Welding →				
0.26% wt	130	60	-	-	-	-	-
	130	1100	$2.7\ 10^{17}$	0.07	0.08	0.23	0.14
	300	Weld at 11 sec	← Welding →				

Table 6.3: Calculated film thickness (in μm) for the e.p. films when DBDS was used as the additive.

Percentage of DBDS	Load (kg)	Test Time (s)	Average [N Δx] (S atoms.cm^{-2})	"t" = calculated film thickness (μ m) assuming structure			
				S	FeS	$FeSO_4$	α Fe_2O_3
0.88% wt	130	60	$1.6\ 10^{16}$	0.004	0.005	0.014	0.008
	130	1100	$2.2\ 10^{16}$	0.006	0.007	0.018	0.011
	180	Starting of welding	-	-	-	-	-
0.26% wt	130	60	← No sulphur detected, only Si →				
	130	1100	$3.5\ 10^{17}$	0.09	0.11	0.30	0.18
	200	10 sec	← Welding →	-	-	-	-
	300	Welding	-	-	-	-	-

Table 6.4: Calculated film thickness (in μ m) for the e.p. films when DPDS was used as the additive.

Percentage of DBMS	Load (kg)	Test Time (s)	Average [N. Δx] (S atoms.cm^{-2})	"t" = calculated film thickness (μm) assuming structure			
				S	FeS	$FeSO_4$	α Fe_2O_3
1.74% wt	130	60	$3.7\ 10^{16}$	0.009	0.011	0.031	0.019
	130	1100	$7.1\ 10^{16}$	0.018	0.021	0.060	0.036
	140	60	$1.4\ 10^{16}$	0.004	0.005	0.012	0.007
1.00% wt	130	9	Welding	-	-	-	-
0.26% wt	130	< 60	Welding	-	-	-	-

Table 6.5: Calculated film thickness (in μm) for the e.p. films when DBMS was used as the additive.

Deuteron Beam Energy	Rate of energy loss with thickness (keV. μ m^{-1}) for the element or compound targets				
	Fe	S	FeS	$FeSO_4$	αFe_2O_3
2.00 MeV	98.56	34.32	66.43	50.90	80.12
1.90 MeV	101.08	35.33	68.23	52.48	82.36
1.80 MeV	103.67	36.43	70.15	54.09	84.83

Table 6.6: Rate of energy loss with thickness for a deuteron beam.

Samples		2.00 MeV Incident Deuteron Beam		1.90 MeV Incident Deuteron Beam		1.80 MeV Incident Deuteron Beam	
		Rate of Energy Loss (MeV)	Final Energy (MeV)	Rate of Energy Loss (MeV)	Final Energy (MeV)	Rate of Energy Loss (MeV)	Final Energy (MeV)
Thin film of S on Ag	*	$4.46\ 10^{-3}$	1.996	$4.59\ 10^{-3}$	1.995	$4.74\ 10^{-3}$	1.995
Medium film of S on Ag	*	$11.67\ 10^{-3}$	1.988	$12.01\ 10^{-3}$	1.988	$12.39\ 10^{-3}$	1.988
Thick film of S on Ag	*	$16.82\ 10^{-3}$	1.983	$17.31\ 10^{-3}$	1.983	$17.85\ 10^{-3}$	1.982
Thin film of $FeSO_4$	**	$6.11\ 10^{-3}$	1.994	$6.30\ 10^{-3}$	1.994	$6.49\ 10^{-3}$	1.994
Medium film of $FeSO_4$	**	$67.19\ 10^{-3}$	1.933	$69.27\ 10^{-3}$	1.931	$71.40\ 10^{-3}$	1.929
Thick film of $FeSO_4$	**	$136.92\ 10^{-3}$	1.864	$141.17\ 10^{-3}$	1.859	$145.50\ 10^{-3}$	1.855

Table 6.7: Calculated energy losses and final values of the energy of the incident deuteron beam when leaving either the sulphur or the $FeSO_4$ films of the reference and calibration samples respectively.

(*): Reference samples.

(**): Calibration samples.

This demonstrates that the standards do in fact satisfy the criteria mentioned above.

6.3 The Relevance of Penetration Depth to the Microanlaysis of E.P. Films

When examining films by the E.P.M.A., the effective depth of penetration of the electron beam, "x" measured in metres, may be valued (in the case of an element) from the following equation:

$$x = 1.1\ 10^{-14}\left(\frac{A}{Z}\right)\left(\frac{E^2}{\rho}\right)(m) \qquad \text{.....(6.4)}$$

where E is the energy of the incident electron beam in electron volts, ρ is the density of the considered element and $\left(\frac{A}{Z}\right)$ is the ratio of the atomic weight to the atomic number of the element.

If the specimen is a chemical compound the term $\left(\frac{A}{Z}\right)$ becomes $\left(\frac{A}{Z}\right)_{wt}$ and it is expressed as follows:

$$\left(\frac{A}{Z}\right)_{wt} = \frac{\sum_{i}^{n} A_i \quad (A_i/Z_i)}{\Sigma A_i} \qquad \text{.....(6.5)}$$

Thus equation 6.4 could be re-written, in a general form, as:

$$x = 1.1\ 10^{-14}\left(\frac{A}{Z}\right)_{wt}\left(\frac{E^2}{\rho}\right)(m) \qquad \text{.....(6.6)}$$

Using equation 6.6, the effective depth probed by a 15 keV E.P.M.A. beam is evaluated for the elements and the compounds of interest. The results, which are displayed in Table 6.8, suggest that if the formed film of iron-sulphur is less than 1 μ m thick, then the

electron beam will penetrate into the substrate giving rise to spurious measurements.

6.4 Prediction of the Mass Composition from (d,p) Reactions and Electron Probe Microanalysis (E.P.M.A.)

Looking at the calculated film thickness found for the different examined samples (cf.Tables 6.1 to 6.5) and, taking into consideration the values of the effective depth of penetration determined for the main elements and compounds of interest (cf.Table 6.8), one must infer that the electron beam penetrates right through the formed films, and, thereby analyses a part of the substrate as well as the films.

	Element or compound probed					
	Ag	Fe	S	FeS	$FeSO_4$	αFe_2O_3
Effective Depth Probed (μm)	0.54	0.68	2.39	1.09	1.71	0.99

Table 6.8: Effective depth probed by a 15 keV E.P.M.A. beam.

Using equation (6.6) to derive the expression which would give the average energy loss per film thickness and, assuming that the penetrated steel substrate is pure iron, the depth of the probed substrate is easily evaluated.

The average energy loss per film thickness (eV/m) is expressed as follows:

$$\frac{dE}{dx} = \frac{1}{1.1\ 10^{-14}\left(\frac{A}{Z}\right)_{wt}}\ \rho\left(\frac{1}{2E}\right) \qquad \text{.....(6.7)}$$

Once the depth of the probed substrate is calculated, the total composition of the two detected elements (ie Fe and S) is deduced, then the calculated values are compared to those experimentally found with the use of the E.P.M.A.

To show how the procedure was carried out, the calculations developed on one of the calibration samples (e.g. Thick film of $FeSO_4$) are shown below. The thickness, t, found for that film is 2.69 μm (cf. Table 6.1).

The rate of energy loss per thickness film of $FeSO_4$, when analysed by a 15 keV incident electron beam, is found by developing the equation (6.7):

$$\left(\frac{dE}{dx}\right)_{FeSO_4} = \frac{1}{1.1\ 10^{-14}\left(\frac{A}{Z}\right)_{FeSO_4}} \rho_{FeSO_4} \frac{1}{2(15)\ 10^3}$$

which gives $\frac{dE}{dx} = 4.384\ \frac{keV}{\mu m}$

Therefore the energy loss (E.L.) suffered by the incident beam after passing through the 2.69 μm film of $FeSO_4$, is:

$$(E.L.) = \frac{(2.69\ \mu m)(4.384)\ keV}{1\ \mu m} = 11.79\ keV$$

Thus, just before entering the substrate, x, the beam will have an energy, E', which is the difference between the initial energy, E, and the energy loss, E.L.:

$$\therefore\ E' = E - (E.L.)$$

that is $E' = (15 - 11.79)$ keV $= 3.21$ keV.

Consequently the effective depth probed into the substrate by the 3.21 keV beam is found by using equation (6.6), which becomes after the terms were replaced by their respective values:

$$x_{sub} = (1.1\ 10^{-14})(2.1477)\frac{(3.21\ 10^{3})^{2}}{7.86} = 3.097\ 10^{-8}\text{m}$$

$$x_{sub} = 0.031\ \mu\text{m}.$$

The relative depths are shown diagrammatically below:

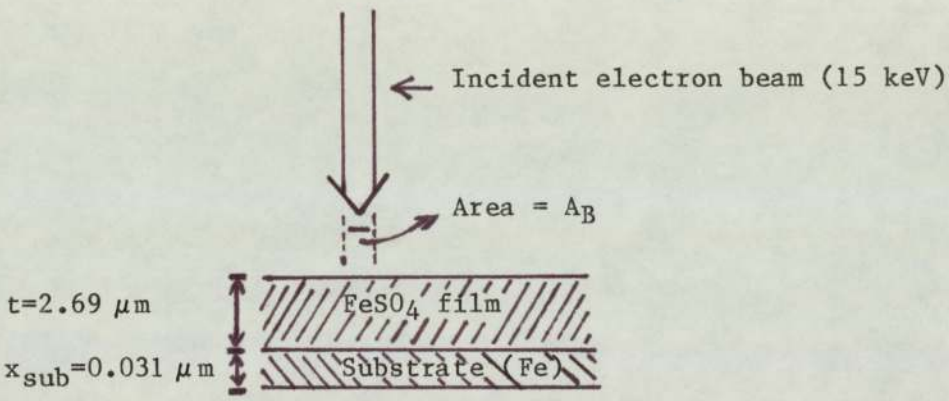

Figure 6.1

- Volume of $FeSO_4$ "probed", $V_{FeSO_4} = t(A_B) = (2.69)A_B$

- Volume of the Fe substrate "probed", $V_{Fe} = {}^{x}A_B = (0.031)\ A_B$

As the density is equal to the ratio of the mass to the volume, one can use this statement to work out the respective masses.

$$\therefore\ M_{FeSO_4} = \rho_{FeSO_4} \cdot V_{FeSO_4} = (2.97)(2.69)A_B \triangleq (7.99)A_B \quad \text{.....(6.8)}$$

and

$$M_{Fesub} = \rho_{Fe} \cdot V_{Fe} = (7.86)(0.031)A_B \triangleq (0.24)A_B \quad \text{.....(6.9)}$$

In the $FeSO_4$ film, the respective masses of Fe, S and O are defined as follows:

$$\text{Mass of Fe} = M_{FeSO_4} \frac{\text{(Atomic weight of Fe)}}{\text{(Mol. weight)}_{FeSO_4}} \quad \ldots\ldots(6.10)$$

$$\text{Mass of S} = M_{FeSO_4} \frac{\text{(Atomic weight of S)}}{\text{(Mol. weight)}_{FeSO_4}} \quad \ldots\ldots(6.11)$$

$$\text{Mass of O} = M_{FeSO_4} \frac{4\text{(Atomic weight of O)}}{\text{(Mol. weight)}_{FeSO_4}} \quad \ldots\ldots(6.12)$$

which will take the following results after replacing the terms by their respective values:

$$\text{Mass of Fe} = (2.94)A_B \quad \ldots\ldots(6.13)$$

$$\text{Mass of S} = (1.69)A_B \quad \ldots\ldots(6.14)$$

$$\text{Mass of O} = (3.37)A_B \quad \ldots\ldots(6.15)$$

Now the total mass of Fe probed is equal to the mass of Fe from the $FeSO_4$ film (equation 6.13) plus the mass of the iron of the substrate (equation 6.9):

$$\therefore \text{ Total Mass of Fe "probed"} = (2.94)A_B + (0.24)A_B$$

$$\text{Total Mass of Fe "probed"} = (3.18)A_B \quad \ldots\ldots\ldots(6.16)$$

Thereby the total mass composition of the three elements detected by the beam is equal to the sum of their respective mass (cf. equations 6.16, 6.14 and 6.15):

$$\therefore \quad \text{General Total Mass} = (3.18 + 1.69 + 3.37)A_B$$

$$\text{General Total Mass} = (8.24)A_B \qquad \text{.....(6.17)}$$

Consequently, the percentage of the mass composition for each detected element is easily found:

i) Iron:

$$\% \text{ Fe} = \left[\frac{\text{Total Mass of Fe "probed"}}{\text{General Total Mass}}\right] 100 \qquad \text{.....(6.18)}$$

Therefore,

$$\text{Fe} = \left[\frac{(3.18)A_B}{(8.24)A_B}\right] 100 = 38.59\%$$

ii) Sulphur:

$$\% \text{ S} = \left[\frac{\text{Mass of S "probed"}}{\text{General Total Mass}}\right] 100 \qquad \text{.....(6.19)}$$

$$\Longrightarrow \quad \text{S} = \left[\frac{(1.69)A_B}{(8.24)A_B}\right] 100 = 20.51\%$$

iii) Oxygen:

$$\% \text{ O} = \left[\frac{\text{Mass of O "probed"}}{\text{General Total Mass}}\right] 100 \qquad \text{.....(6.20)}$$

$$\Longrightarrow \quad \text{O} = \left[\frac{(3.37)A_B}{(8.24)A_B}\right] 100 = 40.90\%$$

Similar procedures are employed for the determination of the percentage composition of the other films used as standard samples. The results together with the observed values for these reference and calibration specimens, are summarised in Table 6.9. This reveals that the agreement between the calculated and observed values is most satisfactory.

The latest observation is taken as a good reference for calculating the percentage of the mass composition for each of the three main films (ie sulphur, FeS and $FeSO_4$) formed on the wear scars produced when elemental sulphur and organo-sulphur additives are tested on the 4-ball machine. Thus a summary of the calculated values alongside with the ones experimentally recorded on the E.P.M.A. for the analysed samples, is presented in Table 6.10. The comparison between the calculated and the observed values leads to the following observations:

(i) On the whole, there is a fair agreement between the results.

(ii) In the case of using 0.25% wt elemental sulphur as the additive, the $FeSO_4$ structure seems more predominant with the exception near the welding region where the FeS structure appears to prevail.

(iii) The same phenomenon is observed when 1.00% wt DBDS is used as the additive. The $FeSO_4$ film appears to be the major constituent part of the surface layers. But however, near the welding region and, even though the complete data is not available, it can be speculated that the FeS structure is the one more likely to prevail.

Samples	Predicted Mass composition				E.P.M.A. Results			
	S (% wt)	Fe (% wt)	Ag (% wt)	O (% wt)	S (% wt)	Fe (% wt)	Ag (% wt)	O (% wt)
Thin film of S on Ag	4.79	-	95.21	-	6.25	-	87.00	-
Medium film * of S on Ag	12.48	-	87.59	-	13.70	-	80.00	-
Thick film of S on Ag	17.97	-	82.03	-	← Not Analysed →			
Thin film of $FeSO_4$	1.41	95.76	-	2.83	← Not Analysed →			
Medium film ** of $FeSO_4$	13.93	58.39	-	27.68	14.00	56.00	-	30.00
Thick film of $FeSO_4$	20.51	38.59	-	40.90	24.16	28.06	-	47.78

Table 6.9: Comparison of the predicted mass compositon with the E.P.M.A. results.

(*): Reference Samples (**): Calibration Samples

Additive	Load (kg)	Test Time (s)	Predicted Elemental Composition assuming structure						E.P.M.A. Results		Possible Structure
			S Film		FeS Film		$FeSO_4$ Film		S (%wt)	Fe (%wt)	
			S (%wt)	Fe (%wt)	S (%wt)	Fe (%wt)	S (%wt)	Fe (%wt)			
0.25% wt Elemental Sulphur	130	60	1.16	98.83	1.31	98.70	1.18	96.47	10.71	86.58	?
	130	1100	10.95	89.05	10.54	89.46	10.42	68.84	7.46	49.43	$FeSO_4$
	200	60	32.21	67.79	26.78	73.22	20.53	38.53	17.31	74.32	FeS
	300	60	7.46	92.54	7.46	92.54	7.25	78.44	16.71	78.87	$FeSO_4$
	300	300	28.18	71.82	24.54	75.54	19.84	40.61	22.50	70.67	FeS
1.00% wt DBDS	130	15	2.72	97.28	2.94	97.06	2.85	91.46	*	*	?
	130	60	-	-	-	-	-	-	3.61	90.70	?
	130	1100	13.21	94.91	4.86	95.14	4.84	85.49	7.30	87.80	$FeSO_4$
	140	60	6.23	96.11	3.57	96.43	3.64	89.07	9.97	89.50	$FeSO_4$
	200	60	6.27	93.73	5.83	94.17	6.04	81.91	20.58	74.19	$FeSO_4$
	300	60	8.20	91.80	7.82	92.18	7.96	76.15	17.09	72.40	$FeSO_4$?
	400	60	7.46	92.54	7.10	92.90	7.22	78.37	18.36	68.27	$FeSO_4$?
	720	60	11.81	88.19	11.16	88.84	11.00	67.04	15.34	41.33	$FeSO_4$/ FeS
	820	60	5.08	94.92	5.21	94.79	5.19	84.46	*	*	-
	870	starting	Welding ←		No sulphur detected			→	1.14	95.17	-
0.26% wt DBDS	130	1100	2.72	97.28	2.59	97.41	2.71	91.88	3.60	95.50	?
0.88% wt DPDS	130	60	0.15	99.85	0.17	99.83	0.17	99.49	5.32	71.13	?
	130	1100	0.23	99.77	0.23	99.78	0.21	99.38	5.78	22.09	?
0.26% wt DPDS	130	1100	3.51	96.49	3.57	96.43	3.55	89.36	3.26	84.20	$FeSO_4$
1.74% wt DBMS	130	60	0.40	99.64	0.36	99.64	0.36	98.90	*	*	?
	130	1100	0.70	99.30	0.70	99.30	0.68	97.90	6.11	54.46	?
	140	60	0.15	99.85	0.17	99.83	0.57	98.26	*	*	-

Table 6.10: Comparison between calculated elemental composition predicted from the interpretation of the calculated film thickness and the E.P.M.A. mass composition results.

(*): Not analysed

(iv) In the event of employing 0.26% wt DBDS, DBMS and DPDS as the additives, none of the films seem more likely than any other. This is due to the very low value of the thickness of the layers evaluated from the (d,p) experiments.

6.5 The Interpretation of the Rutherford Backscattering Results from Surface Reacted Films

The conclusion drawn in the previous chapter states that the deuteron-proton stripping reactions are more adequate in this field than R.B.S.. Although the latter has shown some positive sign by detecting sulphur in some samples, practical factors have limited the results to be exploited efficiently.

The results listed in Table 5.6 reveal that, in the case of using either 0.25% wt elemental sulphur or 1.00% wt DBDS as additives, the probability of detecting the sulphur element belonging to the surface layers increases with the applied load. In other words, the probability gets higher when the formed films becomes thick. The theory of the technique (54) suggests that the probability of backscattering (ie the cross-section) is proportional to the square of the atomic number (Z) of the target. This makes the detection of light elements (e.g. S) of heavy substrates (e.g. Fe) very difficult unless the amount of the former is considerable.

However, when the detection is very positive, one has to know the exact composition of the film layers in order to work out their different thicknesses by applying a computer curve-fitting programme to the experimental results. This programme is based on an analytical solution to backscattering spectra (55), and one of the needed input

data is the chemical symbols of the target, which, in this case, indicates the films developed on the wear scar. More precisely during the elaboration of the programme, the elements in the target input must be specified as a function of depth. Therefore, several iterations of input are necessary before a perfect matching of the various thicknesses to the observed spectrum is reached.

This has been achieved for the thick and medium $FeSO_4$ calibration films as it can be seen in Figures 6.2 and 6.3 respectively. The dotted curves are the experimental spectrum, whilst the solid curves represent the theoretical fit. Both fittings can be regarded as most satisfactory.

Efforts to fit R.B.S. spectra of two samples were carried out. The description of these samples is as follows:

	Additive	Load	Test Time
Sample N° 1	0.25% wt Elem. Sulp	130 kg	1100 seconds
Sample N° 2	1.00% wt DBDS	400 kg	60 seconds

From the different analyses carried out in this research, the structure of the layers appears to be composed by a mixture of chemical compounds. As a result of this, it is not practically possible to input the right chemical formula during the elaboration of the computer-programme. Nevertheless, by assuming that the layers are mainly composed of FeS, attempts to match the spectra 1 and 2 were carried out, and the final results are shown in Figures 6.4 and 6.5 respectively. As it can be seen, both theoretical fits, which are represented by the solid

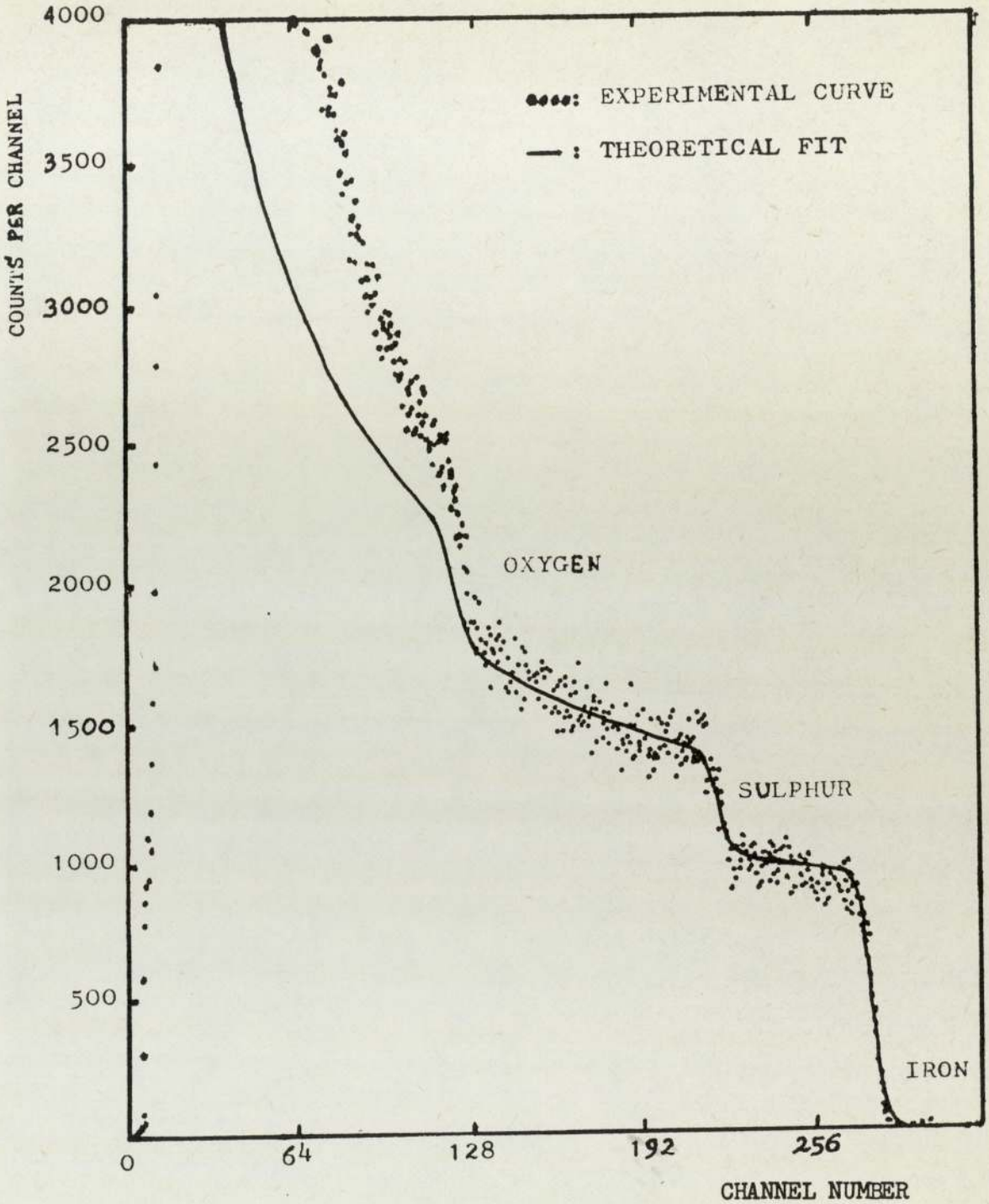

FIG. 6.2 EXPERIMENTAL RESULTS FOR R.B.S. OF THE THICK $FeSO_4$ CALIBRATION FILM.

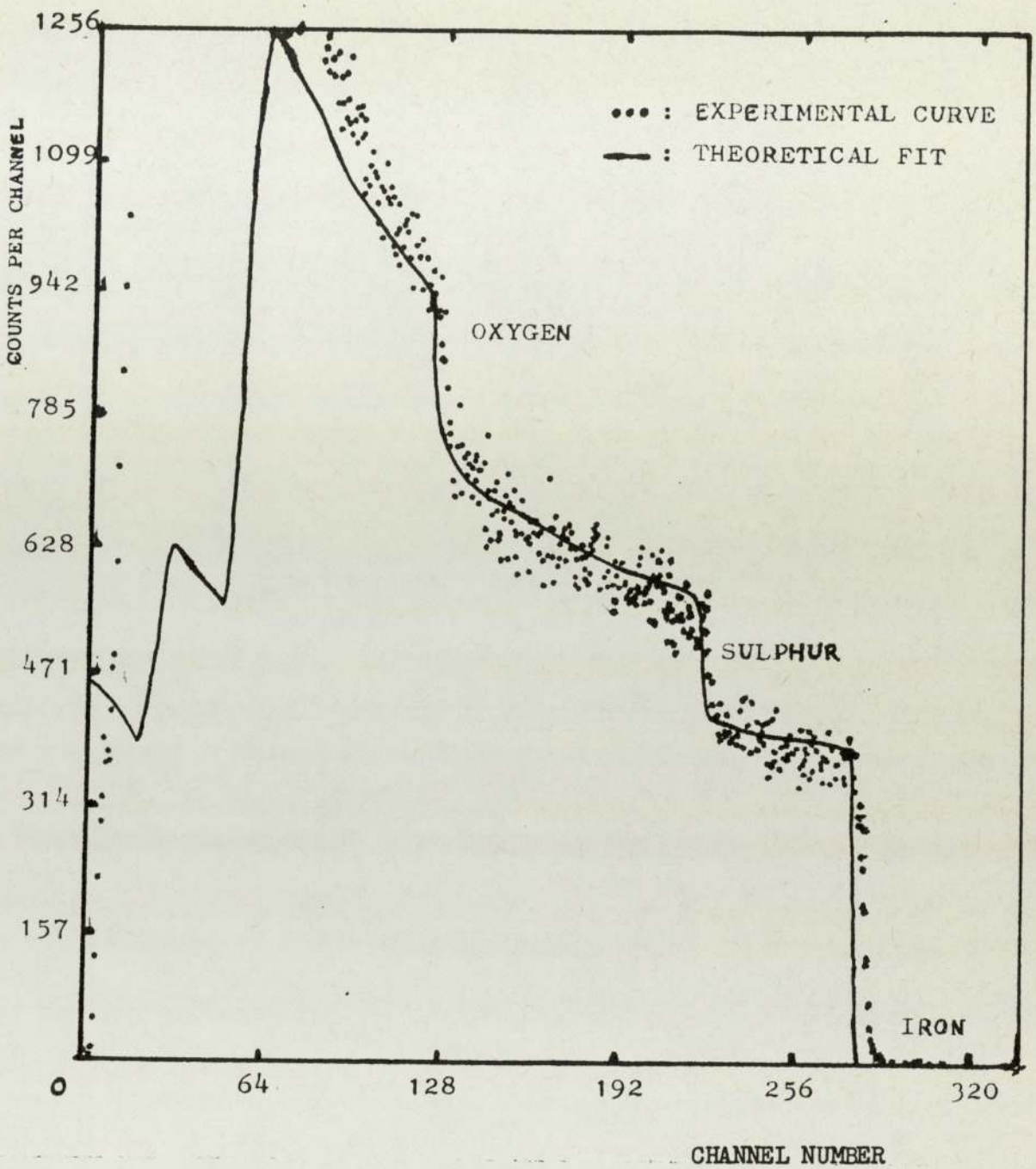

FIG. 6.3 EXPERIMENTAL RESULTS FOR R.B.S. OF THE MEDIUM $FeSO_4$ CALIBRATION FILM.

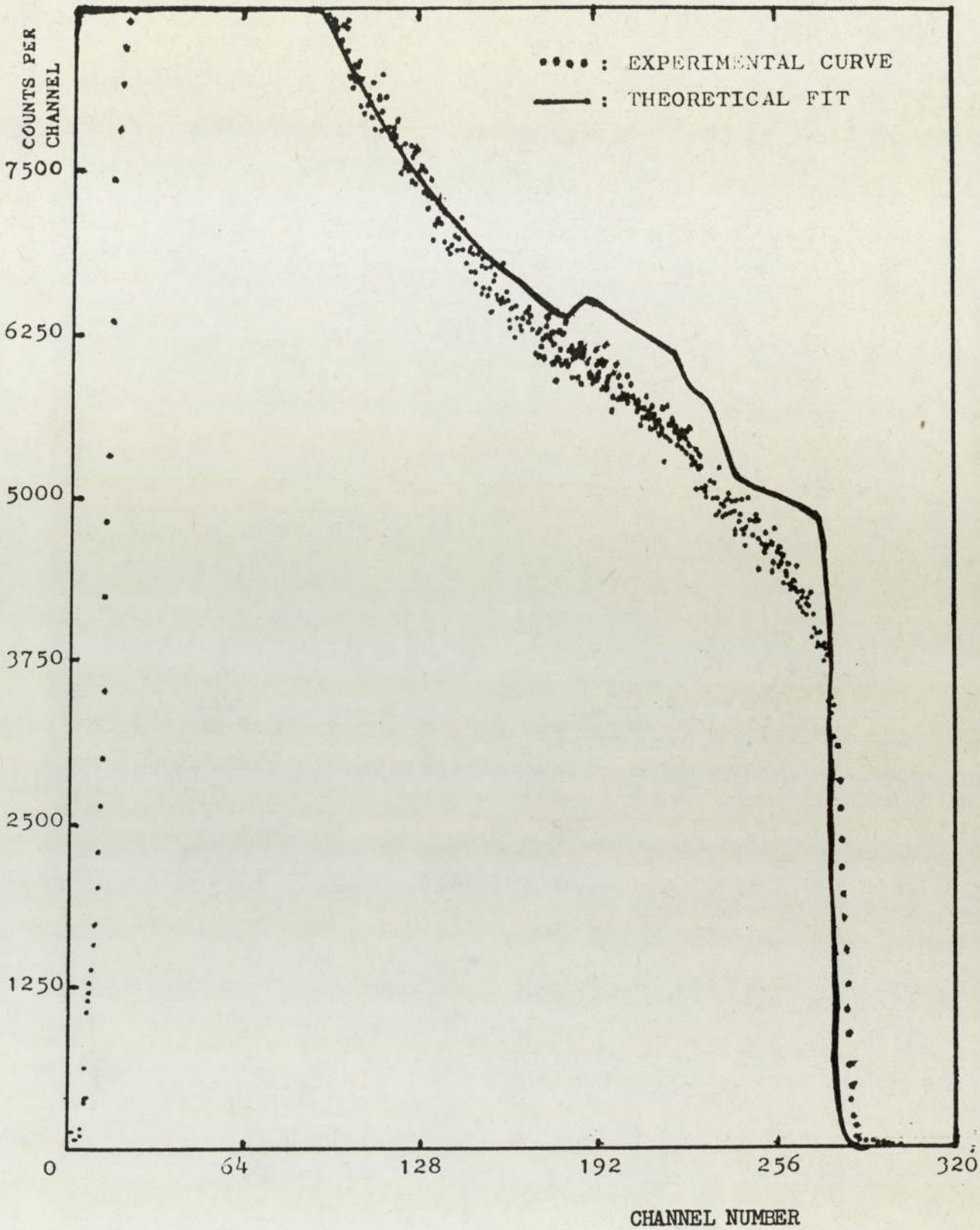

FIG. 6.4 EXPERIMENTAL RESULTS FOR R.B.S. OF THE SAMPLE N. 1 : (0.25 % wt ELEM. SULPHUR, 130 KG, 1100 SECONDS).

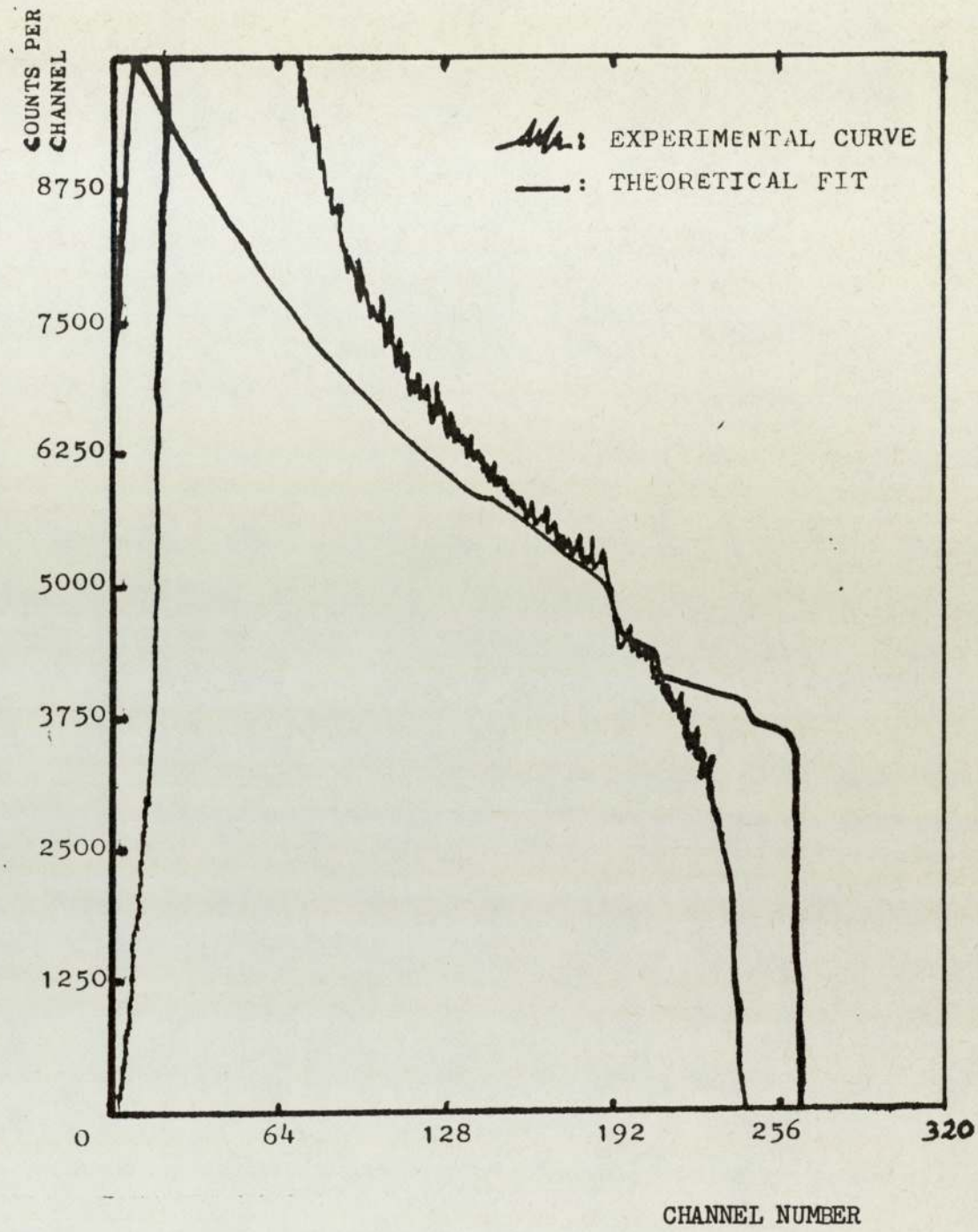

FIG. 6.5 EXPERIMENTAL RESULTS FOR R.B.S. OF THE SAMPLE N. 2 : (1.00 % wt DBDS, 400 KG, 60 SECONDS).

lines, are very unsatisfactory, and this is even after several iterations of data input. This demonstrates and confirms that the surface layers are formed by a mixture of compounds namely FeS, $FeSO_4$ and αFe_2O_3 with different degrees of predominance for each sample. This observation has substantially contributed to the withdraw of attempting the computer curve-fitting. As a general conclusion, R.B.S. is not recommended for detecting sulphur or mainly iron substrates unless the e.p. film is very thick.

6.6 Proposed Mechanisms of A.W. and E.P. Film Formation

Although the existence of films formed during wear tests using a four-ball machine has been confirmed by conventional physical methods of analysis, there is very little reference in the literature about the distribution and thickness of these layers. As stated earlier, the thickness is still one of the unknown parameters in this field. The load-carrying action of the additives could be determined by the properties and the thickness of the layers produced during the tests. Thus one of the most important results of this investigation is the achievement of the evaluation of the thickness by interpretating the results from different methods of analysis, namely conventional techniques coupled with a nuclear microprobe (ie deuteron-proton stripping reactions).

R. C. Coy (8) reported that the reacted layers on the scars formed with 1.00% wt DBDS additive, were very thick under the e.p. region. He predicted a value between 2 to 4 μm in thickness for these layers. Utilising the E.P.M.A. to detect the sulphur element and to measure both its concentration and distribution over the worn surfaces produced by a series of oil containing organic disulphides, Allum and

Forbes (10) observe that in the a.w. region very little sulphur was present, whilst in the e.p. region, large quantities of sulphur were detected. The analyses revealed that the sulphur distribution was uneven. These authors (10) assumed that the layers of the worn areas were mainly composed by FeS compound and in addition, they estimated that the maximum thickness of these layers was between 0.3 to 0.5 μm. Using Auger Electron Spectroscopy (A.E.S.) incorporated with argon-iron sputtered technique, McCarrol and his colleagues (23) built up an approximate composition profile of the surface region of the wear scars formed with two sulphur-containing compounds, DBDS and di-tert-nonyl polysulphide. They observed that the sulphur decreased gradually with increasing depth, then stayed constant below a depth of around 0.01 μm. They concluded that iron sulphide results from the reaction taking place between the additive and the metal, and also the magnitude of the reacted layers was in the order of 10^{-2} to 10^{-1} μm.

In conclusion, the calculated film thickness of the FeS layer produced by the three aromatic sulphide (Tables 6.3, 6.4 and 6.5) are comparable to the estimation made by Allum and Forbes (10), and also by McCarrol et al.. As a result of this, the prediction made by Coy (8) appears somewhat exaggerated. As the calculated values were the source of the predicted mass compositions carried out, and which they were comparable to those found experimentally by using the E.P.M.A., one can conclude that the evaluation of the thickness concluded in this research is very realistic.

The 4-ball standard one minute tests indicate that Risella 32 on its own, presents a mediocre a.w. performance and has no e.p. activity. The addition of the sulphur compounds into the lubricant has mainly

been beneficial to the e.p. regime. During the a.w. regime, the additives manifest, to a certain extent, the same performance produced by the oil. Therefore this signifies that during this period, they contribute very little, and this result only justifies the already-known poor a.w. activity of the sulphur additives (56). At the end, it is worth mentioning again the similarity of the a.w. performance achieved between the monosulphides (ie elemental sulphur and DBMS) on one hand, and between the disulphides (ie DBDS and DPDS) on the other hand.

As mentioned above, these additives turned out to be more efficient under the e.p. regime, which means that they were able to increase the seizure load of the lubricant. However, the increasing order observed for the e.p. effectiveness of the four sulphur additives tested, was found as follows:

DBMS < DPDS < Elemental Sulphur < DBDS

Considering just the organic sulphides, the above rating satisfies the proposed statement made by Forbes and Reid (11) in which, they assert that the monosulphides and the mercaptans are less reactive than the corresponding disulphides.

Concerning the assessment of these four additives by the use of the 4-ball machine, the nearest published work was carried out by Sethuramiah, Okabe and Sakurai (35), who mixed the additives into a medicinal grade white oil at a concentration of 0.294% weight sulphur (9.17 millimoles of sulphur per 100 gms of blend) compared to 0.25% weight sulphur into a white mineral oil (7.8 millimoles of sulphur per 100 gms of blend) used in this work. Table 6.11 displays the weld loads

Additives	Weld Load (kg)	
	Thesis	Sethuramiah et al
Elemental Sulphur	340	280
DPDS	220	180
DBDS	920	200
DBMS	160	180

Table 6.11: Comparison of weld load for a series of four sulphur additives at a concentration of 0.25% weight sulphur in a white mineral oil (Thesis) and 0.294% weight sulphur in a medicinal grade white oil (Sethuramiah et al).

obtained for these additives by Sethuramiah et al, and also those obtained in this research. [The load refers to the machine, ie the total applied load in kg]. The Table shows that the additives have comparable final seizure loads, except in the case of DBDS, where the corresponding values are very different (920 kg "Thesis" for 200 kg "Sethuramiah").

The repeated test for all the additives using the "one-ball-on-three" flats geometry for preparing the suitable samples to be analysed on the E.P.M.A. and by the nuclear microprobes, has produced similar results for the performance achieved by each additive. Table 6.12 shows the e.p. load range and the weld load related to the elemental sulphur and DBDS additives used at a concentration of 0.25% weight sulphur, for both geometries. Therefore these results provide a very strong supporting evidence of the long e.p. activity found for DBDS in this research. [Forbes (10 and 56) reported that a failure load of 2045 kg was recorded during the FALEX test on DBDS additive used at a concentration of 0.59% weight sulphur in a liquid paraffin]. From these results, it seems that the base oil has an effect on the performance of the e.p. activity of the additive. The other possibility could also be due to the high critical temperature of the additive.

As a result of the high e.p. load range shown by DBDS during the tests, and knowing from the theory (56) that the bulk oil collapes when the temperature, (which is a function of the applied load), reaches a certain value, therefore the recording of the lubricant temperature could be taken as a simple "gauge" for drawing a picture of the film formation, particularly during the a.w. and e.p. regimes. Furthermore,

Additives	E.P. Load Range (kg)		Weld Load (kg)	
	Ball	Flat	Ball	Flat
Elemental Sulphur	70-300/320	≙70-300	340	320
DBDS	90-900	≙90-850	920	870

Table 6.12: Comparison of the e.p. load range and the weld loads obtained by using the two geometries, (ie "ball-on-a-3-balls" and "ball-on-3-flats"), for the elemental sulphur and DBDS additives, at a concentration of 0.25% weight sulphur.

to support the explanations put forward, it is essentially to refer to the comments and conclusions drawn during the application of the different techniques employed as complementary to each other throughout the programme of this research.

6.6.1 A.W. Film Formation

The shape of the temperature versus time (cf. Figures 3.7 to 3.10) obtained during the experiments, suggests that the reaction occurring between the additive and the metal asperities is very low. Consequently the reacted film builds-up very smoothly until reaching its maximum value then stays constant. This is confirmed by the S.E.M. results where the corresponding pictures show the presence of fine tracks, and also by X.R.D. technqiue, which indicates that the FeS is the main component forming these tracks. Furthermore, the slow reactivity of the additive leads to a small presence of sulphur on the tracks which means that the resultant film is very thin. This FeS layer is less than 50A° in thickness for being not detectable by the deuteron-proton stripping reactions. Thus the sulphide layer formed during the a.w. regime is too thin to act as a protective film, and this explains the poor a.w. activity of the sulphur additives.

6.6.2 E.P. Film Formation

During the e.p. regime, the bulk temperature rises linearly with time until reaching its equilibrium value before welding takes place (cf. Figures 3.11, 3.12, 3.13 and 3.14). This rapid increase of the temperature indicates that a chemical reaction is taking place between the oil film and the surface. This results by some irregularities in the

film formation, which can be clearly seen from the S.E.M. pictures. The critical temperature and its corresponding time together with the lapse of time taken before welding occurs, have a great effect on the film generation and, also, could be used as useful parameters for comparing the e.p. reactivity of each additive. It is worth noting that the measure of the heat generation would have been a better parameter but, unfortunately the recording of the former was not available in the apparatus used. None-the-less, the measurement of the bulk oil temperature, which is the only practicable parameter available, does not put doubts on the credibility of the interpretation of the results.

The values listed in Table 3.4 suggest that the e.p. effectiveness follows the increasing order:

DBMS < DPDS < Elemental Sulphur < DBDS

This finding corroborates the order of the activity found previously by the use of the standard one-minute test.

The results presented in Table 3.4, also, suggest the similarity between the film formed by the elemental sulphur and DBDS additives on one hand, and by DBMS and DPDS additives on the other hand.

The critical temperature values recorded for the elemental sulphur and DBDS are higher than those found for DBMS and DPDS (cf. Table 3.4). Furthermore, the time corresponding to the equilibrium temperature is found to be less for the first named two additives than for the second group. This means that the chemical reaction occurring in the case of the elemental sulphur and DBDS is faster than the one

happening in the case of DBMS and DPDS. Therefore, the first named additives present a fast rate of formation which ends up by a formation of a strong protective film. The S.E.M. coupled with the energy dispersive analyser, indicates that the film is composed of thick scattered "lumps" of material (or islands) mainly made from a mixture of iron and sulphur. The X.R.D. results show that FeS, $FeSO_4$ and $\alpha\ Fe_2O_3$ compounds compose these "islands" and their vicinities. The comparison between the E.P.M.A. results and the predicted elemental mass composition, from the calculated film thickness, suggest that the film is mainly composed by a mixture of FeS and $FeSO_4$ with a predominance of the second compound, except near the welding region where FeS structure appears to prevail. This very important conclusion could be explained by referring to the postulated sequence of reactions put foward by Rowson and Wu (57 and 58) during their investigation on the pitting of EN31 steel in the presence of sulphur. The authors stated that when the bulk oil temperature is around 100°C, the following sequence of reactions occurred:

$$\text{(i)}\quad Fe + S \longrightarrow FeS \xrightarrow[\text{in air}]{\text{Trituration}} FeSO_4 \qquad \ldots\ldots(6.21)$$

$$\text{(ii)}\quad FeS + S \xrightarrow{\simeq 175°C} FeS_2 \qquad \ldots\ldots(6.22)$$

$$\text{(iii)}\quad FeS_2 + O_2 \xrightarrow{\text{heat}} FeS + SO_2 \qquad \ldots\ldots(6.23)$$

Therefore, following all the results of the recording of the bulk oil temperature, especially the measurement of the temperature versus load (Figure 3.6), and taking into consideration the above equations proposed by Rowson and Wu, the film generated during the e.p. regime, by the elemental sulphur and DBDS additives could be explained by the above-mentioned reactions, which in this case, occurred in two stages:

$$\text{(i)}\quad Fe + S \longrightarrow FeS \xrightarrow[\text{in air}]{\text{Trituration}} FeSO_4 \qquad \ldots\ldots(6.24)$$

$$\text{(ii)}\quad FeS + S \xrightarrow{\triangleq 175°C} FeS_2 \xrightarrow{O_2\ (\text{heat})} FeS + SO_2 \qquad \ldots\ldots(6.25)$$

Thus, equation (6.24) shows why there is a predominance of $FeSO_4$ structure before welding, whilst equation (6.25) justifies the prevalence of FeS structure near the welding region.

Furthermore the thickness of the FeS layer formed is found to be between 0.04 to 1 μm, whilst the $FeSO_4$ layer is between 0.10 to 2.70 μm in thickness.

As stated above, DBMS and DPDS additives display a very slow rate of reaction which, in turn, does not favour the formation and preservation of the protective layer. The calculated thickness indicates that the formed layers are very thin (e.g. FeS layer between 0.005 to 0.010 μm). This result indicates that the equilibrium between the film generation and the wear process, is not reached. This is due to the slow adsorbtion of the additives onto the surface which does not accelerate the formation of the adsorbed layer in order to ensure a good separation of the surface asperities. Consequently, as the pressure gets higher, the thin protective layer is easily broken leaving the surfaces in a large metallic contact area, and this results by the destruction and the removal of the material which appears on the S.E.M. pictures as "craters".

CHAPTER SEVEN

CONCLUSION AND FURTHER WORK

7.1 Conclusion

The introduction of high energy charged particles, especially deuteron-proton stripping reactions, for the investigation of thin films formed during wear tests using a four-ball machine, has been very satisfactory and, the interpretation of the results together with the combination of those from the more conventional physical methods of analysis, has led to the evaluation of the thickness of the surface layers formed during the tests. The measurement of these very thin films formed on EN 31 steel is itself an achievement and, also, is very important. The results has led to a better understanding of the mechanisms of the a.w. and e.p. film formation.

To sum up, the main conclusions drawn from the work described in this volume are as follows:

i) the e.p. effectiveness of the four sulphur additives follows this increasing order:

DBMS < DPDS < Elemental Sulphur < DBDS

ii) The evaluation of the thickness of the films formed on the scars is very realistic. The films generated under the a.w. regime are less than 50 A° thick, whilst in the case of films formed under the e.p. conditions, the thickness of the surface layers depends strongly on the nature of the

sulphur additives used. When the elemental sulphur and DBDS are employed, the thickness of the FeS layer formed is found to be between 0.04 and 1 μm, whilst the $FeSO_4$ structure is between 0.10 and 2.70 μm. In the case of DBMS and DPDS additives, the films generated are very thin (of the order of 10^{-2} μm to 10^{-3} μm).

iii) The film thickness has been shown to be a very useful parameter in the prediction of the elemental mass composition, which, in turn, was the source of ascertaining the dominance between the FeS and $FeSO_4$ structures observed on the e.p. films.

7.2 Futher Work

Following the important results concerning the mechanisms of the a.w. and e.p. film formation, it would be very interesting to investigate the effects of oxygen on the load-carrying action of the sulphur additives. The oxygen seems to be one of the chemical factors controlling the film formation. Auger Electron Spectroscopy (A.E.S.), by its capability of analysing surface layers of very few Angström in thickness, X-ray Photoelectron Spectroscopy (X.P.S.), by its ability of giving the chemical environment of the elements detected on surface layers, and Mössbauer Spectroscopy, by its sensitivity of evaluating the ratio of the different valencies that Fe might possess in the film, would be useful techniques to apply as a complement to the ones already used in this programme, in order to get further insight on the proposed mechanisms.

APPENDIX

FEASIBILITY STUDY OF THE USE OF NEUTRON ACTIVATION ANALYSIS (N.A.A.) IN TRIBOLOGICAL RESEARCH

It was hoped that following the recommendations made in the MSc Project Report (59), Neutron Activation Analysis (14 MeV) would be used as a means for estimating the sulphur compounds which might be formed in the collected wear debris.

A.1 Theory of Neutron Activation Analysis (N.A.A.)

A.1.1 General Principles

When a sample is irradiated by a flux of neutrons some of its stable isotopes will capture a neutron, producing a radioactive isotope with characteristic disintegration properties (60). The type of radiation emitted (usually beta particles or gamma rays), the energy spectrum of the radiation emitted and the half-life of the induced radioactivity will lead to the identification of the elements present in the sample.

Each natural element in a sample consists of one or more stable isotopes present in well known fractional abundancies. Consequently several types of isotope-producing reactions are possible corresponding to each isotope and to the energy of the bombarding neutron.

Thus the number of radioactive isotopes of a certain type present after irradiation of a given element depend upon the quantity of that element in the sample, the neutron flux, the irradiation and post-irradiation time intervals.

A.1.2 Neutron Activation Analysis with Fast Neutrons

The current literature (61) indicates that there is no activation of sulphur using 3 MeV neutrons or thermal neutrons flux from a generator. The availability of Fast Neutrons (14 MeV) produced from the Van De Craaff accelerator in Aston University led to the feasibility of using them as a means for estimating the sulphur compounds which might be formed in the wear debris. Fast neutron capture by the nucleus of an atom causes heavy particles (either neutrons, protons or alpha-particles) to be emitted from the nucleus, and produces new isotopes with lower numbers:

e.g.: $Al^{27}(n,\alpha)Na^{24} \xrightarrow{15\ hrs} Mg^{24} + \beta^- + \gamma$

$Si^{30}(n,\alpha)Mg^{27} \xrightarrow{9.6\ mins} Al^{27} + \beta^- + \gamma$

$Fe^{56}(n,p)Mn^{56} \xrightarrow{2.58\ hrs} Fe^{56} + \beta^- + \gamma$

$S^{34}(n,p)P^{34} \xrightarrow{12.6\ sec} S^{34} + \beta^- + \gamma$

Dealing with Fast Neutrons for an activation analysis, one is limited in the sensitivity. The main limitations are due to the low cross-section of the reaction and the low neutron flux. The neutron flux is fixed by the accelerator used for irradiating the samples. Then the problem is to find out the size of the samples to give a reasonable activity, bearing in mind that the samples collected during wear tests are very small (1 μg to 50 mg). Therefore a survey and theoretical calculations were conducted to estimate the practical detection limit to the sulphur element when being analysed by Fast Neutrons (14 MeV).

A.2 Calculations of the Practical Detection Limit

Before doing the calculations of the practical detection limit, a survey was conducted in order to find out the most sensitive reactions occurring for the sulphur when being bombarded by Fast Neutrons with energies of 14 MeV. Once the sensitive reactions were known (ie also the cross-sections known), therefore the practical sensitivity was easily computed.

The literature survey (61, 62, 63) indicates that there are only two sensitive reactions for the sulphur element. Thus Table A.1, which was compiled from this investigation, displays these two reactions and their interference encountered in N.A.A. with 14 MeV [flux $=10^9$ neutrons per cm^2 per seconds]. In this Table, the column "activity" is estimated from graphs given in the reference 61.

As a result of this, the practical limit of detection from both reactions was evaluated for a neutron flux of 10^7 n/cm^2/sec, which is the maximum flux given by the Van De Craaff accelerator at Aston University. The results obtained are listed in Table A.2. Some useful notes for an understanding on the calculations are presented below:

1. The weight, W, of the sulphur element is assumed to be 1 μg.

2. The equation used for the activity of the sulphur, A, is as follows (59, 60, 61):

$$A = \frac{N_{AV}\ W}{M} f\ \sigma\phi \left[1 - e^{\frac{-(0.693)t_{irr}}{T_{\frac{1}{2}}}} \right] \qquad \text{.....(A.1)}$$

where N_{AV} = Avogadro's Number (=6.023 10^{23} atoms/g)

M = Atomic weight of sulphur 34

f = Fractional abundance of the isotope

σ = Cross-section of the reaction of interest expressed in cm^2

t_{irr} = Irradiation time (in minute) given in Table A.1.

$T_{\frac{1}{2}}$ = Half life of the radioisotope produced (in minute)

3. The count rate per weight, C, is given by the equation:

$$C = A.E \qquad \text{.....(A.2)}$$

Where A is the activity and E is the efficiency of the detection, which is assumed being 47% for the gamma transition and 20% for the scintillation N_aI counter.

4. The counting standard deviation is assumed to be 10%, that is 100 total counts.

5. The practical detection limit for the sulphur is given by the equation below:

$$P = \frac{100 \text{ (counts/min)}}{C \text{ (counts/min/ } \mu g)} \qquad \text{.....(A.3)}$$

Isotope determined & percentage abundance	Most Sensitive Reaction, its cross-section σ(mb) and Product half-life $T_{\frac{1}{2}}$	Gamma Energy, (MeV) and Percentage	Interference Reactions	Activity for Saturation cps/g. Element	Irrad. Time (min)	Counting Time (min)
S^{34}(4.20)	S^{34} (n, α) Si^{31} σ = 138 mb $T_{\frac{1}{2}}$ = 157.20 min	1.26 MeV ($\doteq$1.00%)	P^{31}(n, p)Si^{31}	3.78	$\doteq$45	45
	S^{34} (n,p) P^{34} σ = 85 mb $T_{\frac{1}{2}}$ = 0.21 min	2.13 MeV (25%)	Cl^{37}(n, α)P^{34} σ = 52.4 mb $T_{\frac{1}{2}}$ = 0.21 min	21.977	<5 ($\doteq$2)	<5 ($\doteq$2)

Table A.1: Most sensitive reactions and interfering reactions for the sulphur encountered in Activation Analysis with 14 MeV (flux = 10^9 neutrons/cm^2/sec).

A.3 Conclusion

The values found for the sensitivity (Table A.2) are far from the actual mass of the wear debris collected during the tests. Therefore there is a limitation of the size for the specimens, and it is not recommended to use the N.A.A. (14 MeV) for detecting sulphur in the collected wear debris.

Reaction	t_{irr} (min)	σ (mb)	$T_{\frac{1}{2}}$ (min)	Activity "A" (dis/min/ μ g)	C = A.E (counts/min/ μg)	Limit detection (mg)
$S^{34}(n, \alpha)Si^{31}$	45	138	157.20	0.0111	$1.04\ 10^{-3}$	95.88
$S^{34}(n,p)P^{34}$	2	85	0.21	0.038	$3.57\ 10^{-3}$	28.01

Table A.2: Calculation for the practical sensitivity (assuming W = 1 μ g).

REFERENCES

1. A. Cameron, "Principles of Lubrication", Longmans, (1966).

2. "Lubrication: Theory and its Application", Published by B.P. Trading Ltd, (1969).

3. B. Pugh, "Practical Lubrication: An Introductory Text", Mewnes-Butterworth, (1970).

4. "Lubrication and Lubricants", Edited by E. Braithwaite, Elsevier Publishing Company, (1964).

5. E. A. Evans, "Lubricating and Allied Oils", 4th Edition, Chapman and Hall, (1963).

6. "Principles of Tribology", Edited by J. Halling, Mac Millan Press, (1978).

7. M. Billett, "Industrial Lubrication", Pergamon Press, (1979).

8. R. C. Coy, "Physical Analysis of Worn Surfaces Formed Under Extreme-Pressure Lubrication Conditions", PhD Thesis, Dpt of Physics, Aston University in Birmingham, (1973).

9. G. D. Boerlage, "Four-ball Testing Apparatus for Extreme-Pressure Lubricants", Engineering, 136, pp 46-47, London, (1933).

10. K. G. Allum and E. S. Forbes, "The Load-Carrying Mechanism of Organic Sulphur Compounds - Application of Electron Probe Microanalysis", ASLE Transactions, 11, pp 162-175, (1968).

11. E. S. Forbes and A. J. D. Reid, "Liquid Phase Adsorption/Reaction Studies of Organo-Sulphur Compounds and Their Load-Carrying Mechanism", ASLE Transactions, 16, pp 50-60, (1973).

12. R. C. Coy and T. F. J. Quinn, "An application of Electron Probe Microanalysis and X-Ray Diffraction to the Study of Surfaces Worn Under Extreme Pressure Lubrication", Proc. Inst. Mech. Engrs, 186, Pt 35, pp 62-68, (1972).

13. R. C. Coy and T. F. J. Quinn, "The Use of Physical Methods of Analysis to Identify Surface Layers Formed by Organo-Sulphur Compounds in Wear Tests", ASLE Transactions, 18(3), pp 163-174, (1976).

14. E. B. Greenhill, "The Lubrication of Metal by Compounds Containing Sulphur", Journal Institute of Petroleum, 34, pp 659-669, (1948).

15. W. Davey and E. D. Edwards, "The Extreme-Pressure Lubricating Properties of Some Sulphides and Disulphides, in Mineral Oil, as Assessed by the 4-ball Machine", Wear, 1, pp 291-304, (1957/1958).

16. E. H. Loeser, R. C. Wiquist and S. B. Twiss, "Cam and Tappet Lubrication. IV- Radioactive Study of Sulphur in the E.P. Film", Proceeding of the Annual Meeting of the American of Lubrication Engineers, New York, April, (1959).

17. D. Godfrey, "Chemical Changes in Steel Surfaces During Extreme-Pressure Lubrication", ASLE Transactions, 5, pp 57-66, (1962).

18. K. G. Allum and J. F. Ford, "The Influence of Chemical Structure on the Load-Carrying Properties of Certain Organo-Sulphur Compounds", J. Inst. Petrol., 51, pp 145-161, (1965).

19. K. G. Allum and E. S. Forbes, "The Load-Carrying Properties of Organo-Sulphur Compounds. The Influence of Chemical Structure on Anti-Wear Properties of Organic Disulphides", J. Inst. Petrol., 53, pp 174-185, (1967).

20. M. R. Phillips, M. Dewey, D. D. Hall, T. F. J. Quinn and H. N. Southworth, "The Application of Auger Electron Spectroscopy", Vacuum, 26 (10 and 11), pp 451-456, (1976).

21. R. J. Bird and G. D. Galvin, "The Application of E.S.C.A. to the Study of E.P. Films on Lubricated Surface", Wear, 37, pp 143-167, (1976).

22. J. J. McCarroll, R. W. Mould, H. B. Silver, M. L. Sims, "Auger Electron Spectroscopy of Wear Surfaces", Nature, 266, (1977).

23. M. Tomaru, S. Hironaka and T. Sakurai, "Effects of Oxygen on the Load-Carrying Action of Some Additives", Wear, 41, pp 117-140, (1977).

24. M. Tomaru, S. Hironaka and T. Sakurai, "Effects of Some Chemical Factors on Film Failure Under E.P. Conditions", Wear, 41, pp 141-155, (1977).

25. H. Okabe, H. Nishio and M. Masuko, "Tribochemical Surface Reaction and Lubricating Oil Film", ASLE Transactions, 22(1), pp 65-70, (1979).

26. K. Meyer, H. Berndt, and B. Essiger, "Interacting Mechanisms of Organic Sulphides with Metallic Surfaces and Their Importance for Problems of Friction and Lubrication", Applications of Surface Science, 4, pp 154-161, (1980).

27. H. Blok, "Theoretical Study of Temperature Rise at Surfaces of Actual Contact Under Oiliness Lubricating Conditions", Inst. Mech. Engr., General Discussion on Lubrication, Vol 2, pp 222-235, (1937).

28. H. Blok, "Seizure-Delay-Method for Determining the Seizure Protection of E.P. Lubricants", S.A.E. Journal (Transactions), 44(5), pp 193-200, (1939).

29. J. C. Jaeger, "Moving Sources of Heat and the Temperature at Sliding Contacts", Proceeding Royal Society of New South Wales, 76, pp 203-224, (1942).

30. T. B. Lane, "The Flash Temperature Parameter: A criterion for Assessing E.P. Performance on the Four-Ball Machine", Journal Institute of Petroleum, 43, pp 181-183, (1957).

31. "Extreme Pressure Properties: Friction and Wear Tests for Lubricants: Four-Ball Machine", Designation IP 239/77, IP. Standards for Petroleum and Products, Part 1, Vol 2, pp 1-13, Institute of Petroleum, London, (1977).

32. R. S. Fein, "Transition Temperatures with Four-Ball Machine", ASLE, Transactions, 3(1), pp 34-39, (1960).

33. A. A. Manteuffel and G. Wolfram, "A Method for Studying the Effect of Extreme-Pressure Additives on Rubbing Metal Surfaces", ASLE, Transactions, 3(2), pp 157-164, (1960).

34. A. Sethuramiah, H. Okabe and T. Sakurai, "Critical Temperatures in E.P. Lubrication", Wear, 26, pp 187-206, (1973).

35. J. F. Archard, "The Temperature of Rubbing Surfaces", Wear, 2, pp 438-455, (1958/1959).

36. J. R. Hughes, "The Shell Four-Ball E.P. Lubricant Tester", Proceedings of the Conference on Lubrication and Wear, Inst. Mech. Engrs., pp 575-602, (1957).

37. B. D. Cullity, "Elements of X-Ray Diffraction", Addison-Wesley Publishing Company, (1978).

38. Gudrun A. Hutchins, "Electron Probe Microanalysis", Spragne Electric Company, Research and Development Laboratories, Noth Adams, Massachusetts.

39. D. N. Poole and P. M. Martin, " Electron Probe Microanalysis: Instrumental and Experimental Aspects", Metallurgical Reviews, (1969).

40. S. J. B Reed, "Electron Probe Analysis", Cambridge Press, (1975).

41. P. Duncumb, "Quantitative Microprobe Analysis", (Private Communication), Tube Investments Research Laboratories, Hinxton Hall, Saffron Walden, Essex.

42. W. J. M. Salter, "Manual of Quantitative Electron Probe Microanalysis", Structural Publications, London, (1970).

43. "Information for Users of the Birmingham Radiation Centre", Edited by D. R. Weaver, Paper N°. BRC-76/01, Birmingham University, (1976).

44. "New Uses of Ion Accelerators", Edited by J. F. Ziegler, Plenum Press, New York, (1976).

45. W. D. Mackintosh and J. A. Davies, "Rutherford Scattering and Channeling - A Useful Combination for Chemical Analysis of Surfaces", Analytical Chemistry, 41(4), pp 26A-35A, (1969).

46. M. Peisach and D. O. Poole, "Analysis of Surfaces by Scattering of Accelerated Alpha Particles", Analytical Chemistry, 38(10), pp 1345-1350, (1966).

47. I. V. Mitchell, "Rutherford Backscattering", Phys. Bulletin, 30, pp 23-25, (1979).

48. L. Quaglia, G. Robaye, M. Cuypers and J. N. Barrandon, "Analyse par Reaction Nucleaire de l'Oxygene et du Carbone en Couche Mince a la Surface des Metaux", Nuclear Instruments and Methods, pp 315-324, (1969).

49. E. A. Wolicki and A. R. Knudson, "Nuclear-Detection Method for Sulphur in Thin Films", Int. J. Appl. Rad. Isotopes, pp 429-433, (1967).

50. H. R. Saad, Z. A. Saleh, N. A. Mansour, E. M. Sayed and I. I. Zaloubovsky, "Investigation of the Reaction $S^{32}(d,p)S^{33}$ in the Deuteron Energy Range 1.5-2.5 MeV", Nuclear Physics, 84, pp 629-640, (1966).

51. C. F. Williamson, J. P. Boujot and Jean-Picard, "Tables Range and Stopping Power of Chemical Elements for Charged Particles of Energy 0.5 to 500 MeV", Rapport C.E.A.-R.3042, Centre d'Etudes Nucleaires de Saclay, France.

52. R. A. Jarjis, "Nuclear X-section Data for Surface Analysis", Vol II, Dpt. of Physics, University of Manchester, (Dec. 79).

53. G. Weber and L. Quaglia, "Oxygen Carbon and Nitrogen Determination by Means of Nuclear Reactions", J. of Radioanalytical Chemistry, 12, pp 323-333, (1972).

54. D. A. Thompson and W. D. Mackintosh, "Stopping Cross-Sections for 0.3 to 1.7 MeV Helium Ions in Silicon Dioxide", Journal of Applied Physics, 42(10), pp 3969-3976, (1971).

55. J. F. Ziegler, R. F. Lever, J. K. Hirvonen, "Computer Analysis of Nuclear Backscattering", Ion Beam Surface Layer Analysis, Edited by O. Meyer, G. Linker and F. Kappeler, Vol. 1, Plenum Press, New York, (1976).

56. E. S. Forbes, "Anti-Wear and Extreme-Pressure Aditives for Lubricants", Tribology, 3, pp 145-152, (1970).

57. D. M. Rowson and Y. L. Wu, "Physical Analysis of Pitting in Rolling and Sliding Discs", Performance and Testing of Gear Oils and Transmission Fluids, Edited by R. Tourret and E. P. Wright, Heyden and Son Ltd on behalf of the Institute of Petroleum, London, (1981).

58. D. M. Rowson and Y. L. Wu, "The Effect of the Additive Chemistry of Elemental Sulphur on the Contact Fatique Life of Steel EN31", Wear, 70, pp 373-381, (1981).

59. A. Azouz, "A Study of the Feasibility of Using N.A.A. and Mossbauer Spectroscopy in Tribological Research", MSc. Project Report, Dpt of Physics, Aston University in Birmingham, (1978).

60. "Guide to Activation Analysis", Edited by W. S. Lyon Jr, Robert E. Krieger Publishing Company, New York, (1972).

61. S. S. Nargolwalla and E. P. Przbylowicz, " Activation Analysis with Neutron generators", A Wiley-Interscience Publication, (1973).

62. "Compilation of Neutron Reaction and Total Cross-Sections at 14 MeV", Project N° 7360, Task N° 736005, Texas Nuclear Corporation.

63. S. C. Mathur and G. Oldham, "Interferences Encountered in 14 MeV Neutron Activation Analysis", Nuclear Energy, (1967).

Vacuum/volume 31/numbers 10–12/pages 593 to 596/1981
Printed in Great Britain

0042-207X/81/100593-04$02.00/0

An investigation of extreme pressure films formed during wear tests

D M Rowson and A Azouz, *Tribology Group, Department of Physics, University of Aston in Birmingham, UK*

An investigation of the thin films formed during tests using a four-ball machine with two extreme pressure additives (elemental sulphur and DBDS) has been undertaken. Several physical methods of analysis have been used to give information about the structure and thickness of such films. In particular, data obtained using Electron Probe Microanalysis (EPMA) are compared with those from a nuclear technique using charged particle stripping reactions [(d,p) reactions] and with those from Rutherford Backscattering with 2 MeV alpha-particles.

1. Introduction

Various techniques of analysis, among them Scanning Electron Microscopy (SEM), Electron Probe Microanalysis (EPMA), X-ray Diffraction (XRD), Photo-Electron Spectroscopy (ESCA) and Optical Microscopy combined with sectioning and microhardness testing have already been used to investigate the formation and role of surface films formed during wear tests using a four-ball machine[1–5].

Direct examination of the films formed when using extreme-pressure additives, is limited due to their thinness, although indirect information can be obtained by examination of the debris formed during running.

The aim of the work reported in this paper was to study the feasibility of using high energy charged particle beams to investigate the structure and formation of extreme-pressure (EP) surface films formed on EN31 steel when elemental sulphur was used as an extreme-pressure additive in a white mineral oil lubricant. The particle beams were produced in the Dynamitron Accelerator at the Joint Radiation Facility operated jointly by the University of Aston and the University of Birmingham. Two types of analytical technique were investigated. In the first, the incident beam consisted of alpha-particles and in the second the incident beam consisted of deuterons.

1.1. Rutherford backscattering using alpha-particles. This technique involves bombarding the sample with alpha-particles of known energy E_0 and measuring the energy of the alpha-particles after they have been scattered by interaction with the nuclei of the sample[6].

1.2. Deuteron proton stripping reactions. The procedure consists of bombarding the sample with an energetic deuteron beam and of measuring the energy spectrum of the protons produced by the induced nuclear reaction.

The reaction yield Y, at the incident energy E_d, may be written as[6]

$$Y_p(\theta) = n(N\ \Delta x)\sigma_{(\theta,E_d)}\Omega \tag{1}$$

so that

$$(N\ \Delta x) = \frac{Y_p(\theta)}{n\ .\ \Omega\sigma_{(\theta,E_d)}} \tag{2}$$

where $(N\ \Delta x)$ is the number of target atoms per square centimetre; n is the number of incident deuterons; $\sigma_{(\theta,E_d)}$ is the differential cross-section (for the angle θ and at energy E_d) and Ω is the solid angle sampled by the detector.

2. Experimental details

Wear tests were conducted on a four-ball machine using either the conventional geometry of ball on three balls or ball on three flats in which the contact geometry was identical to the conventional mode. The test specimens were EN31 steel hardened to 850 VPN and the test lubricant was a white mineral oil, Risella 32. Two additives were used in the lubricant, elemental sulphur at 0.25 wt% and dibenzyl-disulphide (DBDS) at 1.0 wt%. Tests were conducted for the standard time of 1 min over a range of loads from 40 900 kg in order to determine the regions of EP action.

At selected loads further tests were conducted for a range of running times to investigate the dependance of EP film formation on time and with temperature of the lubricant and also so that sufficient wear debris could be collected for subsequent analysis.

In addition, thick, medium and thin films of $FeSO_4$ were prepared by reacting clean samples of the EN31 into sulphuric acid for 5, 1 and 0.5 min respectively to provide calibration specimens and reference samples of pure sulphur deposited on substrates of pure silver were also studied.

The wear scars, wear debris and calibration specimens were studied by a variety of analytical techniques and the results are presented below.

3. Results

Figure 1 shows the results for standard tests of 1 min duration indicating that the elemental sulphur has a detrimental effect on wear scar diameter below a load of 60 kg and has a beneficial EP action from 70 to 300 kg load whilst DBDS has a beneficial EP action from 90 to 900 kg load.

Selected specimens prepared in the EP-region and the non-EP-region using both additives were then examined under the scanning electron microscope (SEM) and elemental surface maps were obtained from the induced X-rays which showed that the surfaces consisted of iron and sulphur as expected. X-ray Photoelectron Spectroscopy (XPS) gave the results shown in Table 1, which show that when using sulphur as the additive the product is iron sulphate in the anti-wear-region but a mixed sulphate and sulphide in the EP-region, whereas when DBDS was used as the additive the product was iron sulphate in the EP-region.

Selected specimens were also analysed using EPMA with an incident electron beam energy of 15 keV and the results are presented in Table 2. The results show that, with the exception of the thick reference sample of iron sulphate, the percentages for iron were greater than expected (and the percentages for sulphur were correspondingly less) from the inferred compositions as given by XPS. This will be discussed in the next section.

The reaction $^{32}S(d, p)^{33}S$ was studied using an incident deuteron beam energy of 2 MeV. A typical spectrum of proton yield vs energy is shown in Figure 2. Using equation (2), the average number of sulphur atoms per square centimetre of surface was calculated and these results are presented in Table 3 for both the specimens and reference samples.

The feasibility of using Rutherford backscattering to study the product films was also investigated. No sulphur could be detected in the wear films generated when using sulphur as the additive nor in the films generated when using DBDS as the additive except for the sample produced at a load of 400 kg and a running time of 1 min. However, sulphur and oxygen were identified in the thick and medium reference films of iron sulphate. Figure 3 shows the

Table 1. Results of the XPS examination of selected specimens

Additive	Load (kg)	Test time (s)	Fe_{2P}	Fe_{3P}	O_{1S}	FeS	Sulphate	Sulphur or organic sulphide
0.25 wt"„ sulphur	40	60	×	\	\	×	\	×
	130	1100	×	\	\	\	\	\
	300	60	\	\	\	\	\	\
1.0 wt"„ DBDS	130	1100	×	\	\	×	\	×
Thick iron sulphate reference sample			×	\	\	×	\	×

Table 2. Results of the EPMA examination of selected specimens.

Additive	Load (kg)	Test time (s)	S (wt"„)	Fe (wt"„)	Ag (wt"„)
0.25 wt"„ sulphur	40	60	0.1	96.1	
	130	1100	3.0	86.0	
	300	60	19.9	81.9	
1.0 wt"„ DBDS	130	1100	7.3	87.8	
	140	60	10.0	87.5	
	300	60	17.1	72.4	
	400	60	13.6	91.4	
Thick film of $FeSO_4$			24	28	
Medium film of $FeSO_4$			14	56	
Medium film of S on Ag			13		80
Thin film of S on Ag			6		87

-, indicates not detected.

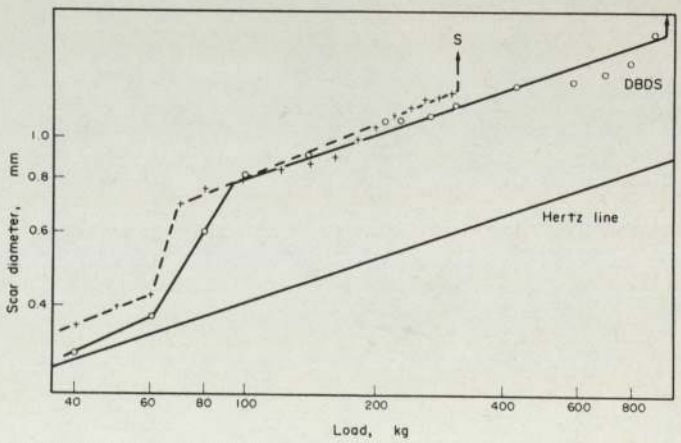

Figure 1. Scar diameter against load for the standard 1 min tests.

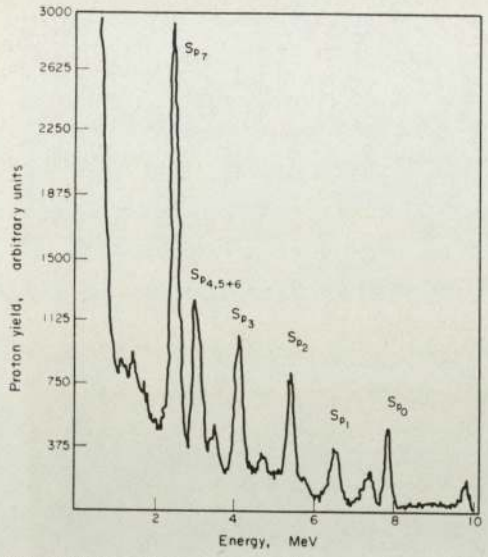

Figure 2. Typical spectrum of proton yield vs energy for an EP film (0.5 wt"„ sulphur, 300 kg, 60 s).

Table 3. Results of the $^{32}S(d, p)^{33}S$ examination and RBS examination of selected specimens

Additive	Load (kg)	Test time (s)	$^{32}S(d, p)^{33}S$ Average $N\,\Delta x$ (S atoms cm^{-2})	RBS Average $N\,\Delta x$ (S atoms cm^{-2})
0.25 wt"„ sulphur	40	60		
	130	60	1.2×10^{17}	
	130	1100	1.1×10^{18}	
	300	60	7.3×10^{17}	
1.0"„ DBDS	130	15	2.8×10^{17}	
	130	1100	4.9×10^{17}	
	140	60	3.7×10^{17}	
	400	60	5.3×10^{17}	7.8×10^{17}
Thick film of $FeSO_4$			3.2×10^{18}	5.0×10^{18}
Medium film of $FeSO_4$			1.6×10^{18}	4.4×10^{18}
Thick film of S on Ag			1.9×10^{18}	*
Medium film of S on Ag			1.3×10^{18}	*
Thin film of S on Ag			4.9×10^{17}	*

– Indicates no sulphur detected; * Indicates specimen not analysed.

experimental spectrum for the thick film of iron sulphate and the solid curve is the best theoretical fit found. The theoretical curve enabled the calculation of the number of sulphur atoms per square centimetre of surface and these results are also given in Table 3.

4. Discussion

The effective depth probed by an EPMA beam may be estimated[7]

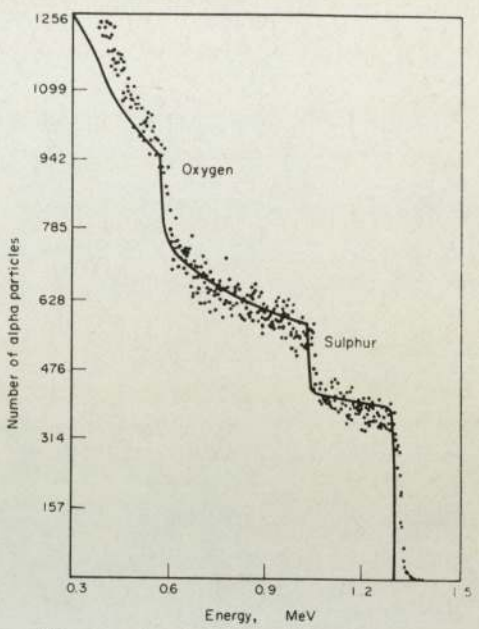

Figure 3. Experimental results for RBS of a thick film of $FeSO_4$. Solid curve is best theoretical fit using 5×10^{18} sulphur atoms cm^{-2} of surface.

(in the case of an element) from the equation

$$x = 1.1 \times 10^{-12} \frac{A}{Z} \frac{E^2}{I} \times 10^2 \text{ (m)} \tag{3}$$

where E is the energy of the incident electron beam in electron volts, I is the density of the element, and A and Z are the atomic weight and atomic number of the element respectively.

In the case of a compound the term (A/Z) in equation (3) must be changed to $(A/Z)_{wt}$ which is given by

$$(A/Z)_{wt} = \frac{\sum_1^n A_i(A_i/Z_i)}{\sum_1^n A_i}. \tag{4}$$

For a 15 keV beam Table 4 shows the effective depth probed in various elements and compounds relevant to this work. From this table one can see that if a film of iron sulphur compounds formed by action of the EP additive is less than about 1 μm thick, then the beam will penetrate into the substrate giving rise to spurious quantitative measurements.

With the $^{32}S(d, p)^{33}S$ reaction, on the other hand, one must ensure that the film is sufficiently thin so as not to appreciably reduce the energy of the deuteron beam, so that the cross-section, $\sigma(E)$, may be considered as a constant. For an initial beam energy of 2 MeV, Table 5 shows the rate of energy loss with thickness for various elements and compounds relevant to this work, where for compounds

$$dE/d(Ix) = \sum_1^n A_i \left(\frac{dE}{d(Ix)}\right)_i \Big/ \sum_1^n A_i \tag{5}$$

Table 4. Effective depth probed by a 15 keV EPMA beam

Element or compound	Fe	S	FeS	$FeSO_4$
Effective depth probed (μm)	0.68	2.39	1.09	1.71

Table 5. Rate of energy loss with thickness penetrated for a deuteron beam (keV . μm^{-1})

Deuteron beam energy	Rate of energy loss with thickness (keV . μm^{-1})			
	Fe	S	FeS	$FeSO_4$
2.0 MeV	98.6	34.3	66.4	50.9
1.9 MeV	101.1	35.3	68.2	52.5
1.8 MeV	103.7	36.4	70.1	54.1

Table 6a. Calculated film thickness (in μm) from the $^{32}S(d, p)^{33}S$ results of Table 3

Additive	Load (kg)	Test time (s)	Calculated film thickness (μm) assuming structure S	FeS	$FeSO_4$
0.25 wt% sulphur	40	60			
	130	60	0.03	0.04	0.10
	130	1100	0.28	0.33	0.93
	300	60	0.19	0.23	0.62
1.0 wt% DBDS	130	15	0.07	0.09	0.24
	130	1100	0.13	0.15	0.41
	140	60	0.10	0.11	0.31
	400	60	0.14	0.16	0.45
Thick film of $FeSO_4$			*	*	2.69
Medium film of $FeSO_4$			*	*	1.32
Thick film of S on Ag			0.49	*	*
Medium film of S on Ag			0.34	*	*
Thin film of S on Ag			0.13	*	*

– Indicates no sulphur detected; * Indicates not analysed.

Table 6b. Calculated film thicknesses (in μm) from the RBS results of Table 3

Additive	Load (kg)	Test time (s)	Calculated film thickness (μm) assuming structure S	FeS	$FeSO_4$
1.0 wt% DBDS	400	60	0.20	0.24	0.66
Thick film of $FeSO_4$			*	*	4.25
Medium film of $FeSO_4$			*	*	3.74

Since the cross-section $\sigma(E)$ does not change markedly in the range 1.9 2 MeV for either the P_0 or the P_2 peaks (i.e. for an energy loss of ~100 keV), Table 4 implies that the EP product films containing sulphur should be less than 1.5 2 μm thick in order to apply equation (2) to the results in order to calculate the number of sulphur atoms per square centimetre in the films ($N\,\Delta x$).

The thickness of the film can be calculated from the value of $N\,\Delta x$ by assuming a structure from XPS or XRD data along with values for the density and then using

$$t = \frac{N\,.\,\Delta x\,.\,\text{mol wt}}{N_A l} \times 10^{-2}\ (\text{m}) \qquad (6)$$

where N_A is Avogadro's number.

Applying this equation to the data in Table 3 gives Tables 6(a and b) and shows that the thick $FeSo_4$ film gives a film thickness, t, of ~2.7 μm whilst for the thin sulphur film the thickness is ~0.13 μm showing that the standards do in fact satisfy the criterion mentioned above.

Similarly taking the sample formed using DBDS at 130 kg (18 min) gives a film of $FeSO_4$ of thickness 0.41 μm when this specimen was analysed by EPMA (Table 2) the result was 87.8% Fe and 7.3% S. This was due to the electron beam penetrating the film, thereby analysing part of the substrate as well as the film. One can readily calculate the depth of substrate probed by the electron beam after it has passed through the $FeSO_4$ film.

Equation (3) shows that the rate of loss of energy with depth is given by

$$dE/dx = \frac{l}{1.1 \times 10^{-14}} \cdot \frac{Z}{A} \cdot \frac{1}{2E} \qquad (7)$$

Integration of equation (7) shows that the incident beam of 15 keV will lose 1.95 keV on passing through a film of 0.41 μm of $FeSO_4$. Hence the beam entering the substrate has an energy of 13.05 keV which from equation (1) will penetrate 0.51 μm into the steel (which is assumed to be pure iron). The total mass of Fe, S and O can now be calculated assuming that the beam does not diverge within the material. Such a calculation predicts a detected composition of 85.4% Fe and 4.9% S. In view of the simplifying assumptions made in the calculation, the agreement between the calculated and observed values is most satisfactory.

5. Conclusion

This work has shown the feasibility of using high energy charged particles beams, in conjunction with more usual physical methods of analysis to investigate the structure and formation of extreme-pressure surface films formed during tribological tests. The work indicates that such films are typically between 0.05 and 0.5 μm thick consisting of FeS and/or $FeSO_4$ when using elemental sulphur or DBDS as the EP additive.

References

[1] R C Coy and T F J Quinn, *Proc Instn Mech Engng*, **186**, 35, 62–68 (1972).
[2] R C Coy and T F J Quinn, *ASLE Trans*, **18** (3), 163–174 (1975).
[3] K G Allum and E S Forbes, *ASLE Trans*, **11**, 163–175 (1968).
[4] R J Bird and G D Galvin, *Wear*, **37**, 143–167 (1976).
[5] R C Coy, PhD thesis, University of Aston in Birmingham (1973).
[6] *New Uses of Ion Accelerators* (Edited by J F Ziegler). Plenum Press, New York (1975).
[7] L S Birks, *Electron Probe Microanalysis*. Wiley, New York (1971).

J.M. GEORGES (Editor)
Microscopic aspects of adhesion and lubrication, pp. 763—778

A COMPARISON OF TECHNIQUES FOR SURFACE ANALYSIS OF EXTREME PRESSURE FILMS FORMED DURING WEAR TESTS.

A.AZOUZ and D.M.ROWSON
Tribology Group, Department of Physics, University of Aston in Birmingham, Birmingham B47ET, U.K.

ABSTRACT

Previous investigations of the formation and role of surface films, developed during wear tests using extreme-pressure additives, have used a number of physical methods of analysis. In order to extend the information given by such techniques, the present work also employed some methods of nuclear analysis, which have not been previously widely used in tribological research. The two main nuclear techniques used were Rutherford Backscattering (RBS) using 2 MeV alpha-particles and charged particle stripping reactions using deuterons [(d,p) reactions].

The results obtained using these new methods of analysis are discussed and compared with the information obtained using other methods of physical analysis, such as X-ray photoelectron spectroscopy, electron probe micro-analysis and electron and optical microscopy. The different methods of analysis used are shown to be complementary leading to a better understanding of the structure and formation of such films.

1. INTRODUCTION

The study of the film formed during wear tests using a 4-ball machine can lead to a better understanding of the mechanism of the action of the additives used. Therefore the determination of the chemical composition of the worn surfaces is one of the priorities in the investigation. Thus several analytical techniques have already been used but the identification and measurement of these surface layers is still not fully completed. These techniques include Scanning Electron Microscopy (SEM), Electron Probe Microanalysis (EPMA), X-ray Diffraction (XRD), Photoelectron Spectroscopy (ESCA) and Optical Microscopy (refs.1-5). The main problem of the analysis is the thinness of the films formed.

Fig.1 shows the main types of analytical techniques used in surface sciences. The development of some nuclear techniques as a means for surface analysis has led to the feasibility of applying such methods in tribological research where

there is very little reference in the literature.

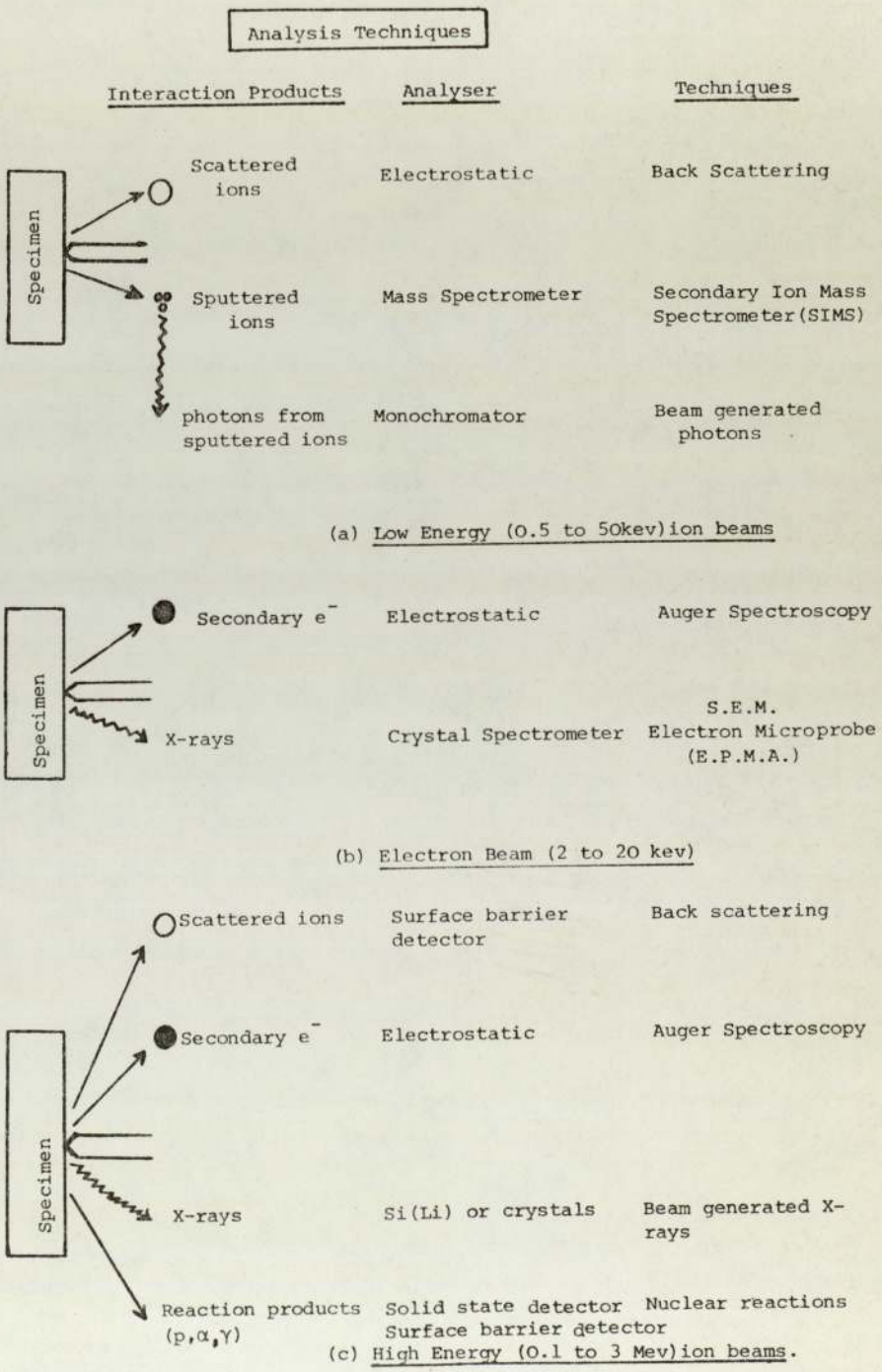

Fig.1: Comparison of Analytical techniques subdivided by incident beam energy.

This report shows the great advantage of combining these new techniques with the previous ones to get the maximum information of the film thickness of the worn surfaces.

The criteria for choosing a new analytical technique must be based on the following factors :

1. Nature of the specimen.
2. Element of interest and its percentage in the sample.
3. Availability of the analytical equipment.
4. Probability of the induced reactions taking place.
5. Advantages over other techniques (sensitivity, non-destructivity and cost).

These requirements led to the use of only two high energy particle beams as a means for investigating the extreme pressure (EP) surface films formed on EN31 steel when sulphur compounds were used as EP additives in a white mineral oil lubricant. The first type of incident beam used were alpha-particles and the second type were deuterons. The particle beams were produced in the Dynamitron Accelerator at the Joint Radiation Facility operated by the University of Aston and the University of Birmingham.

2. EXPERIMENTAL METHODS

A 4-ball machine was used for testing the anti-wear (AW) and EP properties of the additives (ref.6) using either the conventional geometry of ball on three balls or ball on three flats in which the contact geometry was identical to the conventional mode. The test specimens were made from EN31 steel hardened to 850 ± 10 VPN. Tests were carried out using Risella 32 as the base oil and the additives studied were elemental sulphur at 0.25wt%, dibenzyl disulphide(DBDS), dibenzyl mono-sulphide (DBMS) and diphenyl disulphide (DPDS) at various concentrations. The running time was one minute for each load except for some selected loads where the time was extended to enable the investigation of the dependence of EP film formation on time and with temperature and also to permit the collection of a sufficiently large quantity of wear debris for X-ray diffraction analysis.

3. RESUDTS AND DISCUSSION

3.1. Standard Test

In this part of the investigation, the concentration per weight for the additives was chosen so that the same sulphur concentration was present in the lubricant plus additive. 0.25% wt of elemental sulphur was dissolved into the Risella 32 whilst 0.885% wt, 1.0%wt and 1.74%wt were respectively used for DPDS, DBDS and DBMS. Table 1 displays the load range of the AW and EP regions obtained for these additives and fig.2 shows the graphs of the scar diameter versus the

applied loads.

TABLE 1

AW and EP load range of the additives used

Additives	AW load range (kg)	E.P.load range (kg)
0.25%wt elemental sulphur	up to 60	70 - 300
0.885%wt DPDS	up to 60	80 - 200
1.0%wt DBDS	up to 60	90 - 900
1.74%wt DBMS	up to 60	80 - 140

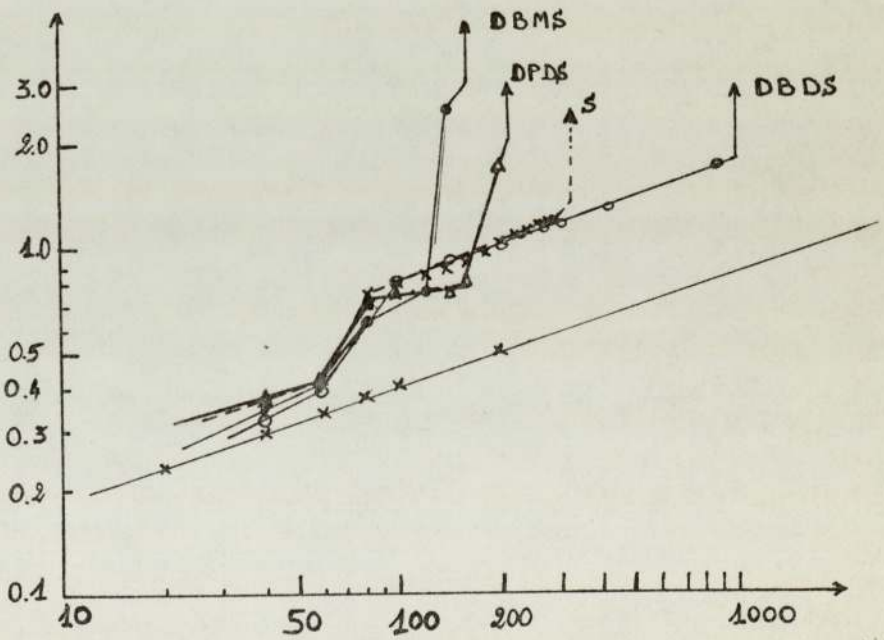

Fig.2: Scar diameter vs load for the standard 1 min tests.

The worn surfaces formed during the AW and EP regime were examined under the scanning electron microscope (SEM) coupled with an energy dispersive X-ray analysis (KEVEX). Fig.3 shows the micrographs of these areas when sulphur was used as the additive whilst Fig.4 represents the X-ray distribution of the main elements of interest covering the scars.

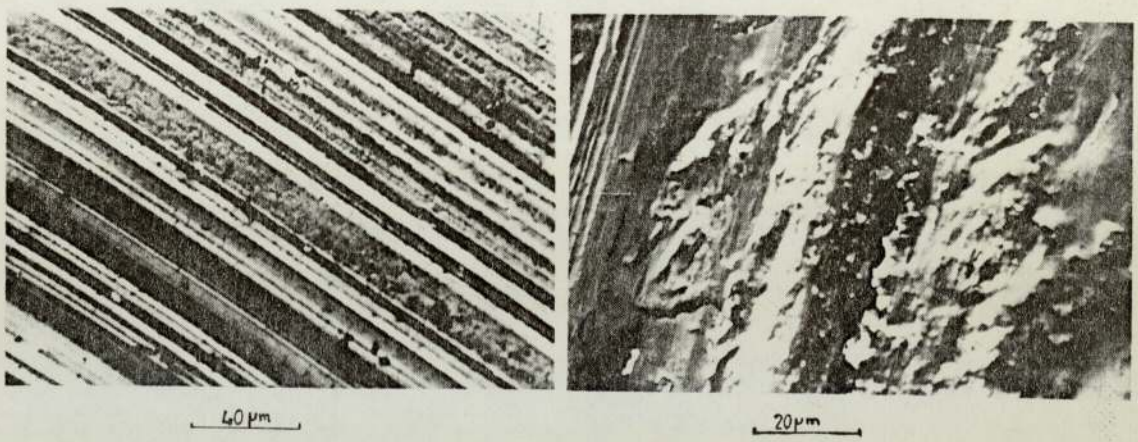

a) b)

Fig.3. Electron pictures of the worn surfaces obtained when sulphur was used as the additive for 1 min run: a) AW region b) EP region.

a) Sulphur X-ray image of the AW region

b) Sulphur X-ray image of the EP region

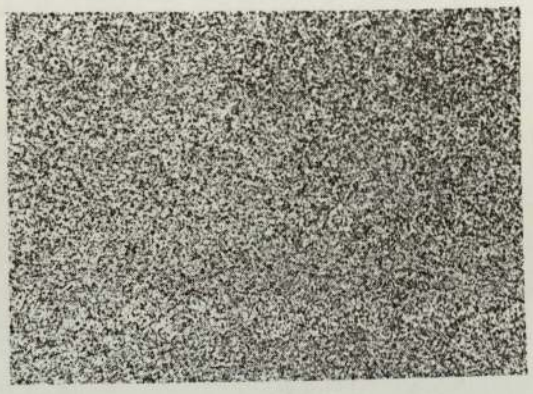

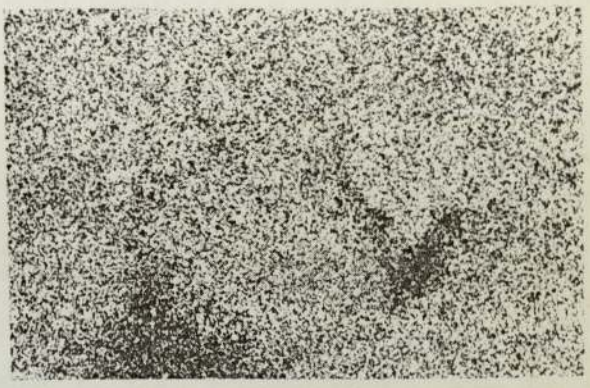

c) Iron X-ray image of the AW region

d) Iron X-ray image of the EP region

Fig.4. X-ray distribution of sulphur and F_e of the worn surfaces when sulphur was used as the additive.

From these photographs one can conclude that :

- There is distinction between the formation of the AW and EP films.
- For the AW region, the film is smooth and composed of fine tracks mainly formed by sulphur and iron adjacent to each other.
- For the EP region, the film is a thick solid layer and there is no regularities as in the AW film. A strong presence of sulphur located near to the iron suggests the formation of islands on the surface.

3.2. Temperature work

The temperature of the bulk oil plus the elemental sulphur additives was recorded by immersing a thermocouple wire into the bowl holding the balls while the test was carried out. Fig.5 shows the graph of the measured temperature versus the applied load and the results reveal the linear dependence between them.

log not linear

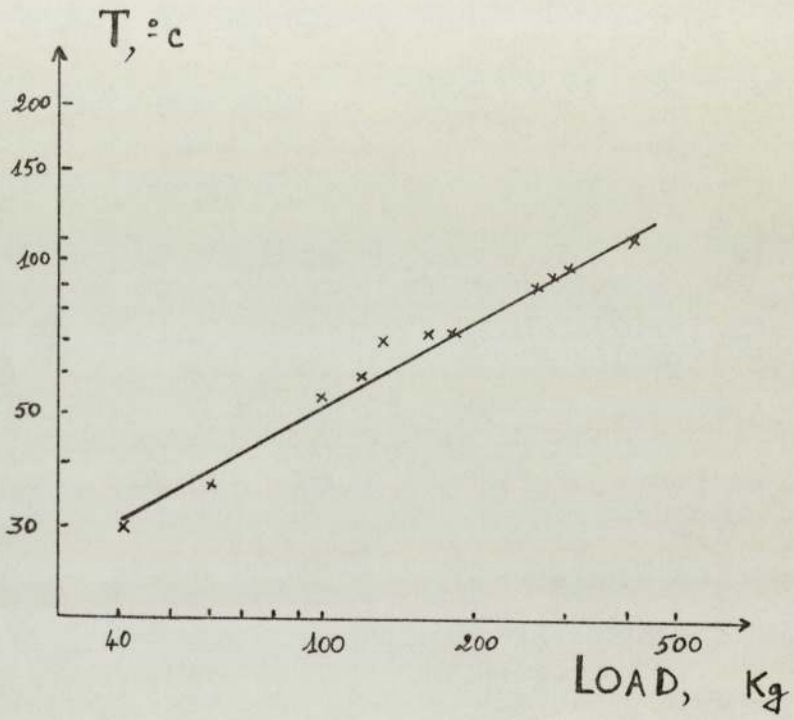

Fig.5. Temperature versus load

To study the formation of the AW and EP films, two loads from each corresponding region were selected and the temperature variation with running time was recorded. The results are displayed in Fig.6 and 7.

For the AW experiment, the temperature initially rises rapidly but then approaches a maximum value of 105°C after a period of 55 minutes and then stays constant for several hours. This suggests that the film builds up smoothly and also explains its regularities. At the end of the experiment, the scar was analysed using the SEM and the micrograph (Fig.8) shows the presence of the fine tracks but much wider than after 1 min running. The uniform striations of the film are still observed therefore increasing the running time does not affect the tribo-chemical effect on the adjacent layers formed by sulphur and iron. The scoring appears when the oil film is reduced and this confirms the physisorption theory predicted for the AW regime by previous work on the 4-ball machine (Ref.6).

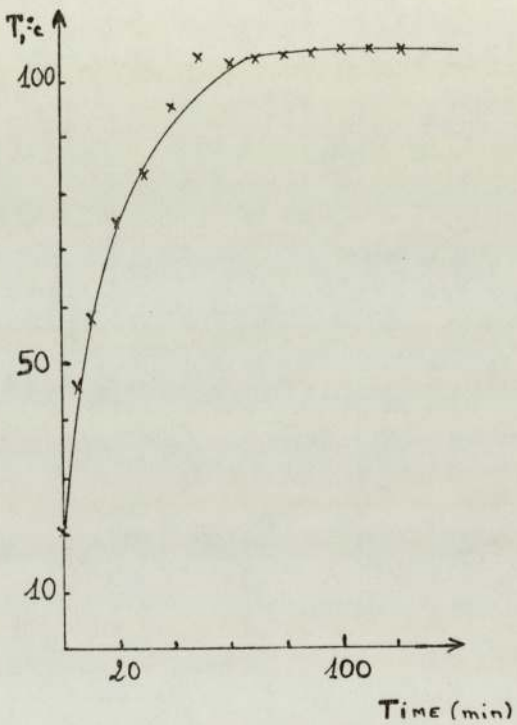

Fig.6. Temperature versus time of an A.W.load

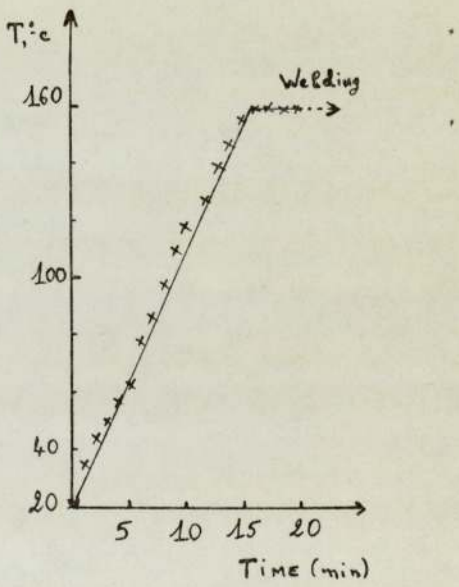

Fig.7. Temperature versus time of an EP load

For the EP experiment, the temperature rises linearly until reaching an equilibrium value of around 150°C in 19 min then one min later welding occurs. The film build up is not uniform and this implies that a chemical reaction is taking place between the oil film and the surface. The welding occurs when the iron sulphide film can no longer protect the surfaces from coming into metallic contact.

3.3. X-ray Diffraction (XRD) and X-ray Photoelectron Spectroscopy Analysis (XPS)

The earlier work (ref.5) has shown that XPS analysis did not detect any FeS in the EP region when DBDS was used as the additive. The elements detected were Fe_{3p}, O_{1s} and sulphate. In that paper, the different calculations were done by assuming that FeS and sulphate were the main compounds of the film after taking into consideration XRD analysis. To justify this assumption, further

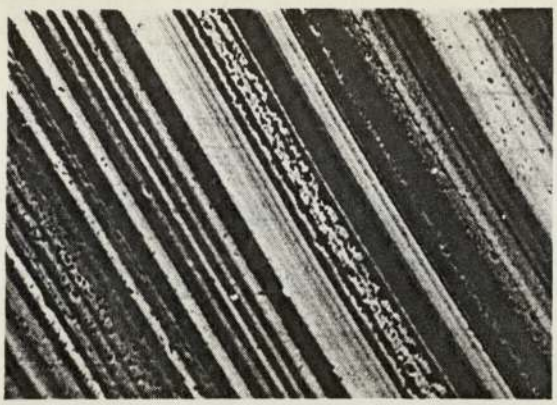

(a)

(b)

Fig.8. Electron picture and X-ray image distributions of the AW region for a long running time.

a) Micrograph of the worn surface.

b) Sulphur X-ray image.

c) Iron X-ray image.

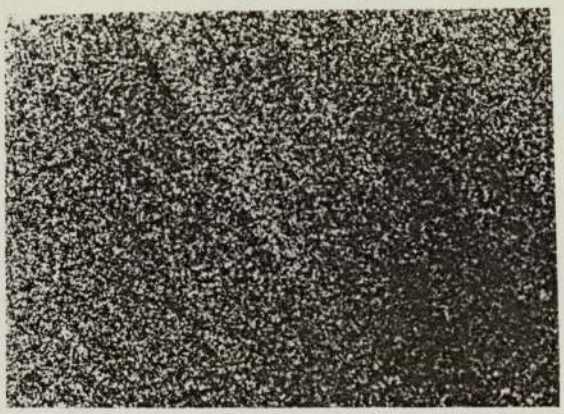

(c)

40 μm

analyses were carried out on wear debris at two different loads within the EP range by the means of XRD and also scars were examined by the X-ray glancing angle method. The possible identifications from the "d" values are FeS and F_eSO_4. The results obtained are summarised in Table 2.

A literature survey has been conducted for the Fe_{3p} information given by XPS and the concluding evidence (ref.7) proves that F_e^{2+} does have a spectrum state denoted by Fe_{3p} and so far there has not been any electronic configuration Fe_{3p} detected for F_e^{3+}. Therefore F_e^{2+} must be related to FeS. Meyer et al(ref.8)

TABLE 2
Results obtained in the EP region by using XRD, XPS and X-ray glancing angle method when DBDS was used as the additive

Element or compound		
XRD	XPS	X-ray glancing angle
FeS and $FeSO_4$	Fe_{3p}, O_{1s} and sulphate	FeS

have detected a very fine dispersed layer of FeS by using X-ray diffraction and Mössbauer Spectroscopy. Bird and Galvin (ref.4) have identified FeS by means of Electron Spectroscopy Chemical Analysis. Therefore, this corroborates the presence of FeS and substantiates the previous calculations.

XPS has also failed to detect FeS in the AW region when elemental sulphur was used as the additive whilst X-ray diffraction analysis shows traces of the compound in addition to Fe_2O_3. These results are shown in Table 3.

TABLE 3
Result obtained in the AW region by using XRD and XPS when elemental sulphur was used as the additive.

Element or compound	
XRD	XPS
- FeS - Fe_2O_3 - αFeO_3	- Fe_{3p} - O_{1s} - sulphate

For the EP, there is a good agreement between the results when both methods of analysis were used except that in addition XRD gave αFe and XPS gave Fe_{2p} (cf Table 4).

3.4 Nuclear Analysis

Rutherford Backscattering (RBS) (refs.5,9,10) and deuteron-proton stripping reaction [(d,p) reaction] (refs.9,11,12) were applied to study the surfaces films formed during wear by organo-sulphur compounds used as additives. Hence elemental sulphur was the main priority of the investigation. A brief description of the experimental procedures involved is given below :

In the case of RBS, the worn surfaces were bombarded by an incident alpha-particles beam energy of 2Mev then the recoil energy was measured and the number

TABLE 4

Results obtained in the EP region by using XRD and XPS when elemental sulphur was used as the additive.

Element or compound	
XRD	XPS
- FeS	- (??) Fe_{2p} ; Sulphur or organic sulphide
- αFe	- Fe_{3p}
- (??) Fe_2O_3	- O_{1s}
- -	- FeS, sulphate

of particles scattered was counted for a range of time between 15 and 20 min by means of a silicon surface barrier detector. Hence the identity and number of atoms present on the scar was determined. Fig.9 shows a typical spectrum when sulphur is detected.

For the $^{32}S(d,p)^{33}S$ reaction, a 2MeV deuteron beam was used to bombard the specimens and the energy spectrum of the protons produced by the induced nuclear reaction was measured using the same detector described above except that a Ni foil was placed in front of it to stop the elastically scattered deuteron and alpha-particles from (d,α) reactions. A typical spectrum of proton yield vs energy is shown in Fig.10. The detection angle was between 170° and 176° for both cases.

Selected specimens prepared in the AW and EP regions using the four additives at various concentrations were examined and the results were compared with the EPMA data reported previously (ref.5) and with further work. The results are summarised in Table 5.

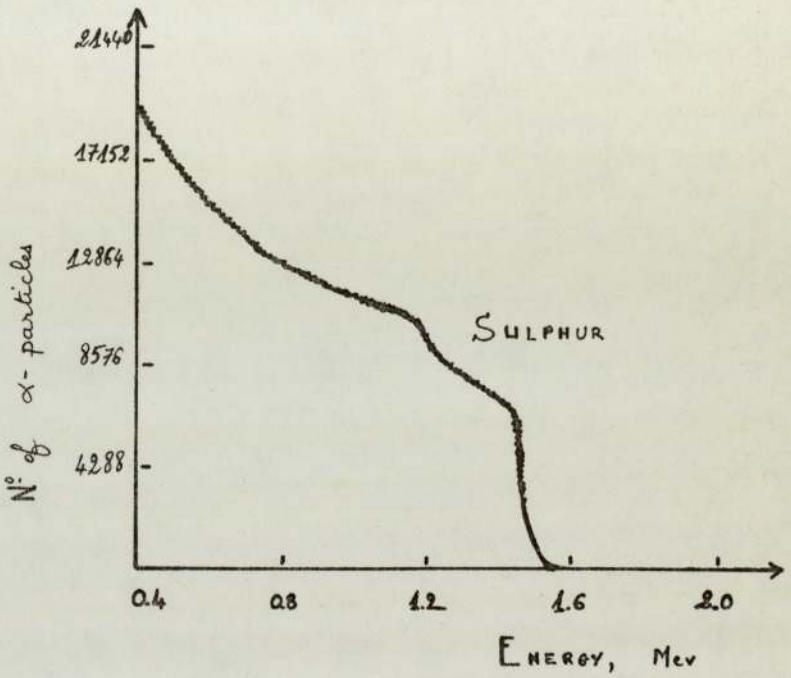

Fig.9: Experimental results for RBS of an EP film (0.25 wt% sulphur. 300 kgs, 300s.)

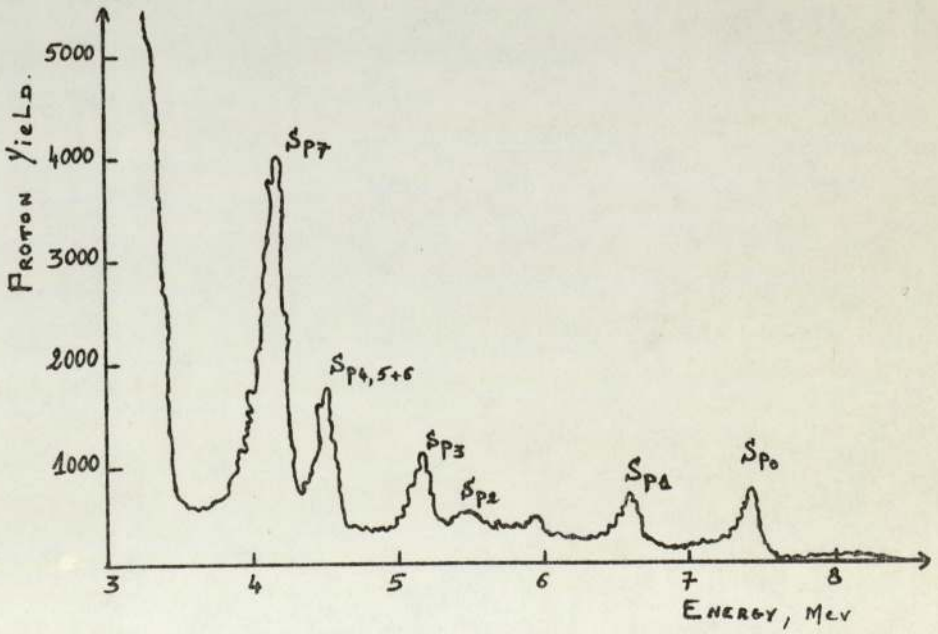

Fig.10: Typical spectrum of proton yield vs energy for an EP film (0.25 wt % sulphur, 300 kgs, 300s.)

TABLE 5

Results of EPMA, RBS and $^{32}S(d,p)^{33}S$ reaction

Additive	Load (kgs)	time (sec)	EPMA S (% wt)	EPMA Fe (% wt)	RBS Possible detection of sulphur	$^{32}S(d,p)^{33}S$ "t" = Calculated film thickness (μm) assuming structure (*) S	FeS	$FeSO_4$
wt 0.25% S	40	60	0.1	96.1	x	-	-	-
	130	60	10.7	86.5	x	0.03	0.04	0.10
	130	1100	3.00	86.0	x	0.28	0.33	0.93
	200	60	15.4	70.2	✓	0.83	0.83	2.71
	300	60	19.9	81.9	x(?)	0.19	0.23	0.62
	300	300	27.5	70.0	✓	0.73	0.86	2.41
wt 1.00% DBDS	130	15	-	-	x	0.07	0.09	0.24
	130	60	-	-	x	x(?)	x(?)	x (?)
	130	1100	7.3	87.8	x	0.13	0.15	0.41
	140	60	10.0	87.5	x	0.10	0.09	0.24
	300	60	17.1	72.4	x	0.17	0.20	0.57
	400	60	13.6	91.4	✓	0.19	0.22	0.62
wt 0.26% DBDS	130	60	3.6	88.7	x	x	x	x
	130	1100	3.6	95.5	x	0.07	0.08	0.23
	300	11	←		welding			→
wt 0.26% DPDS	130	60	4.1	90.2	x	x	x	x
	130	1100	3.23	81.2	x	0.09	0.11	0.30
	300		←		welding			→

- Indicates specimen not analysed; x Indicates no sulphur detected;
✓ Indicates sulphur detected.

$$(*)\ t = \frac{Y_p(\theta)}{n\Omega\sigma_{(\theta E_o)}} \cdot \frac{\text{Mol.wt}}{N_A \rho} \cdot 10^{-2}\,m \qquad \text{(ref.5)}$$

where $Y_p(\theta)$ = reaction yield; n = number of incident deuterons; $\sigma_{(\theta,E_o)}$ = differential cross-section (for the detection angle at 2 Mev); Ω = solid angle sampled by the detector; N_A = Avogadro's number; ρ = density of the compound.

In the calculations of the film thickness from the (d,p) results, the cross-section $\sigma(E)$ was considered constant. The earlier work (ref.5) has shown that in the range of 1.9 - 2 Mev, $\sigma_{(E)}$ does not change for either p_o or p_7 sulphur

peaks. Therefore the EP product films containing sulphur should be less than 1.5 - 2μm in order to apply the above equation. Hence $^{32}S(d,p)^{33}S$ reaction technique is suitable for such thin films where the energy loss is small (∿100 kev).

Table 5 shows that, in the case of RBS the probability of detecting sulphur is higher when the film becomes thick. The theory of the technique (ref.10) suggests that the probability of backscattering(i.e.the cross-section) is proportional to the square of the atomic number(Z) of the target. This makes the detection of light elements on heavy substrates very difficult unless the amount of the former is considerable. Hence, RBS is not recommended for detecting sulphur on mainly iron substrates unless the EP film is thick. The calculations from the results of RBS and EPMA for thick films show a good agreement between these two techniques (ref.5.).

4. CONCLUSION

It has been shown that no one analytical technique is suitable to give a total picture of the thickness and chemical composition of AW and EP films formed during 4-ball tests. However, conventional physical methods of analysis coupled with RBS and [d,p] reactions have proved satisfactory. The $^{32}S[d,p]^{33}S$ reaction is most useful for thin-to-medium films of sulphur products where the reaction cross-section remains sensibly constant. RBS however, is more suitable for thick films (those in which the [(d,p)] reaction starts failing) but the thickness of EP films normally formed is too thin for RBS to be of practical use in analyses for sulphur films on steel substrates. Similar considerations can be made for EPMA in that EP films are normally too thin for the beam to be stopped within the film and the analysis is therefore missed by the detection of the substrate material.

ACKNOWLEDGMENTS

One of the authors (A.Azouz)wishes to thank Dr.Terence F.J.Quinn for his assistance during the final stage of this report.

REFERENCES

1 K.G. Allum and E.S. Forbes, ASLE Transactions, 11 (1968) 162-175.
2 R.C. Coy and T.F.J. Quinn, ASLE Transactions, 18, 3 (1975) 163-174.
3 R.C. Coy and T.F.J. Quinn, Proc. Instn. Mech. Engng, 186, 35 (1972) 62-68.
4 R.J. Bird and G.D. Galvin, Wear, 37 (1975) 143-167.
5 D.M. Rowson and A. Azouz, An Investigation of Extreme Pressure Films formed during Wear Tests, 5th Interdisciplinary Surface Science Conference, Liverpool April 6 - 9, 1981, Vacuum (in press).
6 IP Standards for Petroleum and its Products, Part I, Section 2, Applied Science Publishers, 1975.
7 C.E. Moore, Atomic Energy Levels, Circular 467, National Bureau of Standards (U.S.A.)
8 K. Meyer, H. Berndt and B. Essiger, Applications of Surface Science, 4 (1980) 154-161.
9 J.F. Ziegler (Ed.), New Uses of Ion Accelerators, Plenum Press, New York, 1975.
10 D.A. Thompson and W.D. Mackinstoh, Journal of Applied Physics, 42, 10 (1971) 3269-3976.
11 E.A. Wolicki and A.R. Knudson, U.S. Naval Research Laboratory, Washington D.C. (1966).
12 G. Weber and L. Quaglia, Journal of Radioanalytical Chemistry, 12 (1972) 323-333.

DISCUSSION

Furey - I found your results most interesting. It is important in boundary lubrication to use whatever tools we can to learn about the detailed nature of surface films. Of course, the mere presence of a particular compound in the contact zone doesn't necessarily mean that it is "the" effective wear-reducing surface film. Based on what you have just presented (since the full paper is not yet available), what compound or compounds appear to be essential for anti-wear/anti-scuff action of the sulfur-containing additives studied ?

Another question : also is there any evidence of organic or polymeric films in the contact zone ?

Azouz - The authors thank Prof. Furey for his most pertinent comment and fully agree that the mere presence of a particuliar compound is not necessarily indicative of the only mode of surface protection. Our work would suggest that the essential compound appearing on the films formed by organo - sulphur additives is FeS. This was identified by X-ray diffraction in the extreme pressure region. In the Anti-wear region, although X-ray photoelectron spectroscopy did not detect FeS, it showed the presence of Fe_{3p} which we believe is related to Fe^{2+} (see Table 3). The Fe^{2+} state is the valence state of iron in FeS. This confirms the results found by other workers as stated in this paper (refs. 4 and 8).

In reply to this second question, we would state that so far no organic or polymeric film has been detected in the contact zone under A.W. conditions. Under E.P. conditions, there is some tentative evidence of the formation of organic sulphide as shown by X.P.S. (see table 4).

Richmond - Could you explain why you did not translate your measurements of temperature into rates of heat generation which would seem to be a parameter relevant to the fonction ?

Azouz - The authors agree with Mr Richmond that the rate of heat generation would be a very useful parameter for film generation. However, we did not use such rate of heat generation since the only measurement available was for the bulk oil temperature and previous work on the pitting of EN31 steel in the presence of sulphur (ref. B1 and B2) has shown that it is the bulk oil temperature which determines the relevant sulphur-iron reaction to form either FeS or FeS_2 respectively below or above 175°C. This agrees with the experimental results quoted in this paper.

References :
B1. D.M. Rowson and Y.L. Wu, Wear, 70(1981) 373.381
B2. D.M. Rowson and Y.L. Wu, Physical Analysis in Rolling and Sliding Discs, Proceedings of the Institute of Petroleum, London October 1980, 79-90.